PROGRESS REPORT

AEC Grant No. AT(11-1)1422

"Determination of Body Composition In Vivo"

NASA Grant No. Y-NGR-50-002-051

"Applications of the Direct Photon Absorption
Technique for Measuring Bone Mineral
Content In Vivo"

August 1, 1969

John R. Cameron, Ph.D.
Principal Investigator
University of Wisconsin
Department of Radiology
Madison, Wisconsin 53706

Preface

The reports found on the following pages represent the research efforts at the Bone Measurement Laboratories of the University of Wisconsin during the past year. We are pleased to have been joined by Dr. John M. Jurist in September, 1968. Some of the reports by Dr. Jurist represent work which was started at the University of California, Los Angeles.

Research support for the bone measurement laboratories comes from a variety of sources, these are: United States Atomic Energy Commission through Contract AT(11-1)-1422, the National Aeronautics and Space Administration through Grant Y-NCR-50-002-051, the University of Wisconsin (Funds 101-9301 and 101-9302), the NASA Institutional Grant to the University of Wisconsin Graduate School, and the NIH Institutional Grant to the University of Wisconsin Medical School. Because of the interlocking nature of this support it was decided to include all reports in a single volume.

Some of the recipients of this volume may be interested in earlier reports from our laboratory and a list of these will be found after the table of contents together with a list of papers that have been published in the open literature. Copies of some of these reports and papers are still available.

This research has obviously involved quite a few people as indicated by the authors of the various reports. I would like to thank all of these individuals for their cooperation and for the stimulation I have received working with them.

I also want to acknowledge with thanks the help of Mrs.
Freida Binder who was a technician in our laboratories
during the past year and who has now returned to Vienna,
Austria. Mrs. Binder was most helpful in our research and
we will miss her.

We also wish to acknowledge the help and cooperation
of the staff of the following institutions:

Manor House, Madison, Wisconsin

St. Bernards School, Middleton, Wisconsin

Mendota State Hospital, Madison, Wisconsin

Sisters of Notre Dame Infirmary, Elm Grove, Wisconsin

TABLE OF CONTENTS

Table of Contents (continued-pg. 2)

Bibliography of Past Progress Reports of Research at the
University of Wisconsin on Bone Mineral Content and Body Composition

Partly Supported by: USAEC Contract No. AT (11-1)-1422
NASA Contract No. Y-NGR-50-002-51
NASA Institutional Grant to the University
of Wisconsin - #144-6161

1. Sorenson, J.A. and Cameron, J.R., Body Composition Determination by Differential Absorption of Monochromatic X-Rays, USAEC Report COO-1422-1, (1965).

2. Cameron, J.R., et al, Ash Weight vs. Bone Mineral Content by Direct Photon Absorption Technique, USAEC Report, COO-1422-2, (1965).

3. Cameron, J.R., et al, Longitudinal Studies of Bone Mineral Content by the Photon Absorption Technique, USAEC Report, COO-1422-3, (1965).

4. Cameron, J.R., et al, Factors Affecting the Measurement of Bone Mineral Content by the Direct Photon Absorption Technique, USAEC Report, COO-1422-4, (1965).

5. Cameron, J.R. and Sorenson, J.A., Improved Instrumentation for Bone Mineral Measurement In Vivo, USAEC Report, COO-1422-5, (1965). (Presented to the First International Conference on Medical Physics, Harrogate, England, Sept., 1965)

6. Cameron, J.R. and Sorenson, J.A., Bone Mineral Measurement by Improved Photon Absorption Technique, USAEC Report, COO-1422-6, (1965). (Presented to Conf. on Progress in Development of Bone Densitometry, NASA, Washington, D. C., March, 1965).

7. Sorenson, J.A., Judy, P., Witt, R. and Cameron, J.R., Progress in the Measurement of Bone Mineral Content by the Direct Photon Absorption Technique, USAEC Report, COO-1422-7, (1966).

8. Sorenson, J.A. and Cameron, J.R., Body Composition Determination by Differential Photon Absorption Technique, USAEC Report, COO-1422-8, (1966).

9. Sorenson, J.A., Witt, R.M. and Cameron, J.R., Progress in Development of a Bone Equivalent Material, USAEC Report, COO-1422-9, (1966).

10. Judy, P.F., Raffii, A.S., Cameron, J.R. and Sorenson, J.A., New Bone Mineral Scanners, USAEC Report, COO-1422-10, (1967).

11. Smith, E.L., Cameron, J.R. and Sorenson, J.A., In Vivo Bone Mineral Measurements of the Rat Femur, USAEC Report, COO-1422-11, (1967).

12. Judy, P.F., Cameron, J.R. and Sorenson, J.A., Effect of the Measurement of Bone Mineral of I-126 Contamination of I-125, USAEC Report, COO-1422-12, (1967).

13. Mazess, R.B., Cameron, J.R. and Sorenson, J.A., Precision and Accuracy of Bone Mineral Determination, USAEC Report, COO-1422-13, (1967).

14. Witt, R.M., Judy, P.F., Cameron, J.R. and Sorenson, J.A., Instruction Manual for Semi-Automatic Bone Measuring System, USAEC Report, COO-1422-14, (1967).

15. Sorenson, J.A. and Cameron, J.R., Reliability of Measuring Changes in Bone Mineral Content as a Function of the Precision of the Measurement, USAEC Report, COO-1422-15, (1967).

16. Sorenson, J.A. and Cameron, J.R., Data Recording System for Bone Mineral Measurements, USAEC Report, COO-1422-16, (1967).

17. Sorenson, J.A., Raffii, A.S. and Cameron, J.R., Bone Mineral Content As A Function of Bone Diameter In Cortical Bone, USAEC Report, COO-1422-17, (1967).

18. Suntharalingam, S., Judy, P.F., Witt, R.M., Cameron, J.R. and Sorenson, J.A., A Moldable Soft Tissue Equivalent Material, USAEC Report, COO-1422-18, (1967).

19. Witt, R.M., Raffii, A.S., Cameron, J.R. and Sorenson, J.A., Modification to Computer Program To Determine Bone Mineral Content, USAEC Report, COO-1422-19, (1967).

20. Sorenson, J.A. and Cameron, J.R., A Reliable In Vivo Measurement of Bone Mineral Content, USAEC Report, COO-1422-20, (1967). (Reprint from The Journal of Bone and Joint Surgery, Vol. 49-A, No. 3, pp. 481-497, April, 1967).

21. Cameron, J.R. and Sorenson, J.A., Measurement of Bone Mineral by the Direct Photon Absorption Method: Principles and Instrumentation, USAEC Report, COO-1422-21, (1968).

22. Sorenson, J.A. and Cameron, J.R., Measurement of Bone Mineral by Direct Photon Absorption Method: Experimental Results, USAEC Report, COO-1422-22, (1968).

23. Mazess, R.B., Cameron, J.R. and Sorenson, J.A., A Comparison of Radiological Methods for Determining Bone Mineral Content, USAEC Report, COO-1422-23, (1968).

24. Sorenson, J.A. and Briggs, R.C., Transmission Scanning with Tc-99m and Cs-137, USAEC Report, COO-1422-24, (1968).

25. Smith, E.L., Clark, J.L. and Cameron, J.R., Remineralization of a Fractured Tibia, USAEC Report, COO-1422-25, (1968).

26. Sorenson, J.A. and Cameron, J.R., Comparison of I-125, Pb-210, and Am-241 as Radiation Sources for Bone Mineral Measurement, USAEC Report, COO-1422-26, (1968).

27. Clark, J.L. and Sorenson, J.A., Bone Mineral Measurement with a Line Printer Output and Desk-top Calculator Computations, USAEC Report, COO-1422-27, (1968).

28. Kianian, Kianpour and Sorenson, J.A., Program For Bone Mineral Computations Using General Electric Time-Sharing Service, USAEC Report, COO-1422-28, (1968).

29. Sorenson, J.A., Mazess, R.B., Smith, E.L., Clark, J.L., and Cameron, J.R., Bone Mineral Content and Diameter vs. Age in the Radius and Humerus of Normal Subjects, USAEC Report, COO-1422-29, (1968).

30. Mazess, R.B., Estimation of Bone and Skeletal Weight by the Direct Photon Absorptiometric Method, USAEC Report, COO-1422-30, (1968). (From the "Symposium on Skeletal Mineralization" at the annual meeting of the Am. Assoc. of Physical Anthropologists, Detroit 1968).

31. Sigmon, B.A., Distribution of Bone Mineral in the Femur, USAEC Report, COO-1422-31, (1968). (From the Symposium on Skeletal Mineralization, Am. Assoc. of Physical Anthropologists, April 24, 1968, Detroit).

32. Cameron, J.R., Mazess, R.B. and Sorenson, J.A., Precision and Accuracy of Bone Determination by Direct Photon Absorptiometry, USAEC Report, COO-1422-32, (1968).

33. Smith, E.L., Jr., Felts, W. L., The Effects of Physical Activity on Bone, USAEC Report, COO-1422-33, (1968). (Presented at the Symposium on Skeletal Mineralization, Am. Assoc. of Physical Anthropologists, Detroit, 1968).

34. Smith, E.L., Kempke, W.G., Seireg, Ali, Cameron, J.R., In Vitro Measurements of Bone Volume by Air Displacement, USAEC Report, COO-1422-34, (1968).

35. Bartok, S.P., Witt, R.M. and Cameron, J.R., Radiation Effects on Bone Mineral Content, USAEC Report, COO-1422-35, (1968).

36. Witt, R.M., Sorenson, J.A. and Cameron, J.R., Construction of an Iodine-125 Photon Source Using an Improved Source Holder, USAEC Report, COO-1422-36, (1968).

37. Judy, P.F., Sorenson, J.A. and Cameron, J.R., An Estimation of Variance of Bone Mineral Content Measurement, USAEC Report, COO-1422-37, (1968).

38. Judy, P.F., Cameron, J.R. and Sorenson, J.A., A Description of the Bone Mineral Content Measurement with a Modulation Transfer Function, USAEC Report, COO-1422-38, (1968).

39. Mazess, R.B. and Cameron, J.R., A Portable Scanning System with Direct Readout for Absorptiometric Determination of Bone Mineral Content, USAEC Report, COO-1422-39, (1968).

40. Witt, R.M., Sorenson, J.A. and Cameron, J.R., An Improved Linear Bone Mineral Scanner, USAEC Report, COO-1422-40, (1968).

UNIVERSITY OF WISCONSIN
BONE MINERAL BIBLIOGRAPHY

1. Cameron, J.R., Grant, R.M., and MacGregor, R., An Improved Technique for the Determination of Bone Mineral Content In Vivo., Radiology 78: 111, January, 1962. (Abstract).

2. Cameron, J.R., Sorenson, J.A., Measurement of Bone Mineral In Vivo: An Improved Method, Science 142, 230-232, 1963. (Reprint in 1965 AEC Progress Report)

3. Mazess, R.B., Cameron, J.R., O'Connor, R., and Knutsen, D., Accuracy of Bone Mineral Measurements, Science, Vol. 145, 388, No. 3630, July 24, 1964.

4. Sorenson, J.A. and Cameron, J. R., Body Composition By Differential Absorption by Monochromatic X-rays, Symposium of Low-Energy X- and Gamma Sources and Applications. Institute of Tech. Research Institute, Chicago, Illinois, October 20-21, 1964.

5. Cameron, J.R. and Sorenson, J.A., Bone Mineral Measurement by Improved Photon Absorption Technique, Conference on Progress in Development of Methods in Bone Densitometry, NASA, #SP-64, Washington, D.C., March, 1965.

6. Cameron, J.R. and Sorenson, J.A., The Measurement of Bone Mineral and Body Composition In Vivo, IVth Nordic Meeting on Clinical Physics, Hanko, Finland, September, 1966.

7. Cameron, J.R. and Sorenson, J.A., Bone Mineral Measurement In Vivo Using Monoenergetic Photons From A Radioactive Source, Proceedings of The Symposium on Biomedical Engineering, Marquette University, Milwaukee, Wisconsin, June 1966.

8. Sorenson, J.A. and Cameron, J.R., A Reliable In Vivo Measurement of Bone Mineral Content, The Journal of Bone and Joint Surgery, Vol. 49-A, No. 3, April, 1967.

9. Clark, J.L., Cameron, J.R. and Sorenson, J.A., A Reliable Method of Measuring Bone Mineral In Vivo, Society of Nuclear Medical Technologists Symposium, Chicago, Illinois, Nov., 1967. (talk)

10. Briggs, R.C., Wilson, E.B. and Sorenson, J.A., Combined Emission-Transmission Scanning of the Skeleton, Radiology, Vol. 90, No. 2, pp. 348-350, February, 1968.

11. Cameron, J.R. and Whedon, G.D., editors, Proc. Conference on Progress in Methods of Bone Mineral Measurement, Spons. by NIH-NIAMD, In press, Feb., 1968.

Articles included in these proceedings:

12. Cameron, J.R. and Sorenson, J.A., Measurement of Bone Mineral by the Direct Photon Absorption Method: Principles and Instrumentation

13. Sorenson, J.A., Cameron, J.R. and Mazess, R.B., Measurement of Bone Mineral by the Direct Photon Absorption Method: Experimental Results.

14. Mazess, R.B., Cameron, J.R. and Sorenson, J.A., A Comparison of Radiologic Methods for Determining Bone Mineral Content.

    (The above three articles are in the 1968 Progress Report)

15. Cameron, J.R., Mazess, R.B., and Sorenson, J.A., Precision and Accuracy of Bone Mineral Determination by Direct Photon Absorptiometry, Investigative Radiology, 3 (3), 141, May-June, 1968. (Included in the 1968 USAEC Progress Report)

16. Mazess, R.B., Cameron, J.R., and Sorenson, J.A., Measurement of Skeletal Status; Use of Direct Absorptiometry, Symposium of the Anthropology of Bone, American Assoc. for the Advancement of Science, Dec., 1968, Dallas, Texas. (Talk)

17. Sorenson, J.A., Briggs, R.C. and Cameron, J.R., ^{99m}Tc Point Source for Transmission Scanning, Journal of Nuclear Medicine, Vol. 10, No. 5, pp. 252-253, May, 1969.

18. Cameron, J.R., Jurist, J.M., Sorenson, J.A., Mazess, R.B., Evaluation of Skeletal Status in Humans, Preprints of the 1969 Annual Scientific Meeting of the Aerospace Medical Association, Aerospace Medical Association, Washington, D.C., pp. 130-131, 1969, text of a paper delivered at the meeting, May 7, 1969, San Francisco, California.

19. Smith, E.L., Jurist, J.M., Babcock, S.W., and Cameron, J.R., Detection of Osteoporosis by Measurement of Monoenergetic Photon Absorption, Eighth International Congress of Gerontology, Abstract Volume, Abstract of a paper to be delivered at the Congress, Aug. 26, 1969, Washington, D.C.

PUBLICATIONS ON MEASUREMENT OF MECHANICAL PROPERTIES OF BONE

1. J.M. Jurist, W.A. Selle: Acoustical detection of osteoporosis, The Physiologist, 8:203 (Aug. 65), abstract of a paper delivered at the 17th Autumn Meeting of the American Physiological Society, Aug. 26, 1965, Los Angeles, California.

2. W.A. Selle, J.M. Jurist: Acoustical detection of senile osteoporosis, Proceedings of the Society for Experimental Biology and Medicine, 121:150 (Jan. 66).

3. W.A. Selle, J.M. Jurist: Acoustical measurement of bone density, Federation Proceedings, 25:577 (Mar.-Apr. 66 Part I), abstract of a paper delivered at the 50th Annual Meeting of the Federation of American Societies for Experimental Biology, Apr. 15, 1966, Atlantic City, New Jersey.

4. W.A. Selle, J.M. Jurist: Detection of osteoporosis by a new technique, Archives of Physical Medicine and Rehabilitation, 47:568 (Aug. 66), abstract of a paper delivered at the 44th Annual Session of the American Congress of Physical Medicine and Rehabilitation, Sept. 1, 1966, San Francisco, California.

5. W.A. Selle, J.M. Jurist: The onset of postmenopausal osteoporosis as studied by a new technique, Journal of the American Geriatrics Society, 14:930 (Sept. 66).

6. W.A. Selle, J.M. Jurist: Osteoporosis and the menopause, OB/GYN Digest, 9:33 (Apr. 67).

7. J.R. Cameron, J.M. Jurist, J.A. Sorenson, R.B. Mazess: Evaluation of skeletal status in humans, Preprints of the 1969 Annual Scientific Meeting of the Aerospace Medical Assoc., Aerospace Medical Association, Washington, D.C., pp. 130-131, 1969, text of a paper delivered at the meeting, May 7, 1969, San Francisco, California.

8. J.M. Jurist: Ulnar vibratory properties, Proceedings of the Conference on Progress in Methods of Bone Mineral Measurement, text of a paper delivered at the conference, Feb. 17, 1968, Bethesda, Maryland, in press.

9. J.M. Jurist, J.R. Cameron: Measurement of bone resonant frequency in vivo, Proceedings of the Second International Conference on Medical Physics, abstract of a paper to be delivered at the conference, Aug. 12, 1969, Boston, Massachusetts, in press.

10. J.M. Jurist, E.L. Smith, S.W. Babcock, J.R. Cameron: In vivo estimation of bone elasticity by measurement of ulnar resonant frequency, Eighth International Congress of Gerontology, Abstract Volume, abstract of a paper to be delivered at the congress, Aug. 26, 1969, Washington, D.C., in press.

SUMMARY OF DATA ON THE BONE MINERAL OF THE RADIUS IN NORMALS

by John R. Cameron

The following graphs and tables present summaries of data on normal individuals measured in the University of Wisconsin Bone Mineral Laboratory from the period 1965-March 1969. Although we have measured a variety of bones, these data are all for the radius mear midshaft and essentially all of them were for the left arm. We feel these data may be of interest to other groups using the same technique. It should be noted that all of these data are for whites, we have relatively little information on other races.

Since these data were collected over a number of years, various individuals have contributed to this summary. These are: James A. Sorenson, Richard B. Mazess, John M. Jurist, Philip F. Judy, Robert M. Witt, Everett L. Smith, Joyce Clark Fischer, Mira Binder, Kianpour Kianian, Matt Weber, Ali Raffii, Siva Suntharalingam, and Frances Lin. We wish to express our thanks to these individuals.

HEIGHT AND WEIGHT OF NORMAL MALE SUBJECTS

Age Category (yrs)	Height (in)			Weight (lb)		
	mean	std dev	N	mean	std dev	N
6	47.7	1.9	15	50.6	5.5	15
7	50.4	2.0	26	57.3	8.3	26
8	53.3	2.9	23	63.3	15.0	23
9	55.4	2.4	24	72.9	15.6	24
10	57.2	2.2	29	80.2	17.0	30
11	59.0	2.0	25	85.7	11.7	25
12	61.3	3.3	18	104.4	22.3	17
13	62.1	3.8	14	112.2	26.1	16
14	66.1	2.6	11	127.9	17.0	11
15-16	68.9	2.9	43	149.9	21.6	43
17-19	71.5	2.6	37	164.0	24.8	37
20-29	70.2	3.1	78	167.5	26.7	78
30-39	70.2	2.3	43	171.3	25.5	44
40-49	69.8	2.9	43	172.5	22.1	42
50-59	69.1	2.7	21	169.5	21.9	23
60-69	68.9	3.5	32	165.9	37.0	33
70-79	68.7	3.2	14	161.8	26.8	18
80-89	---	---	---	142.5	16.4	13

HEIGHT AND WEIGHT OF NORMAL FEMALE SUBJECTS

Age Category (yrs)	Height (in)			Weight (lb)		
	mean	std dev	N	mean	std dev	N
6	48.5	2.5	12	51.3	8.4	12
7	50.7	2.4	19	55.5	8.6	19
8	53.0	3.6	16	60.4	8.5	16
9	54.2	2.9	20	68.9	13.6	20
10	56.3	2.4	23	75.7	13.3	23
11	59.4	2.2	19	91.3	19.8	20
12	63.0	3.0	14	98.4	16.7	14
13	63.4	2.2	16	102.6	16.6	16
14	65.4	2.5	16	119.5	17.9	16
15-16	65.5	2.4	37	123.7	13.3	37
17-19	65.2	3.0	62	128.2	20.2	62
20-29	64.7	2.6	67	130.1	23.1	67
30-39	64.8	2.7	22	143.7	24.1	22
40-49	62.7	3.4	31	139.0	23.6	31
50-59	63.6	2.2	34	142.7	26.6	35
60-69	62.9	2.9	34	135.3	23.7	40
70-79	63.2	2.6	39	136.4	24.2	58
80-89	62.8	2.7	13	120.0	17.4	38
90-99	---	---	---	124.4	22.3	7

BONE MINERAL CONTENT OF THE RADIAL MIDSHAFT OF NORMAL MALE SUBJECTS

Age Category (yrs)	N	Age (yrs)		BM (g/cm)		Dia (cm)		BM/Dia (g/cm²)	
		mean	std dev	mean	std dev	mean	std dev	mean	std dev
6	15	6.0	---	0.48	0.06	0.96	0.09	0.49	0.04
7	26	7.0	---	0.51	0.07	1.00	0.09	0.51	0.04
8	23	8.0	---	0.56	0.08	1.02	0.10	0.54	0.05
9	24	9.0	---	0.58	0.06	1.05	0.11	0.56	0.04
10	30	10.0	---	0.64	0.09	1.11	0.11	0.58	0.07
11	25	11.0	---	0.69	0.11	1.13	0.13	0.61	0.05
12	18	12.0	---	0.76	0.12	1.20	0.13	0.63	0.06
13	16	13.0	---	0.79	0.12	1.26	0.12	0.63	0.05
14	11	14.0	---	0.87	0.14	1.28	0.13	0.68	0.06
15-16	43	15.4	0.6	1.08	0.16	1.41	0.15	0.76	0.07
17-19	37	17.5	0.7	1.20	0.16	1.46	0.19	0.82	0.06
20-29	80	24.5	3.0	1.29	0.17	1.48	0.14	0.87	0.07
30-39	45	33.6	2.7	1.32	0.15	1.49	0.13	0.89	0.06
40-49	43	44.1	3.0	1.31	0.14	1.49	0.13	0.88	0.08
50-59	24	55.0	3.0	1.33	0.16	1.51	0.12	0.88	0.07
60-69	35	63.9	3.1	1.24	0.23	1.56	0.18	0.79	0.11
70-79	19	74.5	2.9	1.27	0.19	1.56	0.15	0.82	0.12
80-89	13	84.1	2.6	1.19	0.23	1.57	0.19	0.76	0.11

BONE MINERAL CONTENT OF THE RADIAL MIDSHAFT OF NORMAL FEMALE SUBJECTS

Age Category (yrs)	N	Age (yrs)		BM (g/cm)		Dia (cm)		BM/Dia (g/cm^2)	
		mean	std dev	mean	std dev	mean	std dev	mean	std dev
6	12	6.0	---	0.44	0.08	0.93	0.11	0.48	0.05
7	20	7.0	---	0.45	0.06	0.91	0.09	0.50	0.05
8	16	8.0	---	0.49	0.05	0.93	0.08	0.53	0.04
9	20	9.0	---	0.55	0.07	0.97	0.10	0.56	0.04
10	23	10.0	---	0.57	0.09	1.00	0.11	0.57	0.05
11	20	11.0	---	0.65	0.12	1.08	0.10	0.60	0.09
12	14	12.0	---	0.73	0.10	1.13	0.16	0.65	0.08
13	16	13.0	---	0.74	0.09	1.16	0.11	0.64	0.05
14	16	14.0	---	0.86	0.10	1.20	0.11	0.71	0.04
15-16	37	15.4	0.5	0.87	0.08	1.20	0.09	0.73	0.05
17-19	62	18.0	1.0	0.92	0.11	1.23	0.11	0.75	0.06
20-29	68	22.9	2.7	0.94	0.11	1.23	0.12	0.76	0.05
30-39	22	33.9	3.1	1.00	0.13	1.29	0.14	0.77	0.05
40-49	31	44.0	3.0	0.98	0.10	1.28	0.13	0.77	0.04
50-59	37	55.1	2.8	0.86	0.13	1.23	0.12	0.70	0.07
60-69	43	64.6	2.9	0.80	0.15	1.25	0.16	0.63	0.08
70-79	62	74.1	3.1	0.72	0.12	1.26	0.11	0.57	0.09
80-89	41	83.4	2.7	0.70	0.14	1.29	0.13	0.54	0.09
90-99	9	92.0	2.3	0.71	0.13	1.39	0.07	0.51	0.09

90-99 YR ♀
N = 9

BONE MINERAL (vertical axis): 0, 0.25, 0.5, 0.75, 1.0, 1.25, 1.5

DIAMETER (horizontal axis): 0, 0.3, 0.6, 0.9, 1.2, 1.5, 1.8, 2.1, 2.4

40-49 YR ♂
N = 43

70-79 YR ♂
N = 19

50-59 YR ♂
N = 24

80-89 YR ♂
N = 13

60-69 YR ♂
N = 35

90-99 YR ♂
N =
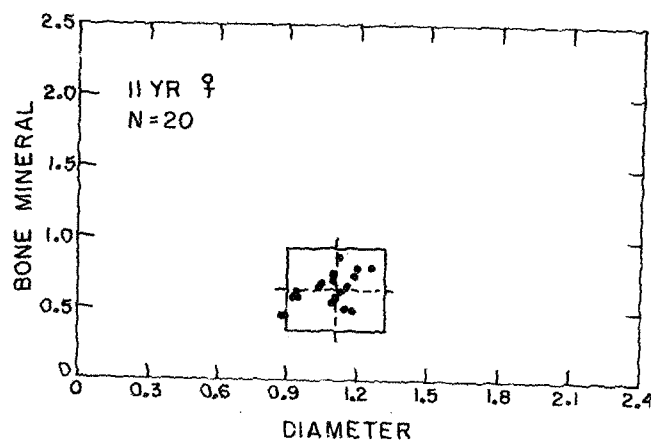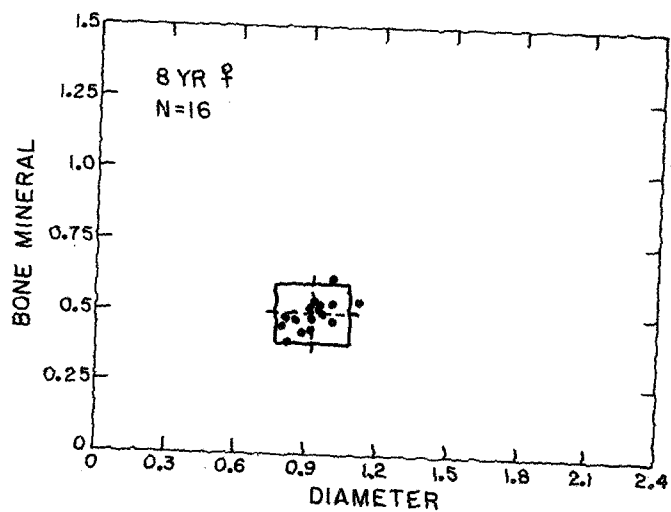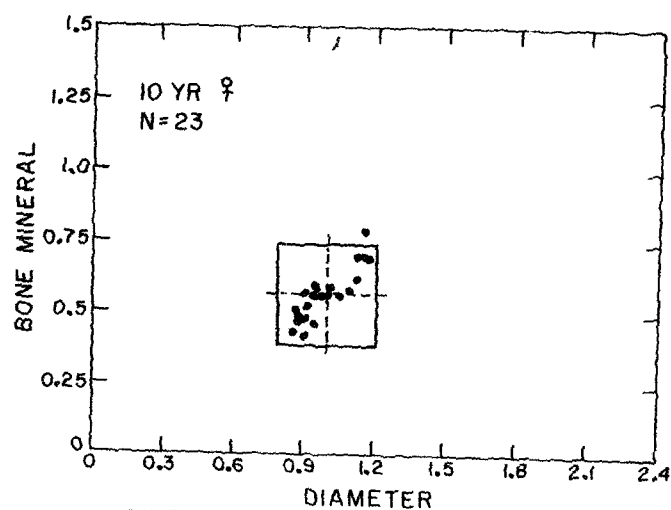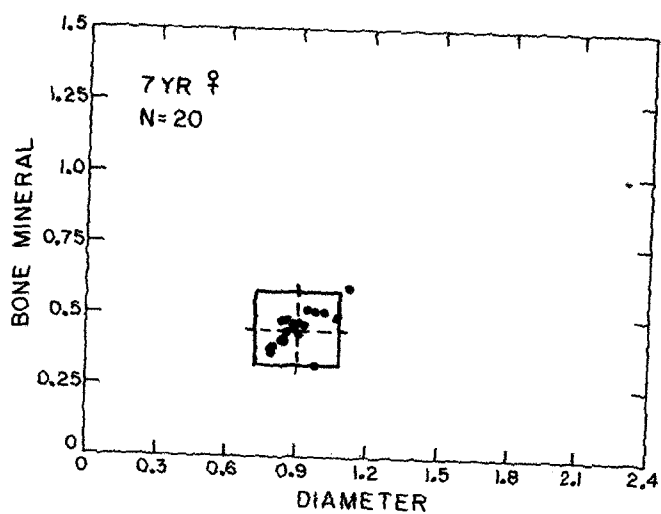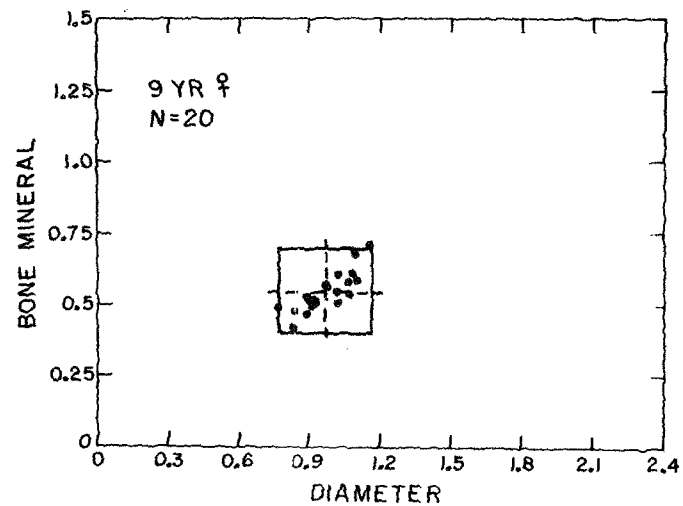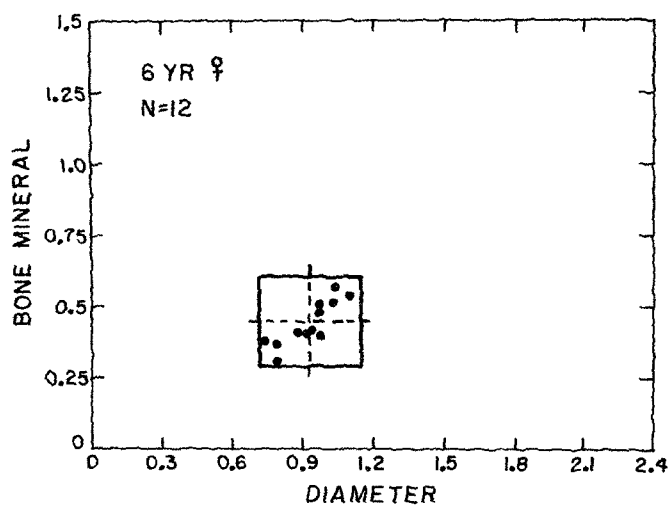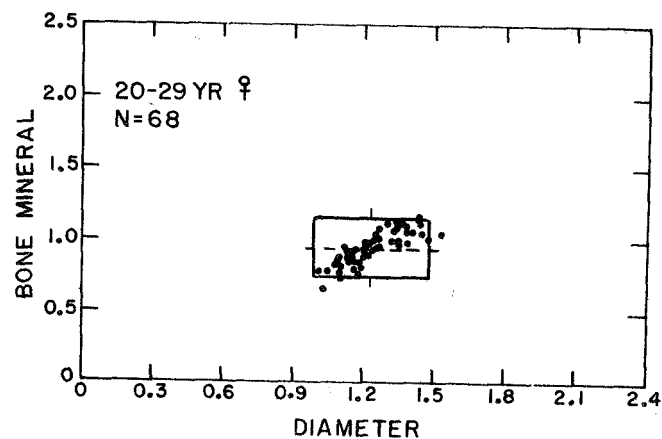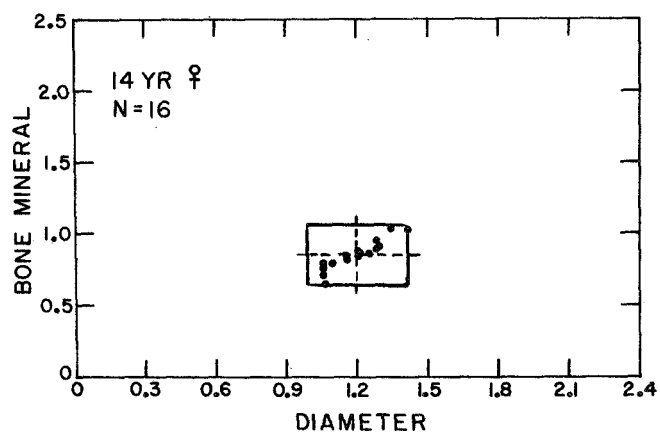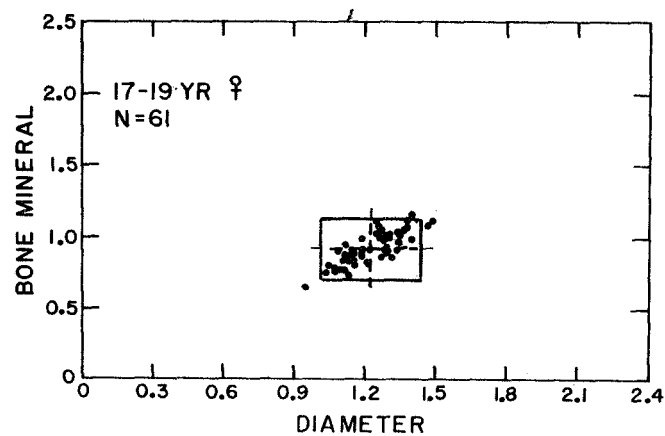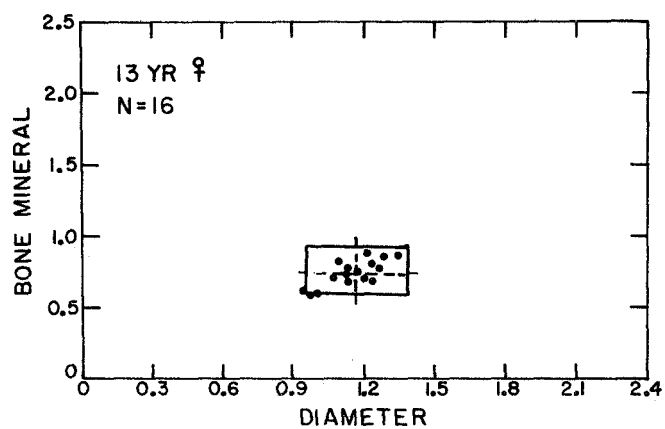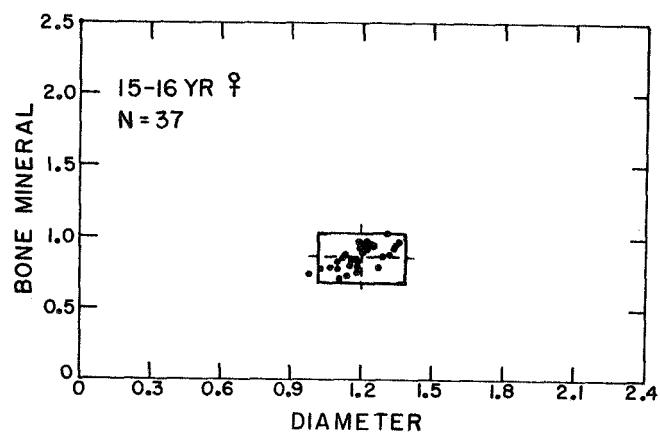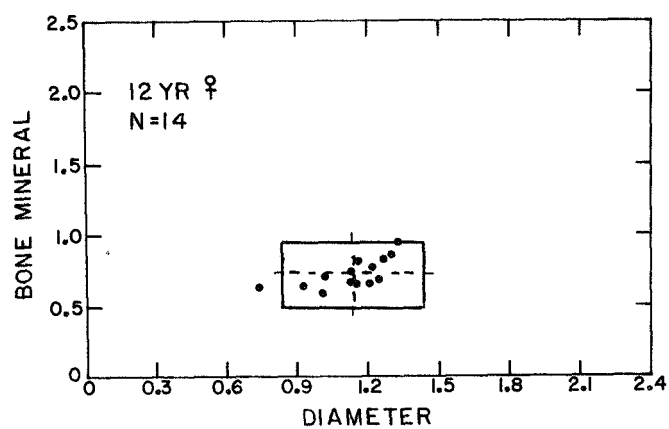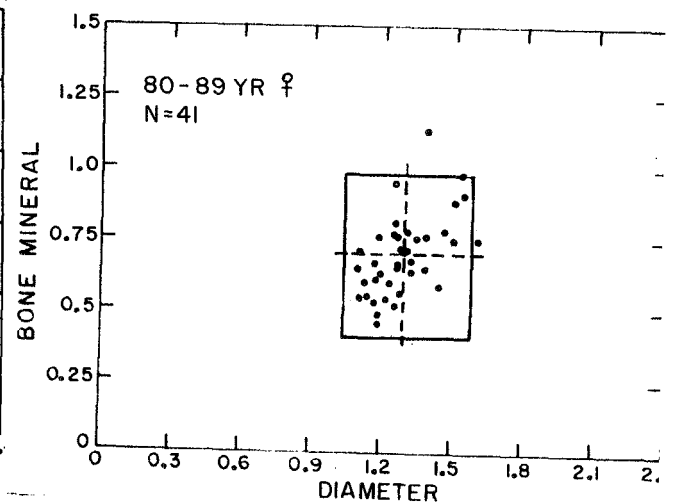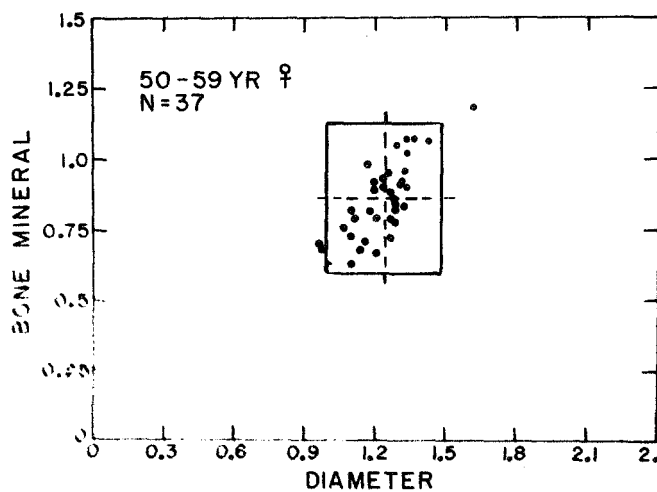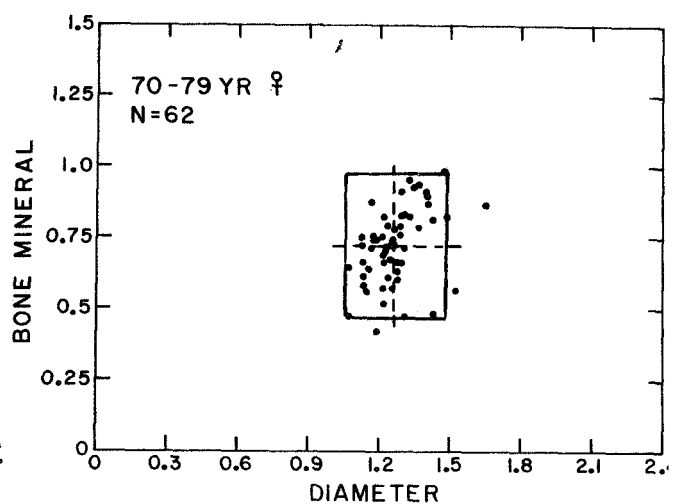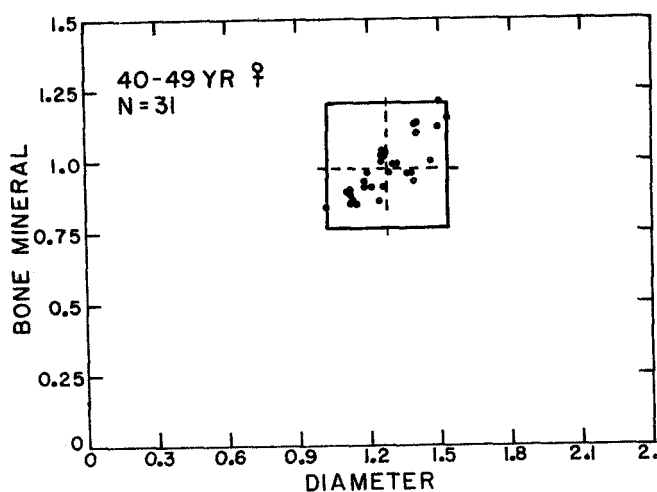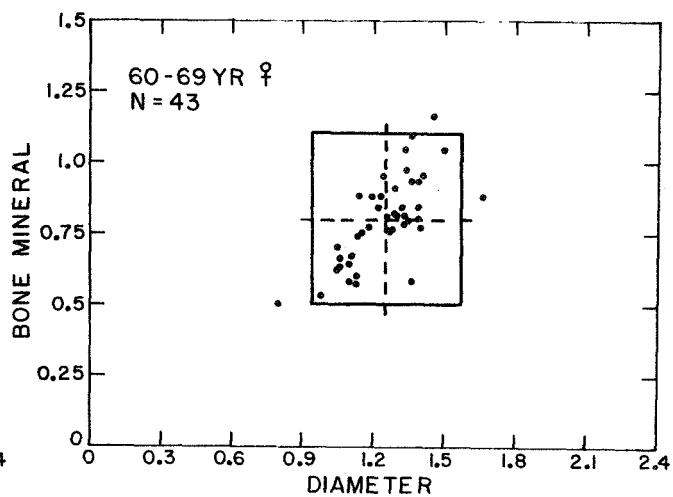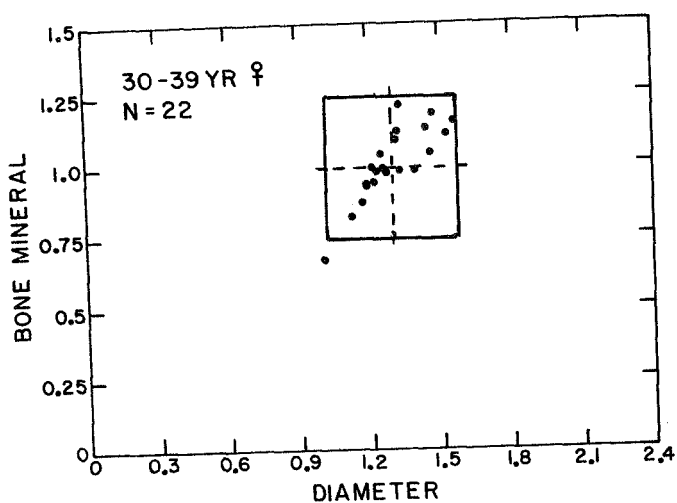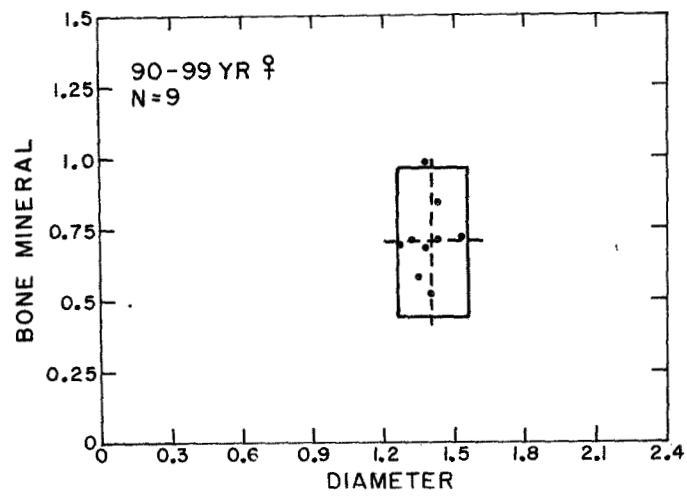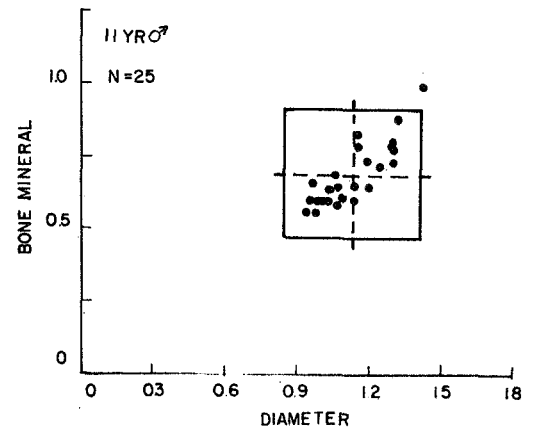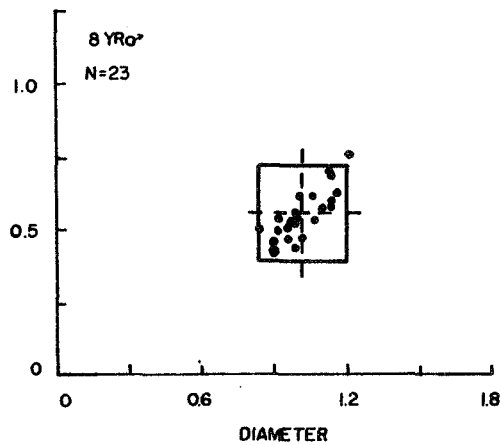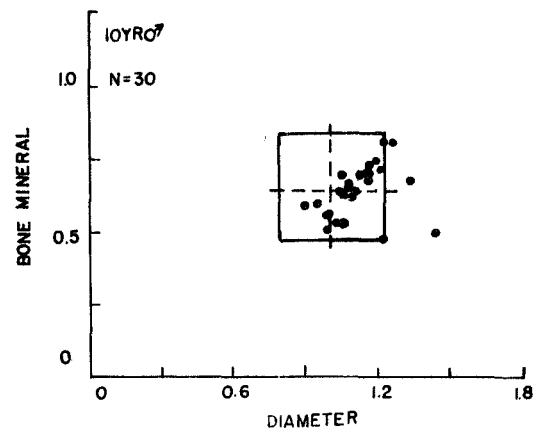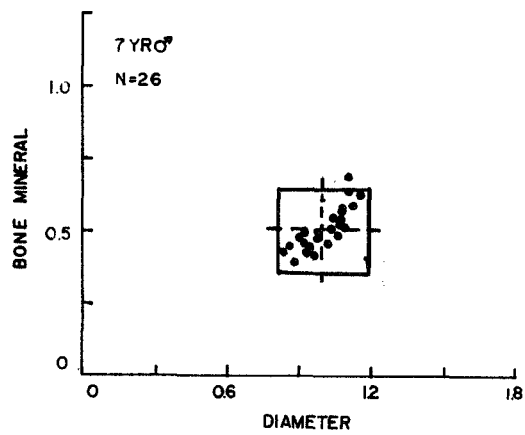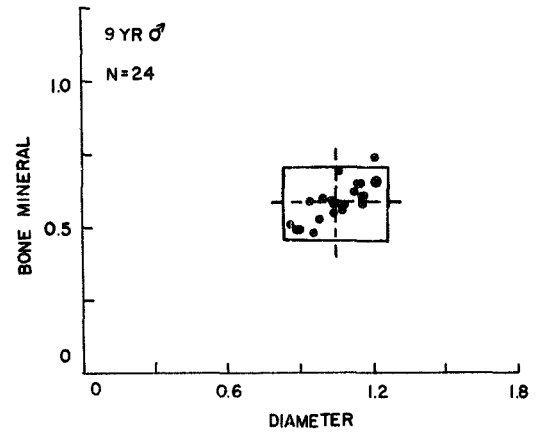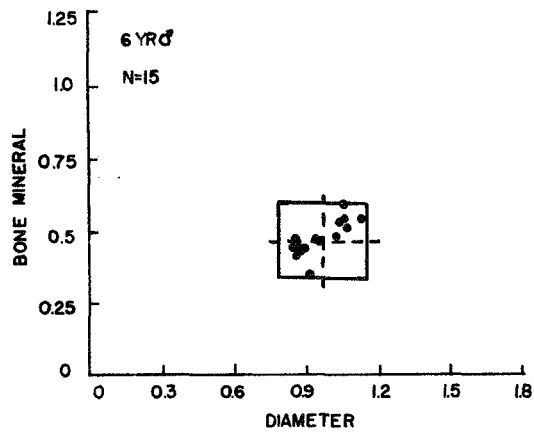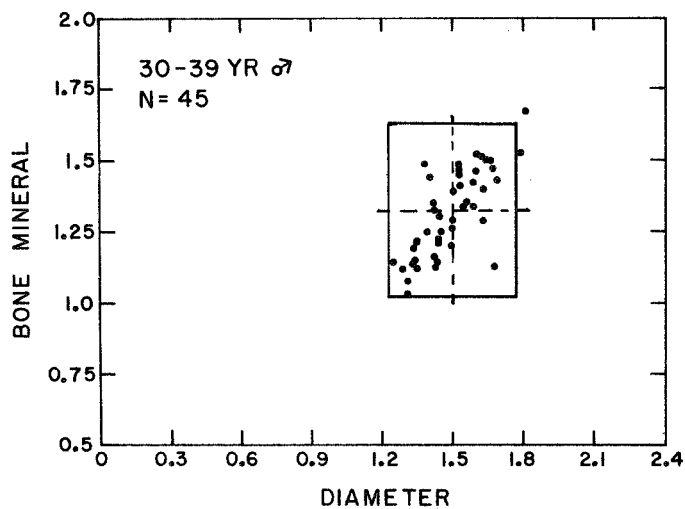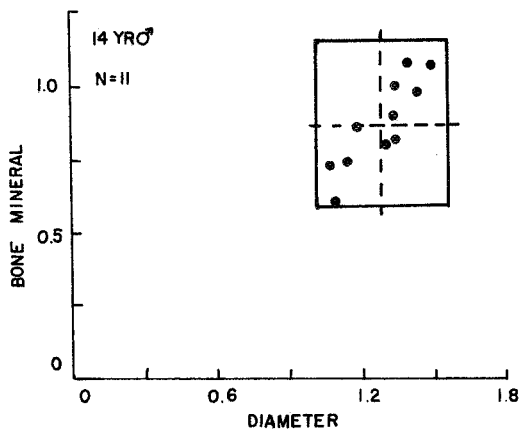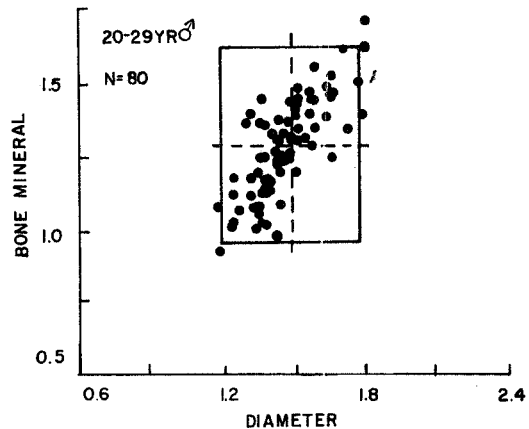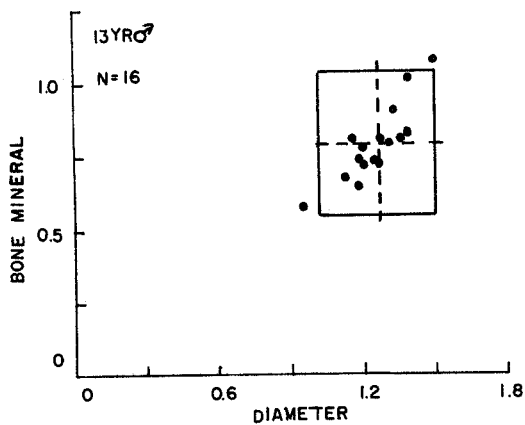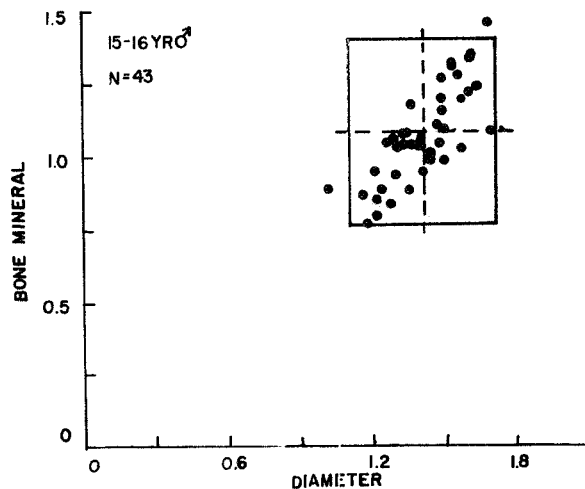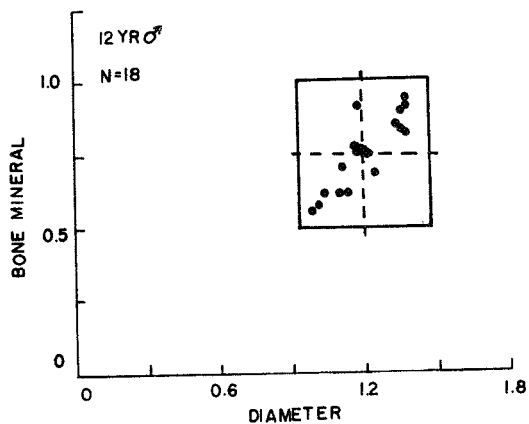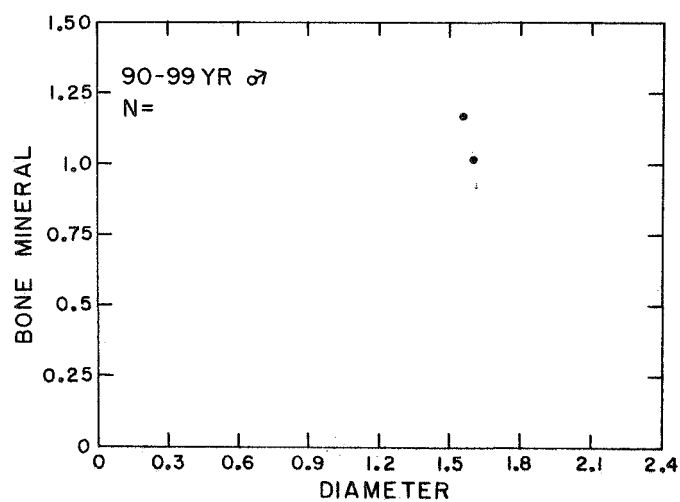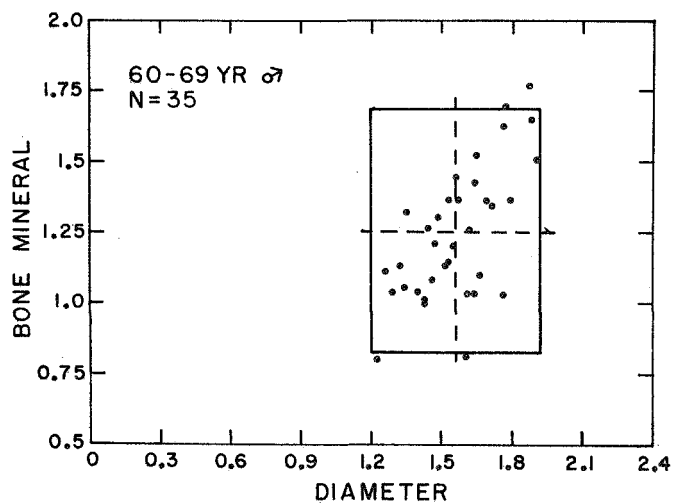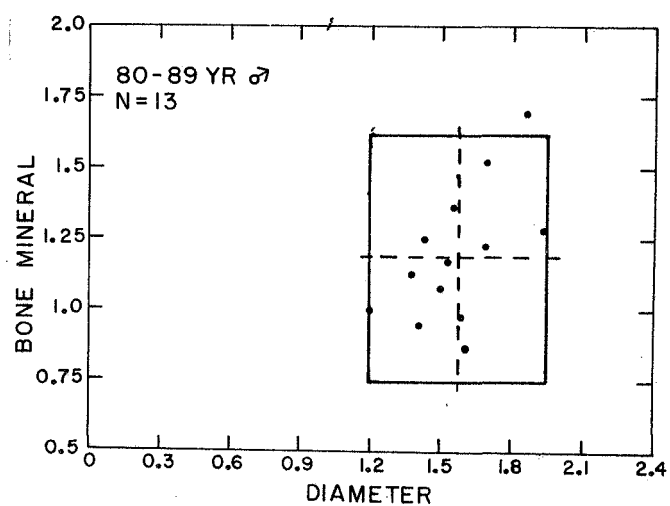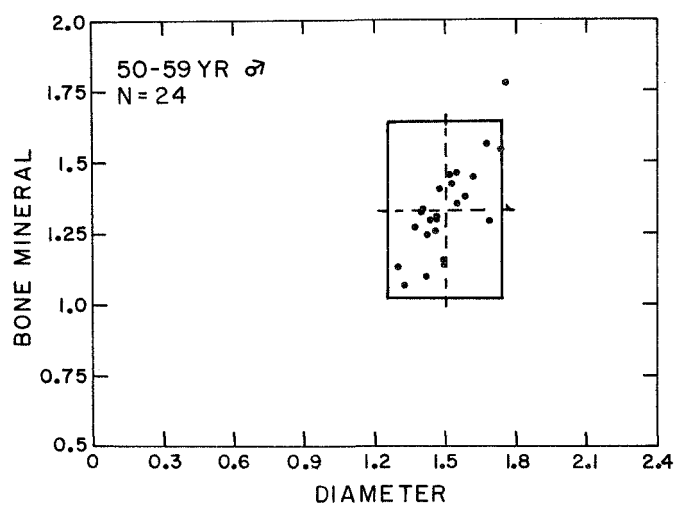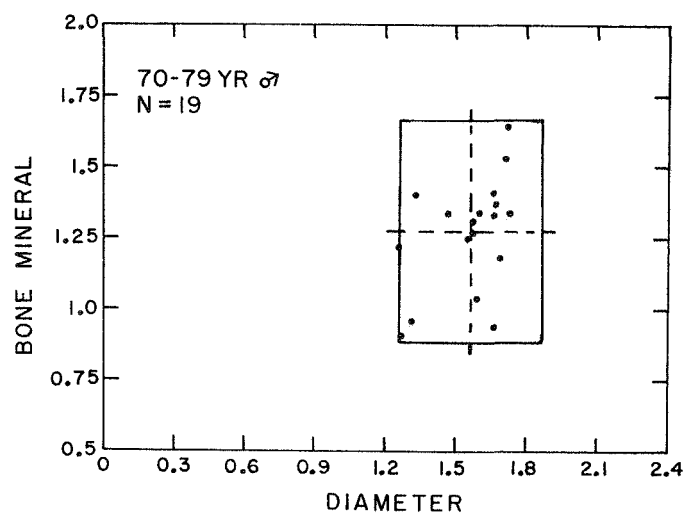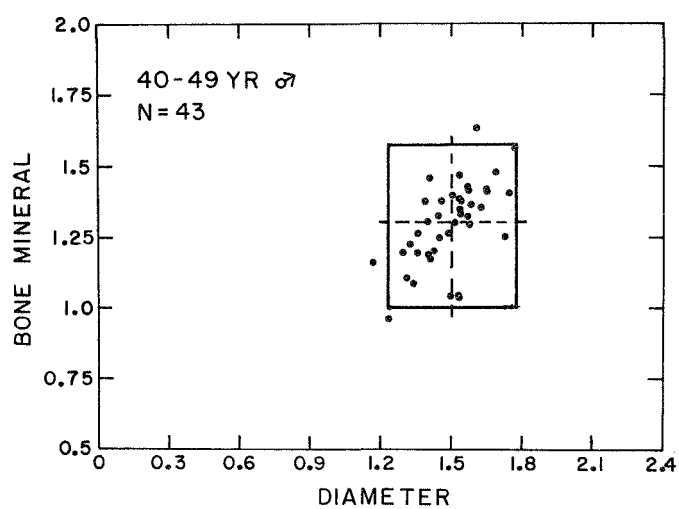
BONE STANDARDS

Robert M. Witt and John R. Cameron

Roentgenographic systems quantitatively determine bone mineral in vivo by comparing the optical density of the roentgenographic image of a bone to the image of a reference step-wedge. Since the method of exposing and developing the film can vary significantly, even under rigid standardization, these systems need to expose the bone reference standard with each roentgenograph (1,2,3). Unlike the roentgenographic systems, the physical nature of the technique to determine bone mineral in vivo developed by Cameron and Sorenson at the University of Wisconsin (4,5) does not need to calibrate individual measurements. The bone mineral is determined by measuring the transmission of a monoenergetic photon beam through the bone in a constant thickness of soft tissue or soft tissue equivalent material with a scintillation detector. The amount of bone mineral, m_B, in the path of the photon beam is related to the transmission count rates according to the following equation:

$$m_B = \rho_B \ln (I_o^*/I) / (\mu_B \; \rho_B - \mu_S \; \rho_S) \qquad (1)$$

where,

I_o^* = transmission counts through constant thickness of soft tissue

I = transmission counts through bone and soft tissue

μ_B = mass attenuation coefficient of compact bone

μ_S = mass attenuation coefficient of soft tissue

ρ_B = density of compact bone

ρ_S = density of soft tissue.

Since the photon beam is monoenergetic, the mass attenuation coefficients are constant, and the amount of bone mineral can

be written as:

$$m_B = C \ln (I_o^*/I) \qquad\qquad (2)$$

where C is a calibration constant which can be determined
from handbook values assuming a known composition of the bone
and soft tissue. The constant C can also be obtained experi-
mentally by measuring bone samples and ashing them to determine
the mass of bone mineral. The quantity, m_B, gives the mass of
bone mineral in the beam at the measuring point. If the beam
is scanned across the bone, m_B can be integrated to give mass
of bone mineral per unit length of bone in units of g/cm.

With this system a bone standard is not necessary for
calibration purposes, but it can be useful to help detect
system errors. Some of these errors which may tend to change
the measured bone mineral are:

1. spectral changes in the source due to filtration
   or contamination

2. changes in the amplifier gain of the analyzer

3. changes in the settings of the lower level and
   window of the analyzer

4. errors in the counting time

5. variation in scanner drive speed

6. variation of the scan speed in different directions
   for reversible scanners.

If a suitable bone-like material could be found, then such a
material could serve as a general standard for the calibration
and the intercomparison of systems located in different labora-
tories.

Various materials have previously been used as a bone
reference standard at the University of Wisconsin. These are:

a calcium carbonate (42%) and paraffin (58%) mixture (6), a
bone ash-muscle equivalent plastic mixture (7), and an aluminum
tube of the approximate dimensions of an adult radius. The
calcium carbonate-paraffin mixture did not have an attenuation
which resembled compact bone and also had sizeable point-to-point
variations because of nonuniformity. The bone ash-muscle equiva-
lent plastic material was apparently inert and easy to machine;
however, the large amounts of bone ash necessary to simulate
the composition of compact bone could not be uniformly mixed
into the plastic (7). Finally, the aluminum tube, which is very
convenient and uniform and presently serves as one of, our stan-
dards, is unsatisfactory since it is not similar to compact bone.

A bone standard material should preferably have the same
linear and mass attenuation coefficients as compact bone in the
energy range of interest (20-100 keV). This implies that the
physical density, electron density, and chemical composition
are similar to compact bone. The material should be stable at
room temperature, simple to produce from commercially available
supplies, and easy to fabricate into phantoms geometrically
similar to human bone. It should be able to withstand normal
handling and shipment.

Since bone is composed of two types of material, organic
and inorganic, it is convenient to consider a two component bone
equivalent material. Compact bone has a composition by weight
of approximately 65% inorganic (hydroxyapatite) and 35% organic
(collagen). A bone equivalent material can be obtained by

mixing in the above proportions two substances which individually resemble hydroxyapatite and collagen. Water is similar to the latter since it has almost the same density and attenuation properties at all photon energies as collagen. The inorganic component is not as easily imitated. Even though hydroxyapatite is widely assumed to be the inorganic bone crystalline material, several calcium containing compounds have been suggested:

1. carbonate-apatite $Ca_{10}(PO_4)_6 \cdot CO_3$
2. tricalcium phosphate hydrate, $Ca_9(PO_4)_6 \cdot (H_2O)_2$
3. hydroxyapatite, $Ca_{10}(PO_4)_6 \cdot (OH)_2.$

Any of the above could be used to simulate the mineral component since they all have approximately the observed molar Ca:P ratio of about 1.67. Obtaining a material with a Ca:P ratio near this value is important since calcium and phosphorous are the two largest contributors to the mass attenuation coefficient of compact bone at low energies (E < 30 keV), Table 1. Unfortunately all three of these Ca containing salts are practically insoluble in water (8,9). Dipotassium hydrogen phosphate, K_2HPO_4, a salt which previously has been used by Meema as a calibration stepwedge (10), is a potential substitute for the bone mineral salt. Since the atomic number of potassium is only one less than that of calcium, the photoelectric absorption of the two elements will be very similar. The K:P ratio is 2.0 which is close to the Ca:P ratio of 1.67 in bone. Moreover, since the effective $\bar{Z}^*$ of K_2HPO_4 is 15.59 and that of hydroxy-

$$* \; \bar{Z}^{2.94} = g_1 Z_1^{2.94} + g_2 Z_2^{2.94} + g_3 Z_3^{2.94} + \ldots\ldots$$

apatite is 15.86, the former should attenuate x-ray photons nearly like the mineral in bone. Finally, K_2HPO_4 is much more soluble in water than any of the above calcium salts. This report discusses the characteristics of a liquid bone equivalent material composed of K_2HPO_4 in water.

Solutions composed of different amounts of anhydrous K_2HPO_4 in water were measured to find a concentration that most resembled compact bone. The attenuation coefficients and physical densities were measured for concentrations ranging from 118g to 160g of K_2HPO_4 per 100 ml of water. The maximum concentration is essentially the solubility limit of K_2HPO_4 in water at $20^\circ C$ (11). The attenuation coefficients for the most concentrated solution were measured with both Am-241 (59.7 keV) and I-125 (27.4 keV) photon sources. The physical densities were obtained by determining the mass of a known volume of the solution.

For both energies, the mass attenuation coefficients of the solution were below the values for compact bone calculated by Spiers (12), Table 2. For I-125 the mass attenuation coefficient was 11% low and for Am-241 it was 6% low. The solution's physical density is 1.72 g/cm^3 which is less than the generally accepted value for compact bone (1.80-1.95 g/cm^3). It is unfortunate that the solubility limit does not permit an increase of K_2HPO_4 which would tend to correct the attenuation coefficient as well as the density.

From Spiers (12) the mass attenuation coefficient for any

compact bone can be written as:

$$\mu_m = \mu/\rho = n_o({}_e\sigma + k\bar{Z}^{2.94}\lambda^3) \qquad (3)$$

where μ_m = mass attenuation coefficient

μ = linear attenuation coefficient

ρ = density

n_o = number of electrons per gram in compound

λ = photon wavelength

${}_e\sigma$ = Compton scatter absorption coefficient per electron

$k = 2.64 \times 10^{-26}$.

Assuming that at low energies (E < 50 keV) the photoelectric cross section is much larger than the Compton cross section, the mass attenuation coefficient at a constant energy depends only on the effective atomic number of the material and becomes:

$$\mu_m \cong C\bar{Z}^{2.94} \qquad (4)$$

where $C = n_o k \lambda^3$.

Using the fractional composition given in Table 3, the effective atomic number for the solution is 13.34. Substituting this value for $\bar{Z}$ into equation 4, the μ_m for the K_2HPO_4 solution falls 11.3% below the value of μ_m obtained with Spiers value for $\bar{Z}$ of 13.9 for compact bone (12). This percent difference agrees with the percent difference between the calculated μ_m for compact bone and the measured μ_m for the K_2HPO_4 solution at energy 27.4 keV. Thus, the solution's lower mass attenuation coefficient can be attributed completely to its lower effective atomic number.

Mass attenuation coefficient measurements were made on four bovine cortical femur slabs. These values are 2% above the

K_2HPO_4 solution at 59.7 keV and 3.4% high at 27.4 keV.

A comparison of the mass attenuation coefficients for this material, calculated attenuation coefficients for ICRU bone (13), Spiers bone (12), and aluminum (13) are given in Figure 1.

The K_2HPO_4 solution has a number of advantages: it is stable indefinitely at room temperature ($20^{o}C$), it can be made reproducibly from commercially available chemical stock, and it produces a uniform mixture. A liquid bone standard has the disadvantage that it must be enclosed in a leak-proof container and, of course, it is not machineable.

Assuming a simple cylindrical model for the shafts of the long bones, phantoms were constructed from three tele-scoping acrylic plastic (methymethacrylate) extruded tubes, Figure 2. The tubes were bonded together with ethyldihydro-chorase. The cavity formed is water tight. A 2-56 machine screw through a threaded hole in the outer tube wall serves as a filler cap. An injection syringe is used to fill or empty the phantom. The phantoms were designed for the Cameron-Sorenson type measuring system and must be scanned in a water bath of constant thickness to simulate the constant soft tissue cover necessary for this technique.

Two different radius-size phantoms have been constructed; one adult male size and the other an adult female size. The converted mineral content and width for the male size radius phantom is quite close to the average values for these para-meters for the 20-29 year male age group, Table 4. Both the bone mineral and the width lie within one standard deviation

of their respective means for this age group.

The female phantom has a "thin cortex" and is over three standard deviations below the mean value for the 20-29 year female age group, but it is typical of values found in osteo-porotic women over age 60. The bone diameter lies within one standard deviation of the mean for both age groups.

Preliminary results for the K_2HPO_4 liquid phantom indicate that its reproducibility is better than our system limit of 2%. These results agree with the long term reproducibility of an earlier phantom containing a tripotassium phosphate in water with a similar solution concentration. This phantom had percent standard deviations of 1.47 for the mineral content and 1.88 for the width for 49 different measurements made over a six month period.

Conclusion

Dipotassium hydrogen phosphate dissolved in water can be used as a bone equivalent material for compact bone. The effective atomic number of the K_2HPO_4 solution is slightly less than the effective atomic number of compact bone, and the solu-bility limit of K_2HPO_4 in water does not permit increasing the concentration. Thus, the K_2HPO_4 solution represents "demineral-ized compact bone".

A number of phantoms have been constructed[**] and will be sent to the various laboratories which measure bone mineral in vivo with the direct photon absorptiometric systems. Such an intercomparison study should reveal any differences between

** A new supply of commercial tubing has been found which is available in more sizes. It is manufactured by Plastruct Inc., Los Angeles, California.

scanning and data processing techniques and could also serve as a common calibration of the systems in the different laboratories in units of grams per centimeter of K_2HPO_4. Work will continue on the interlaboratory comparison study and the development of a trabecular or cancellous bone standard.

REFERENCES

1. Keane, B.E., Spiegler, G., and Davis, R., Brit. J. Radiol., 32 162 (1959).

2. Ömnell, K., Acta Radiol., Supplementum 148, (1957).

3. Mack, P.B., in Progress in Development of Methods in Bone Densitometry, ed. G.D. Whedon, W.F. Neuman and D.W. Jenkins, NASA, SP-6A, pp. 31-46, (1966).

4. Cameron, J.R. and Sorenson, J.A., Science, 142: 230, (1963).

5. Sorenson, J.A. and Cameron, J.R., J. of Bone and J. Surg. 49-A, 481, (1967).

6. Cameron, J.R., Factors Affecting the Measurement of Bone Mineral Content by the Direct Photon Absorption Technique, USAEC Report, COO-1422-4, (1965).

7. Sorenson, J.A., Witt, R.M., and Cameron, J.R., Progress in Development of a Bone Equivalent Material, USAEC Report, COO-1422-9, (1966).

8. Levinskas, G.J. and Neuman, W.F., J. Phys. Chem. 59, 164 (1955).

9. Holt, L.E., La Mer, V.K., and Chown, H.B., J. of Biol. Chem. 64, 509, (1925).

10. Meema, H.E., Harris, C.K., and Porrett, R.E., Radiology 82, 986, (1964).

11. Handbook of Chemistry and Physics, 45th ed., The Chemical Rubber Co., Cleveland, Ohio, (1964).

12. Spiers, F.W., Brit. J. Radiol. 19, 52, (1946).

13. Evans, R.D., In Radiation Dosimetry, (F.H. Attix and W.C. Roesch, eds.), 2nd ed. vol. 2, p. 93, Academic Press Inc., (1968).

TABLE 1 – Fractional Contribution to Mass Attenuation Coefficient

A – Compact Bone (ICRU)[a]; B – K_2HPO_4 – H_2O (1.6: 1.0)

Energy, MeV	.020		.030		.040		.060	
Element	A	B	A	B	A	B	A	B
H	.068	.004	.024	.013	.044	.025	.077	.049
C	.043	–	.073	–	.112	–	.177	–
N	.006	–	.009	–	.012	–	.018	–
O	.122	.116	.159	.160	.207	.221	.286	.343
Mg	.002	–	.002	–	.002	–	.002	–
P	.133	.143	.121	.137	.109	.131	.089	.120
S	.005	–	.004	–	.004	–	.003	–
K	–	.737	–	.689	–	.623	–	.489
Ca	.681	–	.609	–	.510	–	.348	–

a   International Commission on Radiological Units and Protection, Report 10b, 1962, NBS Handbook 85.

TABLE 2 – Mass Attenuation Coefficients, cm^2/g

Energy MeV	Bovine (femur)	Compact bone (femur) Spiers (12)	K_2HPO_4 (1.6 to 1.0)
.0274	1.75	1.89	1.69
.0597	0.319	0.34	0.313

TABLE 3 - Fractional Composition

Element	A Compact Bone (femur) ICRU	B Dipotassium hydrogen phosphate (1.6 K_2HPO_4 to 1.0 H_2O)
H	.064	.047
C	.278	----
N	.027	----
O	.410	.568
Mg	.002	----
P	.070	.109
S	.002	----
K	----	.279
Ca	.147	----

TABLE 4 – Comparison of Phantom to Normal Data

Age Group	Bone Mineral g/cm	Diameter cm
20–29 ♀	0.94 ± 0.11	1.23 ± 0.12
60–69 ♀	0.80 ± 0.15	1.25 ± 0.16
Phantom ♀	0.57	1.25
20–29 ♂	1.29 ± 0.17	1.48 ± 0.14
Phantom ♂	1.25	1.52
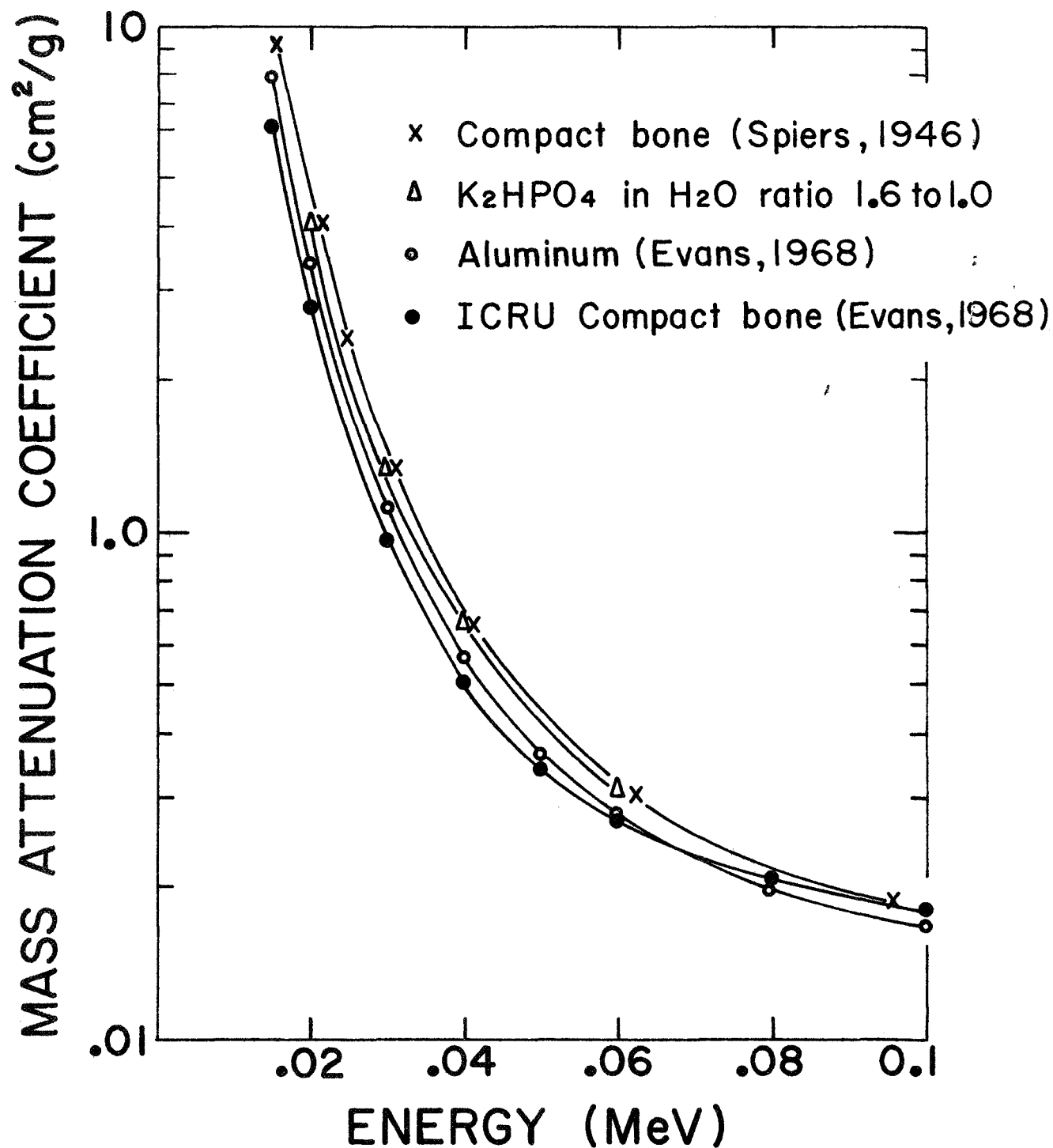
Fig. 1, Logrithm of the mass attenuation verses energy for various materials. ✗ compact bone calculated by Spiers (12), △ K_2HPO_4 in water mixed in a ratio of 1.6 to 1.0, ○ aluminum and ● compact bone with ICRU composition calculated and tabulated in Evans (13).

Drill and tap I-hole for 2-56 M.S.
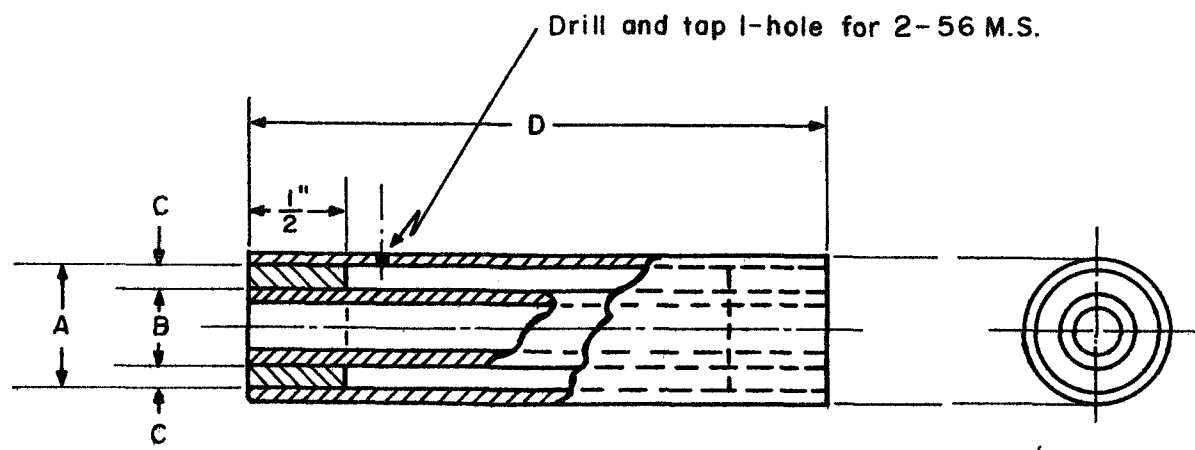
MATERIAL ; EXTRUDED ACRYLIC PLASTIC TUBING. INNER AND OUTER TUBES 1/16" WALLS, SPACER TUBES 1/16" AND 1/8" WALLS

PHANTOM DIMENSIONS			
		MALE	FEMALE
O.D.	A	5/8"	1/2"
I.D.	B	3/8"	3/8"
CORTEX	C	1/8"	1/16"
LENGTH	D	~ 3"	~ 3"
OUTER TUBE		3/4" O.D.	5/8" O.D.
INNER TUBE		3/8" O.D.	3/8" O.D.

Fig. 2, Drawing of telescoping tube phantom and table of dimensions for both male and female adult, radius-size phantoms.

New Methods of Skeletal Status Evaluation in Space Flight

John R. Cameron, Ph.D.
John M. Jurist, Ph.D.
James A. Sorenson, M.S.
Richard B. Mazess, Ph.D.

Medical Physics Section
Department of Radiology
University of Wisconsin Medical Center
1300 University Avenue
Madison, Wisconsin 53706

Abstract

Skeletal status can be evaluated from bone mineral content and bone elasticity measurements. We have developed instrumentation for bone mineral measurement by monoenergetic photon absorptiometry. Bone elasticity is measured by determination of the speed of sound in bone.

Comparison of absorptiometric mineral measurements with ash weights determined on autopsy specimens demonstrated an accuracy of 2-3%; the reproducibility on living subjects over many months is 1-2%.

We are investigating measurement of the speed of sound in bone by timing ultrasound or mechanical impulse propagation, measurement of vibrational phase shift per unit length of bone, determination of "ringing" frequency after a short duration impulse, and measurement of resonant frequency by recording amplitude as a function of frequency. Repeated ulnar resonant frequency measurements indicate a precision of 2-4%.

The above techniques are suitable for evaluation of skeletal status before, during, and after space flight.

Introduction

Measurement of bone mineral content and bone elasticity can provide information on skeletal status. Our laboratory has developed instrumentation for the measurement of bone mineral content by monoenergetic photon absorptiometry. We are now developing techniques for determination of skeletal elasticity _in vivo_ by means of speed of sound measurements in bone.

Photon Absorptiometry

Development of the absorptiometric method started in our laboratory in 1959 following unsuccessful attempts to accurately measure bone mineral content with conventional X-ray films and an optical densitometer. The results obtained by use of the radiographic photodensitometry technique were unsatisfactory for three reasons:

1. The spectrum of the heterogeneous X-ray beam changed in passing through tissue, with softer components being absorbed preferentially.

2. An undetermined amount of scattered radiation struck the film from surrounding soft tissues, affecting the bone image.

3. Film was a poor detector because variations in development

affected results. Also, film has a nonlinear response to
both radiation intensity and energy.

The improved method[3,5] overcame these problems in the following ways:

1. An essentially monoenergetic photon source was used.
Originally we used ^{210}Pb (46.7 keV) and later we used
^{125}I with a tin filter (27.4 keV) or ^{241}Am (59.6 keV).

2. Scattered radiation was essentially eliminated by using a
well collimated beam and detector.

3. The film was replaced by a scintillation detector system.

The basic principles of this method are illustrated in Figure 1.
The bone mineral mass (M_B) at any point in the path of the photon
beam is proportional to $\ln(I_o^*/I)$ when the bone is imbedded in a
uniform thickness of tissue. The measured quantities are the
intensity of the beam through a point of the bone (I) and through
the soft tissue adjacent to the bone (I_o^*). The constant of
proportionality can be calculated from tabulated values of
absorption coefficients since a single well defined energy is used.
Alternatively, the proportionality constant may be determined
experimentally. Note that there is no hardening of the monoenergetic
beam as it passes through the bone and surrounding tissues. Thus,
uncertainties in absorption coefficients are avoided. In contrast,
the X-ray beam used for radiographic photodensitometry has a

continuous, and poorly reproducible, energy spectrum. This leads
to uncertainties in the absorption coefficients; the problem is
exacerbated by beam hardening.

The limb containing the bone of interest is surrounded by a
soft tissue equivalent material in order to simulate a uniform
tissue thickness around the bone (Figure 2). We found either water
or Super Stuff[*] to work well. The source and detector are
mechanically linked and move slowly (about 1 mm/sec) across the
limb (Figure 3). The measured beam intensity depends upon the
absorption characteristics of the material in the beam scan path.
In order to determine the mineral mass across the bone, it is
necessary to integrate M_B across the bone. This can be done
graphically, but it is usually more convenient to take measurements
at fixed intervals across the bone and then to use computer analysis.
Figure 4 illustrates absorptiometric records obtained with different
photon sources on the same subject.

Our method has been evaluated by measuring bones of different
size.[4,16] The ash weight of standard sections cut from the bone at
each measuring site was compared to the absorptiometric measurement
of bone mineral. We found a very high correlation (r more than 0.98)

---

[*]Available from Wham-O Corporation, San Gabriel, California, or
local toy stores.

between ash weight and measured bone mineral content; the error of measurement was less than 3% (Figure 5). Varying the amount and kind of "tissue cover" has little effect on the bone mineral measurement. We have also determined that this method is very reproducible over periods of many months. Typically, the measurement precision is on the order of 1-2%, but this can be improved by scanning several times at a single location and calculating the mean.

Our method is now routinely used at the University of Wisconsin for measurements on patients and normal subjects. More than a dozen other medical centers have adopted this method of skeletal evaluation.

Measurement of the Speed of Sound in Bone

It is well known that the speed of sound in a material is related to both elasticity and density.[13] Thus, measurement of the speed of sound propagation in bone offers a possible estimate of bone elasticity.

Our laboratory is investigating the measurement of the speed of sound in the ulna, tibia, clavicle, mandible, and calvarium. We are using the following approaches:

1. Timing of impulse propagation along the bone. If two

vibration transducers (accelerometers) are strapped to a long bone, the speed of sound can be obtained by measuring the time interval which elapses during passage of a short duration mechanical impulse between the transducers. Alternatively, the speed of ultrasound propagation along the bone can be measured. The large attenuation of ultrasound in bone makes this approach difficult.

2. Measurement of the phase shift per unit length of bone for fixed vibrational frequencies. If a long bone such as the ulna is excited at one end by a sinusoidal vibration of known frequency, the relative phase difference between the outputs of two accelerometers placed on the bone, divided by the distance between the transducers, is proportional to the speed of sound in the bone.

3. Measurement of resonant frequency. The product of resonant frequency and length of a long bone is proportional to the speed of sound in the bone.[8,12] Apparatus used for measurement of resonant frequency in vivo[9] is shown in Figure 6. The resonant frequency is obtained from a recording of the amplitude response as a function of frequency (Figure 7). On repeated resonant frequency determinations, there is a standard deviation of 2-4%; the

variation can be reduced by averaging several measurements.[10] Determination of ulnar resonant frequency has been used for clinical investigations with promising results.[11]

4. Measurement of the ringing frequency of the bone after application of a short duration impulse (Figure 8). The ringing frequency is closely related to the resonant frequency.

Discussion

Bone loss during manned space flight[7] poses two major hazards:

1. Ectopic calcification (especially in the kidney) may occur if mineral mobilization is rapid or prolonged.

2. Severe bone loss will compromise structural integrity of the skeleton.

The danger of kidney stone formation is aggravated by dehydration. Dehydration has been reported on several previous flights.[2] Bone loss resulting from prolonged weightlessness may lead to fractures during stress; fractures could occur during re-entry deceleration or in the subsequent post-flight period if bone loss is irreversible.

There are several possible methods of treating skeletal changes during space flight. Modified physical activity, changes of diet,

or medication may be required. However, the decision to use these procedures should be based on reliable in-flight monitoring of the skeleton. Direct photon absorbtiometry and measurement of bone elasticity afford convenient in-flight monitoring of these critical parameters, and would allow therapeutic action to be taken.

Investigators using a quantitative radiographic method for bone evaluation have reported loss of bone mineral during orbital flight.[14,15] The true extent of this bone loss remains unknown, however, since the radiographic technique used on astronauts is relatively inaccurate (20-30% error) and imprecise and therefore cannot reliably measure small changes.[1,17] Recent advances in radiographic photodensitometry may reduce the error to less than 10%,[6] but in any event radiography can not be conveniently used for in-flight skeletal monitoring since the equipment is bulky, and data would not be available until after the films were processed. Photon absorptiometry and bone resonant frequency measurement overcome these difficulties.

The advantages of the techniques we suggest are summarized as follows:

1. They are highly precise and accurate. The routine precision of absorptiometry is 1-2%, but can probably be reduced to less than 0.5%; the routine precision of the resonant

frequency measurement is 2-4%, but can probably be held to less than 1%.

2. All equipment can be miniaturized for space flight.

3. Results may be analyzed during flight; either on-board or telemetered data reduction is possible for continuous monitoring.

4. The procedures are harmless and innocuous. The radiation dose from absorptiometry is negligible (less than 10 mrad/scan) and is confined to very small areas of the extremities.

5. The procedures are simple, and require little preparation or manipulation. Little training is required to make the measurements.

In conclusion, we feel that these methods are ideally suited for monitoring skeletal status before, during, and after space flight.

References

1. BAKER, P. T., SCHRAER, H., and YALMAN, R. G.: The Accuracy of Human Bone Composition Determined from Roentgenograms. Photogram. Engr. 25:455, 1959.

2. BERRY, C. A.: Preliminary Clinical Report of the Medical

Aspects of Apollos VII and VIII. Aerospace Med. 40:245-254, 1969.

3. CAMERON, J. R., GRANT, R. M., and MacGREGOR, R.: An Improved Technique for the Determination of Bone Mineral Content in Vivo. Radiology 78:111, 1962.

4. CAMERON, J. R., MAZESS, R. B., and SORENSON, J. A.: Precision and Accuracy of Bone Mineral Determination by Direct Photon Absorptiometry. Inv. Radiol. 3:141-150, 1968.

5. CAMERON, J. R., and SORENSON, J. A.: Measurement of Bone Mineral in Vivo. Science 142:230-232, 1963.

6. COLBERT, C., and MAZESS, R. B.: Unpublished Observations, 1968.

7. HATTNER, R. S., and McMILLAN, D. E.: Influence of Weightlessness upon the Skeleton. Aerospace Med. 39:849-855, 1968.

8. JURIST, J. M.: Ulnar Vibratory Properties. Proceedings of the Conference on Progress in Methods of Bone Mineral Measurement, USPHS-NIAMD, Bethesda, in press, 1969.

9. JURIST, J. M.: In Vivo Determination of the Elastic Properties of Bone. I. Theory, Apparatus, and Method of Ulnar Resonant

Frequency Determination. Submitted for publication, 1969.

10. JURIST, J. M.: In Vivo Determination of the Elastic Properties
of Bone. II. Resolution and Precision of the Ulnar Resonant
Frequency Determination. Submitted for publication, 1969.

11. JURIST, J. M.: In Vivo Determination of the Elastic Properties
of Bone. III. Ulnar Resonant Frequency in Osteoporotic,
Diabetic, and Normal Subjects. Submitted for publication, 1969.

12. JURIST, J. M., and SELLE, W. A.: Acoustical Detection of
Osteoporosis. The Physiologist 8:203, 1965.

13. KINSLER, L. E., and FREY, A. R.: Fundamentals of Acoustics,
John Wiley & Sons, Inc., New York, 1950.

14. MACK, P. B., and LaCHANCE, P. A.: Effects of Recumbency and
Spaceflight on Bone Density. Am. J. Clin. Nutr. 20:1194-1205,
1967.

15. MACK, P. B., LaCHANCE, P. A., VOSE, G. P., and VOGT, F. B.:
Bone Demineralization of Foot and Hand of Gemini-Titan IV, V,
and VII Astronauts during Orbital Flight. Am. J. Roent., Rad.
Ther., & Nuc. Med. 100:503-511, 1967.

16. SORENSON, J. A., and CAMERON, J. R.: A Reliable *in Vivo* Measurement of Bone-Mineral Content. *J. Bone Jt. Surg.* 49A:481-497, 1967.

17. VOSE, G. P., HOERSTER, S. A., and MACK, P. B.: New Technics for Radiographic Assessment of Vertebral Density. *Am. J. Med. Elect.* 3:181-188, 1964.
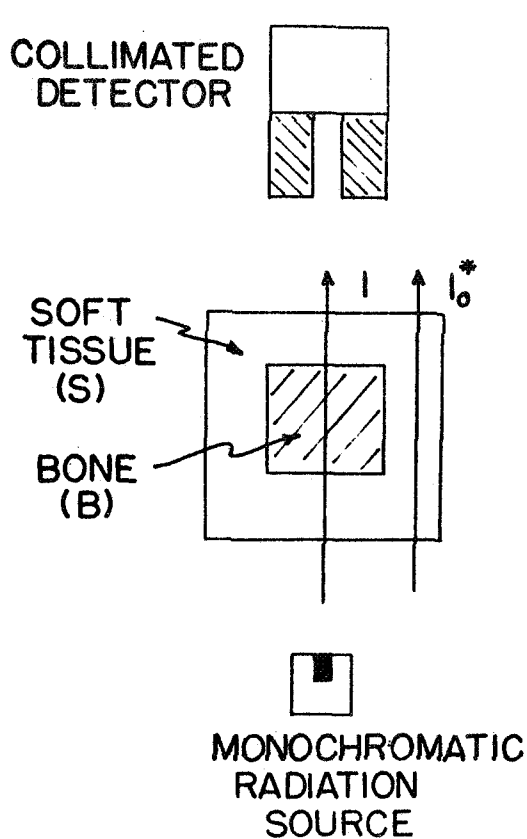
$$M_B = \frac{\rho_B \ln(I_0^*/I)}{(\mu_B\rho_B - \mu_s\rho_s)}$$

= BONE MINERAL MASS
PER UNIT AREA IN
RADIATION BEAM PATH
(GM/CM^2)

μ = MASS ABSORPTION
COEFFICIENT (CM^2/GM)

ρ = MICROSCOPIC
DENSITY (GM/CM^3)

FIGURE 1: Schematic diagram illustrating the basic principles used in measuring bone mineral with a monoenergetic photon source. The bone mineral mass per unit area in the beam path is given by the equation. The measured quantities are I_0^*, the beam intensity through the soft tissue adjacent to the bone, and I, the beam intensity through the bone.
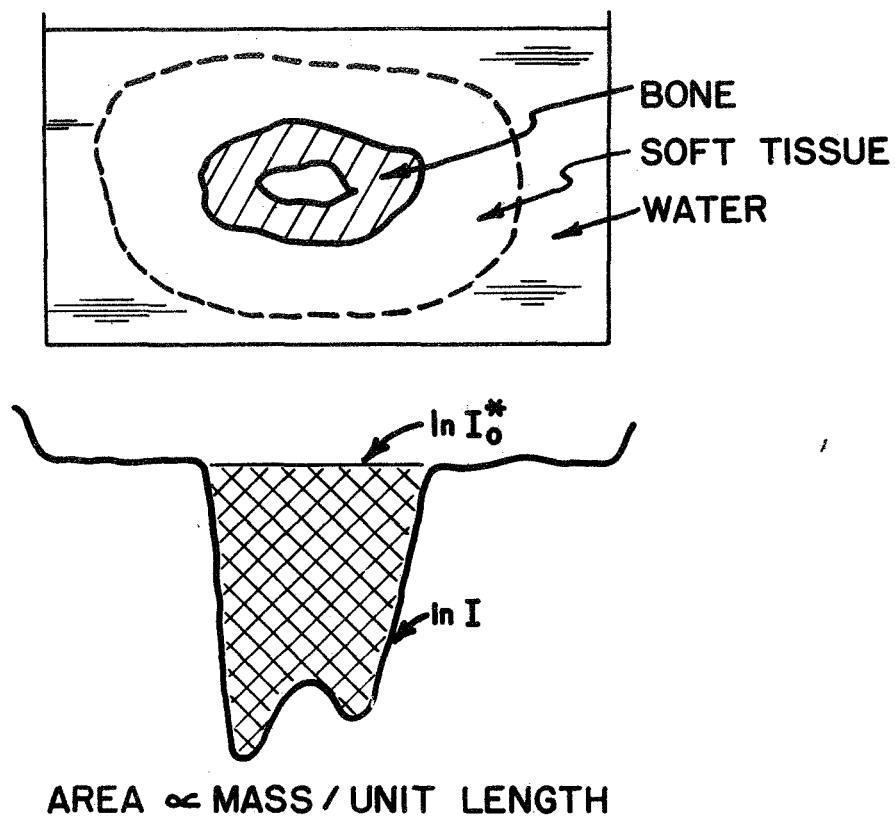
FIGURE 2: Use of soft tissue equivalent material to simulate a constant tissue thickness across the limb. The intensities are plotted on a logarithmic scale; the shaded area is proportional to the mineral mass per unit length of bone.

GAMMA RAY
SPECTROMETER

MECHANICAL
SCANNER

AUTO-TIMER
AND SCALER

ELECTRONIC
COMPUTER

PAPER TAPE
PUNCH
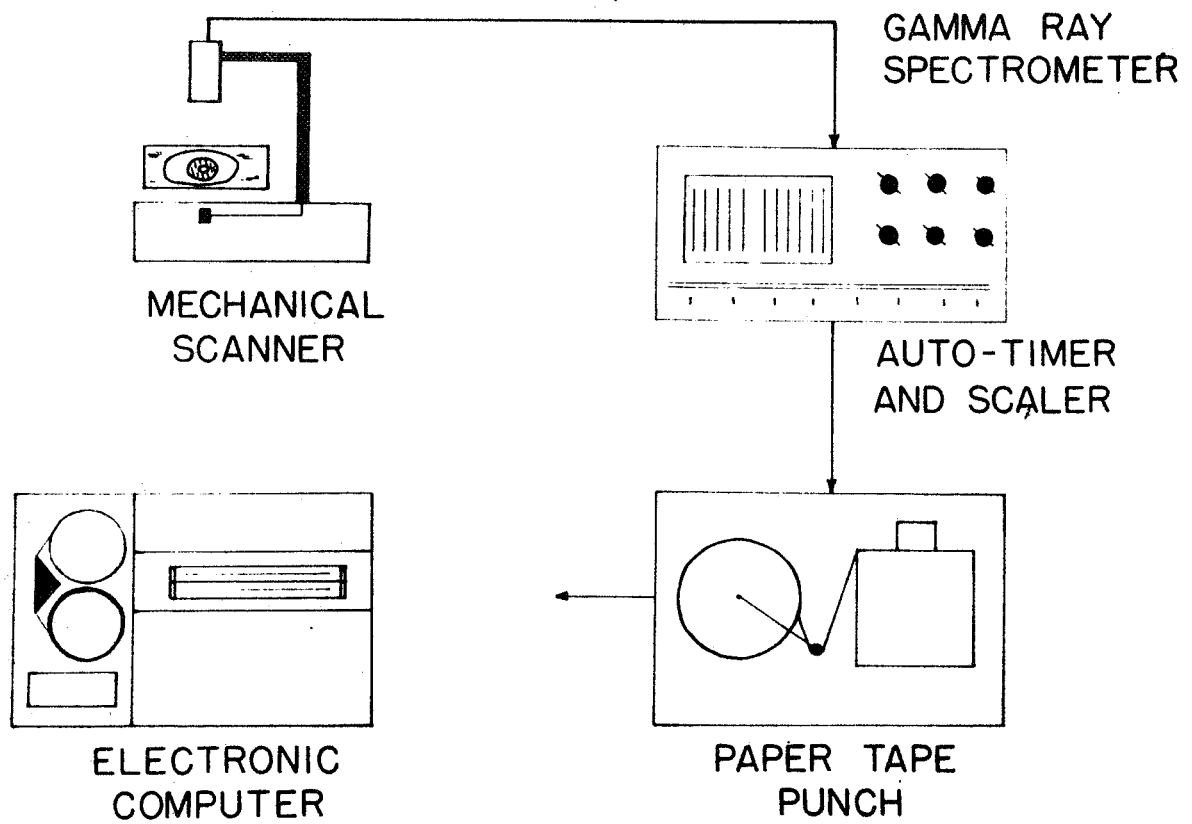
FIGURE 3: Block diagram of the system for measuring bone mineral content.
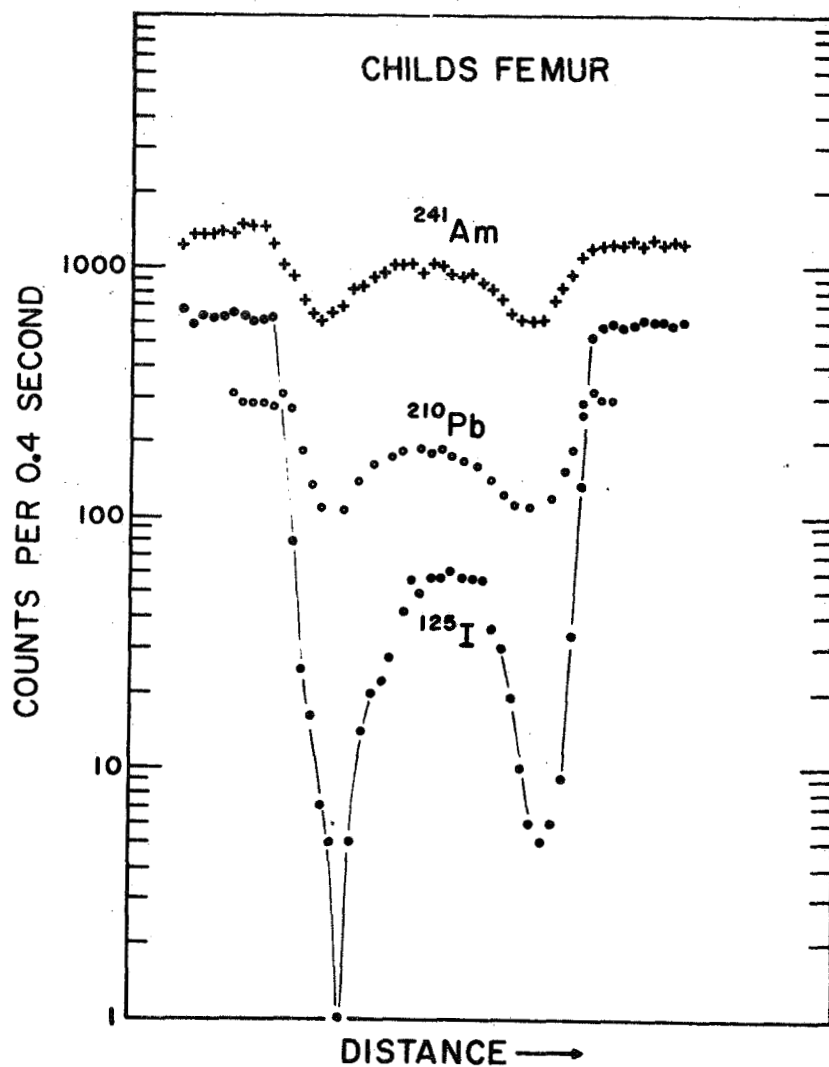
FIGURE 4: Scans of a child's femur using three different photon sources.
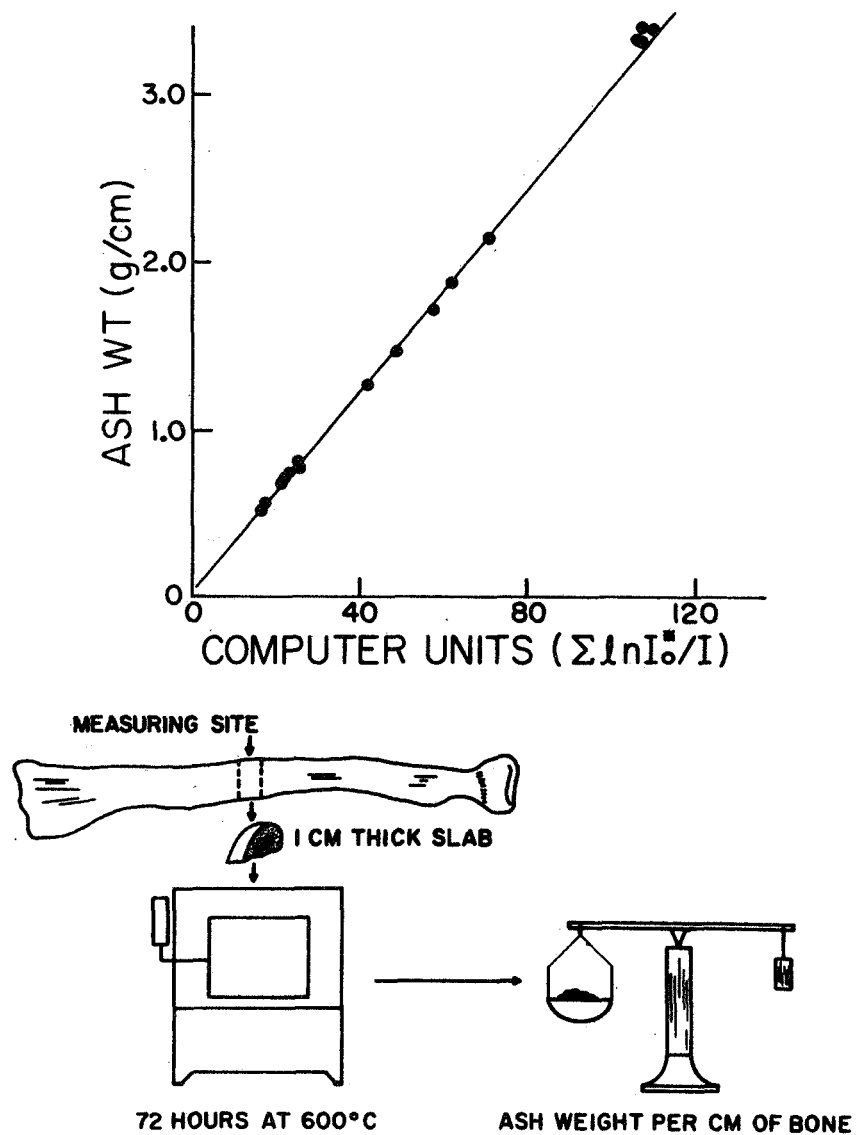
FIGURE 5: Comparison of ash weight of standard bone sections with mineral content obtained from the same sections by the photon absorptiometric technique.
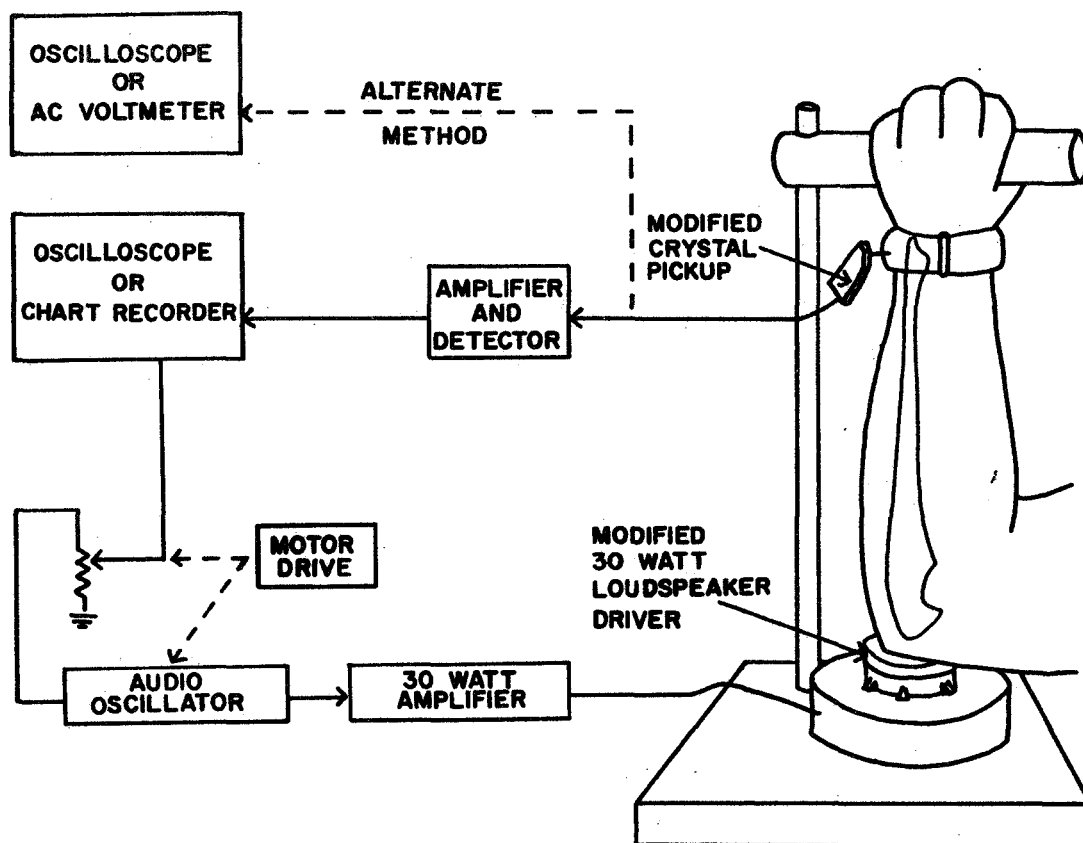
FIGURE 6: Apparatus used to obtain ulnar resonant frequency. The driver is modified by bonding a small lucite piston to the driver diaphragm. The piston contacts the elbow of the subject. The ulnar response is detected by a small crystal accelerometer strapped to the wrist.
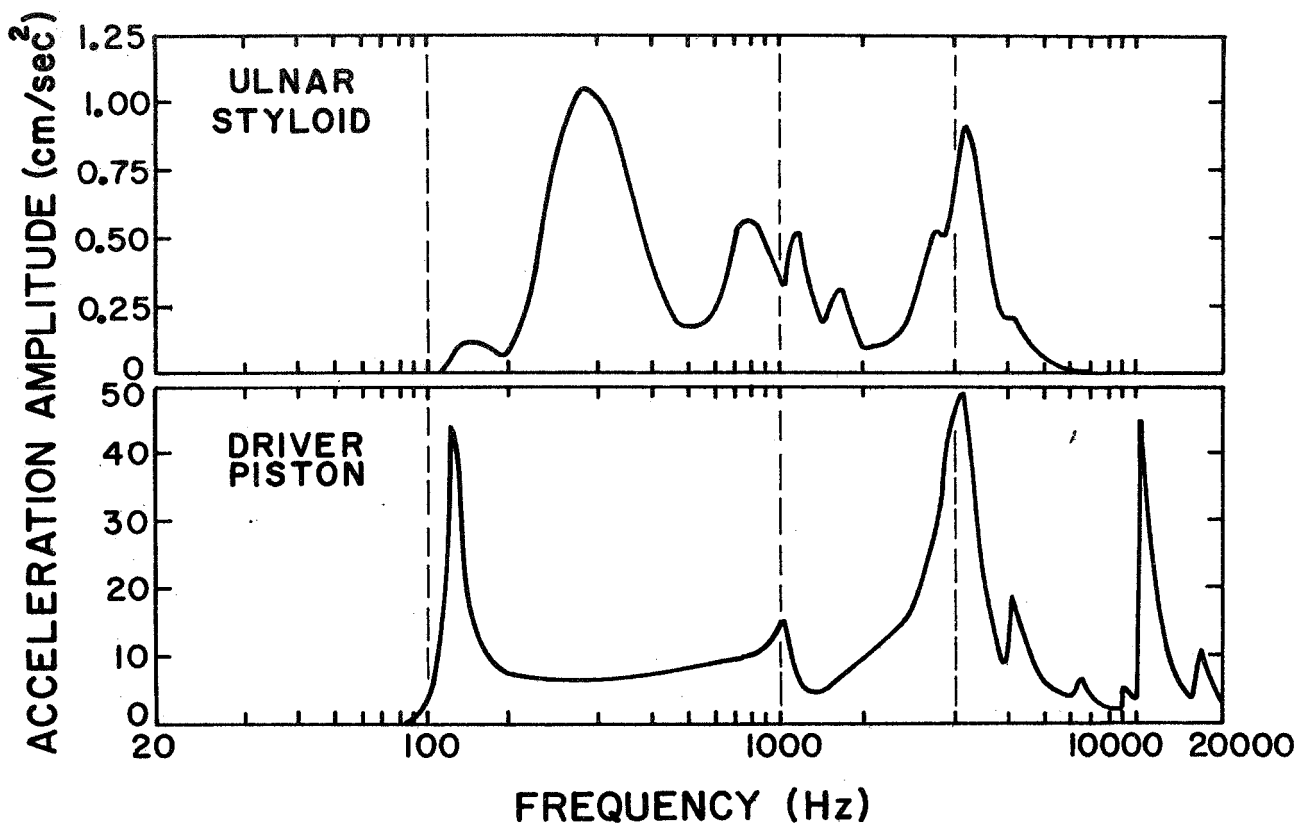
FIGURE 7: Acceleration spectrum of the driver piston (bottom) and of the ulnar styloid (top) for a typical adult. Note the ulnar resonance at about 290 Hz. The resonances at about 130 Hz, 1000 Hz, and 3000 Hz are driver resonances. The resonance at about 10000 Hz is a resonance of the crystal accelerometer.
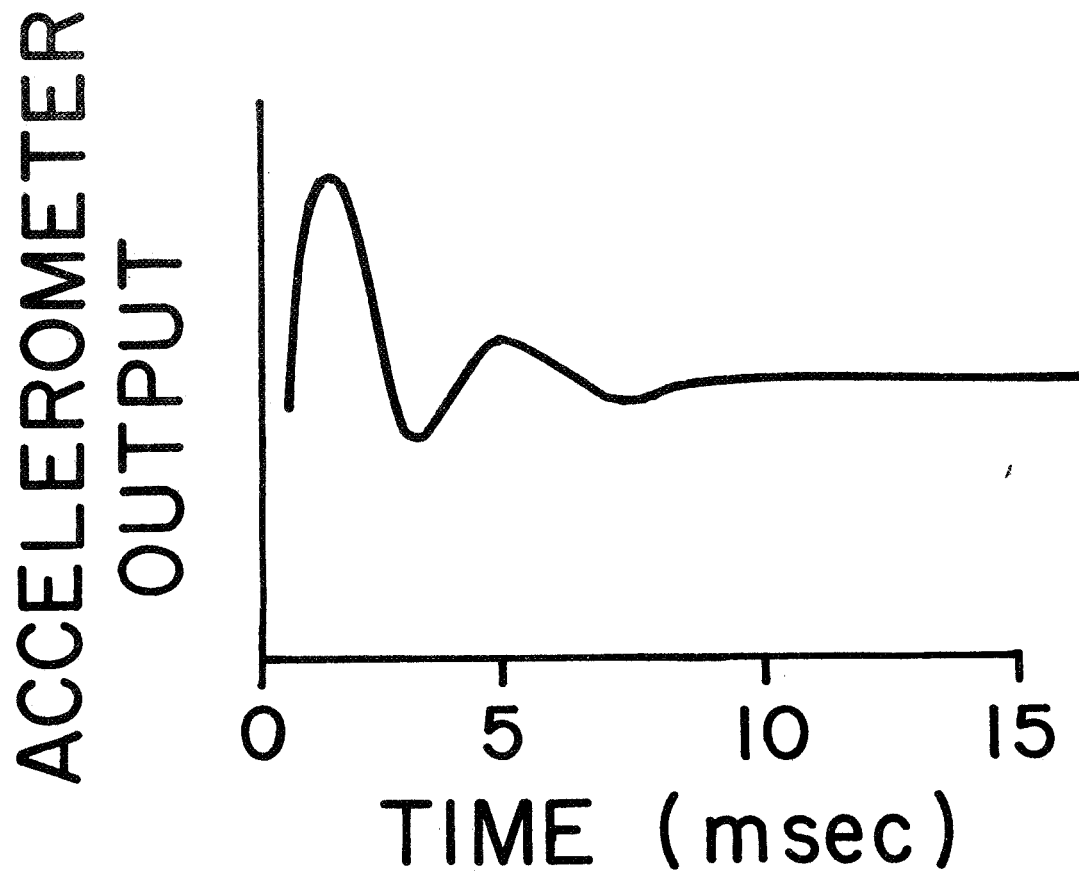
FIGURE 8: Typical acceleration response of the ulna, measured at the wrist, following a short duration impact at the elbow. The frequency of oscillation is about 320 Hz.

Some Physical Methods of Skeletal Evaluation

John R. Cameron, Ph.D.

John M. Jurist, Ph.D.

Richard B. Mazess, Ph.D.

Division of Medical Physics

Department of Radiology

University of Wisconsin Medical Center

Madison, Wisconsin 53706

Abstract

Hypercalciuria, negative calcium balance, and bone loss have been reported in hypodynamic and hypogravic environments. The loss of bone under such conditions is slow, but bone weakness and extraskeletal mineral deposition could occur with prolonged exposure. Precise and accurate measurement methods are necessary to evaluate and control bone loss. Direct photon absorptiometry, using monoenergetic radionuclide sources and a scintillation detector-pulse height analyzer system, provides reliable and sensitive measurement of bone mass. Radiographic photodensitometry is relatively imprecise, inaccurate, and unreliable.

Vibratory measurements of bone are more closely related to the functional status than to the bone mineral mass. Methods of measuring bone quality by determining bone elasticity are being evaluated.

Descriptors

Bone densitometry, Bone elasticity, Bone mass, Bone mineral measurement, Bone quality, Skeletal status.

1. <u>Introduction</u>

Changes in the musculoskeletal system occur in hypodynamic and
hypogravic conditions; these changes, which occur in both bed-bound
patients and astronauts, may lead to medical problems. This report
summarizes some of the major changes, and reviews some newer
physical methods useful in their measurement.

Disuse atrophy is a well-known clinical condition affecting
both muscle and bone following denervation, prolonged bed rest, or
immobilization. For many years investigators have speculated that
weightlessness would have an adverse effect since the forces acting
on the musculoskeletal system would be reduced, particularly in
weight-bearing bones and postural muscles. Of course, only
recently have studies in weightless conditions been possible. The
limited mobility of astronauts suggests that marked alterations may
occur in prolonged flight due to the "disuse" associated with both
weightlessness and relative inactivity.

Bone loss poses two major hazards. First, ectopic mineral
deposits, particularly in the kidney, may occur if bone loss is
rapid or prolonged. Second, severe bone loss can compromise the
structural integrity of the skeleton. Sensitive measurements of
the skeleton are necessitated by these hazards in order to assess

the nature and extent of changes in exposed individuals, and also to evaluate preventive and curative actions.

2. Changes of Skeletal Status

Various medical conditions have been examined, and several experimental techniques utilized, in order to determine the characteristics of bone changes with inactivity. Information has been derived from the study of myopathies, tenotomies, denervation syndromes, prolonged bed rest, fracture healing, as well as partial and total immobilization. In addition weightlessness has been simulated by water or oil immersion for relatively short time periods. Recent reports by other investigators (4,7,14,17,18,23,24,52) have reviewed the major studies. There is an almost uniform indication that hypodynamic conditions, of whatever sort, in both animals and man result in hypercalciuria, negative calcium balance, and bone loss. The extent to which these findings may be ascribed to reduced generalized muscle activity, reduced weight-bearing stress, or altered neural, humoral, or blood flow patterns is still unclear.

Similar results have been obtained in space flight experiments. Mack and co-workers (26,28,29) used radiographic photodensitometry

pre- and post-flight to evaluate bone mineral status. Average
losses of 9, 12, and 14% were reported using os calcis radiographs
of the Gemini IV, V, and VII crews. Losses in the metacarpals,
oddly enough, were greater than those in the os calcis. The
reported losses were not proportional to flight duration (4, 8, and
14 days), and much of the variation between flights was attributed
to differences of calcium intake. Estimated dietary calcium intakes
for the Gemini flights were about 710, 350, and 930 mg/day. Bedrest
studies made by these same investigators supported the role of
dietary calcium in ameliorating bone loss. However, several other
studies have indicated that dietary influences on calcium mobilization
in recumbency are minimal (5). Calcium and nitrogen balance studies
during the Gemini VII mission provided limited information
suggesting negative balance, particularly during the second week of
the 14 day mission (53).

Average bone density losses have been reported for the three
crew members of Apollo VII and of Apollo VIII (3); the average
losses in the two flights were 0.8 and 4% for the os calcis, 1.2
and 10.4% for the distal radius, and 1.4 and 11.7% for the distal
ulna. The individual bone changes ranged from +2 to -16%, and
again the losses did not correspond to flight duration (260 hours
for Apollo VII and 147 hours for Apollo VIII).

The extent of reported bone loss in the Gemini and Apollo crews was many times that expected for a comparable period of total immobilization. Further, the pattern of atrophy at different anatomical locations was variegated, and the losses in general did not correlate with duration of flight. It seems clear that undetermined factors are affecting these bone measurements, and it is possible that the radiographic method used was not sufficiently reliable.

The bone atrophy associated with hypodynamic conditions can reduce skeletal strength if continued for long periods. This is a major problem for older individuals who are subject to the usual loss of bone with age. Bed rest appears to induce a negative calcium balance of approximately 200-300 mg/day, and total immobility, as in poliomyelitis, may double this loss (52). Under severe hypodynamic conditions, the loss might amount to 2-4 g/week, and at least one month would be required for depletion of 1% of the body calcium store. Although atrophy is slow, continued loss would predispose toward fractures. The danger for astronauts could occur during re-entry deceleration. However, if the bone loss is irreversible, it may lead to problems when superimposed on the usual aging loss. This mobilization of bone raises the concomitant problem of abnormal mineral deposition. Such deposits, particularly

urinary calculi, commonly occur in accelerated bone resorption
syndromes, and calculi often have been noted in recumbency and
inactivity.

The implications of bone atrophy in space flight seem
generally adverse; the extent of bone loss predicted from
hypodynamic conditions should not exceed a few percent per month,
even if loss rates during space flight are several times more
severe than during total immobilization. Such bone loss, if
uniform, need not affect the structural integrity of the skeleton
although it might stimulate extraskeletal mineralization. There
are contrasting opinions on the risk and severity of possible
kidney stone formation in space flight (11,38); dehydration,
metabolic alkalosis, and incomplete emptying of the urinary calyces
may exacerbate this problem.

3. Methods of Measuring Skeletal Status In Vivo

Currently there are several practical methods for measurement
of skeletal status which do not require bone biopsy or blood samples.
These methods include direct photon absorptiometry, radiographic
photodensitometry, and measurement of bone vibratory properties.

Measurement of the small rates of bone loss in hypodynamic and

hypogravic conditions necessitates methods which are precise,
accurate, and sensitive; these methods must also demonstrate
long-term reliability. Further, there are changes of soft tissue
composition under these conditions which may affect bone measurements.
For example, shifts of body fluids occur with recumbency, and atrophy
of muscle accompanies disuse (6,41). In space flight, these
problems would be compounded by the marked water loss seen in all
flights to date (3). Alterations in the amount of soft tissue
surrounding a bone, and changes in the fat, water, and muscle
composition of that tissue, could affect measurements of bone
mineral content determined by radiation absorption methods, and
also might modify the measured vibratory properties of bone.

3.1 Direct Photon Absorptiometry

The photon absorptiometric method developed at the University
of Wisconsin over the past 10 years uses the attenuation of a
monoenergetic beam of low energy (20-100 kev) photons as a direct
measure of bone mineral content (8,9,46). The basic principles of
this method are illustrated in Figure 1. The bone mineral mass
(M_B) at any point in the photon beam is proportional to $\ln(I_o^*/I)$
when the bone is embedded in a uniform thickness of soft tissue.
The intensity of the beam is measured through the bone (I) and

through the adjacent soft tissue (I_o^*). The bone mineral content

can be determined at a single point, in a single path across a

bone, or even over an entire anatomic area if serial scans are made.

A low energy radionuclide is used as a source of monoenergetic

photons: ^{125}I (27.4 kev), ^{210}Pb (46.7 kev), and ^{241}Am (59.6 kev)

have been used. Beam intensity is measured with a scintillation

detector-pulse height analyzer system. Scattered radiation is

essentially eliminated by using a narrow, well-collimated beam and

detector. We usually scan across a long bone, typically the radius,

to determine the mineral content of a given cross section. In such

a case, the source and detector are mechanically linked and pass

across the bone at a constant speed (Figure 2). The limb containing

the bone of interest is surrounded by a soft tissue equivalent

material in order to simulate uniform tissue thickness. We found

either water or Super Stuff to work well. Super Stuff is

approximately 95% water and is readily molded; it is available from

Wham-O Corporation, San Gabriel, California or at local toy stores.

The measured beam intensity depends on the absorption

characteristics of the material in the scan path. It is necessary

to integrate the change of beam intensity across the scan path in

order to determine the mineral mass in the path. This is usually

done by recording measurements at fixed intervals across the bone

with a scaler-timer, and then using computer analysis. We have
also developed a direct readout unit which uses analog techniques
to measure the mineral content in the scan path as well as its
width. These values are presented immediately after completion of
a scan; the unit is easily miniaturized and allows convenient
monitoring of mineral content in patients, surveys, or in space
flight.

The accuracy of the absorptiometric method has been
demonstrated on ashed bone sections; section weight was predicted
within about 3% over a wide range of values (10,36). Varying the
thickness and composition (muscle vs. fat) of surrounding tissue
cover has little effect on the measurement (46). The method is
very reproducible over periods of many months. Typical measurement
precision is 1-2%, but this can be improved by scanning several
times at a single location to obtain an average. We are developing
new techniques, using casts of the area of interest, to insure
long-term precision and permit detection of small changes of
mineral content.

The absorptiometric method is simple and involves a minimal
radiation dose (10 mrad/scan). It is now used in at least a dozen
medical centers for clinical and normative skeletal evaluation; the
method has been used to evaluate changes in bed rest (47) and

immobilization (22).

The same equipment used for absorptiometric measurement of
bone suffices to measure soft tissue composition (fat vs.
muscle + water) as well. The composition of a two-component system
can be determined by making absorptiometric determinations at two
selected photon energies (10,45). We are using ^{125}I and ^{241}Am for
these determinations. The measurement of the relative fat content
of phantoms is accurate within about 2%, and measurement precision
is about 1%. This method could be used to monitor dehydration or
edema, fat changes, and muscle atrophy. The photon absorption
method could therefore be used to monitor both soft tissue and bone
changes occurring in hypodynamic or hypogravic conditions.

3.2 Radiographic Photodensitometry

The basic principles underlying radiographic photodensitometry
are the same as for direct photon absorptiometry (27,39,50). The
absorption of radiation by bone mineral is used as a measure of the
mineral mass. However, instead of a monoenergetic radionuclide
source this method uses a conventional X-ray tube, and a radiographic
film is used instead of a scintillation detector. A
photodensitometer is used to measure the optical density of the
radiographic bone image as an indication of the mineral mass. An

extensive annotated bibliography on this method is available (16).

Several problems arise in using this method which are not encountered with direct photon absorptiometry. The radiation from the conventional tube has a continuous energy spectrum, and absorption coefficients for such a beam cannot be well defined. In addition the heterogeneous beam changes in quality (hardens) as lower energy radiation is preferentially absorbed during passage through soft tissue and bone. There is no hardening of a monoenergetic beam, and absorption coefficients are well defined. Furthermore, an undetermined and variable amount of scattered radiation from the surrounding soft tissues affects the radiographic bone image; this does not occur with narrow beam geometry. Also, film usually exhibits a nonlinear response to both radiation intensity and energy.

Precision of a photodensitometer scan is usually quite high and this may have given the deceptive impression that the method itself is highly precise. Variations in film, film development, and film exposure conditions may contribute to large systematic errors. Standard exposure is a critical problem since the energy spectrum of a particular X-ray tube is poorly reproducible, and tubes differ greatly. These errors are partially reduced by using a calibrated wedge as a standard on each film. Investigators using

this technique have sometimes erroneously failed to encase the bone

of interest in a uniform thickness of tissue equivalent material and

to bury the calibration wedge in this material.

Accuracy of radiographic photodensitometry has not been

completely evaluated. Workers using the Pennsylvania State

University technique, largely developed by Mack and associates, have

reported high accuracy on excised bones and on bones with slight

tissue cover. However, on bones with substantial tissue cover the

error of the method is 20-50% (2,43). Mayer et al. (35) concluded

that scattered radiation was a major source of error. When

appropriate methods are used to measure and compensate for

scattered radiation (12), the predictive error of the measurement

is reduced to about 6% on phantoms with moderate tissue cover

(Colbert and Mazess, unpublished observations).

The overall utility of this method may be limited as much by

long-term reliability as by accuracy. Numerous investigators

report the usual precision to be approximately 4-8% (1,25,31,35,37).

Even larger systematic errors are possible unless great care is

taken during film exposure and development (48).

Radiographic photodensitometry has been used in a variety of

clinical and normative investigations. It has been used to assess

bone changes during inactivity, bed rest, and space flight (14,26,

28,29,30).

3.3 Measurement of the Speed of Sound in Bone

Measurement of bone vibratory properties provides a non-absorptiometric method of skeletal evaluation which determines the functional characteristics of bone rather than its mineral mass. Several investigators have related the breaking strength of bone to its mineral content, density, elasticity, size, and shape as well as the age and sex of the propositus (13,32,33,34,49). Since the speed of sound in bone is related to its elasticity and density (21), several laboratories are studying acoustical or vibratory methods of skeletal evaluation. Rich and co-workers (42) exploited the difference between the speed of sound propagation in bone and in soft tissue to build a scanner for measurement of bone quantity. This technique worked reasonably well for compact bone, but the attenuation of ultrasound in bone is so great, especially if any cancellous portions are present, that their technique was impractical. Smith and Keiper (44) measured the elasticity of excised bone segments by a vibratory technique. Hyatt and co-workers (15) obtain the speed of sound in excised bone by ultrasound propagation and relate this measurement to the density and elasticity of the bone sample (Abendschein and Hyatt, to be

published). It is generally recognized that bone is somewhat

inhomogeneous with respect to elasticity (51), but an average or

effective value may be measured.

Our laboratory is developing methods for measurement of the

speed of sound in the ulna, tibia, clavicle, mandible, pelvis, and

calvarium. We are studying the following approaches:

1. Timing of mechanical impulse or ultrasound propagation

   along the bone. If two accelerometers are strapped to a

   long bone, the speed of sound can be obtained by timing a

   short-duration mechanical impulse between the transducers.

   Alternatively, the speed of ultrasound propagation along

   the bone can be measured. However, the large attenuation

   of ultrasound in bone, mentioned previously, makes this

   approach difficult.

2. Measurement of the phase shift per unit length of bone for

   fixed vibrational frequencies. If a long bone such as the

   ulna or tibia is excited at one end by a sinusoidal

   vibration of known frequency, the relative phase difference

   between the outputs of two accelerometers placed on the

   bone, divided by the distance between the transducers, is

   proportional to the speed of sound in the bone at that

   frequency. Since shear waves are excited in the bone, the

dispersion of phase velocity with frequency may be

determined. This gives some information on the distribution

of bone tissue.

3. Measurement of resonant frequency. The product of resonant

frequency and length of a long bone is related to the speed

of sound in the bone (19,20). Apparatus used to measure

ulnar resonant frequency in vivo is shown in Figure 3.

The resonant frequency is obtained from a recording of the

amplitude response as a function of frequency (Figure 4).

On repeated resonant frequency determinations, there is a

standard deviation of 2-4%; the variation can be reduced

by averaging several measurements. Determination of ulnar

resonant frequency has been used for clinical

investigations with promising results.

4. Incorporation of bone into oscillator circuit. This is an

alternate method of measuring the resonant frequency of

the bone. The output from an accelerometer which measures

response of the bone is connected to the input of a power

amplifier which powers the electromagnetic driver used to

excite the bone. The bone is, therefore, essentially the

frequency controlling element of an oscillator circuit.

The frequency of oscillation may be determined by using

the oscillator output to drive a Schmitt trigger connected
to a scaler.

5. Measurement of the transient response of the bone to
application of a short-duration impulse. Analysis of the
transient response by standard engineering methods allows
determination of resonant frequency.

4. Discussion and Conclusions

Bone mineral losses in hypodynamic and hypogravic conditions
probably are relatively slight compared to the total body mineral
stores and major alterations would require long-term exposure.
Findings of major atrophy in pre- and post-flight radiographs are
exceptional, but probably are attributable to the large experimental
error of photodensitometry. The methods used for measuring bone
changes under such conditions must be accurate, sensitive, precise,
and reliable. A medical hazard is presented by ectopic mineral
deposition. This hazard could be magnified by conditions in space
flight. In all situations, the decision for dietary change,
medication, ambulation, or other physical activity should be based
on reliable measurements of bone status. Direct photon
absorptiometry and measurement of bone elasticity afford convenient

measurement of these critical parameters, and in addition photon

absorptiometry can be used to monitor fluid and tissue changes. In

contrast, radiographic photodensitometry is inaccurate on bones

with moderate tissue cover; the possibility of large systematic

errors makes the method very unreliable, even though short-term

precision may be high. We have not discussed the possibility of

utilizing mineral balance as an indication of skeletal status

because of the great difficulties attendant to reliable, complete

determinations. Balance studies are even difficult to use as

research tools in metabolic wards. Although augmented calcium

excretion may be a useful diagnostic tool, it need not reflect the

extent of bone resorption. Neutron activation analysis may be

another useful research tool (40), but the accuracy is unknown and

the difficulties are great.

Newer physical methods are making nondestructive testing of

the musculoskeletal system easier and more reliable. These methods

will probably provide the most useful information when used in

combination. The biomedical import of such information makes the

exclusive use of any single method undesirable.

References

1. ANDERSON, J. B., J. SHIMMINS, and D. A. SMITH. A new technique for measurement of metacarpal density. Brit. J. Radiol. 39:443-450, 1966.

2. BAKER, P. T., H. SCHRAER, and R. G. YALMAN. The accuracy of human bone composition determined from roentgenograms. Photogram. Engr. 25:455-460, 1959.

3. BERRY, C. A. Preliminary clinical report of the medical aspects of Apollos VII and VIII. Aerospace Med. 40:245-254, 1969.

4. BIRGE, S. J., and G. D. WHEDON. Bone. in McCALLY, M. (ed.), Hypodynamics and Hypogravics, New York, Academic Press, 1968.

5. BIRKHEAD, N. C., J. J. BLIZZARD, B. ISSEKUTZ, and K. RODAHL. Effect of exercise, standing, negative trunk and positive skeletal pressure on bed rest-induced orthostasis and hypercalciuria. AMRL-TR-66-6. Wright-Patterson AFB, Ohio, Aerospace Medical Research Laboratories, 1966.

6. BOURNE, G. H., K. NANDY, and M. N. GOLARZ de BOURNE. Muscle and the weightlessness state. in McCALLY, M. (ed.), Hypodynamics and Hypogravics, New York, Academic Press, 1968.

7. BROWSE, N. L. The Physiology and Pathology of Bed Rest, Springfield, Illinois, Charles C Thomas, 1965.

8. CAMERON, J. R., and J. A. SORENSON. Measurement of bone mineral in vivo. Science 142:230-232, 1963.

9. CAMERON, J. R., and J. A. SORENSON. A reliable measurement of bone mineral content in vivo. in Proceedings of the Fifth

European Symposium on Calcified Tissues, Paris, 1969.

10. CAMERON, J. R., R. B. MAZESS, and J. A. SORENSON. Precision
    and accuracy of bone mineral determination by direct photon
    absorptiometry. Inv. Radiol. 3:141-150, 1968.

11. COCKETT, A. T. K., C. C. BEEHLER, and J. E. ROBERTS. Hypodynamic
    urolithiasis: A potential hazard during prolonged weightlessness
    in space travel. School of Aerospace Medicine Review 2-62.
    Brooks AFB, Texas, 1961.

12. COLBERT, C., J. J. SPRUIT, and L. R. DAVILA. Biophysical
    properties of bone: Determining mineral concentration from
    the X-ray image. Trans. N.Y. Acad. Sci., Series II. 30:271-290,
    1967.

13. CURREY, J. D. The mechanical consequences of variation in the
    mineral content of bone. J. Biomech. 2:1-11, 1969.

14. DICK, J. M. Objective determinations of bone calcium levels.
    Aerospace Med. 37:136-139, 1966.

15. FLORIANI, L. P., N. T. DEBEVOISE, and G. W. HYATT. Mechanical
    properties of healing bone by the use of ultrasound. Surg.
    Forum. 18:468-470, 1967.

16. GARN, S. M. An annotated bibliography on bone densitometry.
    Am. J. Clin. Nutr. 10:59-67, 1962.

17. HATTNER, R. S., and D. E. McMILLAN. Influence of weightlessness
    upon the skeleton: A review. Aerospace Med. 39:849-855, 1968.

18. HEANEY, R. P. Radiocalcium metabolism in disuse osteoporosis
    in man. Am. J. Med. 33:188-200, 1962.

19. JURIST, J. M. Ulnar vibratory properties. in _Proceedings of_
     the Conference on Progress in Methods of Bone Mineral
     Measurement, Bethesda, USPHS-NIAMD, 1969.

20. JURIST, J. M., and W. A. SELLE. Acoustical detection of
     osteoporosis. _The Physiologist,_ 8:203, 1965.

21. KINSLER, L. E., and A. R. FREY. _Fundamentals of Acoustics,_
     New York, John Wiley & Sons, Inc., 1950.

22. LUNDBERG, B. J., and B. E. NILSSON. Osteopenia in the frozen
     shoulder. _Clin. Orthop._ 60:187-191, 1968.

23. LYNCH, T. N., R. L. JENSEN, P. M. STEVENS, R. L. JOHNSON, and
     L. E. LAMB. Metabolic effects of prolonged bed rest: Their
     modification by simulated altitude. _Aerospace Med._ 38:10-20,
     1967.

24. McCALLY, M. The pathophysiology of disuse and the problem of
     prolonged weightlessness: A review. AMRL-TDR-63-3.
     Wright-Patterson AFB, Ohio, Aerospace Medical Research
     Laboratories, 1963.

25. McFARLAND, W. Evaluation of bone density from roentgenograms.
     Science 119:810-811, 1954.

26. MACK, P. B., and P. A. LaCHANCE. Effects of recumbency and
     space flight on bone recumbency. _Am. J. Clin. Nutr._ 20:1194-1205,
     1967.

27. MACK, P. B., W. N. BROWN, and H. D. TRAPP. Quantitative
     evaluation of bone density. _Am. J. Roent._ 61:808-825, 1949.

28. MACK, P. B., P. A. LaCHANCE, G. P. VOSE, and F. B. VOGT.
     Review of medical findings of Gemini VII and related missions-

bone demineralization. in A Review of Medical Results of
Gemini 7 and Related Flights, Washington, D.C., NASA Space
Medicine Directorate, 1966.

29. MACK, P. B., P. A. LaCHANCE, G. P. VOSE, and F. B. VOGT. Bone
    demineralization of foot and hand of Gemini-Titan IV, V, and
    VII astronauts during orbital flight. Am. J. Roent. 100:503-511,
    1967.

30. MACK, P. B., R. A. HOFFMAN, and A. N. AL-SHAWI. Physiologic
    and metabolic changes in Macaca nemestrina on two types of
    diets during restraint and non-restraint. II. Bone density
    changes. Aerospace Med. 39:698-704, 1968.

31. MASON, R. L., and C. RUTHVEN. Bone density measurements in
    vivo: Improvement of X-ray densitometry. Science 150:221-222,
    1965.

32. MATHER, B. S. Comparison of two formulae for in vivo prediction
    of strength of the femur. Aerospace Med. 38:1270-1272, 1967.

33. MATHER, B. S. Correlations between strength and other properties
    of long bones. J. Trauma 7:633-638, 1967.

34. MATHER, B. S. The effect of variation in specific gravity and
    ash content on the mechanical properties of human compact bone.
    J. Biomech. 1:207-210, 1968.

35. MAYER, E. H., H. G. TROSTLE, E. ACKERMAN, H. SCHRAER, and O. D.
    SITTLER. A scintillation counter technique for the X-ray
    determination of bone mineral content. Rad. Res. 13:156-167,
    1960.

36. MAZESS, R. B., J. R. CAMERON, R. O'CONNOR, and D. KNUTZEN.

Accuracy of bone mineral measurement. Science 145:388-389, 1964.

37. MORGAN, D. B., F. W. SPIERS, C. N. PULVERTAFT, and P. FOURMAN. The amount of bone in the metacarpal and the phalanx according to age and sex. Clin. Radiol. 18:101-108, 1967.

38. NUNGESSER, W. C. Factors influencing the renal regulation of calcium-implications of prolonged weightlessness. School of Aerospace Medicine Review 2-65. Brooks AFB, Texas, 1965.

39. OMNELL, K. A. Quantitative roentgenologic studies on changes in mineral content of bone in vivo. Acta Radiol. Suppl. 148, 1957.

40. PALMER, H. E., W. B. NELP, R. MURANO, and C. RICH. The feasibility of in vivo neutron activation analysis of total body calcium and other elements of body composition. Phys. Med. Biol. 13:269-279, 1968.

41. PIEMME, T. E. Body fluid volume and renal relationships to gravity. in McCALLY, M. (ed.), Hypodynamics and Hypogravics, New York, Academic Press, 1968.

42. RICH, C., E. KLINK, R. SMITH, B. GRAHAM, and P. IVANOVICH. Sonic measurement of bone mass. in Progress in Development of Methods in Bone Densitometry, Washington, D.C., NASA SP-64, 1966.

43. SCHRAER, H., R. SCHRAER, H. G. TROSTLE, and A. D'ALFONSO. The validity of measuring bone density from roentgenograms by means of a bone density computing apparatus. Arch. Biochem. Biophys. 83:486-500, 1959.

44. SMITH, R. W., and D. A. KEIPER. Dynamic measurement of
    viscoelastic properties of bone. Am. J. Med. Elect. 4:156-160,
    1965.

45. SORENSON, J. A., and J. R. CAMERON. Body composition
    determination by differential absorption of monochromatic
    X-rays. in Proceedings of the Symposium on Low Energy X- and
    Gamma Sources and Applications, Washington, D.C., AEC Report
    ORNL-IIC-5, 1964.

46. SORENSON, J. A., and J. R. CAMERON. A reliable in vivo
    measurement of bone-mineral content. J. Bone Jt. Surg.
    49A:481-497, 1967.   /

47. VOGEL, J. M. Changes in bone mineral content of the os calcis
    induced by prolonged bedrest. Fed. Proc. 28:374, 1969.

48. VOSE, G. P. Factors affecting the precision of radiographic
    densitometry of the lumbar spine and femoral neck. in Progress
    in Development of Methods in Bone Densitometry, Washington, D.C.,
    NASA SP-64, 1966.

49. VOSE, G. P., and A. L. KUBALA. Bone strength-its relationship
    to X-ray determined ash content. Hum. Biol. 31:262-270, 1959.

50. VOSE, G. P., S. A. HOERSTER, and P. B. MACK. New technics for
    radiographic assessment of vertebral density. Am. J. Med. Elect.
    3:181-188, 1964.

51. WALMSLEY, R., and J. W. SMITH. Variations in bone structure
    and the value of Young's modulus. J. Anat. 91:603, 1957.

52. WHEDON, G. D. Osteoporosis: Atrophy of disuse. in RODAHL, K.,
    J. T. NICHOLSON, and E. M. BROWN (eds.), Bone as a Tissue,

New York, McGraw-Hill Book Co., 1960.

53. WHEDON, G. D., L. LUTWAK, and W. NEUMAN. Calcium and nitrogen
    balance. in A Review of Medical Results of Gemini 7 and
    Related Flights, Washington, D.C., NASA Space Medicine
    Directorate, 1966.

COLLIMATED
DETECTOR

$$M_B = \frac{\rho_B \, \ln \, (I_o^*/I)}{(\mu_B \rho_B - \mu_s \rho_s)}$$

= BONE MINERAL MASS
PER UNIT AREA IN
RADIATION BEAM PATH
(GM/CM^2)

SOFT
TISSUE
(S)

BONE
(B)

μ = MASS ABSORPTION
COEFFICIENT (CM^2/GM)

ρ = MICROSCOPIC
DENSITY (GM/CM^3)

MONOCHROMATIC
RADIATION
SOURCE
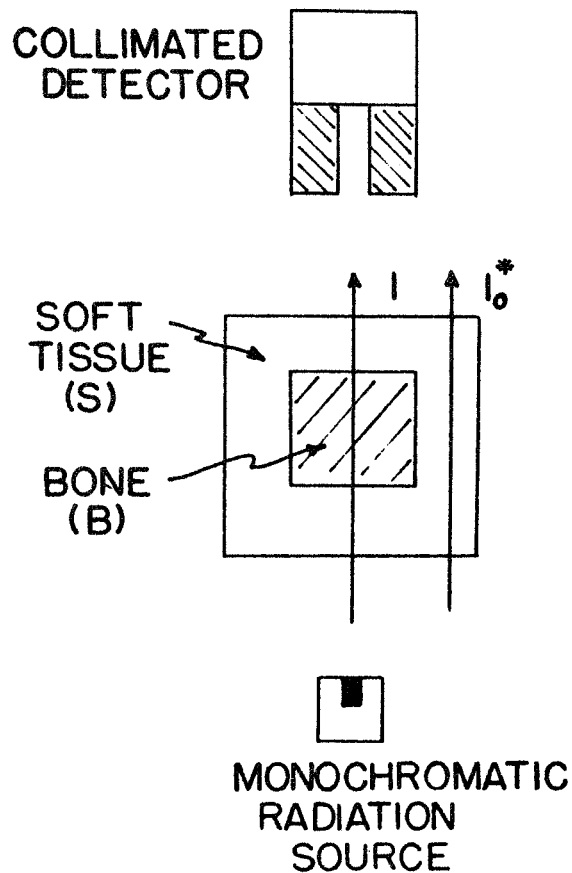
FIGURE 1: Basic principles used in measuring bone mineral with a
monoenergetic photon source. The bone mineral mass per unit area
in the beam path (M_B) is given by the equation. The measured
quantities are I_o^*, the beam intensity through the soft tissue
adjacent to the bone, and I, the beam intensity through the bone.
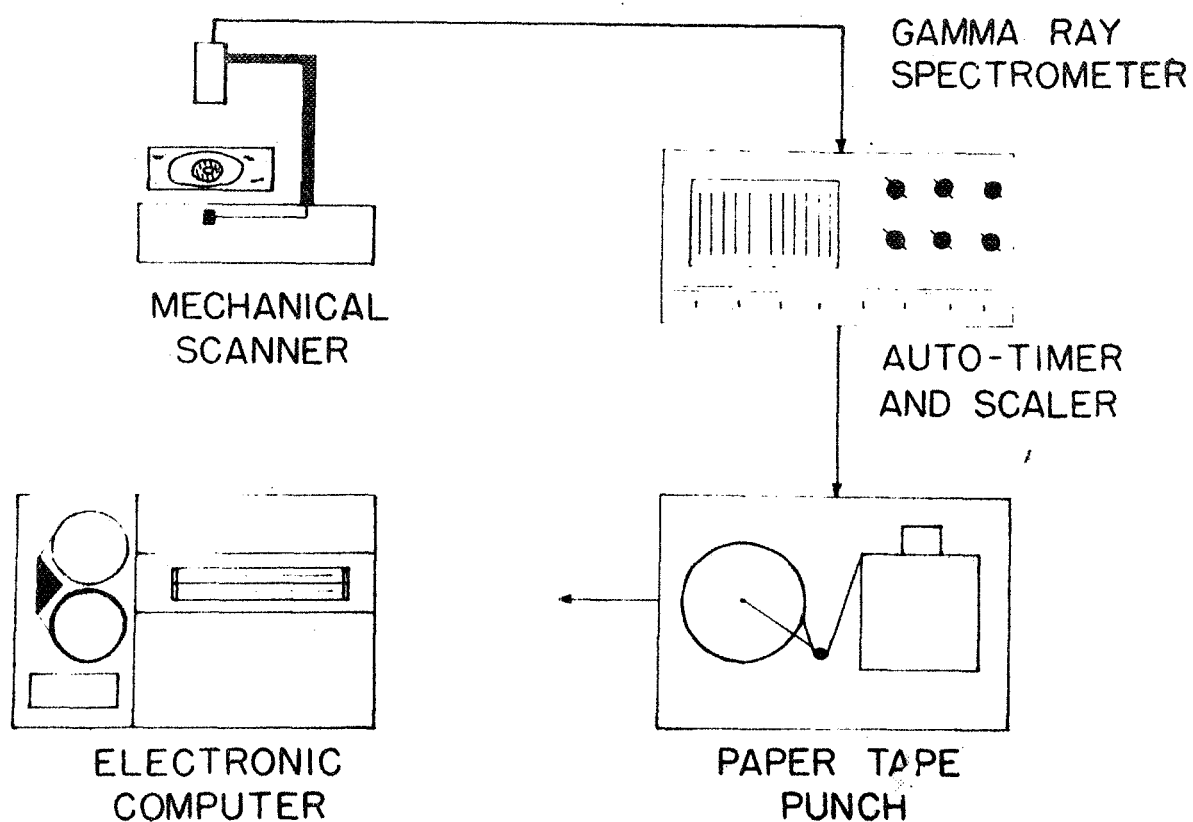
FIGURE 2: System for measuring bone mineral content. Our laboratory is testing a direct readout unit which would allow determination of bone mineral content immediately after completion of a scan.
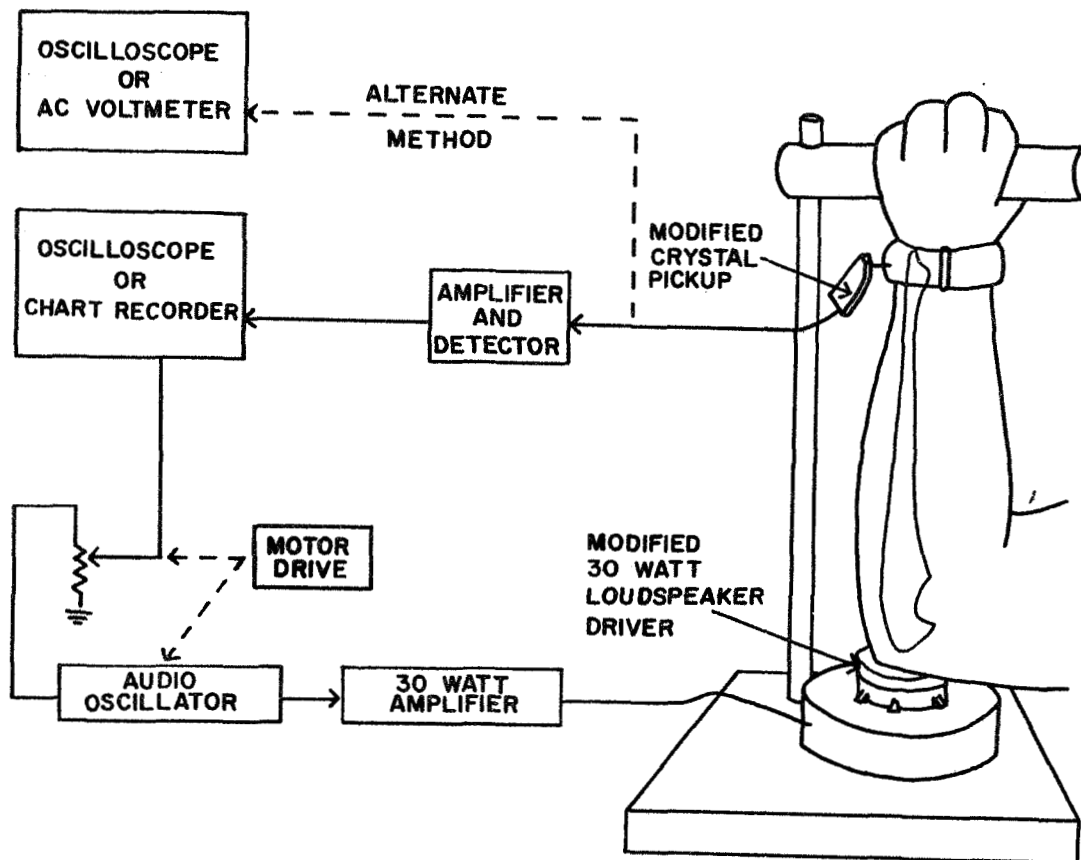
FIGURE 3: Apparatus used for ulnar resonant frequency measurement. The driver is modified by bonding a small lucite piston to the driver diaphragm. The piston contacts the elbow of the subject. The ulnar response is detected by a small crystal accelerometer strapped to the wrist. With changes in the driver support, the apparatus may be used for measurement of tibial resonant frequency (Jurist, to be published).
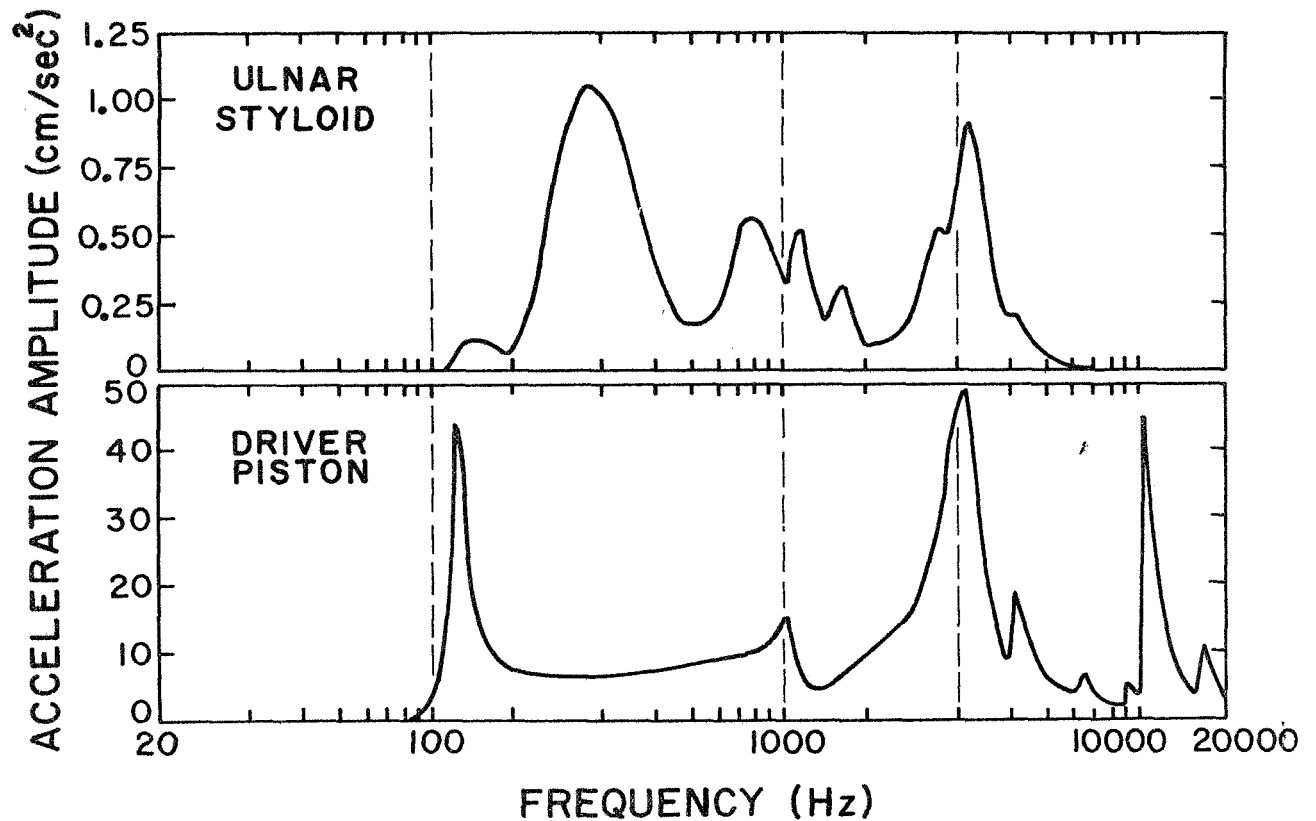
FIGURE 4: Acceleration spectrum of the driver piston (bottom) and of the ulnar styloid (top) for a typical adult. Note the ulnar resonance at about 290 Hz. The resonances at about 130 Hz, 1000 Hz, and 3000 Hz are driver resonances. The resonance at about 10000 Hz is a resonance of the crystal accelerometer.

A Coding System for Clinical and Normative Studies

John M. Jurist

Joyce L. Clark

Kianpour Kianian

1. Introduction

In clinical and normative studies of the skeletal system, we have systematically recorded our data in a form compatible with computer analysis. A simple one-card format, described in a previous report (COO-1422-16), has been satisfactory for recording our measurements until the present time. However, as more and more data are collected from each subject in order to evaluate various factors which may be associated with skeletal status, a more extensive data collection format is required. In addition, many repeated measurements now are made on the same subjects for longitudinal studies. Hence, the new data collection scheme should provide for:

1. Convenient data processing by computer. This requires data storage on punched cards, or as the amount of information increases, on magnetic tape.

2. Recording as much pertinent data as possible from each subject on factors which might be associated with skeletal status.

3. Minimum redundancy of recorded data when repeated measurements are made on the same subject.

4. Maximum convenience of use and minimum possibility of

error in recording or punching data.

5. Sufficient generality to allow use by other laboratories. This facilitates formation of a central registry for quantitative skeletal data. Such a registry would reduce needless duplication of effort by laboratories using comparable measurement techniques.

Our new data collection scheme is consistent with these requirements since:

1. It provides for data recording on standard 80-column punched cards (or card images on magnetic tape).

2. Standard identification and historical data (name, address, sex, etc.) is recorded separately from physical data. Provision is made for recording relevant data (past medical history, height, weight, medication, etc.) in detail.

3. Data are recorded in modular form. Therefore, repeated bone mineral measurements, for example, can be recorded without duplication of data on past medical history, laboratory chemistry values, etc.

4. The data recording sheets are arranged so they may be used directly for keypunching. With our previous system, data were recorded on large file cards, transferred to

coding sheets, and keypunched. Our new system, which allows cards to be keypunched directly from the data forms, eliminates one copying step and thus reduces the probability of making errors. The use of multiple data cards allows a less crowded card format, thus facilitating punching and checking of cards.

5. The data format is sufficiently general to allow another laboratory to use our data for comparative purposes if they use quantitative methods of skeletal evaluation. Additional data card types can be designed for special studies such as skin transparency, the effects of arthritis on the skeletal system, etc.

2. The Data Coding Format

The data card types are listed in the accompanying table. A sample of each coding sheet is included in this report. Each data sheet, except for the first, is used to code one data card. The columns of numbers down the left margin of each sheet indicate the punched card column numbers for the data given. For example, on the header card, columns 1-4 are reserved for the subject number, column 5 is blank, columns 6-7 have 01 punched in them, column 8

is blank, etc. Each card type is represented by a two-digit card identification number in columns 6-7, while each subject is identified by a unique number in columns 1-4.

In some instances, such as columns 9-10 of the header card, coded data is to be punched. Space is provided (in parentheses) to record the raw data for later coding. In the example cited (columns 9-10 of the header card), the measurement location site is coded. For example, a patient in the University of Wisconsin Hospitals would be located at the time of data collection by writing "UW Hosp. Pat." or equivalent in the space provided within the parentheses following "Location Code." When the data sheets are coded for punching, the technician doing the coding would refer to the Location Code List and would find that a patient at the University Hospitals is coded as "11." Consequently the code number 11 would be marked in the space provided after "Location Code." Copies of the code lists are included in this report.

Space is not provided for certain data on a symbol by symbol basis. An example of this is the name of the subject (columns 22-69 of the header card). In these cases, the pertinent alphameric data is provided as needed. There is, however, a column or symbol limitation given at the end of the space for data recording. For example, the name of the subject may be written in

the space provided as long as the limitation of 48 letters, spaces, commas, etc. is observed. Any remaining spaces will be blank on the punched card. Data recorded in this way will not be processed, but will be printed verbatim onto reports or lists when requested.

3. Comments on Data Format

Header and Address Cards: Location code refers to the place where the skeletal evaluation is performed. The referral code is redundant with the location code for investigational controls, but not for patients. The hospital department providing the referral is used for patients of the University of Wisconsin Hospitals.

Personal and Family History Card: The date refers to the date when the data on this card were obtained. The conditions listed under personal history include presently existing conditions. If certain information is not available, the appropriate spaces are left blank.

OB/GYN History Card: Postmenopausal (column 33) refers to either the physiological or surgical menopause. Columns 47-51 refer to the physiological menopause only.

Physical Data, Diagnosis, and Therapy Card: Columns 47-53

are used for pregnant women only. Columns 55-79 refer to current conditions and therapies only. Repeated collection of data for this card may be coded on additional sheets to provide a time sequence of changes in, for example, height or weight.

X-Ray Report Card: Note the limitation of 60 symbols and spaces for the abbreviated list of relevant findings.

Comment Card: This card is used for recording additional information.

Completion Card: This is the last card in the data card deck of each subject.

List of Data Card Types

Card Identification Number	Card Name
01	Header
02	Address
30	Personal and family history
40	OB/GYN history
50	Physical data, diagnosis, and therapy
60	Laboratory data
65	X-ray report
66	Bone mineral scan
70	Resonance data
72	Impact data (long bone)
73	Impact data (skull and mandible)
75	Phase shift data
98	Comment
99	Completion

LOCATION CODE LIST (INITIAL REFERRAL ONLY)

01   UW Staff (investigational control)

02

03

04

05   Mendota Staff (investigational control)

06   Central Colony Staff (investigational control)

07   Manor House Staff (investigational control)

08   Edgewood High School (investigational control)

09   St. Bernard's School (investigational control)

10

11   UW Patient

12   Mendota Patient

13   Central Colony Patient

14   Manor House Patient

15   VA Hospital Patient

16

17

18

19

20

90   Patient of Outside Physician

91

92

93

94

LOCATION CODE LIST (Continued)

95

96

97

98

99   Other

REFERRAL CODE LIST (INITIAL REFERRAL ONLY)

01	Control, UW
02	
03	
04	
05	Manor House Staff
06	Manor House Patient
07	Exercise Study
08	Diet Study
09	La Leche Study
10	Medicine
11	General Surgery
12	Clinical Oncology
13	ENT
14	Ophthalmology
15	Neurosurgery
16	Neurology
17	Orthopedics
18	OB/GYN
19	Dermatology
20	Pediatrics
21	Psychiatry
22	Radiology
23	Rehabilitative Medicine
24	Urology
25	Student Health
26	Arthritis Clinic

REFERRAL CODE LIST (Continued)

27	Radiotherapy
28	Plastic Surgery
29	
30	VA Hospital
90	Outside Physician
91	
92	
93	
94	
95	
96	
97	
98	
99	Other

FRACTURE CODE LIST

01	Left Femoral Neck
02	Left Femoral Shaft
03	
04	
05	Left Tibia
06	Left Fibula
07	Left Os Calcis
08	Left Metatarsal(s) (specify)
09	Left "Hip"
10	Left "Knee"
11	Left "Ankle"
12	Left "Leg"
13	
14	
15	Left Clavicle
16	Left Humerus
17	Left Radius
18	Left Ulna
19	
20	Left "Hand"
21	Left "Elbow"
22	Left "Wrist"
23	Left "Forearm"
24	Left "Arm"
25	Left Metacarpal(s) (specify)
26	Left Phalanx (specify)

FRACTURE CODE LIST (Continued)

27
28
29
30
31 Right Femoral Neck
32 Right Femoral Shaft
33
34
35 Right Tibia
36 Right Fibula
37 Right Os Calcis
38 Right Metatarsal(s) (specify)
39 Right "Hip"
40 Right "Knee"
41 Right "Ankle"
42 Right "Leg"
43
44
45 Right Clavicle
46 Right Humerus
47 Right Radius
48 Right Ulna
49
50 Right "Hand"
51 Right "Elbow"
52 Right "Wrist"

<u>FRACTURE</u> <u>CODE</u> <u>LIST</u> (Continued)

53	Right "Forearm"
54	Right "Arm"
55	Right Metacarpal(s) (specify)
56	Right Phalanx (specify)
57	
58	
59	
60	"Jaw"
61	Skull
62	Mandible
63	Cervical Vertebra
64	Thoracic Vertebra
65	Rib
66	Lumbar Vertebra
67	Sacral Vertebra
68	Coccyx
69	
70	Pubic Ramus
71	
72	
73	"Pelvis"
74	
75	
76	
77	
78	

ACTIVITY CODE LIST

1	Confined to Bed--No Occupation
2	Confined to Wheelchair--No Occupation
3	Confined to Home--No Occupation
4	Sedentary
5	Little Activity
6	Intermediate Activity
7	Moderate Activity
8	Vigorous Activity (athlete, construction worker, etc.)
9	

DIAGNOSIS CODE LIST

001	Myocardial Infarction (MI)
002	Chronic Cor Pumonale
003	Chronic Heart Failure (CHF)
004	Rheumatic Fever
005	Arteriosclerotic Heart Disease (ASHD)
006	Persistent Tachycardia
007	Essential Hypertension
008	Renal Hypertension
009	Hypotension
010	Aortic Calcification
011	Arteriosclerosis
012	Peripheral Vascular Disease
013	Thrombophlebitis
014	Aseptic Necrosis
015	
016	Anemia
017	Chronic Pulmonary Disease
018	Pulmonary Emphysema
019	
020	
021	Pancreatitis
022	Hepatitis
023	Cirrhosis
024	Hepatomegaly
025	"Liver Disease"
026	

DIAGNOSIS CODE LIST (Continued)

027	Diabetes Mellitus
028	
029	
030	Gallstones
031	
032	
033	Gastrectomy
034	
035	Gastric Ulcer
036	Duodenal Ulcer
037	
038	Esophagitis
039	Sprue
040	Steatorrhea
041	Osteomalacia (dietary)
042	Rickets
043	Calcium Deficiency
044	Hypervitaminosis A
045	Pellagra (niacin deficiency)
046	Kwashiorkor (protein deficiency)
047	Scurvy
048	
049	Starvation
050	
051	
052	Alcoholism

DIAGNOSIS CODE LIST (Continued)

053
054   Pyelonephritis
055
056   Glomerulonephritis
057   Nephritis
058   Hydronephrosis
059   Renal Osteodystrophy
060   Chronic Renal Failure
061   Uremia
062   Kidney Stones
063   Cystitis
064
065
066   Leukemia
067   Multiple Myeloma
068   Osteogenic Sarcoma
069   Parathyroid Adenoma
070   Bone Metastases
071   Other Malignancies
072
073
074
075
076   Hypogonadism
077   Castration
078   Amenorrhea

DIAGNOSIS CODE LIST (Continued)

079

080   "Thyroid Disease"

081   Hyperthyroidism

082   Hypothyroidism

083   Hyperparathyroidism

084   Hypoparathyroidism

085

086   Acromegaly

087   Hyperadrenocorticism

088   Addison's Disease (adrenal hypofunction)

089   Cushing's Disease

090

091

092

093   Osteoporosis

094

095   Ankylosing Spondylitis

096   Osteoarthritis

097   Rheumatoid Arthritis, Adult

098   Rheumatoid Arthritis, Juvenile

099   Gout

100

101   Polymyositis

102   Myositis Ossificans

103   Epicondylitis

104   Systemic Lupus Erythromatosus (SLE)

<u>DIAGNOSIS CODE LIST</u> (Continued)

105	Bursitis
106	Scleroderma
107	Polymyalgia Rheumatica
108	Polyarteritis
109	Osteoid TB
110	Osteomyelitis
111	Chronic Brain Syndrome (CBS)
112	Polio
113	Parkinson's Disease
114	Cerebral Arteriosclerosis
115	Epilepsy
116	Cerebrovascular Accident (CVA, stroke)
117	CVA (left) Hemiparesis (spastic)
118	CVA (left) Hemiparesis (flaccid)
119	CVA (right) Hemiparesis (spastic)
120	CVA (right) Hemiparesis (flaccid)
121	Traumatic Quadriplegia
122	Traumatic Hemiplegia
123	Glaucoma
124	
125	Cataracts
126	
127	
128	
129	Pregnant
130	Lactating

THERAPY CODE LIST

001   Unspecified Calcium

002   Unspecified Vitamin D

003   Unspecified Vitamin A

004   Unspecified Iron

005   Unspecified Multivitamin Preparation

006   Unicap (multivitamin)

007

008   Unspecified Thyroid Extract

009   Synthroid (thyroxine)

010   Unspecified Anabolic Steroid

011   Winstrol (anabolic steroid)

012   Dianabol (anabolic steroid)

013

014

015   Unspecified Penicillin

016   Unspecified Sulfa

017   Orinase (antidiabetic)

018   Insulin

019

020

021   Unspecified Diuretic

022   Pitressin (diuretic)

023

024   Digitalis

025   Digoxin (digitalis)

026   Nitroglycerin

THERAPY CODE LIST (Continued)

027	Peritrate (coronary vasodilator)
028	Unspecified Anticoagulant
029	Coumarin
030	Heparin
031	
032	Unspecified Corticoid
033	Prednisone (corticoid)
034	Butazolidin (anti-inflammatory)
035	Indocin (anti-inflammatory)
036	
037	Aspirin or Bufferin
038	Premarin (estrogen)
039	
040	
041	
042	Unspecified Oral Contraceptive
043	Enovid (oral contraceptive)
044	Enovid-E (oral contraceptive)
045	Ortho-Novum (oral contraceptive)
046	Norlestrin (oral contraceptive)
047	Ovulin 28 (oral contraceptive)
048	
049	
050	Dilantin (anti-epileptic)
051	Unspecified Phenobarbitol

X-RAY EXAMINATION CODE LIST

001	Upper GI Series
002	Barium Enema
003	IVP
004	Chest
005	Abdomen
006	Pelvis
007	Skull
008	Cervical Spine
009	Dorsolumbar Spine
010	Lumbosacral Spine
011	Femur
012	Tibia
013	Hand
014	
015	
016	
017	
018	
019	
020	

BONE SCAN SITE LIST

01   Distal 3rd Phalanx, Midlength

02   Medial 3rd Phalanx, Midlength

03   Proximal 3rd Phalanx, Midlength

04   3rd Metacarpal, Midlength

05   Radius, Distal 1/3 (all distances for forearm scans refer to distance relative to ulnar styloid and olecranon)

06   Radius, Midlength

07   Radius, 1.5-3 cm Distal

08   Radius, 4 cm Distal

09   Radius, 8 cm Distal

10   Radius, 12 cm Distal

11   Radius, 16 cm Distal

12   Ulna, Distal 1/3

13   Ulna, Midlength

14   Ulna, 1.5-3 cm Distal

15   Ulna, 4 cm Distal

16   Ulna, 8 cm Distal

17   Ulna, 12 cm Distal

18   Ulna, 16 cm Distal

19   Os Calcis

20   Humerus, Midlength

21

22   Tibia, Midlength

23   Fibula, Midlength

24

25   Femur, Midlength

coded _____
punched _____
proofed _____

HEADER AND ADDRESS CARDS

1-4	Subject Number	___ ___ ___ ___
6-7	01	
9-10	Location Code ___ ___ (	)
12-17	Hospital ID Number ___ ___ ___ ___ ___ ___	
19-20	Referral Code ___ ___ (	)
22-69	Name (Last, First) _____	

_____(48)

71	Sex ___ (M or F)	
72	Race ___ (C, N, or O)	
73	Handedness ___ (L or R)	
75-80	Birthdate (Month, Day, Year) ___ ___ ___ ___ ___ ___	

1-4	Subject Number ___ ___ ___ ___	
6-7	02	
9-15	Home Telephone ___ ___ ___ ___ ___ ___ ___	
17-56	Street Address _____	

_____(40)

58-69	City _____(12)	
71-74	State ___ ___ ___ ___	
76-80	ZIP Code ___ ___ ___ ___ ___	

PERSONAL AND FAMILY HISTORY CARD

1-4	Subject Number	___ ___ ___ ___
6-7	30	
9-14	Date (Month, Day, Year)	___ ___ ___ ___ ___ ___

PERSONAL HISTORY: N if no history of, Y if history of the following conditions (Use comment cards for dates, durations, treatments, etc.)

16	Rheumatoid Arthritis ___
17	Osteoarthritis ___
18	Rheumatism ___
19	Gout ___
20	Height Loss ___
21	Back Pain ___
22	Kidney Stones ___
23	Gastric Ulcer ___
24	Duodenal Ulcer ___
25	Sprue ___
26	Osteomalacia ___
27	Rickets ___
28	Calcium Deficiency ___
29	Steatorrhea ___
30	Chronic Pulmonary Disease ___
31	Liver Disease ___
32	Kidney Disease ___

personal and family history card – continued

33   Hypotension ___

34   Hypertension ___

35   Cardiovascular Disease ___

36   Diabetes ___

37   Parathyroid Disease ___

38   Hypothyroidism ___

39   Hyperthyroidism ___

40   Other Endocrinopathy ___

42-53   Coded Traumatic Fractures ___ ___ ___ ___ ___ ___

           ___ ___ ___ ___ ___ ___ (_____

           _____ _____ _____

           _____ _____)   ,

55-66   Coded Spontaneous Fractures ___ ___ ___ ___ ___ ___

           ___ ___ ___ ___ ___ ___ (_____

           _____ _____ _____

           _____ _____)

FAMILY OSTEOPOROSIS HISTORY: N if non-osteoporotic, Y
      if osteoporotic (based on history of spontaneous
      fractures by age 70)

68   Father ___

69   Mother ___

70   Paternal Grandfather ___

71   Paternal Grandmother ___

72   Maternal Grandfather ___

73   Maternal Grandmother ___

74   Brother ___

75   Sister ___

76   Paternal Uncle ___

personal and family history card - continued

77   Paternal Aunt ____

78   Maternal Uncle ____

79   Maternal Aunt ____

80   First Cousin ____

Comments:

OB/GYN HISTORY CARD

1-4	Subject Number ___ ___ ___ ___
6-7	40
9-14	Date (Month, Day, Year) ___ ___ ___ ___ ___ ___
16	X If Postmenarchial ___
18-19	Start of Menstruation at Age (Years) ___ ___
21-22	Number of Past Pregnancies ___ ___
24-25	Number of Term Pregnancies ___ ___
27-28	Number of Breast Fed Children ___ ___
30-31	Average Lactation Duration (Months) ___ ___
33	X if Postmenopausal ___
35-36	First Oophorectomy at Age (Years) ___ ___
38-39	Second Oophorectomy at Age (Years) ___ ___
41-42	Bilateral Oophorectomy at Age (Years) ___ ___
44-45	Hysterectomy at Age (Years) ___ ___
47-48	Last Regular Menstrual Period at Age (Years) ___ ___
50-51	Duration of Menopausal Symptoms (Months) ___ ___

coded _____
punched _____
proofed _____

PHYSICAL DATA, DIAGNOSIS, AND THERAPY CARD

1-4   Subject Number ___ ___ ___ ___

6-7   50

9-14   Date (Month, Day, Year) ___ ___ ___ ___ ___ ___

16   Body Build Code ___

17   Activity Code ___

19-21   Standing Height (Centimeters) ___ ___ ___

23-25   Sitting Height (Centimeters) ___ ___ ___

27-29   Weight (Pounds) ___ ___ ___

31-32   Left Triceps Skin Fold (Millimeters) __ __

34-36   Resting Heart Rate (Beats/Minute) ___ ___ ___

38-40   Resting Systolic Blood Pressure (mm Hg) ___ ___ ___

42-44   Resting Diastolic Blood Pressure (mm Hg) ___ ___ ___

46   X if Pregnant ___

47-52   Date of Last Menstrual Period Completion (Month, Day, Year) __ __ __ __ __ __

53   X if Taking Supplemental Calcium ___

55-66   Coded Diagnoses ___ ___ ___ ___ ___ ___ ___ ___ ___

           ___ ___ ___ (_____ _____

           _____ _____)

68-79   Coded Therapies ___ ___ ___ ___ ___ ___ ___ ___ ___

           ___ ___ ___ (_____ _____

           _____ _____) Note: The subject should be specifically questioned about the following medications: oral contraceptives, cortisone, thyroid extract, insulin, calcium preparations.

coded _____
punched _____
proofed _____

LABORATORY DATA CARD

1-4	Subject Number ___ ___ ___ ___	
6-7	60	
9-14	Date (Month, Day, Year) ___ ___ ___ ___ ___ ___	
16-19	Photomotogram (Milliseconds) ___ ___ ___ ___	
21-24	Serum Protein Bound Iodine (µg%) ___ ___ . ___	
26-29	Serum Calcium (mg%) ___ ___ . ___	
31-34	Serum Phosphorus (mg%) ___ ___ . ___	
36-39	Serum Glutamate-oxaloacetate Transaminase (Units) ___ ___ ___ ___	
40-43	Serum Glutamate-pyruvate Transaminase (Units) ___ ___ ___ ___	
44-47	Serum Lactic Acid Dehydrogenase (Units) ___ ___ ___ ___	
49-52	Serum Alkaline Phosphatase (K-A Units) ___ ___ . ___	
54-57	Serum Creatinine (mg%) ___ ___ . ___	
59-62	Serum Protein (g%) ___ ___ . ___	
64-67	Urinary Calcium (mg/24 hrs) ___ ___ ___ ___	
69-72	Urinary Phosphorus (mg/24 hrs) ___ ___ ___ ___	
74-76	Urinary 17 Hydroxycorticosteroids (mg/24 hrs) ___ ___ ___	
78-80	Urinary 17 Ketosteroids (mg/24 hrs) ___ ___ ___	

X-RAY REPORT CARD

1-4   Subject Number ___ ___ ___ ___

6-7   65

9-14   Date (Month, Day, Year) ___ ___ ___ ___ ___ ___

16-18   Coded X-Ray Examination ___ ___ ___ (_____

_____)

20-79   Findings _____

_____

_____

_____

_____(60)

BONE MINERAL SCAN CARD

1-4   Subject Number ___ ___ . ___ ___

6-7   66

9-14   Date (Month, Day, Year) ___ ___ ___ ___ ___ ___

16   Isotope (A for ^{241}Am, I for ^{125}I, or P for ^{210}Pb) ___

17   Side Scanned (L or R) ___

19-20   Coded Bone Site Scanned ___ ___ (_____)

22-23   Source Distance (cm from source to fingertip, elbow, heel, or knee, depending on whether scan is of hand or forearm, upper arm, foot or lower leg, or upper leg) ___ ___

25-29   Bone Mineral Content (g/cm) ___ ___ . ___ ___

31-34   Bone Width at Scan Site (cm) ___ . ___ ___

36   Isotope ___

37   Side Scanned ___

39-40   Coded Bone Site Scanned ___ ___ (_____)

42-43   Source Distance ___ ___

45-49   Bone Mineral Content ___ ___ . ___ ___

51-54   Bone Width at Scan Site ___ . ___ ___

56   Isotope ___

57   Side Scanned ___

59-60   Coded Bone Site Scanned ___ ___ (_____)

62-63   Source Distance ___ ___

65-69   Bone Mineral Content ___ ___ . ___ ___

71-74   Bone Width at Scan Site ___ . ___ ___

RESONANCE DATA CARD

1-4	Subject Number ___ ___ ___ ___
6-7	70
9-14	Date (Month, Day, Year) ___ ___ ___ ___ ___ ___

LEFT ULNA:

16-19	L (cm) ___ ___ . ___
21-24	F_o (Hz) ___ ___ ___ ___
26-28	$F_2 - F_1$ (Hz) ___ ___ ___

RIGHT ULNA:

30-33	L ___ ___ . ___
35-38	F_o ___ ___ ___ ___
40-42	$F_2 - F_1$ ___ ___ ___

LEFT TIBIA:

44-47	L ___ ___ . ___
49-52	F_o ___ ___ ___ ___
54-56	$F_2 - F_1$ ___ ___ ___

RIGHT TIBIA:

58-61	L ___ ___ . ___
63-66	F_o ___ ___ ___ ___
68-70	$F_2 - F_1$ ___ ___ ___

IMPACT DATA CARD (Long Bone)

1-4   Subject Number ___ ___ ___ ___

6-7   72

9-14   Date (Month, Day, Year) ___ ___   ___ ___   ___ ___

16   Bone (C for Clavicle, T for Tibia, or U for Ulna) ___

18   Side (L or R) ___

20-23   L (cm) ___ ___ • ___

25-28 F_d (Hz) ___ ___ ___ ___

30-33 α (/sec) ___ ___ ___ ___

35   Bone ___

37   Side ___

39-42   L ___ ___ • ___

44-47 F_d ___ ___ ___ ___

49-52 α ___ ___ ___ ___

54   Bone ___

56   Side ___

58-61   L ___ ___ • ___

63-66 F_d ___ ___ ___ ___

68-71 α ___ ___ ___ ___

coded_____
punched_____.
proofed_____

IMPACT DATA CARD (Skull and Mandible)

1-4   Subject Number ___ ___ ___ ___

6-7   73

9-14   Date (Month, Day, Year) ___ ___   ___ ___   ___ ___

SKULL:

16-19   Head Length (cm) ___ ___ • ___

21-24   Head Breadth (cm) ___ ___ • ___

26-29 F_d (Hz) ___ ___ ___ ___

31-34 α (/sec) ___ ___ ___ ___

MANDIBLE:

36-38   Ramus-Body Angle (^{o}) ___ ___ ___

40-43   Angle Separation (cm) ___ ___ • ___

45-48   Angle Arc Separation (cm) ___ ___ • ___

50-53 F_d (Hz) ___ ___ ___ ___

55-58 α (/sec) ___ ___ ___ ___

PHASE SHIFT DATA CARD

1-4   Subject Number ___ ___ ___ ___

6-7   75

9-14   Date (Month, Day, Year) ___ ___ ___ ___ ___ ___

16   Bone (T for Tibia, U for Ulna) ___

18   Side (L or R) ___

20-23   Length (cm) ___ ___ • ___

25-28   Frequency (Hz) ___ ___ ___ ___

30-32   Wavelength (cm) ___ • ___

34-36   Bone Lag (cm) ___ • ___

38-40   Sensor Lag (cm) ___ • ___

42-45   Frequency ___ ___ ___ ___

47-49   Wavelength ___ • ___

51-53   Bone Lag ___ • ___

55-57   Sensor Lag ___ • ___

59-62   Frequency ___ ___ ___ ___

64-66   Wavelength ___ • ___

68-70   Bone Lag ___ • ___

72-74   Sensor Lag ___ • ___

coded_____
punched_____
proofed_____

COMMENT CARD

1-4   Subject Number ____ ____ ____ ____

6-7   98

9-14   Date (Month, Day, Year) ____ ____ ____ ____ ____ ____

16-17   Comment Card Number for This Date ____ ____

19-78   Comment_____

           _____

           _____

           _____(60)

coded_____ .
punched_____
proofed_____

COMPLETION CARD

1-4   Subject Number ____ ____ ____ ____

6-7   99

9-11   END

/

Quantitative Evaluation of Skeletal Status

in the Rheumatic Diseases

John M. Jurist

Mark N. Mueller

Joyce L. Clark

1. Introduction

As a result of the 1957-1959 US National Health Survey (7), it was estimated that 10,845,000 people in the United States have "arthritis" or "rheumatism." The incidence was only 0.2% for people less than 25 years of age, but was 28.6% for people at least 75 years old. These estimates are not entirely reliable because of sampling difficulties and inadequately defined criteria; it is, however, still apparent that an enormous loss in potential productivity results from disability associated with these diseases.

Rheumatoid arthritis (2) is a chronic, progressive, disabling, systemic disease of the connective tissues. Joint inflammation is the predominant clinical manifestation of this condition. Skeletal changes often associated with rheumatoid arthritis include juxta-articular osteoporosis in the initial stages. Osteoporosis may become generalized in later stages of the disease. Although bone demineralization may be caused by the disease process itself, immobilization resulting from the disease, or anti-anabolic effects of the anti-inflammatory agents (especially corticosteroids) used in its therapy (1,3,5,6), no quantitative or direct study of skeletal status in rheumatoid arthritis has been made.

We propose to measure bone mineral content in a number of

sites such as the distal radius, midshaft of the radius, etc. and
relative bone elasticity in the ulna and tibia in patients with
rheumatoid arthritis. Changes in skeletal status will be studied
on both cross sectional and longitudinal bases as a function of
disease severity and duration, involved joints, and the type and
duration of therapy.

2. Documentation

For this study, two additional data sheets were added to the
coding system previously described for clinical and normative
studies (4). These sheets, samples of which are included in this
report, are used to record data for the medication history and
arthritis study cards.

The medication history card allows recording of relevant data
on three types of medication. Dose strengths are recorded in
appropriate units (milligrams, micrograms, units, etc.) for each
medication type. Space is provided for a record of the duration of
each treatment and the elapsed time (if any) since its
discontinuation.

The arthritis study card provides a record of the severity of
the disease. (A copy of the coding list is included in this report.)

In addition, the card provides a record of pertinent laboratory
data, a summary of the involved joints, and whether or not objective
signs (swelling, radiographic changes, etc.) are found for these
joints.

3. References

1. BERNSTEN, C. R.; FREYBERG, R. H.: Evaluation of status of
   patients with rheumatoid arthritis after five or more years of
   corticosteroid treatment, Bull. Rheum. Dis. 12:261-262, 1961.

2. DECKER, J. L. (ed.): Primer on the Rheumatic Diseases, The
   Arthritis Foundation, New York, 1964.

3. DUNCAN, H.; FROST, H. M.; VILLANUEVA, A. R.; SIGLER, J. W.: The
   osteoporosis of rheumatoid arthritis, Arth. and Rheum. 8:943-954,
   1965.

4. JURIST, J. M.; CLARK, J. L.; KIANIAN, K.: A coding system for
   clinical and normative studies, 1969 Progress Report.

5. McCONKEY, E.; FRASER, G. M.; BLIGH, A. S.: Osteoporosis and
   purpura in rheumatoid disease: Prevalence and relation to
   treatment with corticosteroids, Quart. J. Med. 31:419, 1962.

6. MOLDAWER, M.: *Osteoporosis*, in DACSO, M. (ed.): <u>Restorative</u> <u>Medicine</u> <u>in</u> <u>Geriatrics</u>, Charles C Thomas, Springfield, Ill., 1963.

7. <u>Arthritis</u> <u>and</u> <u>Rheumatism</u>, Health Statistics, Series B, No. 20, US HEW, Washington, D.C., 1960.

MEDICATION HISTORY CARD (Systemic Medication Only)

1-4   Subject Number ___ ___ ___ ___

6-7   35

9-14   Date (Month, Day, Year) ___ ___ ___ ___ ___ ___

16-18   Coded Medication ___ ___ ___ (_____)

20-22   Strength (Per Dose) ___ ___ ___

24   Dosage (Doses Per Day) ___

26-29   Medication Duration (Years, Months) ___ ___ ___ ___

31-34   Time Since Discontinuation (Years, Months) ___ ___ ___ ___

36-38   Coded Medication ___ ___ ___ (_____)

40-42   Strength ___ ___ ___

44   Dosage ___

46-49   Medication Duration ___ ___ ___ ___

51-54   Time Since Discontinuation ___ ___ ___ ___

56-58   Coded Medication ___ ___ ___ (_____)

60-62   Strength ___ ___ ___

64   Dosage ___

66-69   Medication Duration ___ ___ ___ ___

71-74   Time Since Discontinuation ___ ___ ___ ___

ARTHRITIS STUDY CARD

1-4   Subject Number ___ ___ ___ ___

6-7   80

9-14   Date (Month, Day, Year) ___ ___ ___ ___ ___ ___

16   Marital Status (S, D, W, or M) ___

18-21   Time since Disease Onset (Years, Months) ___ ___ ___ ___

23   Coded Disease Severity ___ (_____)

25-27   Erythrocyte Sedimentation Rate (mm/hr) ___ ___ ___

29   X if Nodules Present ___

30   X if Rheumatoid Factor Present ___

32-36   Rheumatoid Factor Dilution ___ ___ ___ ___ ___

INVOLVED JOINTS: N for not involved, L for left side involved, R for right side involved, B for both sides involved; P for pain only, O for objective signs only, B for both subjective and objective signs (involved side(s) first, type last)

38-39   Spine ___ ___

41-42   Shoulder ___ ___

44-45   Elbow ___ ___

47-48   Wrist ___ ___

50-59   MP: (1) ___ ___ (2) ___ ___ (3) ___ ___ (4) ___ ___ (5) ___ ___

61-70   IP: (1) ___ ___ (2) ___ ___ (3) ___ ___ (4) ___ ___ (5) ___ ___

72-73   Hip ___ ___

75-76   Knee ___ ___

78-79   Ankle ___ ___

DISEASE SEVERITY CODE LIST

1   No Impairment of Activity

2   Mild Impairment of Activity

3   Moderate Impairment of Activity

4   Severe Impairment of Activity

In Vivo Determination of the Elastic Properties of Bone

I.   Theory, Apparatus, and Method of Ulnar

Resonant Frequency Determination

John M. Jurist, Ph.D.
Department of Radiology
University of Wisconsin Medical Center
Madison, Wisconsin

1. Introduction

For a number of years, skeletal status has been evaluated by estimation of bone radio-opacity--either visually or with an optical densitometer. This approach has evolved into the sophisticated and highly precise monoenergetic photon absorptiometry techniques of bone mineral measurement (Cameron and Sorenson 1963, Sorenson and Cameron 1967). However, measurement of bone mineral may give an inadequate indication of skeletal status in osteoporosis. Urist, MacDonald, Moss, and Skoog (1963), for example, report the existence of regions of dead, weak bone which are normally or even excessively mineralized in this condition. Thus, bones which appear normal with respect to mineral mass may still be unusually susceptible to fracture. Mather (1967) has demonstrated a correlation between bone elasticity, geometry, and strength. It therefore appears desirable to investigate methods of measuring bone elasticity _in vivo_ as a means of estimating bone quality.

Because the speed of sound in a material is a function of elasticity and density (Kinsler and Frey 1950), measurement of the speed of sound propagation in bone offers one approach to estimation of bone elasticity.

We are investigating the measurement of the speed of sound
in the ulna and in the tibia by the following approaches:

1. Timing of impulse propagation,

2. Measurement of the phase shift per unit length of bone
   for fixed vibrational frequencies,

3. Measurement of resonant frequency by obtaining the
   amplitude response of the bone to vibratory excitation
   of relatively constant amplitude and variable frequency,

4. Measurement of the "ringing frequency" of the bone after
   application of a short-duration impulse.

The ulna is suitable for all four approaches listed above because
it is easily accessible at each end--both the olecranon and styloid
processes are close to the body surface (even in obese subjects).
The tibia, which is now being investigated in our laboratory, has
certain advantages for measurement of ringing or resonant
frequency since it can be easily excited along the middle of the
(subcutaneous) medial surface. Excitation at this location tends
to suppress even harmonics.

For many years, various acoustical or vibratory techniques
have been used for non-destructive testing of materials (Rowe 1949),
but application of these techniques to study of skeletal properties
is relatively recent (Jurist and Selle 1965, Smith and Keiper 1965).

This report deals with the instrumentation used for in vivo
estimation of ulnar elasticity by resonant frequency measurement.

2. Theoretical Basis of Resonant Frequency Measurement

The vibratory properties of a long bone such as the ulna may
be modeled on the fundamental equation describing a vibrating bar:
$F_oL=KC$. In this equation, F_o is the resonant frequency and L is
the length of the bar, C is the speed of sound through thé material
of the bar, and K is a proportionality constant dependent on the
mode of vibration, geometrical factors, and boundary conditions
(Kinsler and Frey 1950).

If transverse modes of vibration are considered, C is
unchanged, but K then includes factors dependent on the shape of
the bar and is usually much smaller than it is for longitudinal
modes. As a first approximation, the ulna may be considered to be
a cylindrical tube with an outside diameter equal to 5% of its
length and an inside diameter equal to 3.3% of its length. It is
attached to rigid supports at each end by hinges. The values of K
are then 0.5000 and 0.0235 for the fundamental longitudinal and
transverse modes of vibration, respectively. It is recognized that
the ulna is not a uniform cylinder, and the joints do not act as

true hinges. Thus, the actual K values for the ulna may vary considerably from these estimates. In addition, since the ulna is not symmetrical about its long axis, K values for fundamental transverse resonances may vary with the plane of vibration. These considerations will be evaluated in later reports.

If the bar is excited by a constant amplitude sinusoidal driving force of variable frequency, it will exhibit a maximum response or "resonance" at a frequency, F_a, which is approximately equal to the resonant frequency, F_o. More explicitly, $F_o = F_a \sqrt{2Q^2/(2Q^2-1)}$, where Q is a measure of damping or frictional losses in the vibrating system. Since the ulnar Q is typically 2.7-3.6 when measured in vivo, F_o is usually 2-4% larger than F_a. To a first approximation, correction for Q may be neglected, and F_o set approximately equal to F_a.

The relationship $F_o L = KC$ may be exploited to determine the elastic properties of long bones because $C^2 = Y/\rho$, where Y is the average value of Young's modulus over the cross section of the bone, and ρ is the average density. The density term includes any muscle or connective tissues which may be coupled to the bone. However, the acoustical impedance of bone is so much larger than that of soft tissue that any coupling effects are small. The

ratio Y/ρ is identical to the ratio of Young's modulus integrated
over the cross section of the bone to the linear density (mass per
unit length) of the bone. Since the linear density of a long bone
is proportional to the mineral content expressed in terms of mineral
mass per unit length (Cameron, Mazess, and Sorenson 1968), the
linear density may be estimated by monoenergetic photon
absorptiometry (Cameron and Sorenson 1963). If the shape and
boundary conditions of the bone under consideration are assumed to
be constant, then the vibrational mode is fixed and $F_o L$ is thus
proportional to $\sqrt{Y/\rho}$. The validity of this assumption is discussed
in the following paper.

3. Instrumentation

The apparatus used to measure ulnar resonant frequency is
shown in Figure 1. The oscillator-amplifier combination powers
the modified loudspeaker driver with a variable frequency signal.
The response of the ulna to excitation at the olecranon process is
monitored at the styloid process by means of a seismographically
mounted crystal pickup. Figure 2 shows the arm support, driver,
and detector in detail.

In practice, the length L of the ulna is measured with a

metric rule. A response spectrum is obtained by scanning a frequency range and recording the response as a function of frequency. In this case, F_a, the frequency of maximum amplitude response, may be taken directly from the record. Alternatively, F_a is determined by tuning the oscillator to obtain maximum response on the monitoring oscilloscope. Since, to a first approximation, the frequency of maximum amplitude response is equal to the resonant frequency ($F_a \gtrsim F_o$), the product $F_o L$ may be calculated in order to obtain a quantity proportional to $\sqrt{Y/\rho}$. In practice, $F_o L$ is usually 4000-8000 Hz-cm for healthy subjects, and 1200-4500 Hz-cm for patients with symptomatic osteoporosis.

Figure 3 shows a typical response spectrum for a normal subject. This figure clearly demonstrates a resonance peak at about 250 Hz, but does not show any other resonances. Additional resonances are often observed which may be either overtones or fundamental frequencies of different modes of vibration (Figure 4).

4. Instrumentation Characteristics

Figure 5 shows the amplitude of piston vibration, measured optically, of the unloaded driver for frequencies of 50-400 Hz. Observation of the piston vibrational amplitude at higher

frequencies shows the driver to have a resonant frequency of about 750 Hz. This frequency is much higher than the ulnar resonant frequency. The piston vibrational amplitude, measured at constant frequency, is proportional to the input voltage (Figure 6).

Figure 7 shows the crystal pickup voltage as a function of frequency when the pickup is seismographically mounted on the driver piston. There are no pickup resonances in the frequency range of interest (50-400 Hz).

In order to confirm that the resonance shown in Figure 3 was not a resonance of the arm support, the oscillator was tuned until resonance was detected, and then the crystal pickup output voltage was measured for four situations:

1. Subject positioned as shown in Figure 3. In this case, the peak to peak output voltage, V, of the crystal is a function of the vibration conducted from the driver through the subject's arm, through the arm support, and through the arm. $V_{(arm+support+air)} = 4.6$ volts.

2. Subject positioned as above except with elbow about 5 mm above the driver piston. This measures conduction through the arm support and through the air.

$V_{(support+air)} = 0.0$ volts.

3. Subject positioned with elbow on driver piston and with handgrip separated from the arm support. This measures conduction through the subject's arm and through the air. $V_{(arm+air)} = 7.0$ volts.

4. Subject positioned with elbow about 5 mm above the driver piston and with the handgrip separated from the arm support. This measures air conduction only. $V_{(air)} = 0.0$ volts.

These measurements show that most of the driver output reaches the crystal through the forearm of the subject. It should also be noted that the characteristic resonance peak was obtained only when the elbow of the subject was in contact with the driver piston.

5. Discussion and Conclusions

The in vivo determination of bone elasticity has potential value in screening programs for metabolic bone disease, early detection of osteoporosis, and evaluation of skeletal effects of various therapeutic modalities. Mather (1967) has related breaking strength of the femur to age of the subject, bone geometry (which can be determined roentgenographically), and bone elasticity measured in vitro. It appears, therefore, that breaking loads of

bones could be predicted by roentgenographic and vibratory measurement of the living subject if bone resonant frequency proves to be an accurate estimate of bone elasticity.

If C is assumed to be 2880 meters/second (Rich, Klink, Smith, Graham, and Ivanovich 1966), and the ulnar L is assumed to be 30 cm, the model presented previously predicts a fundamental transverse resonant frequency of about 230 Hz. Considering the limitations of the model, the predicted transverse resonant frequency is in reasonable agreement with experimental values, typically 150-300 Hz, obtained with healthy subjects.

The following paper will discuss the precision or reproducibility of the technique. Later papers will consider clinical findings obtained by ulnar resonant frequency measurement and their implications, measurement of tibial resonant frequency, and determination of the speed of sound in bone by phase shift and impulse propagation measurements.

6. Acknowledgments

awarded to the University of Wisconsin by NASA. I wish to acknowledge the many helpful discussions with Dr. Benedict Cassen (UCLA), Dr. Anthony Dymond (UCLA), and Dr. John Cameron (Wis.).

Summary

The relationship between resonant frequency (F_o), length (L), and speed of sound (C) for a long bone is given by $F_o L = KC$, where K is a proportionality constant depending on geometrical factors, boundary conditions, and the mode of vibration. Since the speed of sound in a material is related to elasticity, the elasticity of a long bone such as the ulna may be estimated by determining $F_o L$. The resonant frequency of the ulna is obtained by recording the amplitude response of this bone at the styloid process to sinusoidal vibration applied at the olecranon process as a function of driving frequency. Measurement of ulnar resonant frequency is a promising approach to _in vivo_ estimation of bone elasticity.

References

1. CAMERON, J. R., and SORENSON, J. A., 1963, _Science_, 142:230.

2. CAMERON, J. R., MAZESS, R. B., and SORENSON, J. A., 1968, _Investigative Radiology_, 3:141.

3. JURIST, J. M., and SELLE, W. A., 1965, _The Physiologist_, 8:203.

4. KINSLER, L. E., and FREY, A. R., 1950, _Fundamentals of Acoustics_ (New York: John Wiley & Sons, Inc.), Chaps. 1-3.

5. MATHER, B. S., 1967, _Aerospace Medicine_, 38:1270.

6. RICH, C., KLINK, E., SMITH, R., GRAHAM, B., and IVANOVICH, P., 1966, in _Progress in Development of Methods in Bone Densitometry_ (Washington, D.C.: National Aeronautics and Space Administration), p. 137.

7. ROWE, R. G., 1949, _Vibration Apparatus for Testing Articles_, United States Patent No. 2,486,984.

8. SMITH, R. W., and KEIPER, D. A., 1965, _American Journal of Medical Electronics_, 4:156.

9. SORENSON, J. A., and CAMERON, J. R., 1967, <u>The</u> <u>Journal</u> <u>of</u>
    <u>Bone</u> <u>and</u> <u>Joint</u> <u>Surgery</u>, <u>49A</u>:481.

10. URIST, M. R., MacDONALD, N. S., MOSS, M. J., and SKOOG, W. A.,
    1963, in <u>Mechanisms</u> <u>of</u> <u>Hard</u> <u>Tissue</u> <u>Destruction</u> (Washington, D.C.:
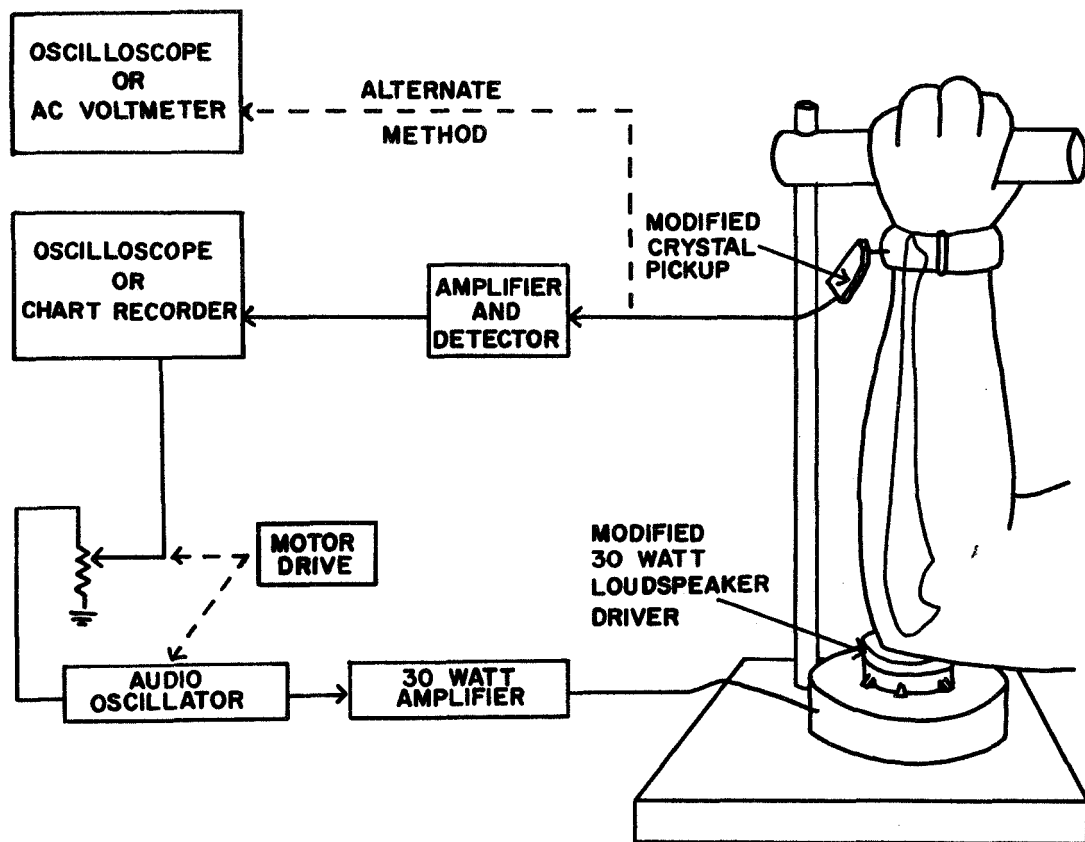   American Association for the Advancement of Science), p. 385.

FIGURE 1: Apparatus used to measure ulnar resonant frequency. The 16Ω Atlas PD-4V driver was modified by addition of a small lucite piston bonded to the diaphragm by epoxy cement. This piston made contact with the elbow of the subject. The vibration pickup (Calrad C-10) was mounted seismographically over the ulnar styloid process with the cartridge stylus strapped to the wrist. The ulnar resonant frequency may be determined by: (1) scanning a frequency range and recording the amplitude response as a function of driving frequency, or (2) tuning the Heath AG-10 audio oscillator to obtain maximum response as measured on the monitoring oscilloscope.
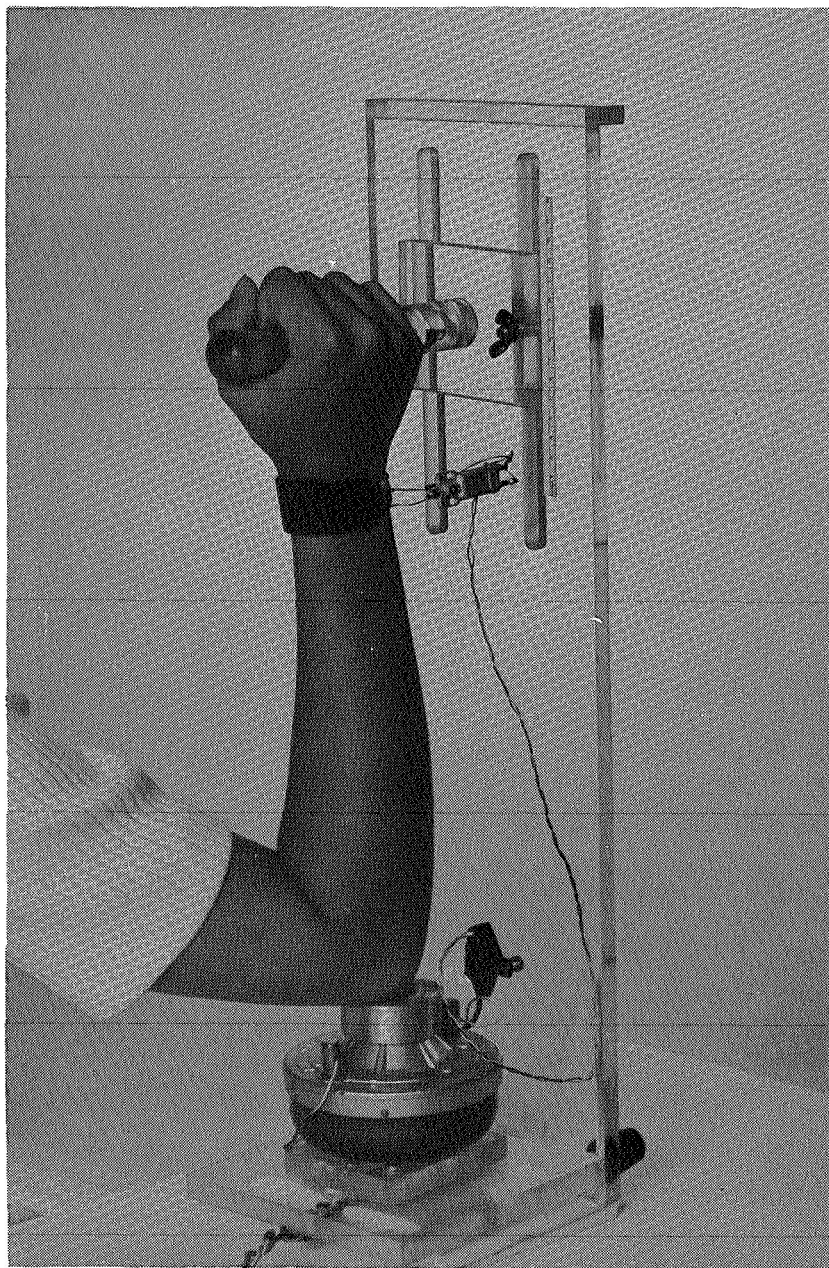
FIGURE 2: Photograph of arm support showing driver and vibration detector.
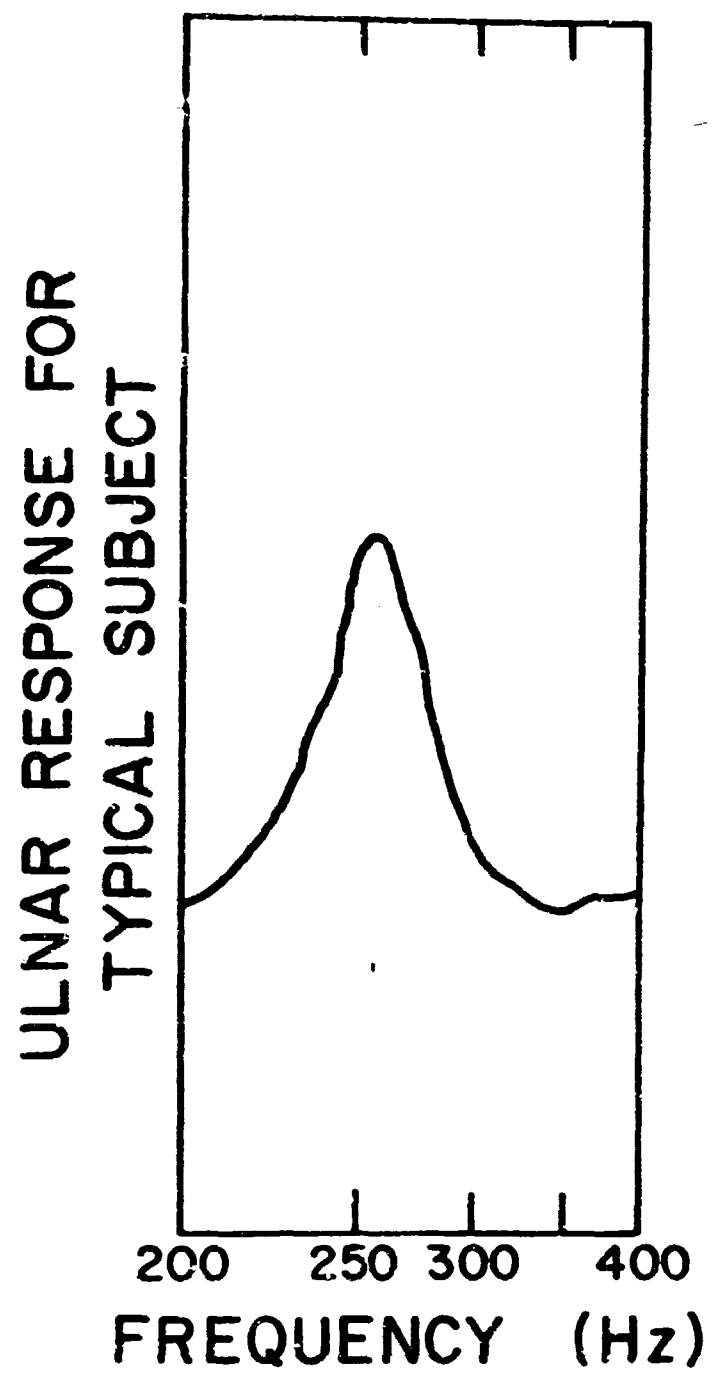
FIGURE 3: Typical ulnar response spectrum for a normal adult. Note the resonance peak at about 250 Hz.
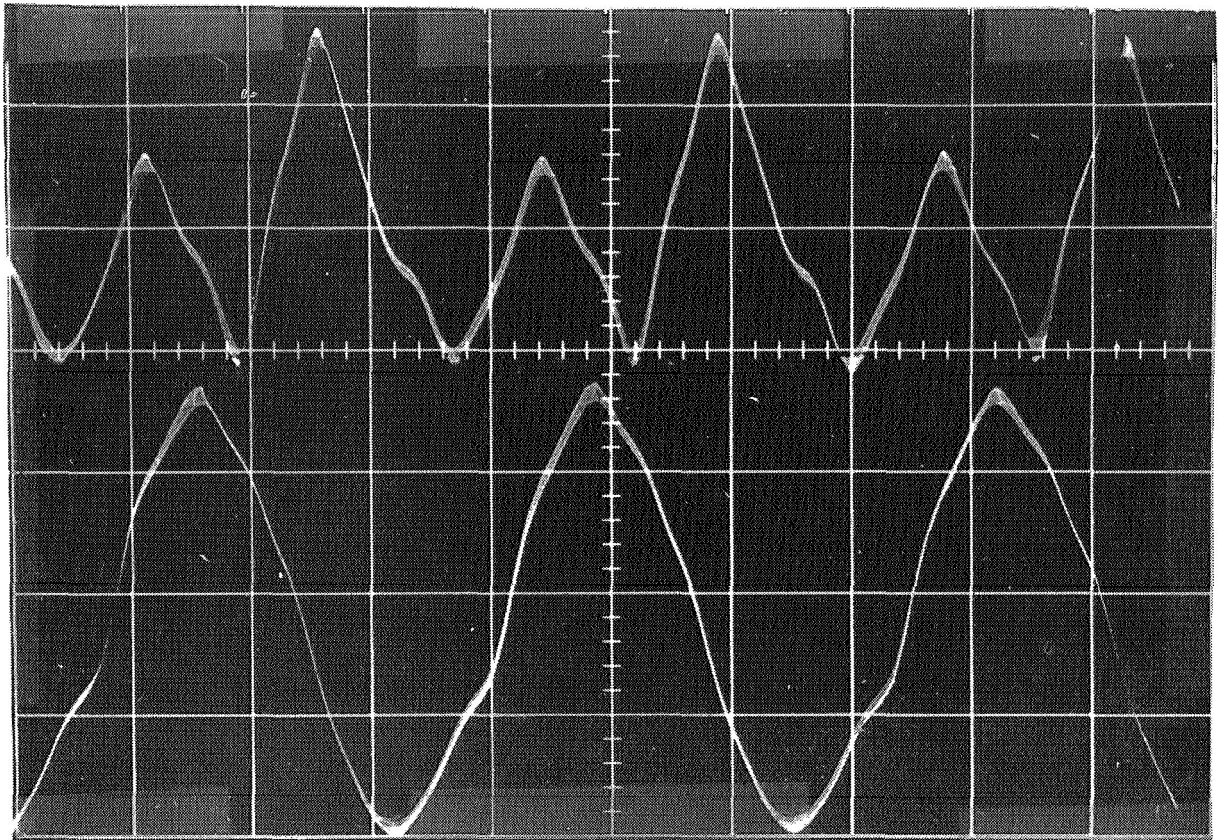
FIGURE 4: Oscilloscope trace showing a 250 Hz response of the ulna (top) to a 125 Hz driving signal (bottom).
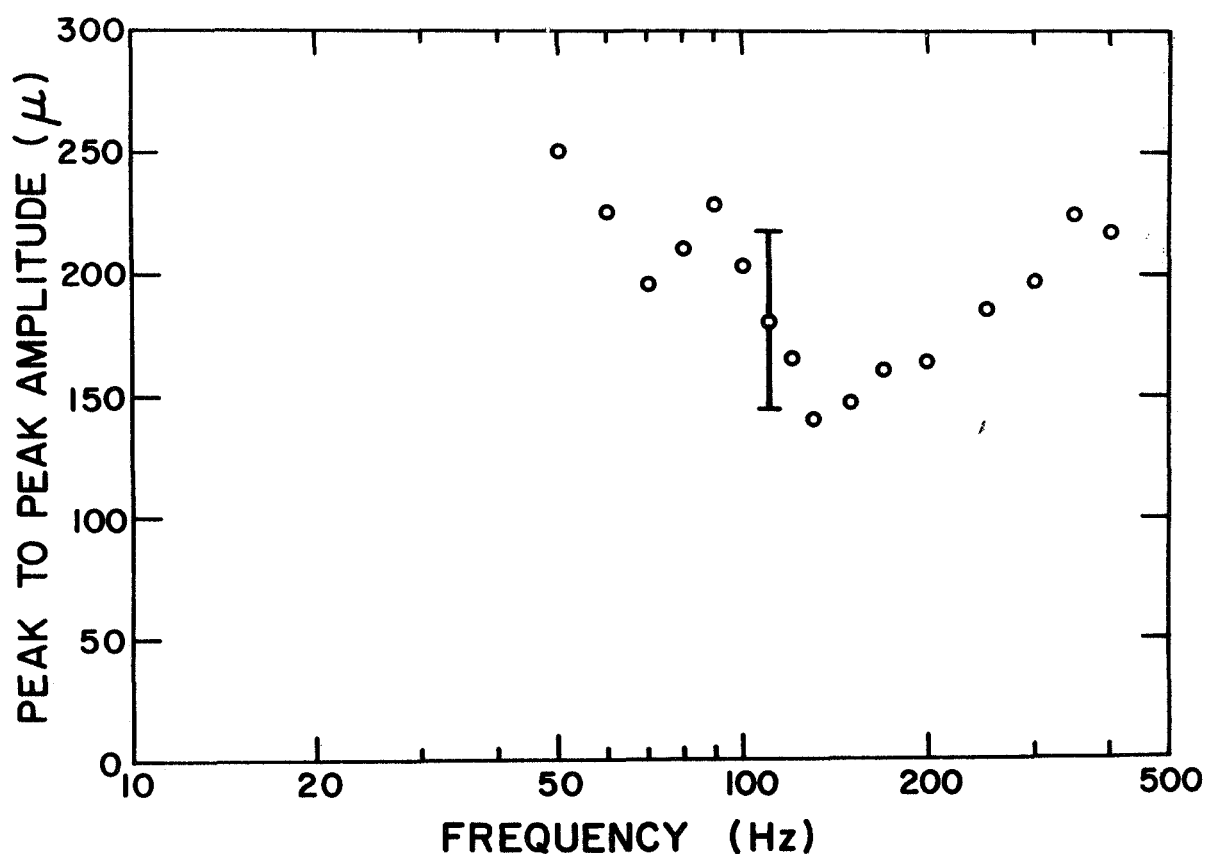
FIGURE 5: Amplitude of vibration of the unloaded driver piston as a function of frequency. The amplitudes were measured optically, and each point represents the mean of 3 determinations. The range bars indicate the largest mean deviation about the mean obtained in the series.
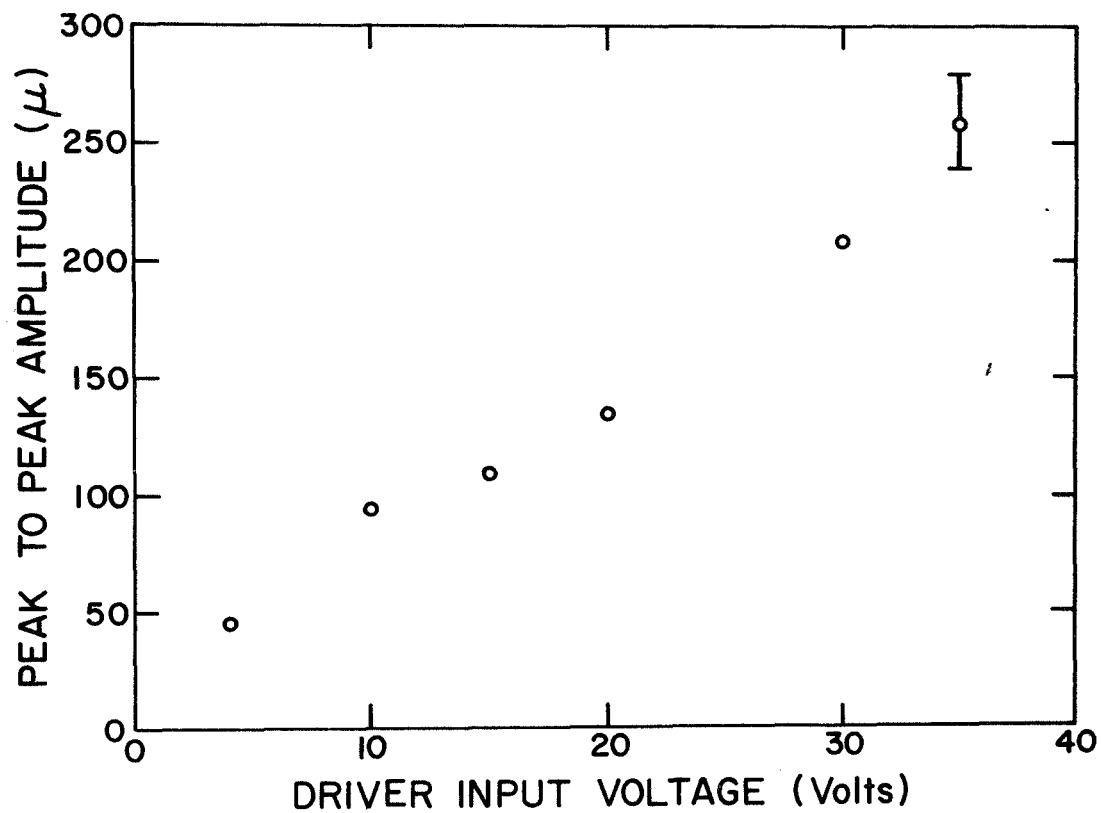
FIGURE 6: Amplitude of vibration of the unloaded piston as a
function of input voltage (peak to peak) at 300 Hz. Each point
represents the mean of 3 determinations. The range bars indicate
the largest mean deviation about the mean obtained in the series.
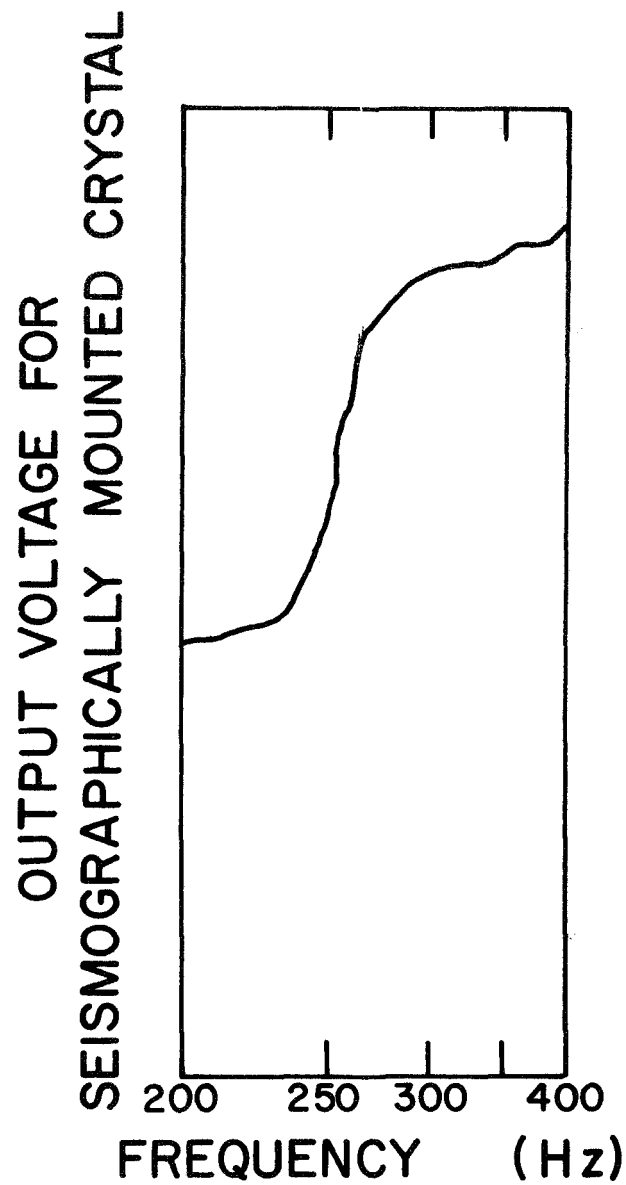
FIGURE 7: Relative output voltage of the crystal pickup as a function of frequency when the crystal is seismographically mounted on the driver piston. Note the difference between this spectrum and the one shown in Figure 3.

In Vivo Determination of the Elastic Properties of Bone

II. Resolution and Precision of the Ulnar

Resonant Frequency Determination

John M. Jurist, Ph.D.
Department of Radiology
University of Wisconsin Medical Center
Madison, Wisconsin

1. Introduction

A preceding paper (Jurist 1969) reported a method of in vivo measurement of ulnar frequency. This paper reports the reproducibility of the technique.

Resonance of the ulna, or any other long bone, may be modeled on the fundamental equation describing a vibrating bar: $F_o L = KC$. In this equation, F_o is the ulnar resonant frequency, L is the ulnar length, C is the speed of sound through the ulna, and K is a proportionality constant dependent on boundary conditions and mode of vibration. Since elasticity (Y) is a function of density (ρ) and the speed of sound ($Y = c^2\rho$), relative ulnar elasticity may be estimated from measurement of F_o and L if K is constant ($Y \propto (F_o L)^2$).

The resonant frequency of the ulna is obtained from measurement of response at the styloid process to vibration applied at the elbow (over the olecranon process). Because of damping, the excitation frequency at which the amplitude response is largest (F_a) is slightly less than the true resonant frequency (F_o). The difference between F_a and F_o, however, is so small that it can usually be neglected.

The reproducibility of the F_a measurement was tested in 2

ways. First, repeated determinations of F_a were made by tuning

the driving oscillator to maximum response. Second, repeated

determinations of F_a were made by recording the response of the

ulna as a function of frequency. During the tests, the forearms

were carefully repositioned in an attempt to keep the mode of

vibration constant. In the first case, the standard deviation

of F_a was about 3%. In the second case, a standard deviation

of about 2% was obtained. Table 1 presents these data in more

detail.

Since the length L of the ulna may be measured with a

precision of approximately 1-2%, the product $F_a L$ has a precision

of 5% or less. Because biological variations are so large, a

precision of 5% is acceptable for comparison of $F_a L$ values of

different subjects. In order to consider changes in elasticity

in the same subject, the length of the ulna may be assumed to be

constant and F_a measurements may be directly compared.

2. Variation of K with Arm Position and Muscle Tension

To determine the effect of repositioning on F_a (which would

alter K), F_a was measured 6-10 times for 2 subjects while the

orientations of their forearms were varied. The standard arm

position was illustrated in the first paper. With maximal wrist supination, K changed in such a way that F_a was increased by about 20%. Maximal volar flexion of the hand reduced F_a by about 10%, while maximal dorsiflexion reduced F_a by about 15%.

Since older subjects measured in a clinical study exhibited varying degrees of muscle spasm as sequelae to strokes, F_a was measured for the 2 experimental subjects with their forearms in the relaxed state and then during maximum gripping effort. Muscle tension increased F_a by about 5%. These findings underscore the importance of forearm positioning and degree of muscle relaxation in determining K.

3. Precision of the F_a Determination

A simple spring-mass-dashpot model may be used for estimation of the precision of the F_a measurement as a function of resonance peak width. For a given uncertainty in amplitude, (ΔA), there exists a corresponding uncertainty in F_a (ΔF_a) (Figure 1). The width of the resonance peak may be formally described in terms of Q_a, where $Q_a = F_a/(F_{2a}-F_{1a})$. As shown in Figure 2, F_{1a} and F_{2a} are the frequencies at which the amplitude response at the styloid process falls to $1/\sqrt{2}$ of its value at F_a. Figure 3 shows the

calculated precision of F_a as a function of amplitude resolution

for various Q_a. For a typical Q_a of 3 and an amplitude resolution

of 2%, the precision of the F_a determination is about 3%. Note

that this is roughly the same value as the standard deviation of

repeated determinations reported in Table 1.

The uncertainty in F_a may be reduced by taking the mean of

repeated measurements. This approach to improving the F_a

determination was tested by recording, at 30 minute intervals,

6 sets of 6 response spectra each from the same subject. Between

spectral recordings, the elbow of the subject was removed from

the driver, but the crystal pickup remained attached to the wrist.

Between each set of 6 spectra, the subject was completely removed

from the apparatus and allowed to rest. Table 2 shows that

although the standard deviation of the individual F_a determinations

was about 2% of the mean value, the standard deviation of the

mean F_a values calculated from each set of 6 recordings was less

than 1%. Since each response spectrum may be recorded in about

15 seconds, averaging several F_a determinations for each subject

is practical.

4. <u>Second Order Correction for</u> F_a

As discussed previously, the frequency of maximum amplitude

response, F_a, is only approximately equal to the resonant

frequency, F_o. Figure 4 shows the correction (D) which must

be applied to F_a as a function of Q_a. Note that, for typical

Q_a of 2.5-3.5, F_a is only 2-4% smaller than F_o. Thus, correction

for the effects of muscle damping, etc. may be made, but these

corrections are of the same order of magnitude as the precision

of F_a. In the experiment which investigated changes in F_a with

muscle tension, Q_a was found to decrease with maximal gripping

effort by about 15% from a resting value of about 2.7.

5. Discussion and Conclusions

The short-term reproducibility or precision of the F_a

determination for normal subjects as reported in this paper

compares favorably with that of the monoenergetic photon

absorptiometry technique of bone mineral measurement (about

2-4% as compared to 1-2%) as reported by Cameron, Mazess, and

Sorenson (1968).

Because the ulna may vibrate in several modes, the simple

damped oscillator model, used to predict the F_a determination

precision and second order correction for finite Q_a, is

inadequate for completely simulating the vibrating ulna.

However, behavior of the ulna when near resonance is similar
to that of a simple damped oscillator. After assigning
reasonable values for Q_a and the amplitude measurement resolution,
this model predicts F_a precision of the same order of magnitude
as found experimentally. Thus, the precision of <u>single</u> F_a
measurements is unlikely to improve over the reported value of
2-4% unless precision of the amplitude measurement is markedly
improved.

Abrams (1968), in a study of fresh and embalmed pig
forelimbs and an embalmed cadaver arm, found embalming to increase
the resonant frequency by a factor of 2 and increase damping by a
factor of 4.5. The embalmed cadaver arm exhibited ulnar
resonances of 65 Hz and 500 Hz. If the embalming process is
assumed to double F_o in the human, it is possible that ulnar
resonance data presented in this series of reports resulted from
measurement of the first overtone and not the fundamental
ulnar resonance. An alternative, and more likely, interpretation
is that the lower resonance reported by Abrams resulted from
interactions of the ulna with the humerus. It should be noted
that accepted bone elasticity and density values predict a
fundamental transverse ulnar resonance of about 230 Hz (Jurist 1969).

6. Acknowledgments

Summary

The reproducibility of the F_a measurement was studied,
and various factors which affect F_a were investigated. The
standard deviation of repeated F_a determinations was found to
be 2-4% in 3 subjects. The precision of F_a was increased by
taking the mean of several measurements. Wrist supination,
volar flexion and dorsiflexion of the hand, and gripping effort
changed F_a by up to about 20% relative to the F_a measurement
under normal conditions by altering boundary conditions (K).
Gripping effort reduced Q_a by about 15% from the resting values
in 2 subjects.

References

1. ABRAMS, C. F., Jr., 1968, A Study of the Transmission of High Frequency Vibration in the Human Arm, M.S. Thesis (Raleigh, North Carolina: North Carolina State University at Raleigh).

2. CAMERON, J. R., MAZESS, R. B., and SORENSON, J. A., 1968, Investigative Radiology, 3:141.

3. JURIST, J. M., 1969, In vivo determination of the elastic properties of bone. I. Theory, apparatus, and method of ulnar resonant frequency determination, Physics in Medicine and Biology, in press.

4. KINSLER, L. E., and FREY, A. R., 1950, Fundamentals of Acoustics (New York: John Wiley & Sons, Inc.), Chaps. 1-3.

Table 1

Reproducibility of the F_a Measurement[*]

Subject	$\overline{F}_a$ (Hz)	σF_a (Hz)	σF_a (%)	N
1	266.4	8.8	3.3	21
2	279.7	8.4	3.0	20
3	298.2	5.8	1.9	36

[*]The F_a for Subjects 1 and 2 were measured at daily intervals by tuning the oscillator to maximum response. The F_a for Subject 3 were obtained by recording the ulnar response as a function of frequency.

Table 2

Increased $\overline{F}_a$ Precision Obtained by Calculating
the Mean of Several Determinations

Set[*]	$\overline{F}_a$ (Hz)	σF_a (Hz)	σF_a (%)
1	294.5	5.4	1.83
2	300.0	3.3	1.10
3	299.0	3.1	1.04
4	300.0	6.9	2.29
5	296.7	5.8	1.96
6	299.0	8.8	2.94
1-6	298.2[**]	2.2	0.73
---	298.2	5.8[***]	1.95

[*]Each set consisted of 6 F_a determinations.

[**]Mean and standard deviation of the $\overline{F}_a$ for each set.

[***]Standard deviation of the 36 individual F_a determinations.
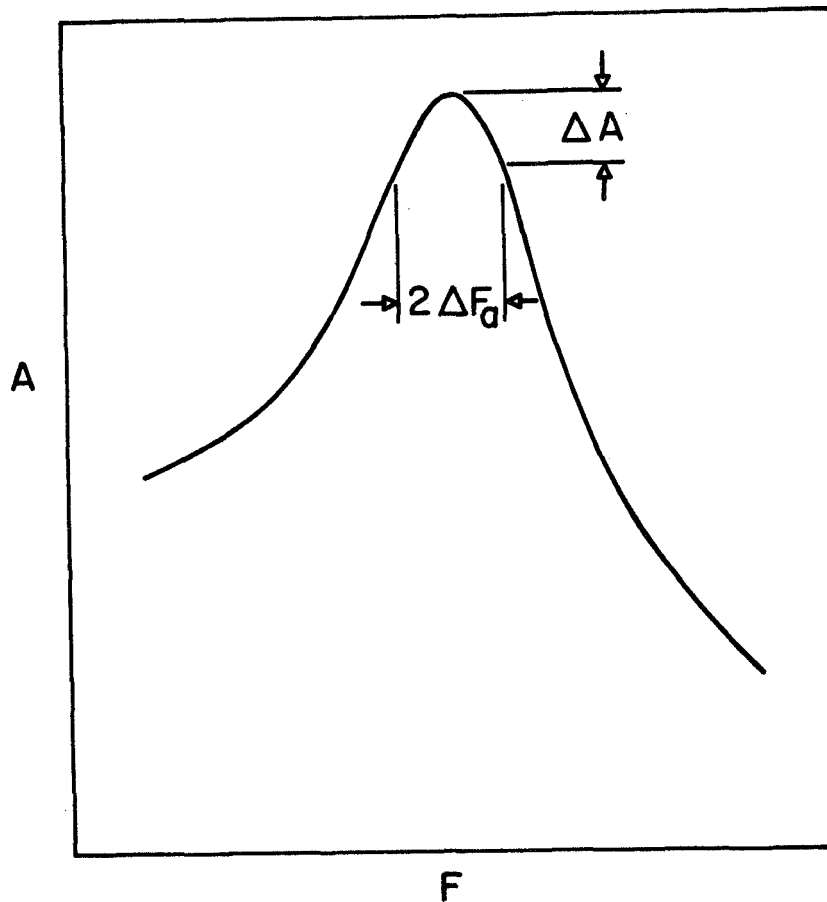
FIGURE 1: Uncertainty (ΔF_a) in the determination of the frequency of maximum amplitude response (F_a) associated with a given resolution (ΔA) in the amplitude response (A) of the ulna.
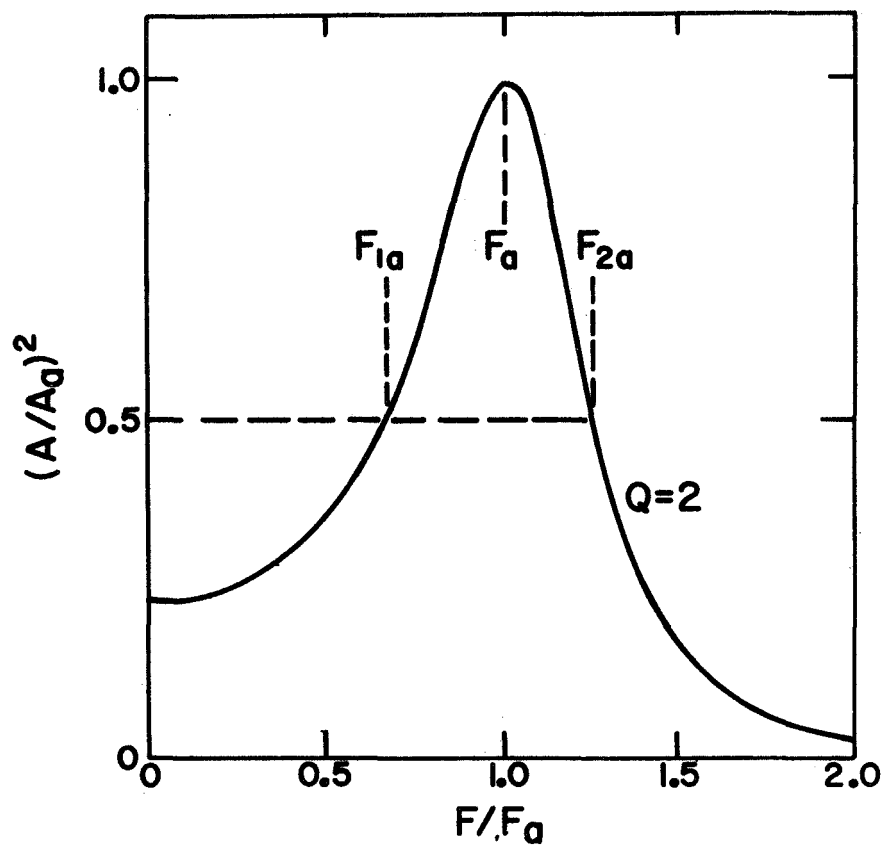
FIGURE 2: Width of a resonance peak. The frequencies F_{1a} and F_{2a} are those for which the vibrational amplitude is $1/\sqrt{2}$ of its value at F_a.
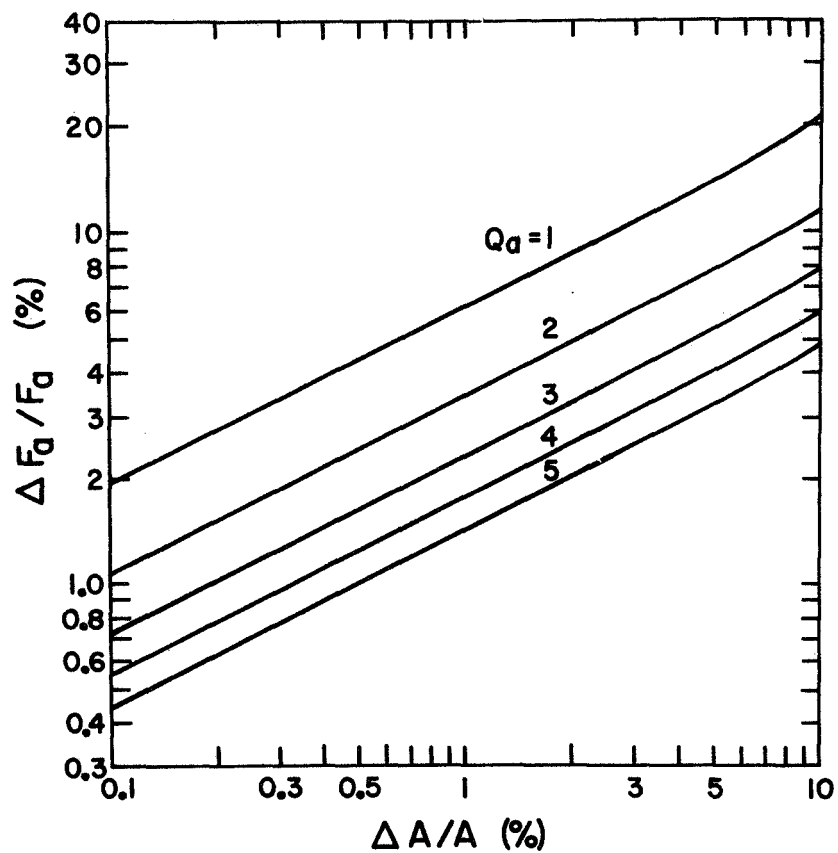
FIGURE 3: Precision of the F_a determination as a function of the amplitude resolution ($\Delta A/A$) and the resonance peak width (Q_a). These data are obtained from a simple damped oscillator model (Kinsler and Frey 1950).
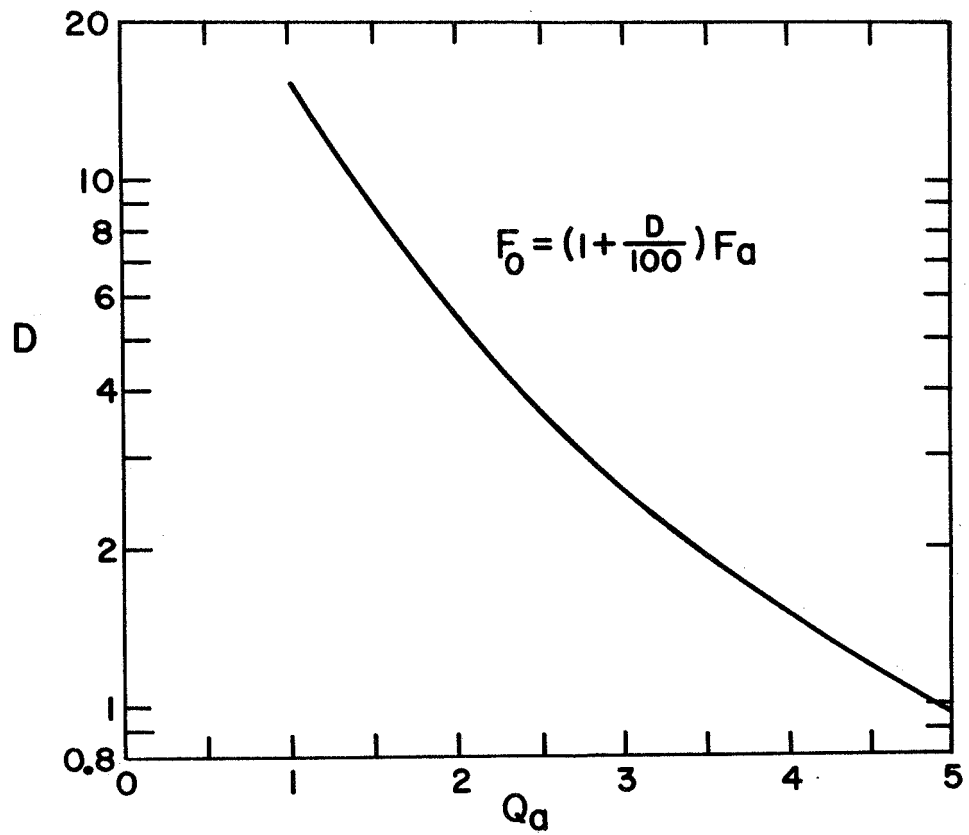
FIGURE 4: Difference (D), expressed as a percentage, between F_o and F_a as a function of Q_a (Kinsler and Frey 1950).

In Vivo Determination of the Elastic Properties of Bone

III. Ulnar Resonant Frequency in Osteoporotic,

Diabetic, and Normal Subjects

John M. Jurist, Ph.D.
Department of Radiology
University of Wisconsin Medical Center
Madison, Wisconsin

1. Introduction

Mather (1967) reported the relationship between bone elasticity and breaking strength. Previous papers in this series (Jurist 1969a, 1969b) described the in vivo estimation of bone elasticity by measurement of ulnar resonance. Measuring resonance of the ulna may therefore provide an indication of bone quality. The product of resonant frequency (F_o) and length (L) of the ulna is proportional to the speed of sound in the ulna. However, the speed of sound is proportional to the square root of elasticity for a given density. Hence, $F_o L$ is a measure of the bone elasticity and should provide an indication of relative skeletal strength or quality.

The resonant frequency is, to within a few percent, equal to the frequency of maximum amplitude response, F_a. Experimentally, F_a may be obtained by recording the amplitude response of the styloid process as a function of driving frequency for excitation applied to the elbow (olecranon process).

2. Materials and Methods

$F_a L$ was measured for 437 clinically normal subjects (ages 6-89

years) and for 28 osteoporotic women (mean age 74 years). The osteoporotic women were age-matched with normal controls. In addition, F_aL was measured for 15 diabetic women (mean age 74 years) who were also age-matched with normal women.

Normal subjects were those without any overt evidence of osteoporosis, and no history of prolonged corticosteroid therapy or immobilization for more than 2 months. Osteoporotic subjects were those with a history of recent vertebral collapse or fracture of the femoral neck with little or no associated trauma. In addition, any osteoporotic subjects with any form of malignancy were excluded from the study. Diabetic subjects were included in the study because diabetes has been reported to be associated with a relatively high incidence of osteoporosis (Boulet and Mirouze 1954).

3. Results

3.1 Normal Subjects

Figures 1 and 2 show that F_aL increases from age 6 to about 15-20 years, and then decreases. The decrease after about 20 years of age occurs at a relatively constant rate in men until

at least 80 years. The F_aL of women decreases in the interval 25-55 years at roughly the same rate as for men. After 55 years, however, F_aL decreases very rapidly (about 1%/year) in women.

The increase in F_aL before adulthood is almost exclusively secondary to growth increasing L in this period (Figures 3 and 4). After adulthood, of course, L is essentially constant. The slight decrease in L with advancing age shown in Figures 3 and 4 probably reflects the smaller stature of subjects born in the Nineteenth Century, and does not, in all likelihood, represent any "shrinkage" with increasing age.*

Figure 5 shows that F_a appears to be relatively constant for 6-12 year old boys, and then decreases steadily. The F_a values for females decrease steadily from age 6 to about 55 years, after which F_a decreases even more markedly (Figure 6).

3.2 Osteoporotic and Diabetic Subjects

Table 1 shows that the mean F_aL for 28 osteoporotic women

---

*The decrease in height often seen with advancing age is the result of increased spinal curvature, vertebral collapse, and inter-vertebral disc degeneration.

is significantly (at the 0.1% level) lower (about 44%) than the mean F_aL of 28 age-matched normal controls. Likewise, the F_aL of diabetic women appears to be about 25% lower than the F_aL of normal women of the same ages. This difference is significant at the 2-5% level.

Tables 1 and 2 show that only about 18% of the osteoporotic subjects have F_aL values greater than 3055 Hz-cm. Similarly, only 18% of the normal subjects have F_aL values less than 3055 Hz-cm. Thus, the osteoporotic women and their age-matched controls could be discriminated with an effectiveness of 82% on the basis of their F_aL values.

3.3 F_aL Distributions

An interesting feature of the distribution of F_aL of women aged 46 or more who are categorized as normal is shown in Figure 7. Note that this distribution is bimodal. The F_aL distributions for normal men or younger normal women, however, were not bimodal. Figure 8, a cumulative distribution of the F_aL distribution for women 46 or more years old, clearly shows that two populations are included in the distribution.

4. Discussion

At present, there is some controversy over whether or not osteoporosis is part of the normal aging process in women. Many investigators believe that bone loss is physiologic and, therefore, not a disease or metabolic error (Garn, Rohmann, and Nolan 1964; Garn, Rohmann, and Wagner 1967). Other investigators, however, argue that bone loss sufficiently severe to lead to spontaneous fractures is abnormal (Urist 1960; Urist, MacDonald, Moss, and Skoog 1963; Vincent and Urist 1961). These authors, however, concede a certain amount of bone loss to accompany aging. The etiological agents involved in development of "pathological" osteoporosis are not well understood, but endocrine disorders, inactivity and associated reduction of skeletal stress, dietary deficiency or malabsorption of calcium have been suggested as factors (Fraser 1962; Nordin 1962; Urist 1960).

Indirect evidence for osteoporosis being a definite abnormality has been presented by Urist et al. (1963), and by Vincent and Urist (1961), but no direct evidence for this contention has been published. The bimodal F_aL distribution shown in Figure 7, however, suggests that there are two, or possibly more, types of bone metabolism in women after the age of about 45 years. For the

first type (Group I in Figure 9), F_aL decreases at about the same

rate after age 45* as it does for men. For the second type (Group

II in Figure 9), F_aL decreases very rapidly after age 45. These

women are future osteoporotics although they have been defined as

clinically "normal" because they have exhibited no independent

evidence of osteoporosis. Figure 7 suggests that about 35% of the

randomly selected population of "normal" women over the age of

45 years fit into the Group II or future osteoporotic category.

Confirmation of this finding awaits results of long-term longitudinal

studies which allow determination of individual rates of skeletal

change.

The observation that about 82% of the osteoporotic women

were discriminated from their age-matched normal controls by

their ulnar F_aL values alone suggests that measurement of F_aL is

of great potential value in screening programs for detecting

---

*The data on which this interpretation is based show only the
separation into two populations after the age of 45. An
association between the menopause and this separation into two
populations is implied, but is not established by the investigation.
The term postmenopausal osteoporosis might be a fallacy caused
by post hoc reasoning.

osteoporosis. Further studies which quantitatively relate strength of the axial skeleton to elasticity and bone mineral content of the appendicular skeleton are now in progress.

The 25% difference between the mean F_aL values of diabetic women and their age-matched controls suggests that, as reported by Boulet and Mirouze (1954), there is indeed an association between diabetes and an increased incidence of osteoporosis.

The simplicity and precision (Jurist 1969b) of the technique for F_aL determination suggests its value for long-term studies of changes in skeletal status.

5. Conclusions

Measurement of F_aL in large numbers of human subjects has allowed establishment of normal values of this parameter as a function of age and sex. The F_aL distribution for clinically normal women more than 45 years of age suggests that about 35% of these women may be developing osteoporosis. Measurement of ulnar F_aL has shown about 82% discrimination of women with symptomatic osteoporosis (fracture of the femoral neck and/or vertebral collapse) from their age-matched normal controls. The

F_aL of women with symptomatic osteoporosis is about 44% lower than that of normal women. Diabetic women have F_aL values which lie between those of normal subjects and patients with symptomatic osteoporosis. Measurement of ulnar F_aL is a promising approach to following development of osteoporosis in aging or immobilized populations on a long-term basis.

6. <u>Acknowledgments</u>

Summary

The product of ulnar resonant frequency and length (F_aL) was measured for 172 normal men, 265 normal women, and for 28 osteoporotic and 15 diabetic women. F_aL was shown to increase for subjects of age 6-20 years and then decrease after about 25 years. After age 55, F_aL of women decreases rapidly (about 1%/year). The distribution of F_aL for randomly selected clinically normal women more than 45 years old is bimodal with about 35% of these subjects in the lower F_aL group. This suggests that rapid bone loss is not a universal phenomenon; the so-called senile or postmenopausal osteoporosis appears to be an abnormality and not a normal concomitant of the aging process. Women with symptomatic osteoporosis have F_aL values averaging about 44% less than those of age-matched controls, while diabetic women have F_aL values between these two extremes. Measurement of ulnar F_aL allows 82% successful discrimination of women with osteoporosis from their age-matched controls. Determination of F_aL offers a promising approach to evaluation of skeletal status and following skeletal changes with immobilization or increasing age.

References

1. BOULET, P. and MIROUZE, J., 1954, Annals of Medicine, 55:674.

2. FRASER, R., 1962, The Journal of Bone and Joint Surgery,
   44B:485.

3. GARN, S., ROHMANN, C., and NOLAN, P., 1964, in Relations of
   Development and Aging (Springfield, Illinois: Charles C
   Thomas), p. 41.

4. GARN, S., ROHMANN, C., and WAGNER, B., 1967, Federation
   Proceedings, 26:1729.

5. JURIST, J. M., 1969a, In vivo determination of the elastic
   properties of bone. I. Theory, apparatus, and method of
   ulnar resonant frequency determination, Physics in Medicine
   and Biology, in press.

6. JURIST, J. M., 1969b, In vivo determination of the elastic
   properties of bone. II. Resolution and precision of the ulnar
   resonant frequency determination, Physics in Medicine and
   Biology, in press.

7. MATHER, B. S., 1967, Aerospace Medicine, 38:1270.

8. NORDIN, B. E. C., 1962, The American Journal of Clinical Nutrition, 10:384.

9. URIST, M. R., 1960, in Bone as a Tissue (New York: McGraw-Hill Book Company), p. 18.

10. URIST, M. R., MacDONALD, N. S., MOSS, M. J., and SKOOG, W. A., 1963, in Mechanisms of Hard Tissue Destruction (Washington, D.C.: American Association for the Advancement of Science), p. 385.

11. VINCENT, P. J. and URIST, M. R., 1961, Clinical Orthopaedics and Related Research, 19:245.

Table 1

$F_a L$ in Postmenopausal Osteoporosis and Diabetes Mellitus

Group	$F_a L$ (Hz-cm) (mean±σ)	N (Pairs)	Age (yrs) (mean±σ)	Δ(%)*	Student's t value	Discriminant $F_a L$ (Hz-cm)**	δ(%)***
Osteoporotic ♀	2557± 852						
Age-matched normal ♀	4549±1622	28	74.0±8.9	44	5.76 (P<0.1%)	3055	18
Diabetic ♀	3042±1227						
Age-matched normal ♀	4072±1448	15	74.5±7.5	25	2.10 (P=2-5%)		

*
$$\Delta = \frac{F_a L(control) - F_a L(ill)}{F_a L(control)} \times 100\%$$

**Value of $F_a L$ which minimizes δ

***
$$\delta = \frac{N_{(ill)} \; \bar{c} \; F_a L \geq discriminant + N_{(control)} \; \bar{c} \; F_a L < discriminant}{N_{(ill)} + N_{(control)}} \times 100\%$$

Table 2

$F_a L$ Discriminant Analysis for 28 Postmenopausal

Osteoporotic and Age-Matched Control Pairs

(Mean Age = 74.0 yrs)

	Clinical Group	
	Control	Osteoporotic
$F_a L \geq 3055$ Hz-cm	23	5'
$F_a L < 3055$ Hz-cm	5	23
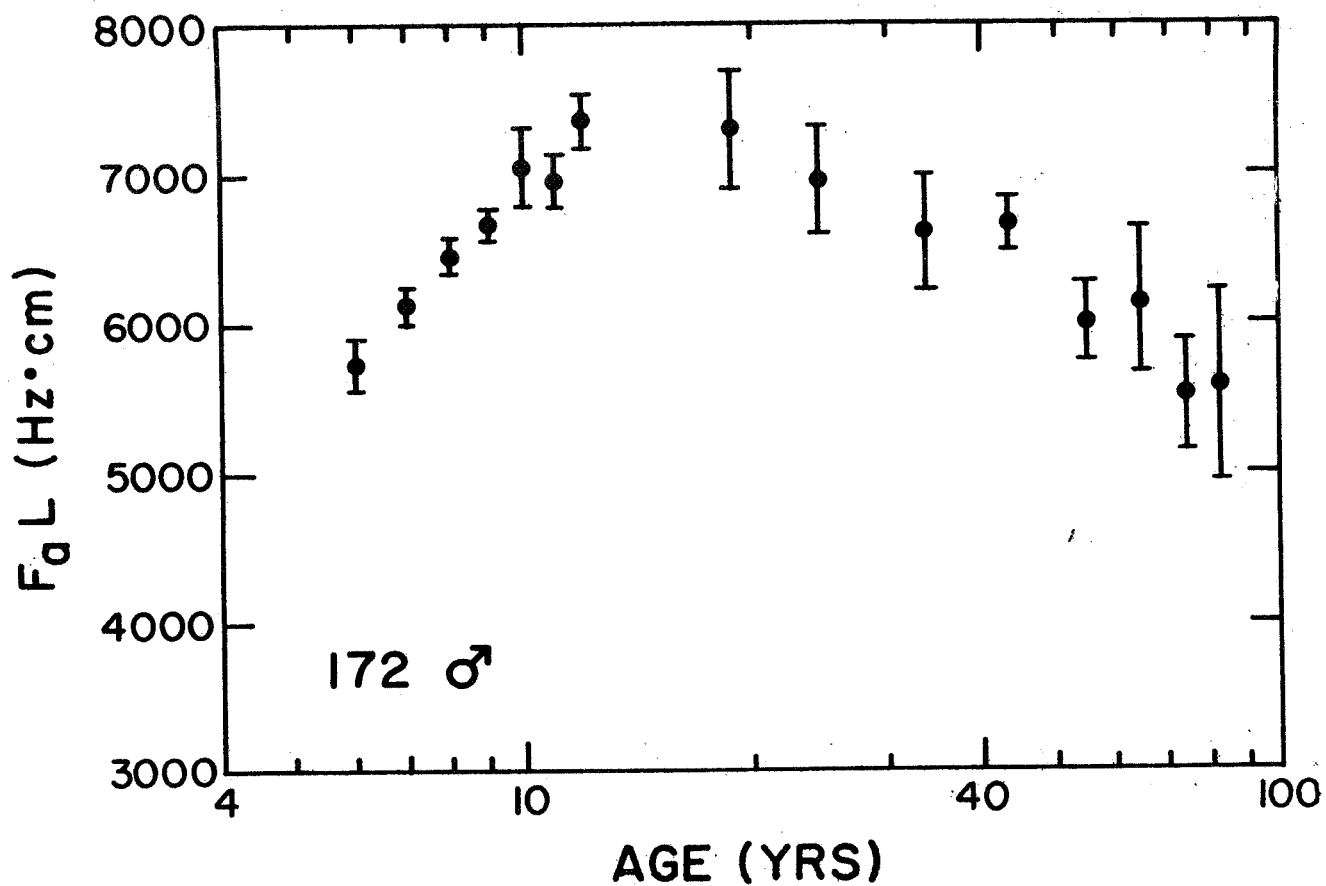
FIGURE 1: Product of ulnar length (L) and frequency of maximum amplitude response (F_a) vs. age for 172 normal males. As in the following 5 figures, the range bars enclose ±1 standard error of the mean for each age category. Age categories were 6, 7, 8, 9, 10, 11, 12, 13, 14, 15-16, 17-19, 20-29, 30-39, 40-49, 50-59, 60-69, 70-79, and 80-89 years.
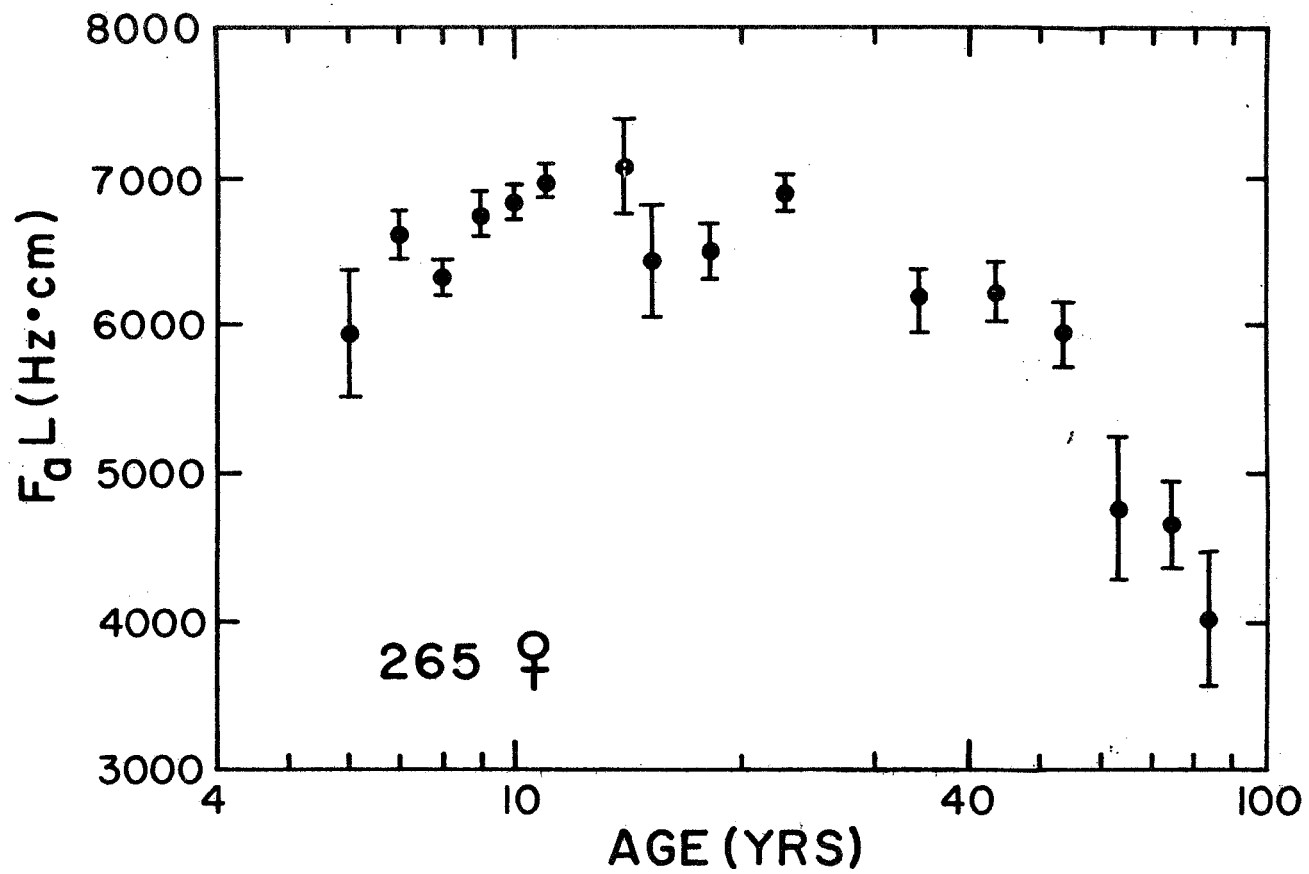
FIGURE 2: F_aL vs. age for 265 normal females.
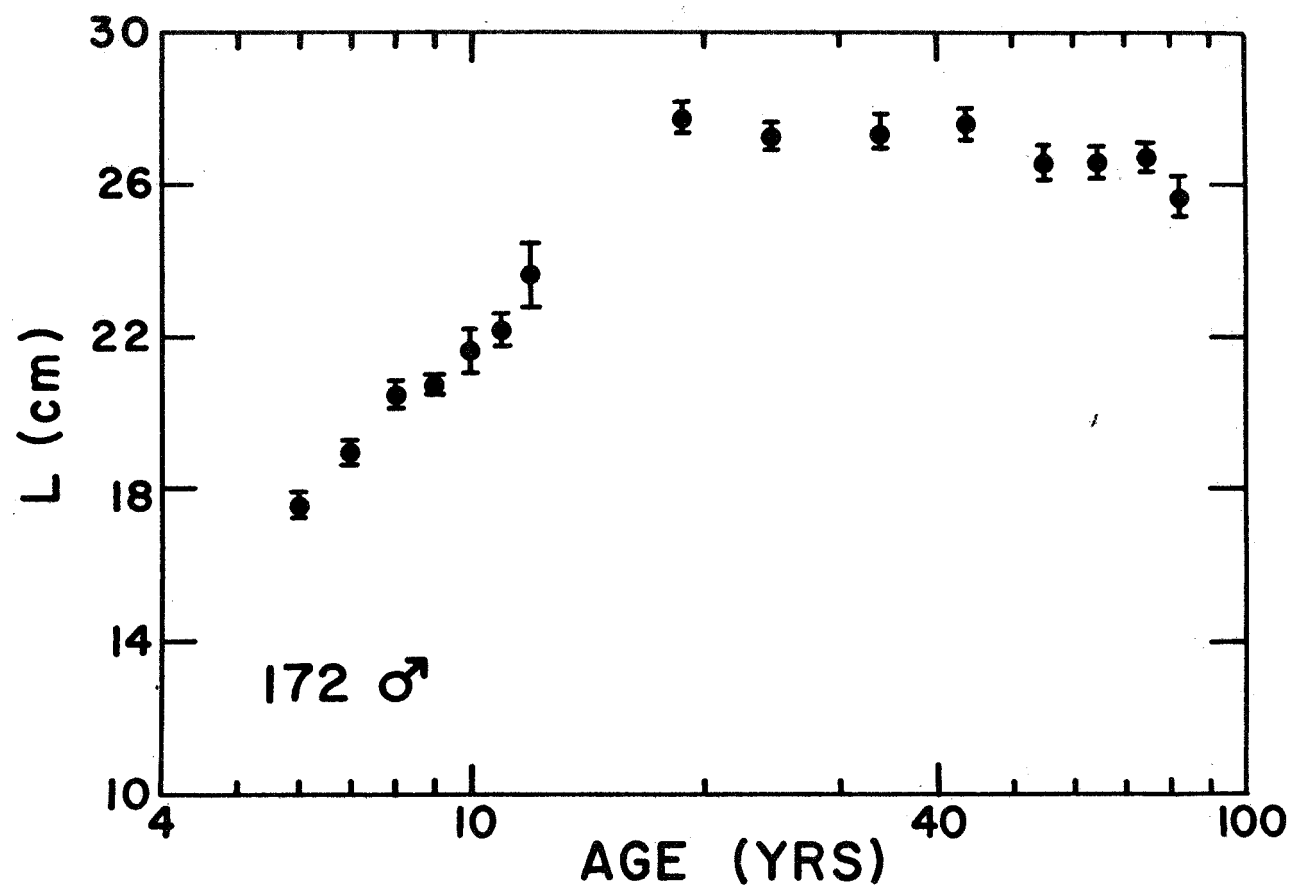
FIGURE 3: L vs. age for normal males.
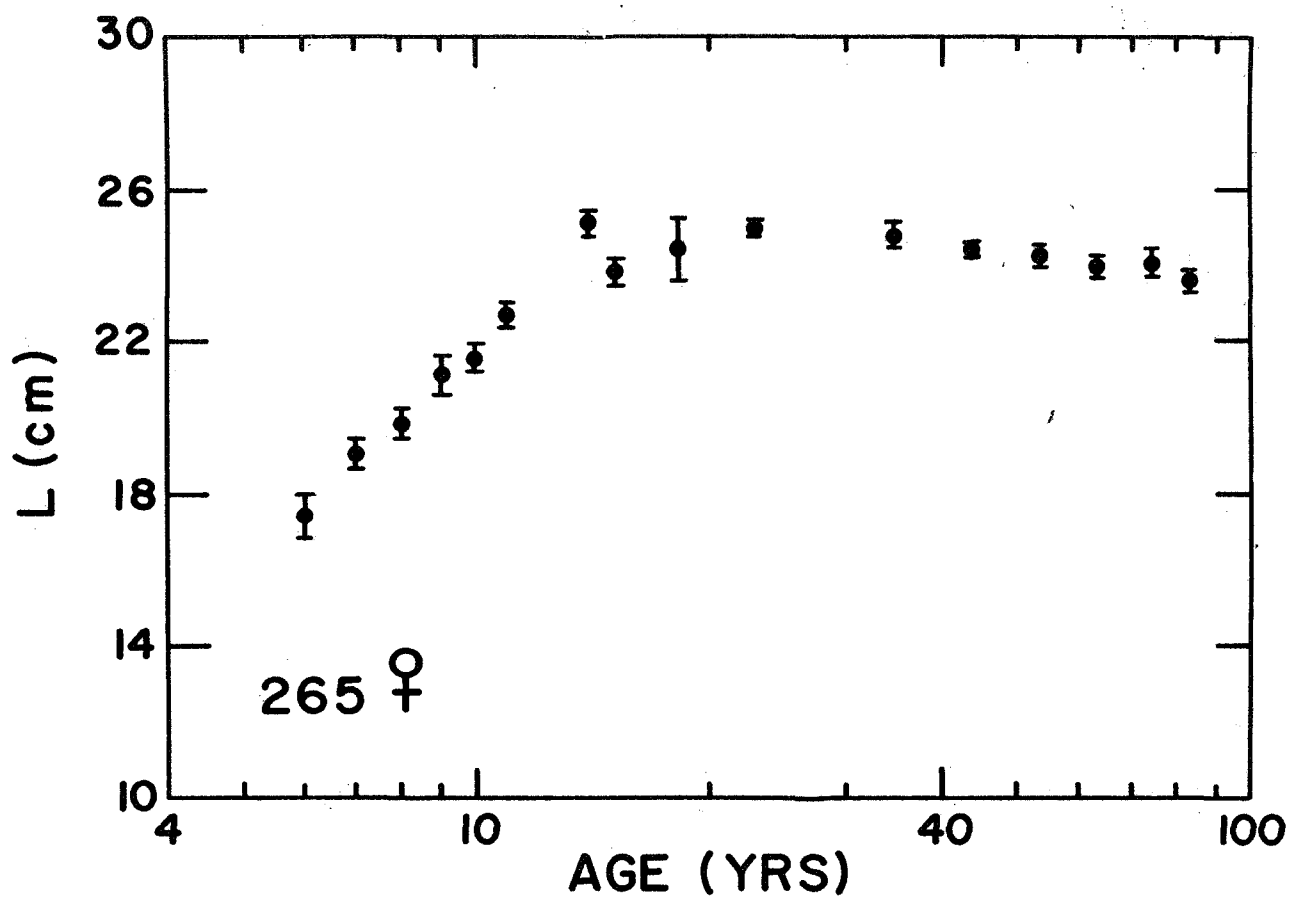
FIGURE 4: L vs. age for normal females.
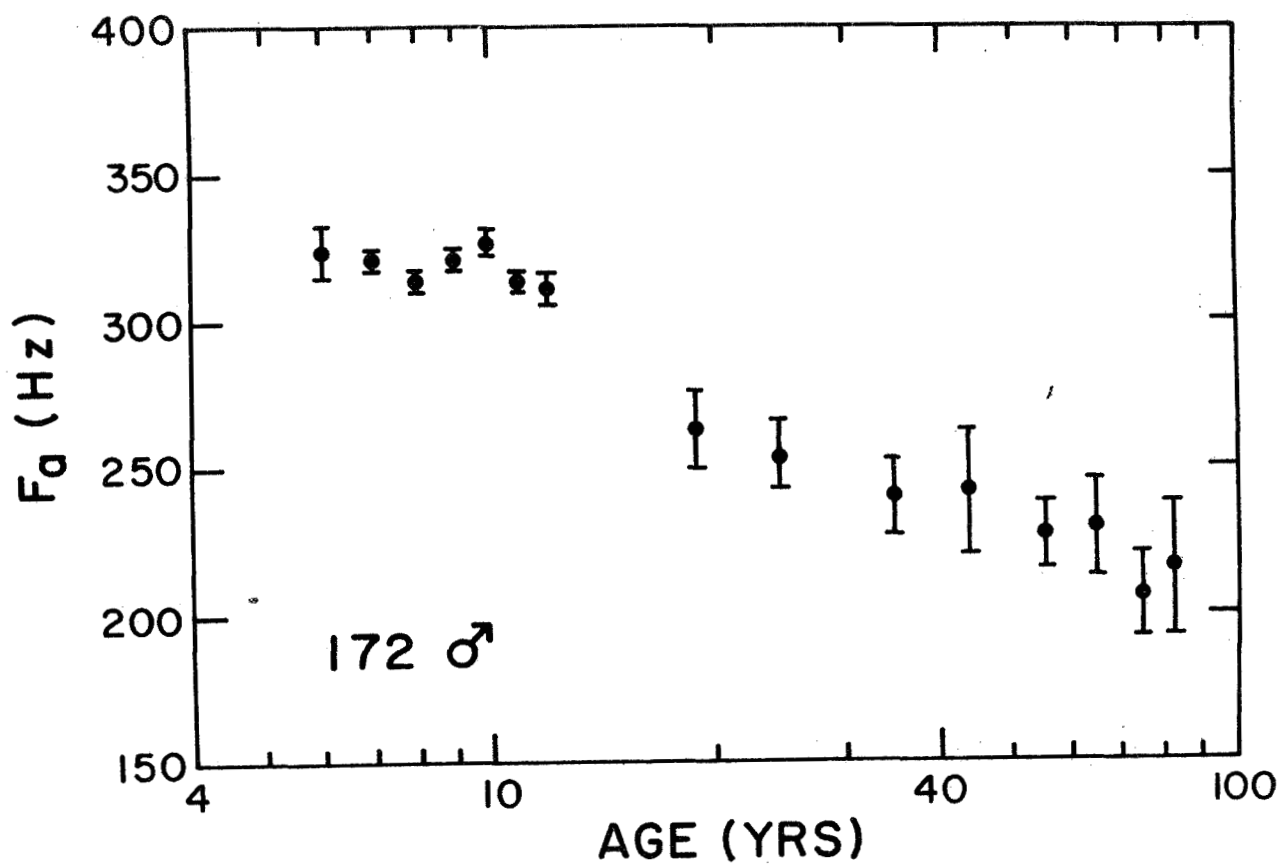
FIGURE 5: F_a vs. age for normal males.
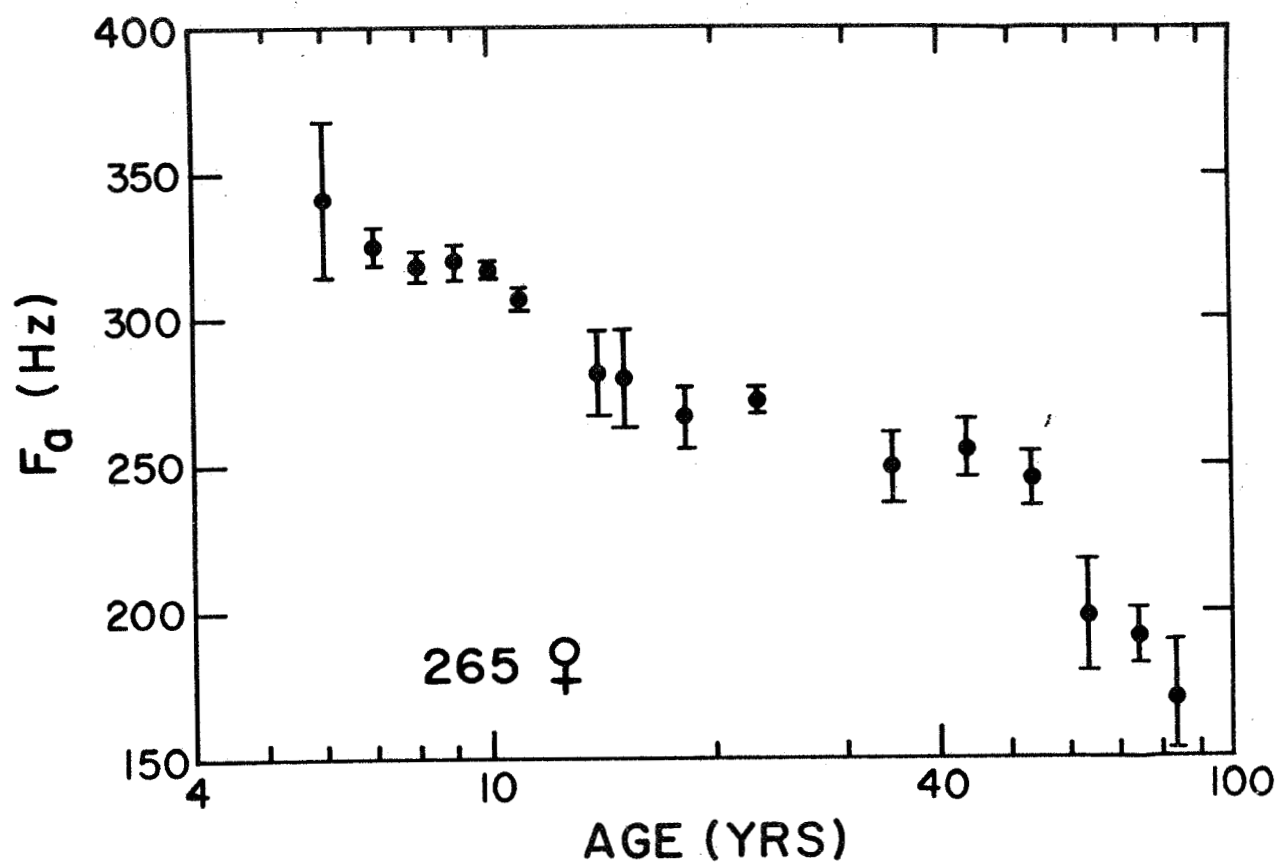
FIGURE 6: F_a vs. age for normal females.
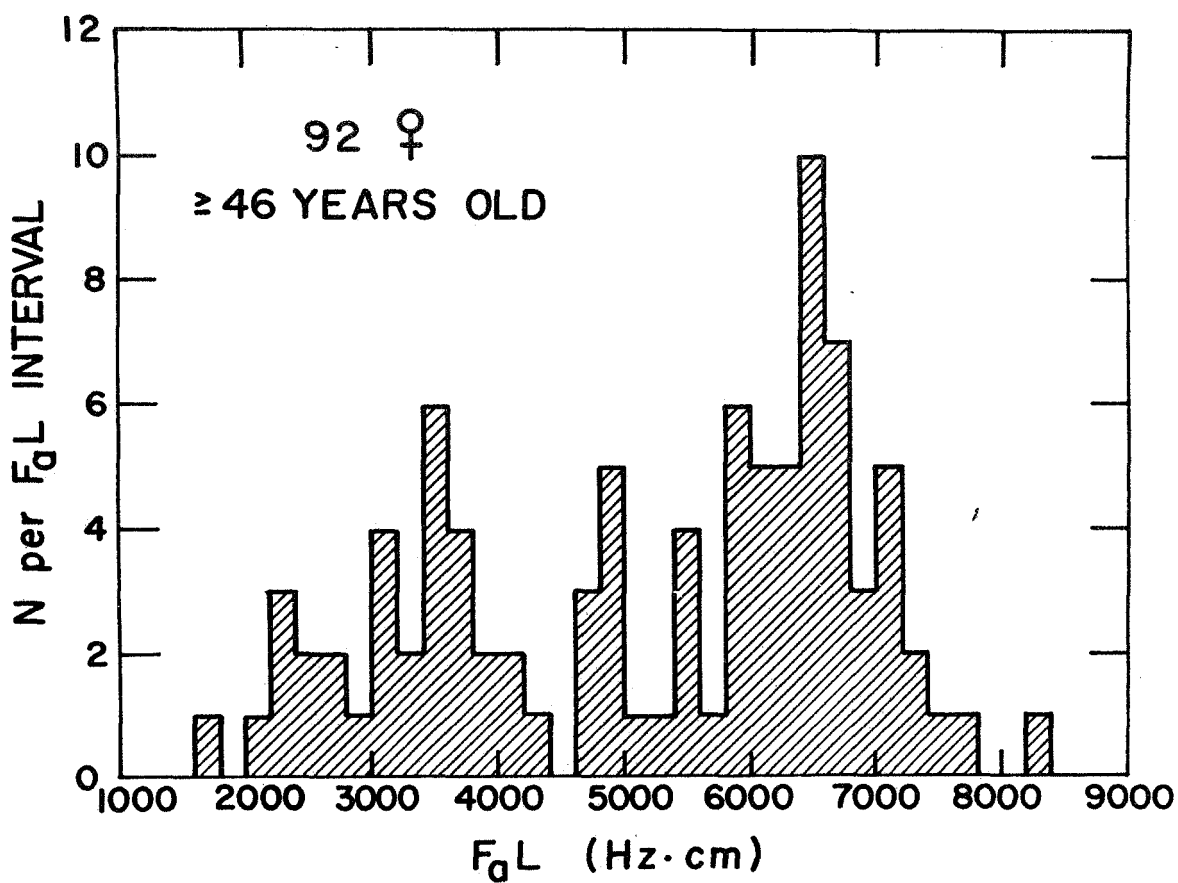
FIGURE 7: Distribution of $F_a L$ for 92 normal women more than 45 years old.
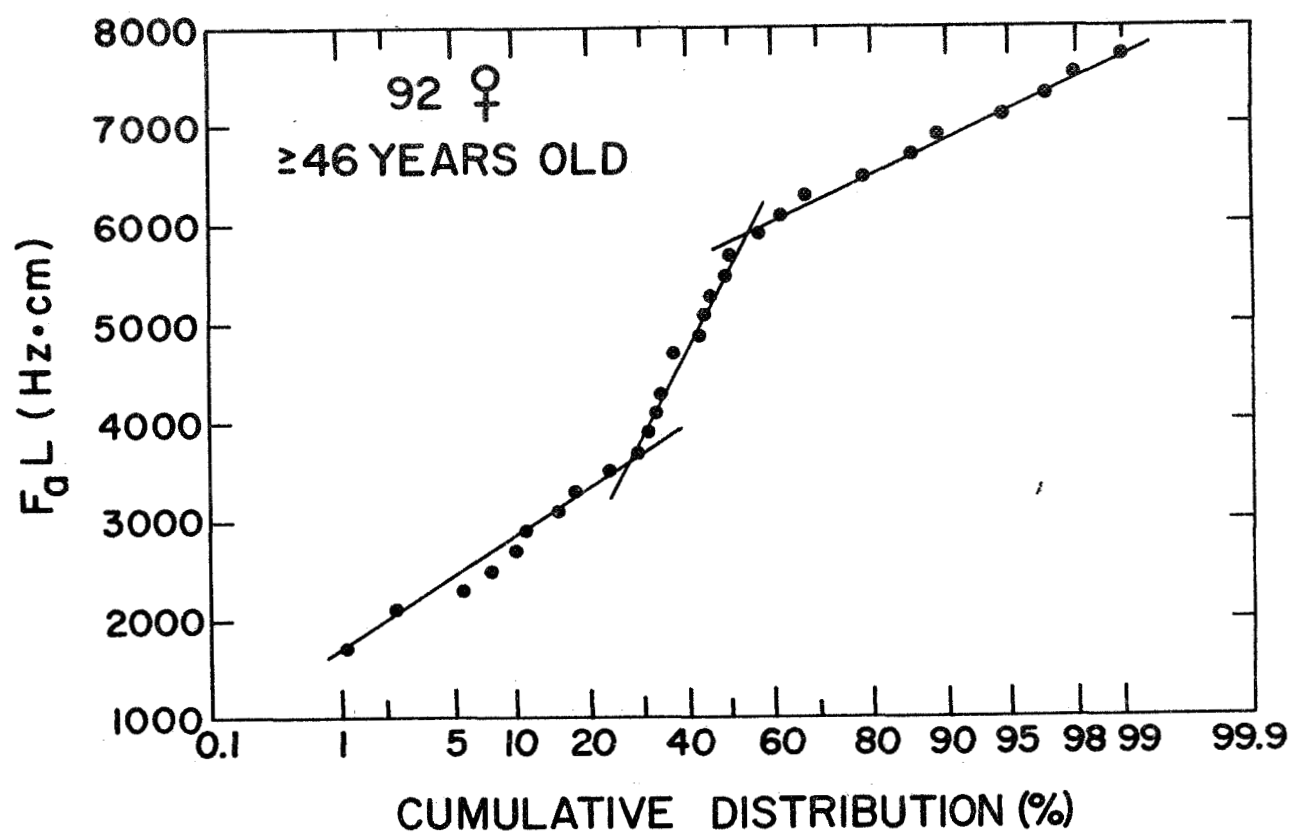
FIGURE 8: Cumulative distribution of F_aL for 92 normal women more than 45 years old.
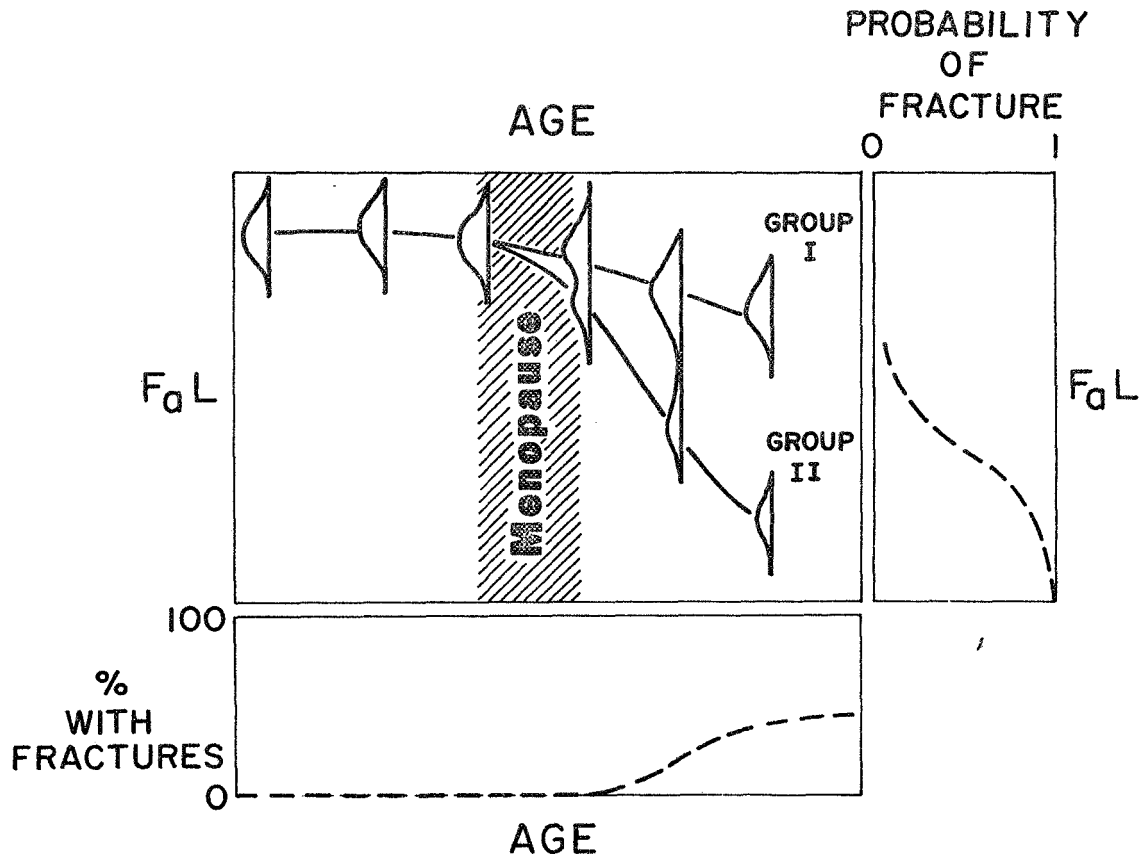
FIGURE 9: Schematic diagram illustrating a possible interpretation of data presented in this paper. With increasing age, the $F_a L$ of most (Group I) women decreases at a rate nearly equal to the rate of decrease for men. However, the $F_a L$ of about 35% of the women (Group II) decreases rapidly after about 45 years of age. One may speculate that this sudden bone loss for the Group II women is triggered by the relatively rapid cessation of gonadal activity which precedes the menopause. At lower $F_a L$ values, skeletal strength is low and spontaneous fractures occur. After the age of about 60 years, most of the Group II women have spontaneous fractures and are diagnosed as osteoporotic. If longitudinal study of large numbers of women permit early identification of those who belong in Group II, it may be possible to discover the various factors involved in osteoporosis.

In Vivo Measurement of Bone Quality

John M. Jurist, Ph.D.

John R. Cameron, Ph.D.

Department of Radiology

University of Wisconsin Medical Center

Madison, Wisconsin

1. Introduction

Various papers describing study of autopsy specimens have shown that the breaking strength of bone is related to the shape of the bone, its elasticity, and the age and sex of the donor[6]. Therefore, it might be useful to be able to measure bone elasticity in vivo as a means of predicting skeletal strength or quality. Since the speed of sound in a material is a function of elasticity and density, it is possible that measurement of the speed of sound in bone will allow estimation of bone elasticity.

Our laboratory, extending a study begun in 1965[3,4], is investigating measurement of the speed of sound in the calvarium, clavicle, mandible, tibia, and ulna. We are using the following approaches:

1. Timing the rate of mechanical impulse propagation along the bone.

2. Measurement of the phase shift per unit length of bone for fixed vibrational frequencies.

3. Measurement of the resonant frequency of the bone by recording amplitude response as a function of vibrational frequency.

4. Determination of the ringing frequency of the bone after

application of a short-duration impulse.

This paper will consider the latter two approaches to estimation of elasticity in the ulna.

2. Theory

A simple model, in which the ulna is treated as a vibrating bar, shows that $F_oL = KC$. In this equation, F_o is the resonant frequency and L is the length of the bar, C is the speed of sound through the material of the bar, and K is a constant of proportionality which depends on the mode of vibration, geometrical factors, and boundary conditions[5].

If transverse modes of vibration are considered, C is unchanged, but K then is a function of the shape of the bar and is much smaller than it is for longitudinal modes.

As an example, the ulna may be considered to be a cylindrical tube with an outside diameter equal to 5% of its length and an inside diameter of 3.3% of its length. We will assume the ends of the "ulna" to be attached to rigid supports by hinges. These hinges simulate the wrist and elbow joints. The proportionality factor K is then given by $K = 0.5N$ and $K = 0.5N^2\pi S/L$ for longitudinal and transverse modes of vibration, respectively. In

both cases, N is an integer. The shape factor, S, is the radius of gyration of the cross section of the tube about its diameter. For a tube with inside and outside diameters as listed above, $K = 0.0235N^2$ for transverse modes of vibration. Note that K is smaller for the fundamental transverse mode by a factor of 21 than for the fundamental longitudinal mode. If C is assumed to be 2880 m/sec[7], and L is assumed to be 30 cm, the model predicts fundamental transverse and longitudinal resonant frequencies of about 230 Hz and 4800 Hz, respectively.

It is recognized that the ulna is not a true cylinder, and the joints do not act as true hinges. In addition, the ulna is not symmetrical about its long axis. Thus, the K value for the fundamental transverse resonance may vary from the estimated value of 0.0235 and may even vary with the plane of vibration. However, the predicted transverse resonant frequency of 230 Hz is in reasonable agreement with experimentally determined values of 150-300 Hz for healthy subjects.

The relationship $F_o L = KC$ may be exploited to determine the elastic properties of the long bones because $C^2 = Y/\rho$, where Y is the average value of Young's modulus over the cross section of the bone, and ρ is the average density. The density term includes any muscle or connective tissues which may be coupled to the bone.

However, at the frequencies of interest, the coupling of soft tissues to bone is small; the effect of the presence of soft tissue may be considered to be on mass loading and damping only[10]. The ratio Y/ρ is identical to the ratio of Young's modulus integrated over the cross section of the bone to the linear density (mass per unit length) of the bone. Since the linear density of a long bone is proportional to the mineral content expressed in terms of mineral mass per unit length[2], the linear density may be estimated by monoenergetic photon absorptiometry[9]. If the shape and boundary conditions of the bone under consideration are assumed to be constant, then the vibrational mode is fixed and $(F_o L)^2$ is thus proportional to Y/ρ .

3. Measurement of Ulnar $F_o L$

The length L of the ulna is measured with an ordinary metric rule. Although $F_o L$ values of different subjects may be compared, the length of the bone may be assumed to be constant for measurements made on the same subject at different times. Thus, F_o measurements may be directly compared in order to consider changes in skeletal quality in the same subject.

3.1 Resonant Frequency Determination

The apparatus used to measure ulnar resonant frequency is shown in Figure 1. The same approach may be used to measure the tibial resonant frequency with minor modifications. The oscillator-amplifier combination powers the modified loudspeaker driver with a variable frequency signal. The response of the ulna to excitation at the olecranon process is monitored at the styloid process by means of a crystal pickup. A small instrumentation accelerometer makes a suitable pickup.

A response spectrum is obtained by scanning a frequency range and recording response as a function of frequency. The response spectrum may show the displacement amplitude, velocity amplitude, or acceleration amplitude depending on whether or not the accelerometer output is integrated twice, once, or used directly. The frequency of maximum displacement amplitude (F_x), velocity amplitude (F_v), or acceleration amplitude (F_a) may be obtained from the record. If the damping or frictional losses in the vibrating system are represented by the "quality factor" or Q, it can be shown that the resonant frequency (F_o) is given by:

$$F_o = F_x/\sqrt{1-1/2Q^2} \, , \quad F_o = F_v \, , \quad \text{and} \quad F_o = F_a\sqrt{1-1/2Q^2} \, .$$

Since the ulnar Q is typically 2.7-3.6 when measured _in vivo_, F_o is usually

2-4% larger than F_x and 2-4% smaller than F_a . To a first

approximation, the correction for Q may be neglected and F_x and F_a

set approximately equal to F_o .

An alternative method for measuring the resonant frequency is

to tune the oscillator to obtain maximum response on the monitoring

oscilloscope.

In practice, the ulnar F_oL is usually 4000-8000 Hz-cm for

healthy subjects, and 1200-4500 Hz-cm for patients with symptomatic

osteoporosis. Tibial resonant frequencies are usually about 75%

as large as ulnar resonant frequencies, while the tibia is usually

about 40% longer than the ulna. Figure 2 illustrates a typical

ulnar response spectrum for a normal subject. Note the resonance

peak at about 290 Hz. Additional bone resonances are often

observed which may be either overtones or fundamental frequencies

of different modes of vibration. In addition, resonances may be

caused by oscillation of the accelerometer-skin system, or may

occur in the driver or in the accelerometer.

3.2 Ringing Frequency Determination

Another way to characterize an elastic system is to measure

the ringing frequency which results from application of a

short-duration impulse. Figure 3 shows a typical recording of the

distal ulnar response to an impact at the elbow. The frequency of oscillation, F_d, is nearly equal to the resonant frequency. The relationship between these two quantities is $F_o = F_d/\sqrt{1-1/4Q^2}$, where Q is the quality factor. The quantity Q may be found from the decay constant: $Q = 0.5\sqrt{1+4\pi^2 F_d^2/\alpha^2}$.

4. Clinical Application

Ulnar $F_a L$ was measured for 437 normal subjects with ages of 6-89 years. In addition, 28 osteoporotic and 15 diabetic women were measured. Recent spontaneous vertebral collapse or femoral fractures associated with little or no trauma were our criteria for defining osteoporosis.

As shown in Figures 4 and 5, $F_a L$ was found to rise until about 15 years of age and then to decrease after about age 20. The $F_a L$ of women was found to decrease at a rate of about 1% per year after the age of 50.

The 28 osteoporotic women exhibited a mean $F_a L$ value about 44% lower than that of their age-matched controls (4550 Hz-cm). This difference is significant at the 0.001 level. The diabetic women had a mean $F_a L$ value moderately lower (25%) than that of their age-matched controls (4070 Hz-cm). Application of the t test

showed this difference to be significant at the 0.02-0.05 level. These findings are summarized in Table I.

Discriminant analysis showed 82% of the women with symptomatic osteoporosis to be below, and 82% of the normal women to be above a discriminant F_aL value of 3060 Hz-cm (Table II).

5. Discussion

The limitations of the simple model of the vibrating ulna which has been presented in this paper are extensive:

1. The model ignores the effects of the soft tissue which surrounds the bone.

2. The effects of limited coupling between the equipment and the ulna, caused by the soft tissue covering the ulna, is ignored.

3. The finite mass of the hand is ignored.

4. The joint characteristics are oversimplified. Joints do not act as true hinges, but allow translational as well as rotational movements to occur.

5. The asymmetry of the ulna is ignored.

Yet, there is evidence that ulnar resonance is being measured:

1. For young, normal subjects, there is an inverse

relationship between F_a and L.

2. Placing a layer of 2 mm thick rubber sheeting between the driver piston and elbow or between the wrist and accelerometer reduces the amplitude of the resonance peak but does not change F_a.

3. The tissues of the forearm, in the relaxed state, do not appear to load the ulna significantly since the $F_a L$ of osteoporotic women, who weigh less than normal[8], is lower than the $F_a L$ of age-matched normal women. One expects mass loading to decrease the resonant frequency, not to increase it.

4. Tightening the muscles of the forearm does appear to change loading of the ulna since maximum gripping effort increases F_a by about 5%.

5. Firmly squeezing the middle of the forearm increases F_a by about 25%.

6. Isolating the handgrip from the rest of the arm support does not alter the resonance peak. Hence, the observed resonance is in the forearm and not in the arm support.

7. The driver resonant frequencies are not shifted appreciably by the presence of the arm; the ulnar resonance appears in a relatively flat region between the driver resonance

peaks (Figure 2).

Since the measurements described in this paper do provide, on an empirical basis, separation of patients with symptomatic osteoporosis from their age-matched controls (Tables I and II), future investigations will be directed toward revising the simplified model presented in this paper so that it more realistically simulates the vibrating forearm.

The finding that the $F_a L$ of diabetic women is lower than that of their age-matched controls (Table I), but not as low as the $F_a L$ of women with symptomatic osteoporosis is consistent with the report of Boulet and Mirouze[1] that diabetes is associated with an increased incidence of osteoporosis.

6. Conclusions

The product of ulnar resonant frequency and length was measured in 437 normal subjects, 28 osteoporotic women, and 15 diabetic women. $F_a L$ was found to decrease after about 20 years of age in both men and women. The mean $F_a L$ of the osteoporotic women was about 44% less than that of age-matched normal women, while the mean $F_a L$ of the diabetic women was intermediate. When normal women were compared with women who had osteoporosis sufficiently

severe to produce spontaneous fractures, the 2 groups could be discriminated with an effectiveness of 82% on the basis of their $F_a L$ values. Although our present understanding of the vibratory properties of the ulna is inadequate from an engineering standpoint, measurement of ulnar resonant frequency is a promising approach to the study of skeletal status.

7. Acknowledgments

References

1. BOULET, P., and MIROUZE, J.: Les ostéoses diabétiques (Ostéoporose et hyperostose). Ann. Med., 55:674-721, 1954.

2. CAMERON, J.; MAZESS, R.; and SORENSON, J.: Precision and Accuracy of Bone Mineral Determination by Direct Photon Absorptiometry. Inv. Radiol., 3:141-150, 1968.

3. JURIST, J.: Ulnar Vibratory Properties. Proceedings of the Conference on Progress in Methods of Bone Mineral Measurement, USPHS-NIAMD, 1969, in press.

4. JURIST, J., and SELLE, W.: Acoustical Detection of Osteoporosis. The Physiologist, 8:203, 1965.

5. KINSLER, L., and FREY, A.: Fundamentals of Acoustics, John Wiley & Sons, Inc., chaps. 1-3, 1950.

6. MATHER, B.: Comparison of Two Formulae for in Vivo Prediction of Strength of the Femur. Aerospace Med., 38:1270-1272, 1967.

7. RICH, C.; KLINK, E.; SMITH, R.; GRAHAM, B.; and IVANOVICH, P.: Sonic Measurement of Bone Mass. Progress in Development of Methods in Bone Densitometry, NASA SP-64, pp. 137-144, 1966.

8. SAVILLE, P., and NILSSON, B.: Height and Weight in Symptomatic Postmenopausal Osteoporosis. Clin. Orthop., 45:49-54, 1966.

9. SORENSON, J., and CAMERON, J.: A Reliable In Vivo Measurement of Bone-Mineral Content. J. Bone Jt. Surg., 49A:481-497, 1967.

10. von GIERKE, H.: Transmission of Vibratory Energy Through Human Tissue. In Glasser, O. (ed.): Medical Physics, Volume III, The Year Book Publishers, Inc., pp. 661-669, 1960.

Table 1

F_aL in Women with Postmenopausal Osteoporosis or Diabetes Mellitus

Group	F_aL (Hz-cm) (mean $\pm \sigma$)	N (pairs)	Age (yrs) (mean $\pm \sigma$)	t Test
Osteoporotic	2560 $\pm$ 850			
		28	74.0 $\pm$ 8.9	5.76 (P<0.001)
Age-matched control	4550 $\pm$ 1620			
Diabetic	3040 $\pm$ 1230			
		15	74.5 $\pm$ 7.5	2.10 (P=0.02-0.05)
Age-matched control	4070 $\pm$ 1450			

Table 2

Discriminant Analysis for 28 Osteoporotic

and Age-Matched Control Pairs

	Clinical Group	
	Control	Osteoporotic
$F_a L \geq 3055$ Hz-cm	23	5
$F_a L < 3055$ Hz-cm	5	23

The mean age of these women was 74 years.
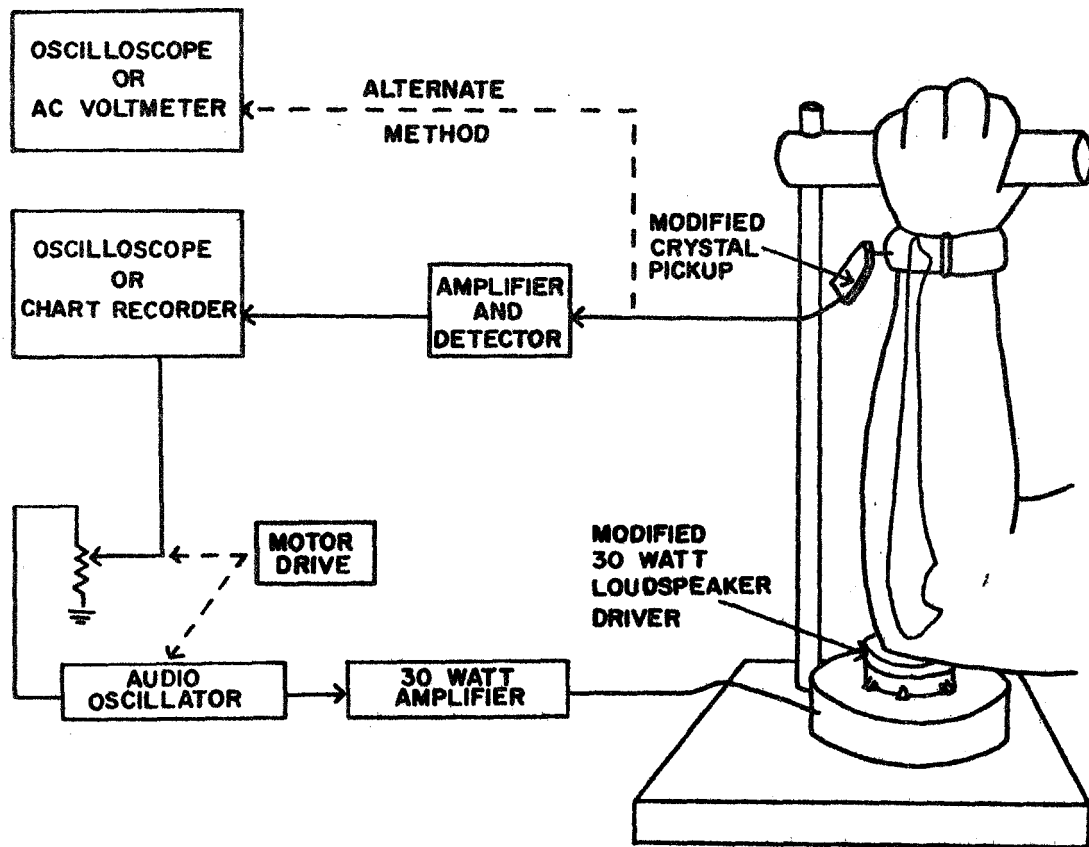
FIGURE 1: Apparatus for measurement of ulnar resonant frequency.
The 16Ω Atlas PD-4V driver was modified by addition of a small
lucite piston bonded to the diaphragm with epoxy cement. The
piston makes contact with the elbow of the subject. The ulnar
response is detected with a small crystal accelerometer strapped
to the wrist. The resonant frequency of the ulna may be determined
by: (1) scanning a frequency range and recording response as a
function of frequency, or (2) tuning the audio oscillator to obtain
maximum response as measured on the monitoring oscilloscope or
voltmeter.
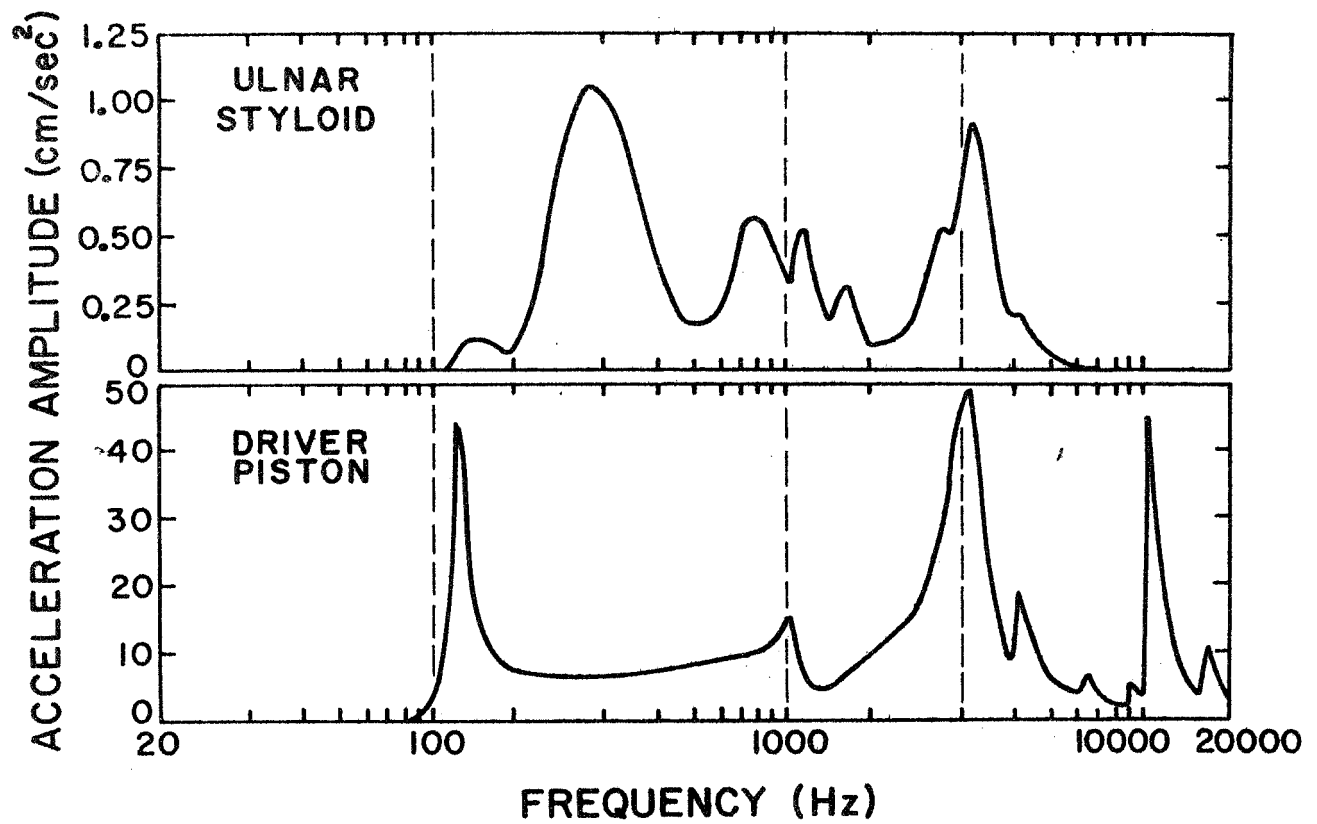
FIGURE 2: Acceleration spectrum of the driver piston (bottom) and of the ulnar styloid (top) for a typical adult. Note the ulnar resonance at about 290 Hz.
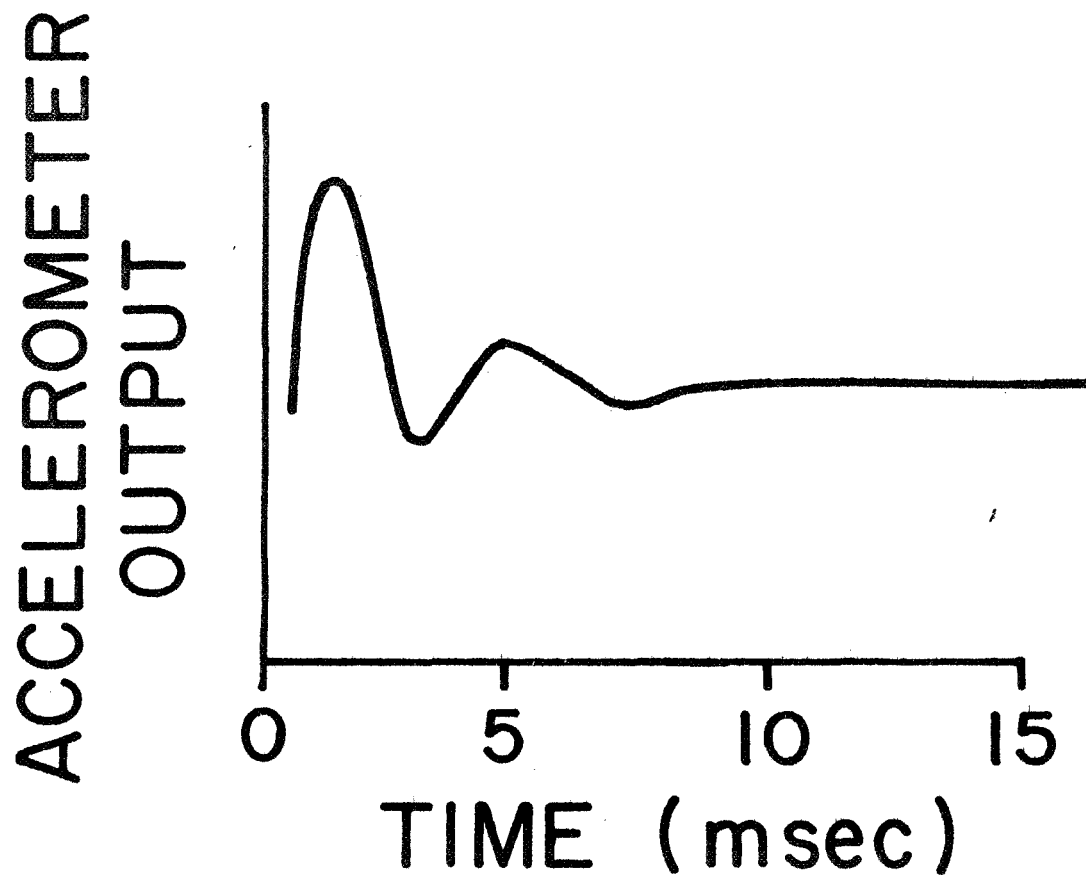
FIGURE 3: Typical acceleration response of the ulna, measured at the wrist, following a short-duration impact at the elbow. The frequency of oscillation is about 320 Hz.
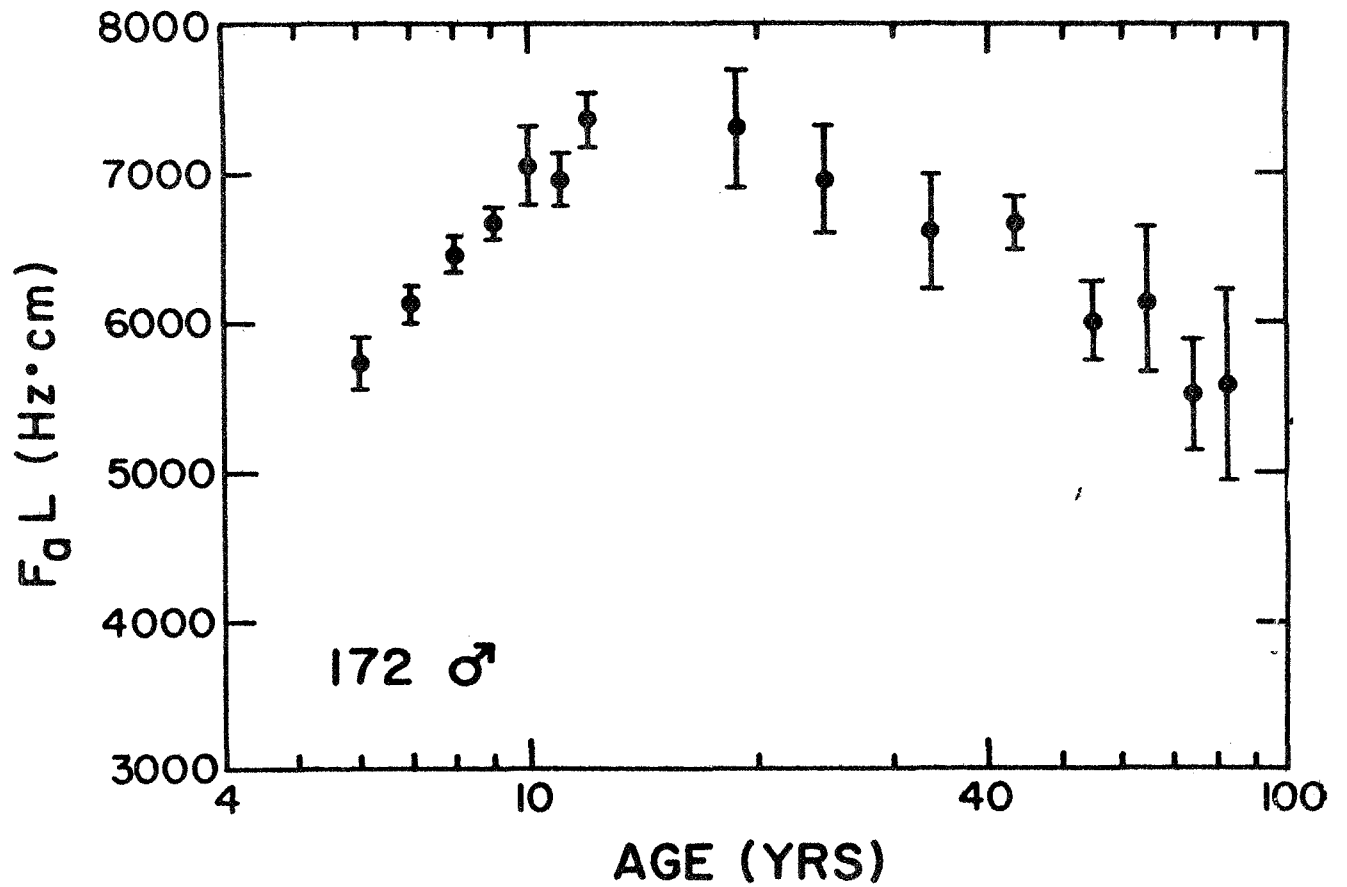
FIGURE 4: Product of resonant frequency and length $(F_a L)$ of the ulna for 172 normal males as a function of age. The range bars enclose ±1 standard deviation of the mean.
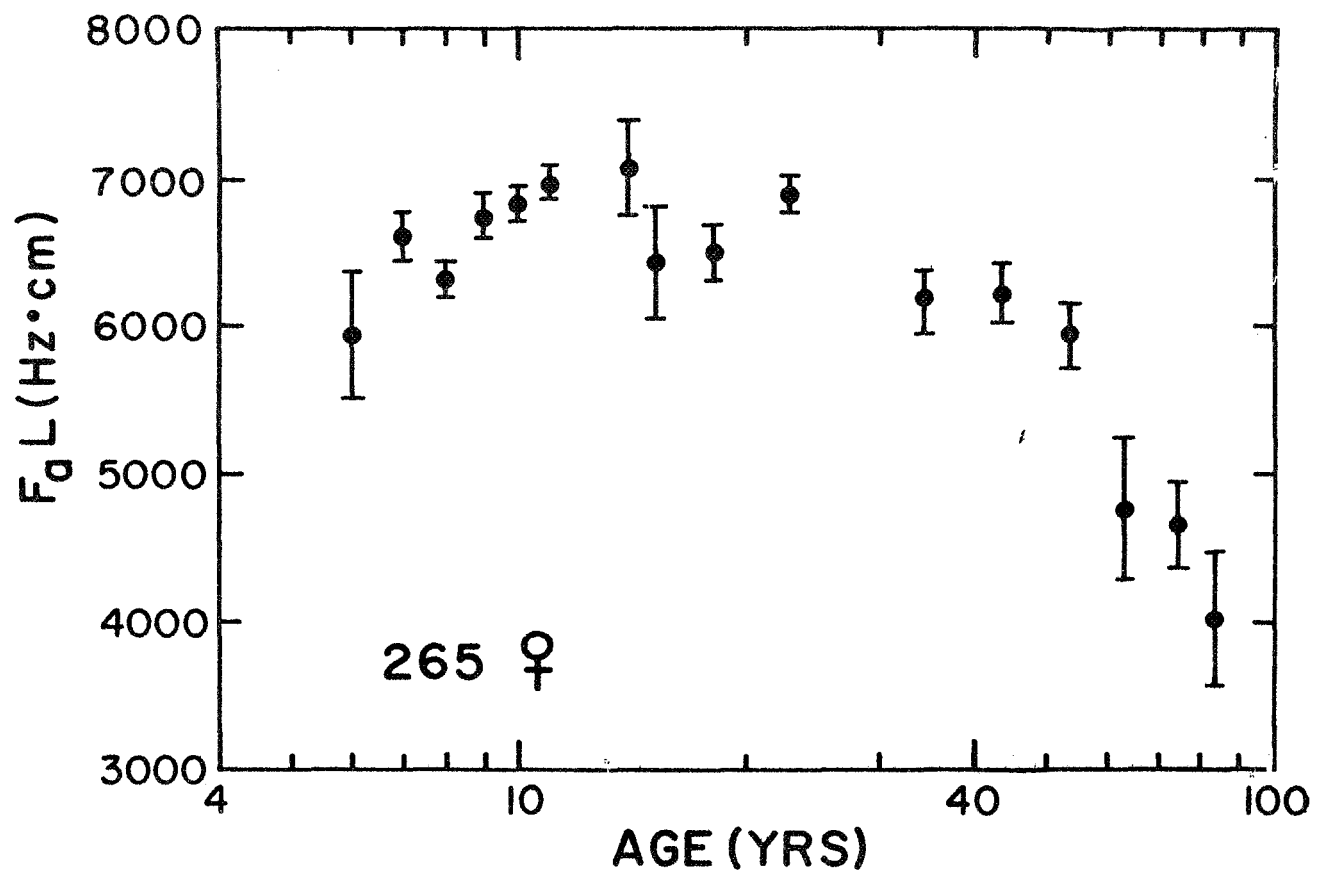
FIGURE 5: F_aL vs. age for 265 normal females.

An Improved Apparatus for Determination <u>in</u> <u>Vivo</u> of Bone Resonant Frequency

by Recording the Vibration Response Spectrum

John M. Jurist

Darrell Loper

Clifford Vought

1. Introduction

Recent experience with determination in vivo of bone resonant frequency has suggested a number of improvements to be incorporated in a second generation apparatus. This report describes progress in the development of such an improved apparatus and contrasts the improvements with the characteristics of the currently used unit.[1]

2. General Discussion of Electronic Apparatus

Our present apparatus requires approximately 25 seconds to sweep a frequency decade. Then, the unit must be reset by backtracking over the same range before another frequency scan can be made. Hence, a total of about 50 seconds is required for each sweep. The improved apparatus uses a faster drive motor so a frequency decade can be scanned in about 10 seconds. In addition, the frequency control (ganged precision potentiometers) can be rotated through 360°. Therefore, no backtracking or resetting is necessary, and a total of only 10 seconds is required for each sweep when repeated sweeps are to be made. The improvement in sweep speed reduces the time the subject must hold still and makes it less likely that inadvertent movement will reduce the response spectrum quality.

The frequency decades used on the existing apparatus are 20-200 Hz and 200-2000 Hz. The transverse resonant frequencies of the ulnae of normal subjects are usually in the range 200-400 Hz, while the resonant frequencies observed in osteoporotic patients are usually in the range 60-150 Hz.[2] Consequently, the frequency range of the existing apparatus must be switched to cover all observed ulnar resonant frequencies, and recording spectra for subjects with ulnar resonances of about 200 Hz is difficult. The improved unit is designed to cover a range of approximately 75-500 Hz in one scan.

The frequency response of the existing oscillator and power amplifier is essentially constant (within ±5%) over the frequency range used, but the driver amplitude response is not (Figure 1). The improved apparatus incorporates a compensation network between the oscillator and power amplifier to flatten the combined oscillator-amplifier-driver frequency response characteristic in the range 50-500 Hz.

The existing apparatus uses the oscillator B+ supply to furnish a reference voltage for the shaft position potentiometer. The output of this potentiometer then drives the X-axis (frequency axis) of the recording device. The B+ voltage supply is not regulated and can vary considerably during short time intervals if line voltage

fluctuates. One is therefore required to repeatedly correct the X-axis scale to a constant full scale deflection either by adjusting the recorder gain or by employing a correction factor when determining the resonant frequency. The improved apparatus uses a regulated (Zener diode) power supply for the shaft position potentiometer reference voltage. Compensation for variable X-axis sensitivity is therefore unnecessary.

At the present time, a simple amplifier, rectifier, and filter combination is used to detect the response of the sensing accelerometer and yield a voltage which is proportional to the amplitude of the accelerometer output voltage. Upon occasion, the ulna will vibrate at a frequency which is a subharmonic or an overtone of the driving frequency; this causes an ambiguity in determination of the resonant frequency. The present unit makes no provision for this possibility. Also, muscle tremor, arterial pulses (the ulnar artery often passes close to the ulnar styloid), etc. are all superimposed on the accelerometer output and affect the quality of the frequency response recording. The improved apparatus will incorporate a narrow bandpass filter in the detector circuit which can track the oscillator output. Thus, all frequency components in the accelerometer output other than the oscillator driving frequency will be rejected.

The new apparatus will also incorporate an integrator circuit so that the velocity amplitude response spectrum of the bone will be recorded rather than the acceleration amplitude response spectrum. Since the frequency of maximum velocity response is identical to the resonant frequency while the frequency of maximum acceleration response only approaches the resonant frequency as a limit when the damping factor becomes infinitesimal, correction for the existence of finite damping (limited Q) will not be necessary.[3]

To summarize, then, the following improvements are to be incorporated in the new apparatus:

1. Faster frequency drive motor,

2. No resetting necessary for repeated frequency scans,

3. Frequencies of 50-500 Hz covered by one scan,

4. Frequency response of oscillator-power amplifier system corrected for frequency response of driver,

5. Regulated reference voltage used for oscillator frequency control shaft position indication,

6. Narrow bandpass filter which tracks oscillator output frequency incorporated into detection circuit, and

7. Integrator circuit incorporated into detector to provide velocity amplitude response measurement.

3. Design of Improved Electronic Apparatus

A block diagram of the improved electronic apparatus is shown in Figure 2.

The output frequency of the oscillator and the center frequency of the bandpass filter will be controlled by identical ganged twin-T networks which use precision capacitors and potentiometers (Figure 3). Balance and trimmer potentiometers are incorporated into each network to allow for precise matching. A small synchronous motor (6 RPM) is connected to the twin-T network potentiometers--thus controlling the frequency setting of these networks. An additional precision potentiometer is ganged on the same shaft in order to provide a shaft position indication (X-axis). The twin-T potentiometers and the shaft position indication potentiometer are aligned in such a way that the frequency setting of the networks and the voltage output of the indication circuit both increase steadily with time for 10 seconds and then reset for the next drive motor revolution.

The oscillator is a solid state device which uses the twin-T network described above to control output frequency. It uses small incandescent lamps as nonlinear elements to stabilize the output. The oscillator circuit is shown in Figure 4.

The compensation network was devised empirically from a

network of capacitors and resistors to provide a relatively flat
driver response characteristic as a function of frequency.

The 10 watt solid state amplifier (class AB power stage)
provides a frequency response characteristic which is flat within
$\pm 25\%$ in the range 15-25000 Hz. The circuit of this amplifier is
shown in Figure 5.

The preamplifier will use a field effect transistor circuit to
provide a high input impedance (10-20 Megohms) for the crystal
pickup (accelerometer). The output of this stage will be amplified
by an integrated circuit operational amplifier (open loop gain of
approximately 10^6) to bring the microvolt level signal from the
accelerometer up to a useful level.

The narrow bandpass filter will use an integrated circuit
operational amplifier with a twin-T network in the feedback loop.
The forward gain of this filter at the center frequency will be
approximately 10.

Another field effect transistor and operational amplifier
circuit will integrate the signal before it is rectified and
filtered by a capacitor. The filter output will provide a voltage
level proportional to the amplitude of the integrated (velocity)
output of the accelerometer. This voltage will be recorded on the
Y-axis of the recording device (X-Y plotter or oscilloscope).

4. The Improved Mechanical System

We are now testing a new arm support for ulnar resonant
frequency measurements. This new support, shown in Figure 6, is
constructed of aluminum channel rather than lucite in order to
reduce material costs and fabrication time.

The Atlas PD-4V driver is mounted transversely to the long
axis of the ulna. Since the ulna resonates in the transverse mode
at frequencies of less than 1000 Hz, this arrangement allows a
greater ulnar amplitude response at resonance than does the previous
(longitudinal excitation) arrangement for given driver power levels.

The driver piston is threaded for attachment of an accelerometer.
This allows convenient determination of the driver frequency response
characteristics under different loading conditions.

5. Discussion

It is anticipated that the improved apparatus will be completed
and ready for extensive testing by September, 1969. At that time,
measurements of both short-term and long-term stability and accuracy
of the apparatus will be made on excised bones. In addition,
estimates of the long-term reproducibility of the ulnar resonant
frequency determination in vivo will be made. Continued testing of

the apparatus will then be performed in a clinical environment in order to evaluate further improvements and simplifications in the procedure for estimation of bone quality.

6. **References**

1. J. M. Jurist: _In Vivo_ Determination of the Elastic Properties of Bone: I. Theory, Apparatus, and Method of Ulnar Resonant Frequency Determination, submitted for publication, 1969.

2. J. M. Jurist: _In Vivo_ Determination of the Elastic Properties of Bone: III. Ulnar Resonant Frequency in Osteoporotic, Diabetic, and Normal Subjects, submitted for publication, 1969.

3. J. M. Jurist and J. R. Cameron: _In Vivo_ Measurement of Bone Quality, _Symposium on Bioengineering in Wisconsin_, March, 1969.
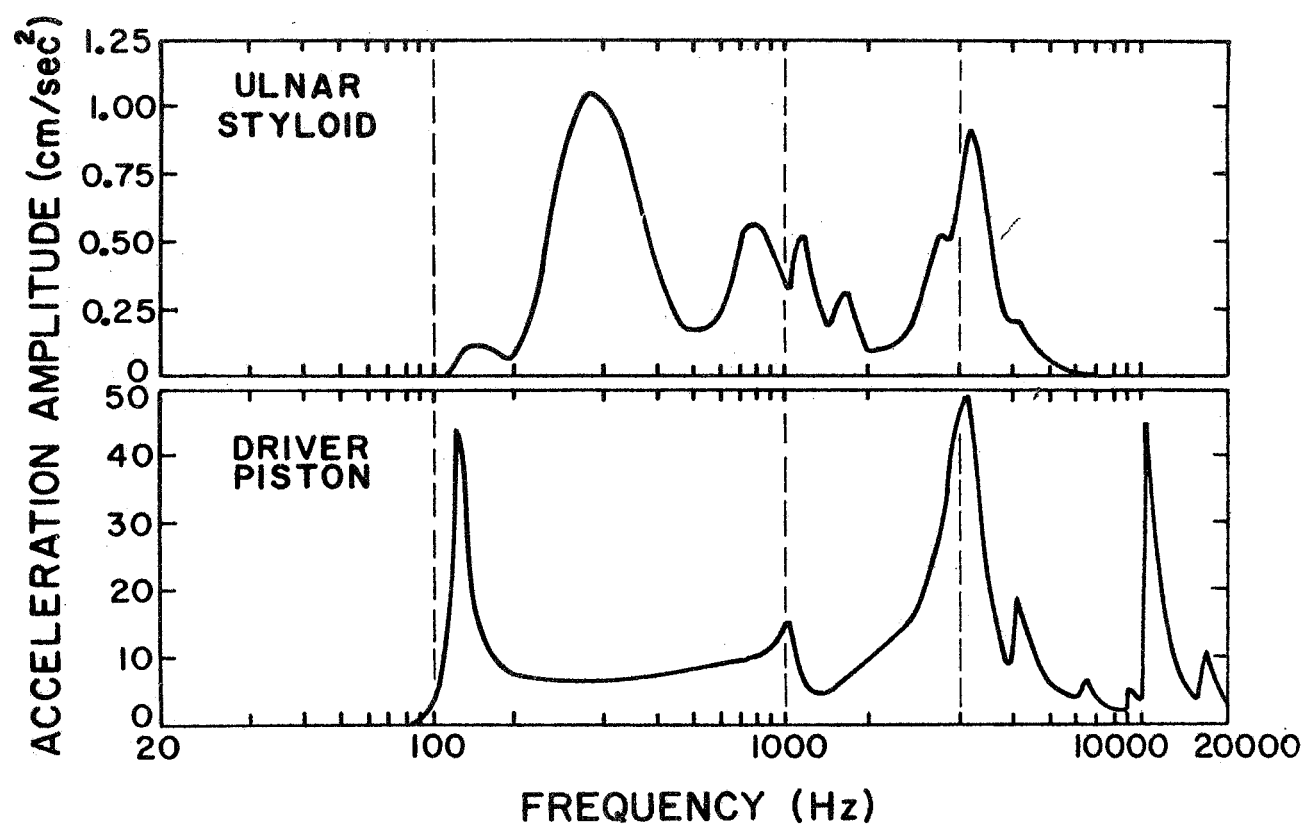
FIGURE 1: Acceleration spectrum of the driver piston (bottom) and of the ulnar styloid (top) for a typical adult. The resonances at 130 Hz, 1000 Hz, and 3000 Hz are in the driver, while the resonance at 10000 Hz is in the accelerometer.
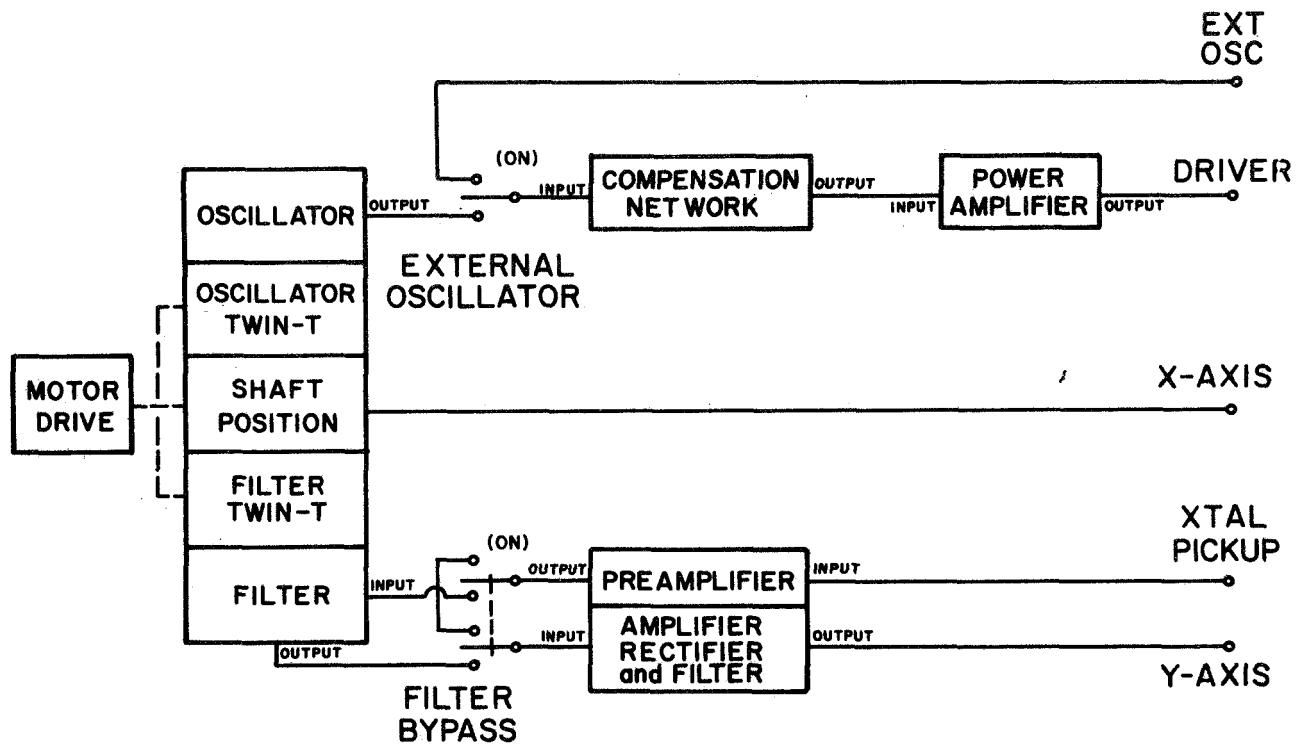
FIGURE 2: Block diagram of the new resonance apparatus.
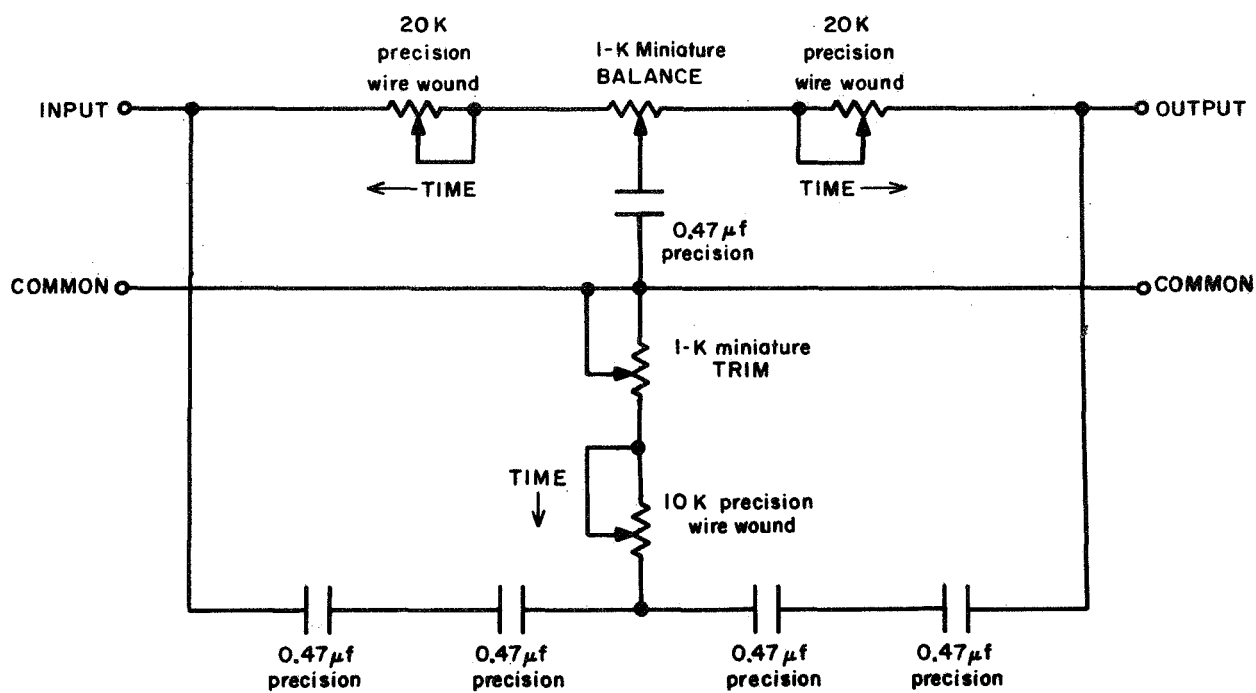
FIGURE 3: Twin-T network used to control the oscillator frequency
and the passing frequency of the filter.
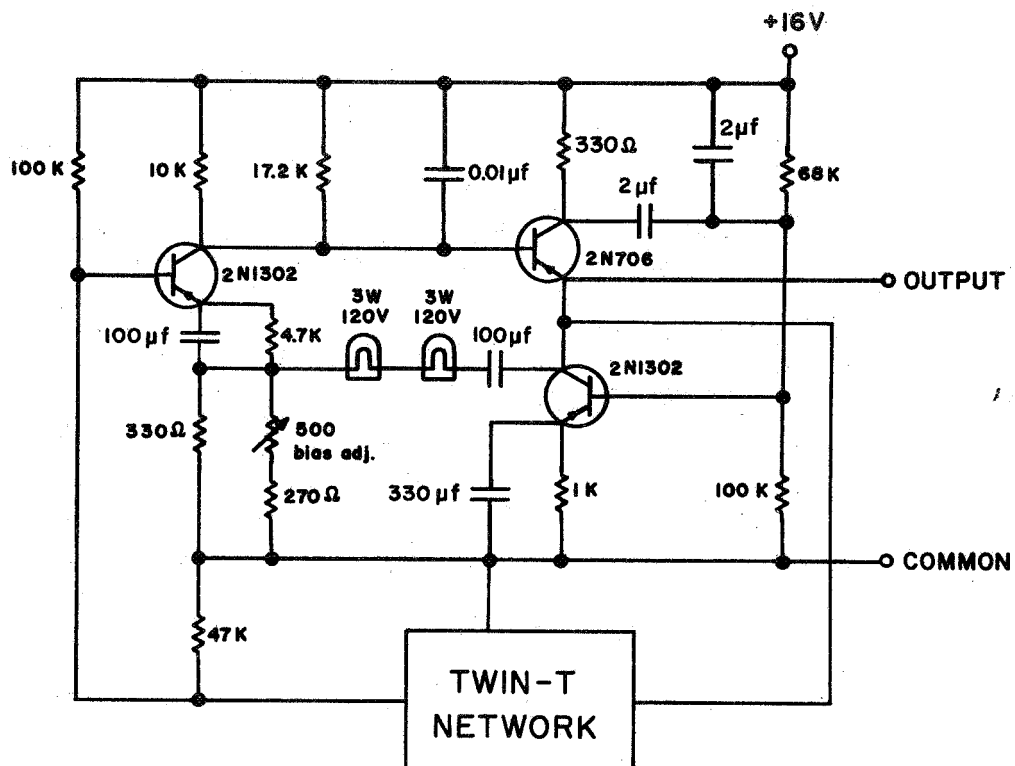
FIGURE 4: Oscillator circuit.
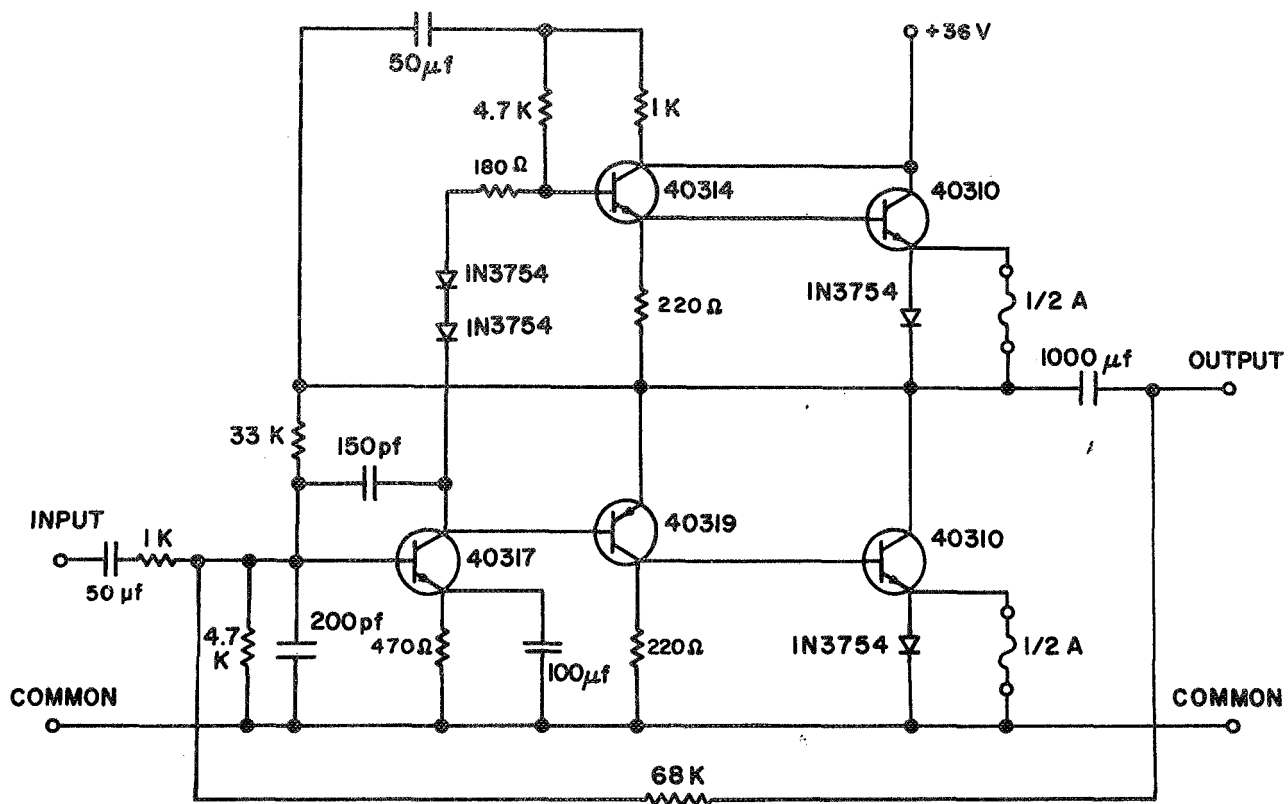
FIGURE 5: Power amplifier circuit.
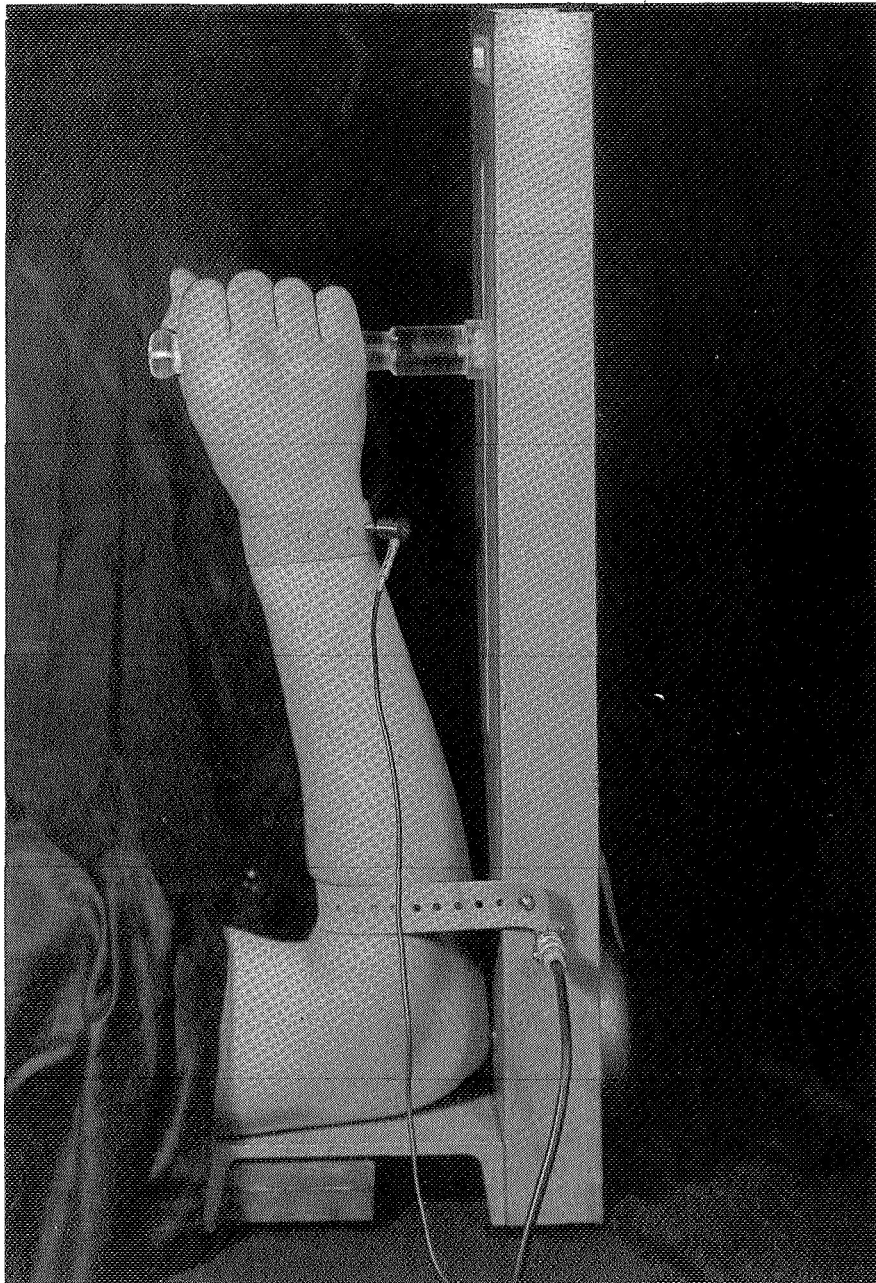
FIGURE 6: Improved arm support. This support is made out of aluminum channel in order to minimize fabrication costs. The rubber strap forces the elbow against the driver piston.

Dynamic Measurement of Young's Modulus for Excised Strips of Bone

John M. Jurist

Charles R. Wilson

1. Introduction

In order to determine the modulus of elasticity of an excised sample of bone, the speed of sound propagation through the bone sample should be determined. Although the speed of sound may be determined in several ways, we are studying exploitation of the resonant properties of bone to obtain this parameter.

2. Theory

The bone sample should be machined into a uniform strip in order to facilitate calculation of the elasticity as a function of density, size, shape, and loading of the sample. Machining of bone samples should be done at low temperatures with the samples kept moist in order to minimize changes in mechanical properties.[2,3]

If the bone sample is machined into a rectangular strip of length 1, width b, and thickness a, where $a < b < 1$, it will be least stiff about its least dimension (a). Hence, the bone strip will vibrate preferentially in a transverse direction with the neutral plane parallel to the plane formed by b and 1.

It can be shown[1] that the periodic solution of the equation of motion of a transversely vibrating bar of uniform cross section is given by

(1) $y = \cos(\omega t+\phi)(A\cosh(\omega X/v) + B\sinh(\omega X/v) + C\cos(\omega X/v) + D\sin(\omega X/v))$

if the material of the bar is homogeneous and if the bending of the

bar is small. In this equation, y is the displacement from the

neutral position of the cross section of the bar at a point X along

its length, ω is the angular frequency of the sinusoidal vibration,

and ϕ is its phase. A, B, C, and D are arbitrary constants

determined by boundary conditions. The factor v is the phase

velocity of transverse wave propagation along the bar, and is given by

(2) $v = \sqrt{\omega c K}$.

The speed of sound propagation through the material of the bar (c)

is defined by

(3) $c = \sqrt{Y/\rho}$.

Y is the effective Young's modulus and ρ is the density of the bar.

K is defined as the radius of gyration of the cross section of the

bar about its neutral axis and, for a bar of rectangular cross

section, is given by

(4) $K = a/\sqrt{12}$.

If the vibrating bar (Figure 1) is assumed to be rigidly

clamped at one end (origin of X-axis) so that the slope and

displacement are zero, the boundary conditions are $y = 0$, and

$\partial y/\partial X = 0$. Substitution of equation (1) into these equations for

$X = 0$ shows that $C = -A$, and $D = -B$. If the latter two equations

are substituted back into equation (1), the equation of motion becomes

(5) $y = \cos(\omega t + \phi)(A(\cosh(\omega X/v) - \cos(\omega X/v)) + B(\sinh(\omega X/v) - \sin(\omega X/v)))$.

If the bar is clamped so that its free length is defined by L,
and if the end at $X = L$ is attached to a point mass M, the boundary
conditions at this end are $\partial^2 y/\partial X^2 = 0$, and $M\partial^2 y/\partial t^2 = YabK^2\partial^3 y/\partial X^3$.
When equation (5) is substituted into these equations at $X = L$, and
the results are combined to eliminate A and B, one obtains

(6) $\cosh\alpha\sin\alpha - \sinh\alpha\cos\alpha - \dfrac{\rho abL}{\alpha M}(1 + \cosh\alpha\cos\alpha) = 0$

after simplification by use of equations (2), (3), and (4). In
equation (6), α is defined by

(7) $\alpha = \omega L/v$.

It is clear that ρabL is the mass of the freely suspended portion
of the bone strip. If the mass of the strip (dimensions a, b, 1)
is defined by m, then $\rho abL = mL/1$. Therefore,

(8) $\cosh\alpha\sin\alpha - \sinh\alpha\cos\alpha - (mL/M1\alpha)(1 + \cosh\alpha\cos\alpha) = 0$.

This transcendental equation was solved by the method of
successive approximations. The first four solutions are listed for
various mL/Ml in Table 1 and plotted in Figure 2. If mL/Ml increases
without limit $(M \rightarrow 0)$, equation (8) reduces to $\cosh\alpha\cos\alpha + 1 = 0$. This
equation describes the limiting case of a bar rigidly clamped at
one end and free at the other $(M \rightarrow 0)$, and has the solutions
$\alpha = 1.8755, 4.6935, 7.8540, 10.9956, \ldots$. Note that the solutions

of equation (8) plotted in Figure 2 approach these limits as $M \rightarrow 0$.
The other limiting case occurs when M is allowed to increase
without limit ($m/M \rightarrow 0$), thus reducing equation (8) to
$\cosh\alpha\sin\alpha - \sinh\alpha\cos\alpha = 0$. This limit corresponds to a bar rigidly
clamped at one end and connected to a rigid support by a hinge at
the other and has the solutions $\alpha = 0$, 3.9265, 7.0686, 10.2102, ...
Again, Figure 2 shows that the solutions of equation (8) approach
these limits as $mL/M1 \rightarrow 0$. Figure 3 illustrates the modes of
vibration which correspond to the solutions for the limiting cases.
The nodal points for the limiting cases are given in Table 2.

3. Method

The basis for determination of Young's modulus for a strip of
bone is now established (Figure 1). If a bone strip of length 1,
width b, thickness a, and mass m is clamped so that a length L
projects freely from the clamp, an accelerometer of mass M may be
mounted on the free end. The allowed values of α may be obtained
from either Table 1 or Figure 2 after mL/M1 is calculated. If the
resonant frequency of the bone strip and attached accelerometer
for a given vibrational mode is defined by F, then it is clear
from equations (2), (3), (4), and (7) that

(9) $Y = 48\pi^2 L^4 mF^2 / a^3 bl\alpha^4$

since $\omega = 2\pi F$.

4. Discussion

It is recognized that a number of assumptions were made in deriving equation (9): Bone is a homogeneous and perfectly elastic material, all deflections are small, the clamp is perfectly rigid (infinite mass), and the load (M) is a point mass. Studies are presently underway in our laboratory to determine the validity of these assumptions.

5. References

1. Kinsler, L. E.; Frey, A. R.: Fundamentals of Acoustics, New York, John Wiley & Sons, Inc., 1950, Chap. 3.

2. Sedlin, E. D.: A rheologic model for cortical bone, Acta Orthop. Scand. Supp. 83:1-77, 1965.

3. Smith, J. W.; Walmsley, R.: Factors affecting the elasticity of bone, J. Anat. 93:503-523, 1959.

Table 1

Allowed α for Various mL/Ml

mL/Ml	α_1	α_2	α_3	α_4
0.0001	0.1316	3.9266	7.0686	10.2102
0.0002	0.1565	3.9266	7.0686	10.2102
0.0005	0.1968	3.9267	7.0686	10.2102
0.0010	0.2340	3.9267	7.0687	10.2102
0.0020	0.2783	3.9268	7.0687	10.2103
0.0050	0.3499	3.9272	7.0689	10.2104
0.0100	0.4159	3.9278	7.0693	10.2107
0.0200	0.4943	3.9290	7.0700	10.2112
0.0500	0.6205	3.9326	7.0721	10.2126
0.1000	0.7358	3.9385	7.0756	10.2150
0.2000	0.8700	3.9500	7.0825	10.2199
0.5000	1.0762	3.9826	7.1026	10.2340
1.0000	1.2479	4.0311	7.1341	10.2566
2.0000	1.4200	4.1111	7.1903	10.2984
5.0000	1.6164	4.2671	7.3184	10.4016
10.0000	1.7227	4.3995	7.4511	10.5218
20.0000	1.7918	4.5127	7.5863	10.6609
50.0000	1.8393	4.6100	7.7218	10.8195
100.0000	1.8568	4.6497	7.7827	10.8976
200.0000	1.8658	4.6713	7.8172	10.9437
500.0000	1.8714	4.6848	7.8393	10.9741
1000.0000	1.8732	4.6894	7.8470	10.9847

Table 2

X Coordinates of Nodal Points

for Different Modes of Vibration

mL/M1 → 0

α	Nodal Points (% of L)			
0.0000	0.0	---	---	'100.0
3.9265	0.0	---	---	100.0
7.0686	0.0	---	55.5	100.0
10.2102	0.0	38.5	69.2	100.0

mL/M1 → ∞

α	Nodal Points (% of L)			
1.8755	0.0	---	---	---
4.6935	0.0	---	---	77.4
7.8540	0.0	---	50.0	86.8
10.9956	0.0	35.6	64.4	90.5
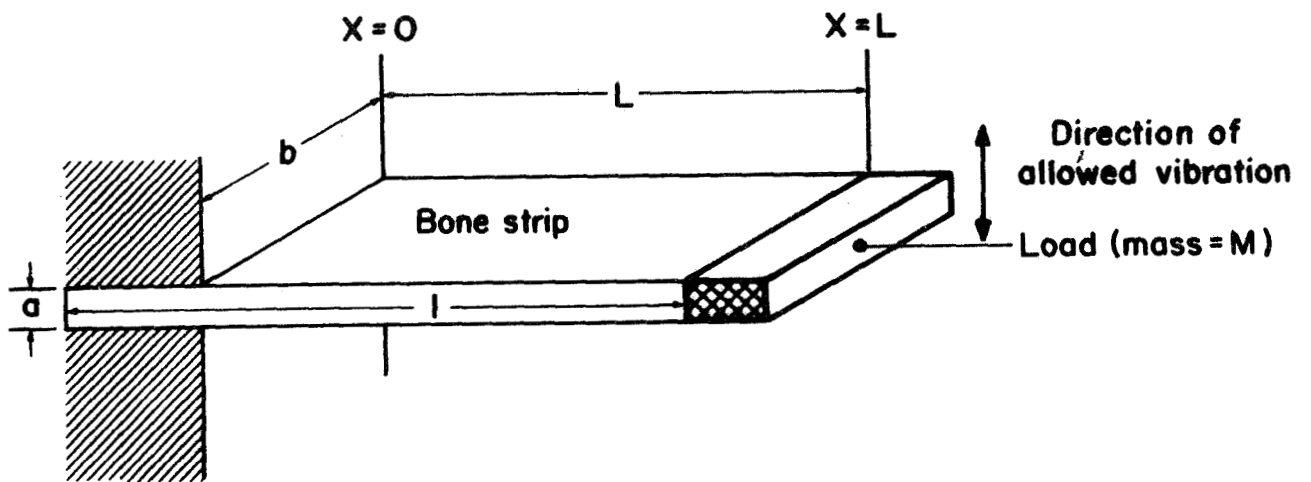
FIGURE 1: Rectangular strip of bone rigidly clamped at $X = 0$ and loaded by a mass M at $X = L$.
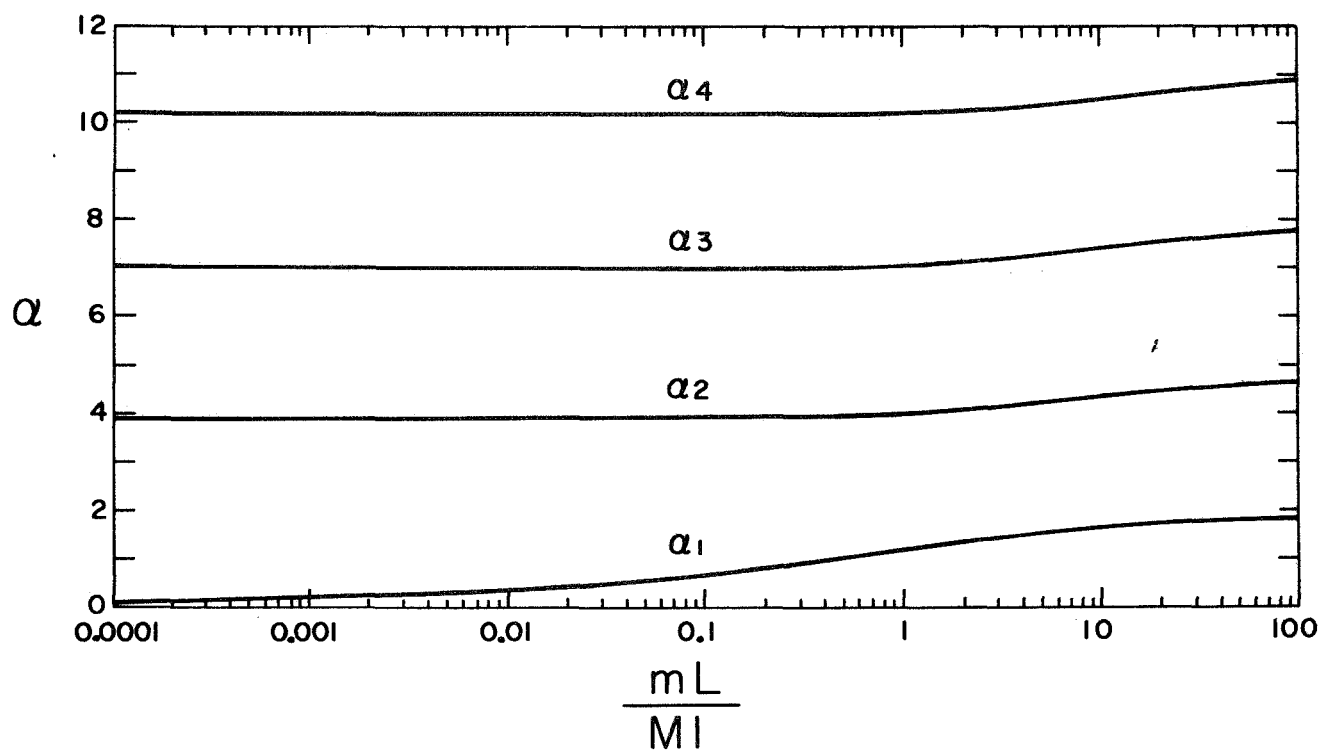
FIGURE 2: Solutions of equation (8) for α as a function of mL/Ml.
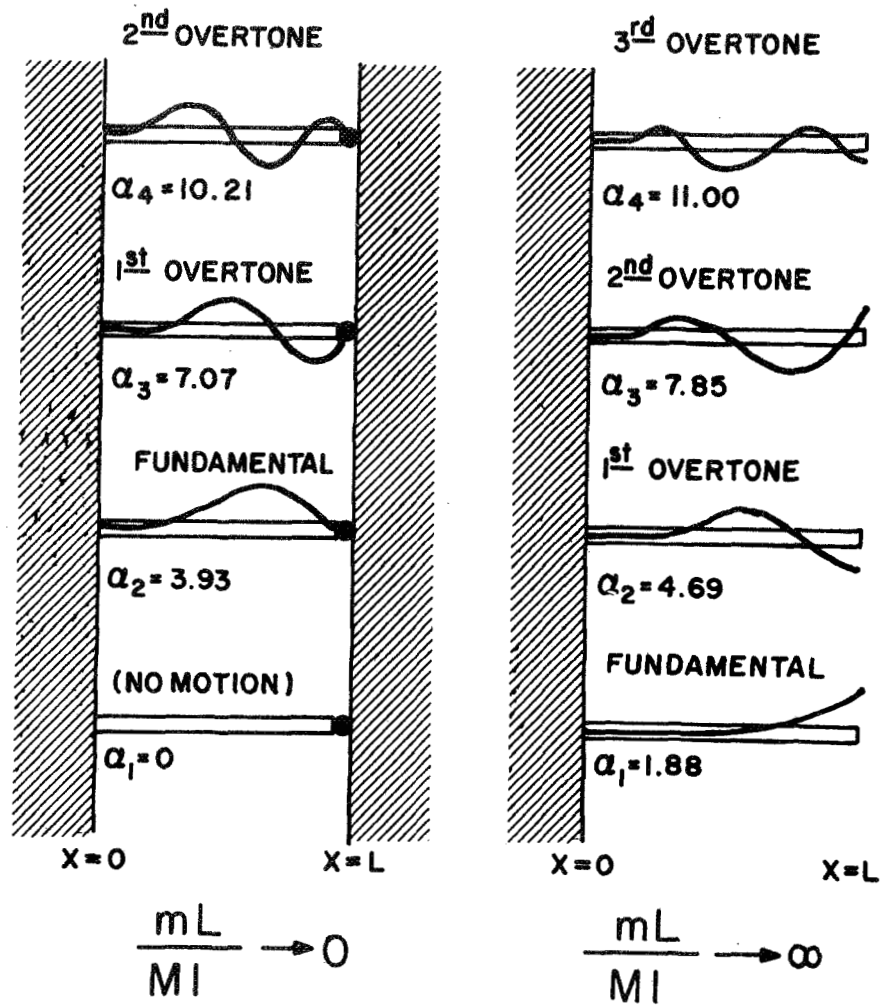
FIGURE 3: Modes of vibration of the bone strip for two limiting cases.

Study of Bone Strain by Holographic Interferometry

By: James M. Hevezi, Ph. D.
     Department of Radiology
     University of Wisconsin
     Madison, Wisconsin

Previous studies from this laboratory (1,2,3) have provided quantitative descriptions of both mineral content of bone, through photon absorptiometry, and bone quality, through resonant fre- quency determinations. In vivo and in vitro studies are possible with these techniques; the results may provide increased knowledge of the properties of bone.

With the advent of the laser as a source of intense, coherent, monochromatic light, and the pioneering experiments of Stroke (4) and others (5) in the fields of laser interferometry and holography, it has become possible to visualize both small displacments of stressed objects (6,7) and their modes of vibration (8). In applying these techniques to biological specimens such as bone, there is an inherent disadvantage in that only studies in vitro can be made. However, information obtained may be important for a more complete knowledge of bone properties.

Holography is not difficult to understand, and is moderately easy to put into practice. Consider a beam of coherent light in which the phase relationships of the wavefronts are known. This beam is split into two beams, one of which illuminates the object to be photographed. A photographic plate intercepts the light reflected from the object. Simultaneously, the second beam (the reference beam) impinges directly on the photographic plate. The reference beam interferes with the beam from the object; an inter- ference pattern is recorded on the photographic plate. Only the

lines and whorls of the interference pattern are perceptible when the plate is developed. However, when a facsimile of the original reference beam is directed onto the plate, the wavefronts which reached the plate from the object are reconstructed. Hence, when looking through the plate, one will see a three dimensional image of the object.

Since the hologram records all of the information contained in a wavefront, the images produced by this technique are very realistic. A number of objects can be examined from different viewpoints, or one can focus at different depths throughout the reconstructed image.

For the purposes of the proposed study, the holographic plate contains all of the information (amplitude and phase) necessary for interferometry. If the plate is exposed twice, one pattern of interference fringes is formed at each exposure. Assuming that the object and plate remain undisturbed between exposures, the fringes will be superimposed on one another further lightening light areas and darkening dark areas. If, however, some part of the object has moved between exposures, the corresponding fringes will have changed their positions. From the resulting pattern, a quantitative determination of the displacement direction and magnitude of each point of the object can be made.

Using this technique on excised bones, one could assess skeletal strain patterns resulting from application of stress to the proximal and distal ends, for example. The stresses at these points may be applied either transversely or longitudinally to the axis of the bone. In addition, strain patterns caused by applying torquing stress may be visualized. This latter study could be applied to the study of spiral fractures of the tibia,

for example.

Observing the interference patterns produced by vibrating bones is another possible application of holographic interferometry. In this case, the motion is such that the interference fringes are moving rapidly through the field of view in synchrony with the vibration. Hence, in practice, the fringes will be blurred for all but the lowest vibratory frequencies. However, if a stroboscopic coherent beam is used to illuminate the vibrating bone, the fringe motion may be arrested if the stroboscopic frequency is equal to or an integral multiple of the frequency of the vibration of the bone. Such a study would allow direct determination of the modes of vibration of bones for different boundary conditions, planes of vibration and excitation points.

BIBLIOGRAPHY

1. Cameron, J.R. and Sorenson, J.A., Measurement of Bone Mineral In Vivo: An Improved Method., Science 142: 230-232, (1963)

2. Sorenson, J.A. and Cameron, J.R., A Reliable In Vivo Measurement of Bone Mineral Content., The Journal of Bone and Joint Surgery, Vol. 49-A, No. 3, (April, 1967)

3. Jurist, J.M., In Vivo Determination of the Elastic Properties of Bone. To be published.

4. Stroke, G.W., An Introduction to Coherent Optics and Holography. Academic Press, New York, 1966.

5. Powell, R.L. and Stetson, K.A., Journal of the Optical Society of America, Vol. 55, p. 1593 (1965).

6. Pennington, K.S., Advances In Holography. Scientific American, Vol. 214, No. 2, p. 1255 (Feb. 1968).

7. Abramson, N., "Interferometric Holography" Without Holograms. Laser Focus, p. 26 (Dec. 1968).

8. Archbold, E. and Ennos, A.E., Vibrating Surface Viewed in Real Time by Interference Holography. Laser Focus, p. 58 (Oct. 1968).

BONE AS THE RESONANT ELEMENT IN A FEEDBACK OSCILLATOR

Charles R. Wilson, Clifford E. Vought and John R. Cameron

Jurist (1969) reported on a method for the determination of the resonant frequency of bone <u>in</u> <u>vivo</u> by obtaining the amplitude response of the bone to vibratory excitation as a function of frequency. A new method for the determination of the resonant frequency is being investigated. Instead of driving the bone through a range of frequencies the bone is incorporated into the circuit of a feedback oscillator. Figure 1 shows the method applied to the ulna. By tapping the elbow a small transient vibration which will include the resonant frequency of the ulna is produced. This vibration is detected by the transducer,[*] the signal is amplified and fedback to the driver[**] which reinforces the resonant frequency if the phase relationships are correct. The bone continues to vibrate and the frequency can be measured by using a scaler or ratemeter as a frequency meter.

The frequency at which oscillations occur for a subject have been in general lower with the present equipment than the resonant frequency determined by finding the maximum amplitude response. A difference is to be expected in that the conditions for their determination are not the same. In the first case, oscillation occurs when the signal from the accelerometer[1] is in the proper phase relationship with the driver vibrations so that reinforcement of the vibrations in the bone can take place. While in the

---

[*] Piezoelectric Accelerometer: Model 2219, Endevco Corporation, Pasadena, California

[**] Ashworth Sound Reproducer Model 250 available from Allied Electronics, Chicago, Illinois

second case the frequency determined at the maximum amplitude
does not depend upon the phase between the accelerometer signal
and the driver vibration.

A series of measurements were made on one subject to check
the reproducibility of the method. Eleven measurements were
made over a period of one week, each measurement was the average
of ten separate frequency determinations. The typical percent
standard deviation of a set of 10 determinations was about 3%.
The standard deviation of the eleven measurements was 1.5%. A
similar study is now being carried out to evaluate the long term
precision of the method.

In one study the frequency was measured by using a ratemeter
and recorder to find the variation in the resonant frequency
under various conditions. Figure 2 shows the ratemeter output
for 84 seconds in which variability was intentionally produced
by moving the arm about to change the contact point of the driver
at the elbow and the accelerometer at the wrist. The maximum
spread is about $\pm$ 4%. By holding the arm stationary the frequency
does not vary more than $\pm$ 3%. The breaks in the curve are those
points at which either the oscillation ceases because of failure
of proper feedback conditions or the bone goes into oscillation
at a different frequency. In general there appears to be three
common modes of vibration for the small number of adult subjects
tested to date. The frequencies are on the order of 200Hz,
1000Hz, and 2200Hz.

A clinical study is now being started to determine the
frequency of oscillation for patients seen in our laboratory

for bone mineral tests. Data is also being collected on normal subjects. Although all the current measurements are on the ulna, the technique has been applied to the mandible, tibia, clavicle and skull.

The equipment for making the measurements is basically simple and inexpensive. Details can be obtained by writing the authors.

REFERENCE

Jurist, John   Determination of Elastic Properties of Bone:

1. Theory, Apparatus and Method of Ulna Resonant Frequency Determination, Physics in Medicine and Biology; to be published.
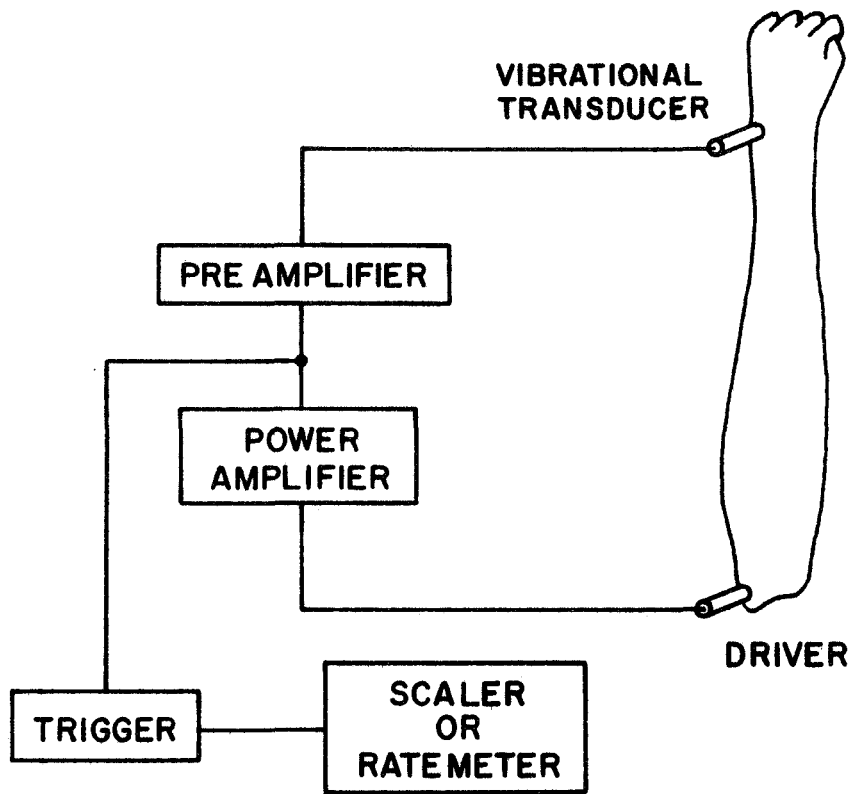
Figure 1 – Block diagram of system
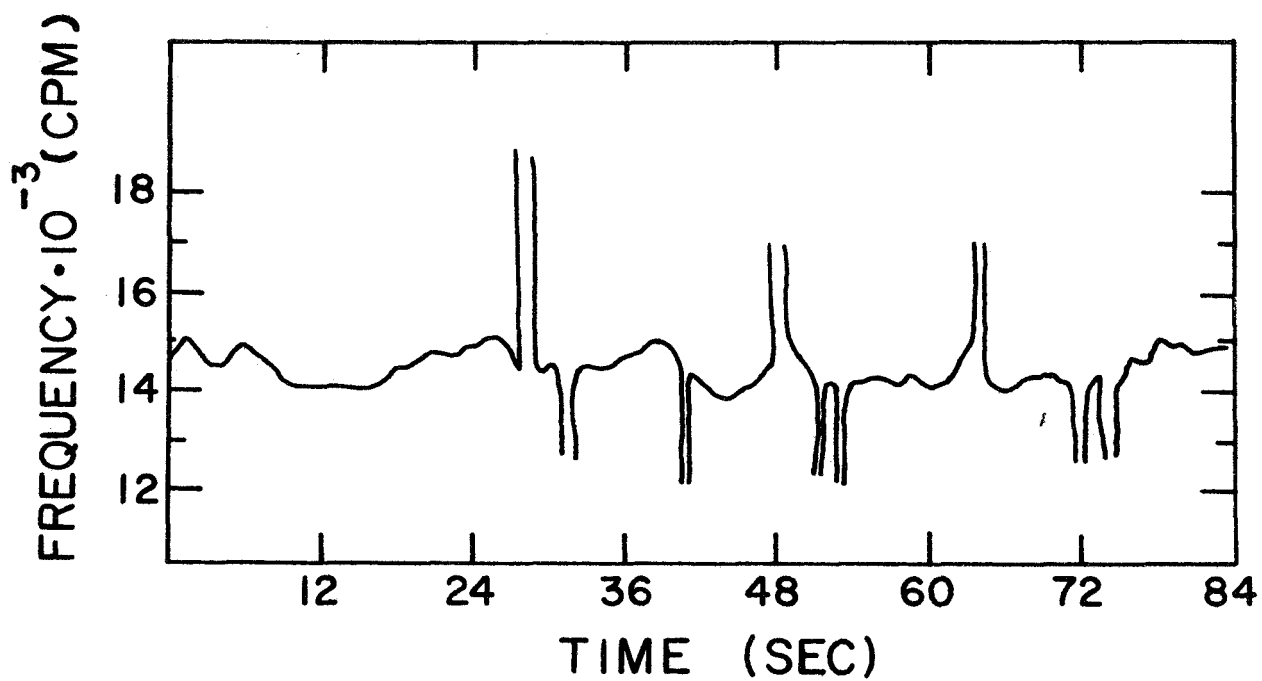
Figure 2 – Frequency of oscillation of ulna for period of 84 sec.

BODY COMPOSITION BY ABSORPTIOMETRY

OF MONOENERGETIC RADIATION

Richard B. Mazess, John R. Cameron and James A. Sorenson

Several authors have indicated that the fractional composition of a multi-component material can be determined through measuring the attenuation of gamma radiation by the substance at several energies. The attenuation of mono-energetic radiation in a single absorber is described by:

$$I = I_o^{-\mu x} \qquad \text{or} \qquad \log I_o - \log I = \mu x \qquad (1)$$

where I is the beam intensity after passing through the absorber, I_o is the initial beam intensity, μ is the mass absorption coefficient (cm^2/g) of the absorber, and x is the mass of the absorber (g/cm^2) in the beam. For a complex absorber the total absorption coefficient (μ_t) at any single energy is the sum of the fractional absorption contributions of the various components of the material:

$$\mu_t = \mu_a f_b + \mu_b f_b \cdots \cdots + \mu_n f_n \qquad (2)$$

where μ_a is the absorption coefficient of component a, and f_a is the fractional contribution of a to the total mass. For a material composed of n components it is possible to derive the fractional composition by solving a series of n equations of the form of (1), and using equation (2), where each equation describes an absorption measurement at a different energy. In practice, however, it is quite difficult to use absorptiometry at different energies for composition of complex mixtures because of the cumulative uncertainties of the measurements at each energy. Moreover, it is difficult to obtain convenient mono-

energetic sources in many of the most useful energy ranges.

We have previously suggested in several publications that absorption measurements at two energies could be used to measure the relative composition of: (1) lean cellular mass versus fat mass in soft-tissue in vivo and (2) organic versus inorganic (mineral) in excised bone. In most of our work to date absorption measurements were done with ^{241}Am (60 kev) or a tin-filtered ^{125}I source (27.4 kev). A conventional single channel analyzer system with scaler/timer and digital output has been used. The ratio of ^{125}I absorption to that with ^{241}Am provides a direct index of relative composition. For example, in bone 100% mineral gives a ratio of 7.0 and 100% collagen 2.0; in soft-tissue 100% lean gives a ration of 2.10 and 100% fat 1.52. In typical dry bone a 2% uncertainty in the ^{125}I/^{241}Am gives a fractional uncertainty of 0.02. In typical human soft-tissue a 2% error in the ratio gives an uncertainty in fractional composition of about 0.06 to 0.07. Thus, soft-tissue composition measurements require absorption determinations of high precision and accuracy.

Our initial work in measuring the collagen-mineral composition of bone was incomplete, but suggested that relative composition could be measured within about 2%. Far more extensive work has been done in evaluating the composition of soft-tissue. Precision and accuracy have been assessed using various soft-tissue phantoms (polyethylene and sodium acetate; paraffin and water) as well as meat samples (fat content determined by lipid extraction). Measurements were made at a

single location in mixtures of known composition. The
uncertainties in the $^{125}I/^{241}Am$ ratio were held to about
1 to 2%; use of water and lard as absorption standards
halved the variability associated with varying measurement
conditions. Fractional composition in these experiments
was estimated within about 0.03 and the correlation coeffi-
cients were about 0.98.

The first applications of absorption methods for soft-
tissue measurement were limited to single point measure-
ments. With careful repositioning the reproducibility of
these measurements was high, and with high total counts the
error of the $^{125}I/^{241}Am$ ratio was held to 0.5%; this allowed
an uncertainty of only 0.02 in the fraction of fat. However,
small variations in positioning of a single point can lead
to large compositional differences in the same person, and
it is difficult to locate corresponding points in any series
of subjects. Consequently a scanning method has been developed
to allow determination of composition in a linear path across
an accessible area, usually the middle of the upperarm. Scan-
ning across a limb aids relocation in the same person, and
facilitates intercomparison among individuals. Repositioning
may alter the total tissue mass scanned but the relative compo-
sition of the limb is fairly uniform thus eliminating a major
source of error. In addition, the scanning procedure permits
direct determination of the lean cellular, fat, and bone mineral
mass at the measurement site. Theoretically a third energy
would be needed to have simultaneous absorptiometric measurement

of bone mineral together with soft-tissue. However, the
absorption coefficient of bone mineral is much greater than
that of soft-tissue and the mineral absorption is sharply
demarcated in the typical scan. This permits separation of
the mineral absorption without use of the third energy.
Typical upperarm scans on a fat person, and on a thin person,
are shown in Figure 1. Immediate reproducibility of these
scans is high; in a series of replicate scans on 63 subjects
the uncertainty for bone mineral content was 2% while that for
soft-tissue absorption was about 0.5%.

There are several problems associated with this new
scanning procedure. Subject movement can seriously affect
results; we find it advantageous to use the average of several
fast-speed scans to minimize this problem. Sources of high
activity are needed to insure adequate counts during the scan
of the tissue and bone. Such sources will give high count
rates with an unattenuated beam and appropriate corrections
must be made for loss of counts due to system deadtime. In
scanning the upperarm we use a detector collimation of 3-mm with
a 100 to 200 mCi source of ^{125}I and 6-mm with a 125 mCi source
of ^{241}Am; the source collimator distance is about 17 cm.
Larger collimation produced problems with scattered radiation.
The radiation from ^{241}Am is monoenergetic but ^{125}I has several
low energy peaks and suitable tin filtering is necessary to
insure a narrow spectrum. Contaminants in ^{125}I sources,
including ^{126}I, may give problems. Brehmstrahlung sources,
or other low energy sources such as ^{109}Cd or ^{210}Pb, may prove
useful. To insure the best precision and accuracy calibration

standards should be used with the same geometry and general conditions as in subject measurement.

Replicate scan determinations of soft-tissue absorption were made on nine subjects after a six-month interval to assess long-term precision. The error for both ^{125}I and ^{241}Am scans was about 2.5%. The ratio of the ^{125}I to ^{241}Am tissue scans was more highly reproducible, indicating that part of the difference between scans at the two times reflected actual changes of soft-tissue mass, most probably due to repositioning. The mean difference between the ratios at the two times was about 1.7%. In two subjects remeasurements were made five times each during a nine month period (Table 1). Even without careful relocation of scan sites it appears that soft-tissue absorption can be determined reliably (2 to 3% error), and the ^{125}I/^{241}Am ratio can be measured with even higher precision (about 1%). An error of this magnitude is negligible with regard to the lean-tissue mass in a limb, but under usual conditions translates into an error of about 3 to 4% in the relative fat content.

. . . .

Table 1 – Repeat measurements at 5 times over a 9-month period in two subjects

Subject		^{241}Am Tissue Scan	^{125}I Tissue Scan	Ratio ^{125}I/^{241}Am
RW	Mean	69.6	144.2	2.070
	SD	1.95	3.72	0.006
	CV	2.80%	2.58%	0.27%
RBM	Mean	104.5	214.2	2.045
	SD	3.07	8.32	0.026
	CV	2.94%	3.88%	1.28%

. . . .

On a standard measured several times the coefficient of variation was about 1.2% for both ^{125}I and ^{241}Am scans, as well as for the $^{125}I/^{241}Am$ ratio. This error amounted to 0.019 units or about .033 in fractional composition.

We are currently studying the composition relationships at different body sites and examining the association of these measurements with total body composition, as measured by whole-body ^{40}K counting, hydrometric body density, and tritium dilution. In 19 subjects measured in preliminary work we found a high correlation (r = 0.98) between the absorptiometric measure of soft-tissue mass and circumference of the upperarm. In these same subjects the $^{125}I/^{241}Am$ ratio was highly negatively correlated (r = 0.91) with the tricaps fatfold measurement (using Lange constant tension calipers).

We do not feel that the absorptiometric measures are merely costly and time-consuming elaborations of anthropometric and fatfold measures, but rather that soft-tissue absorptiometry eliminates the many errors inherent in the latter indirect measures and will provide precise and accurate indications of both local and total body composition. For example it appears that composition of the upperarm in young adults is about 16% fat, 81% lean-tissue, and 3% bone mineral. Similar values might be expected for total body composition. Total soft-tissue, lean-tissue, and bone mineral mass and the relative composition can be measured with very high precision and accuracy; the relative fat composition involves a somewhat greater error.

The absorptiometric measures have already been used to evaluate soft-tissue and compositional changes during low

protein-low calcium diet(see USAEC Report COO-1422-

Further data is being collected to define normative patterns

to aid in clinical and diagnostic applications, and to provide

ancillary information to absorptiometric evaluation of skeletal

status. We are also evaluating use ^{109}Cd to determine the

water and fat content of adipose tissue; this will provide

a clinical and diagnostic index of obesity.
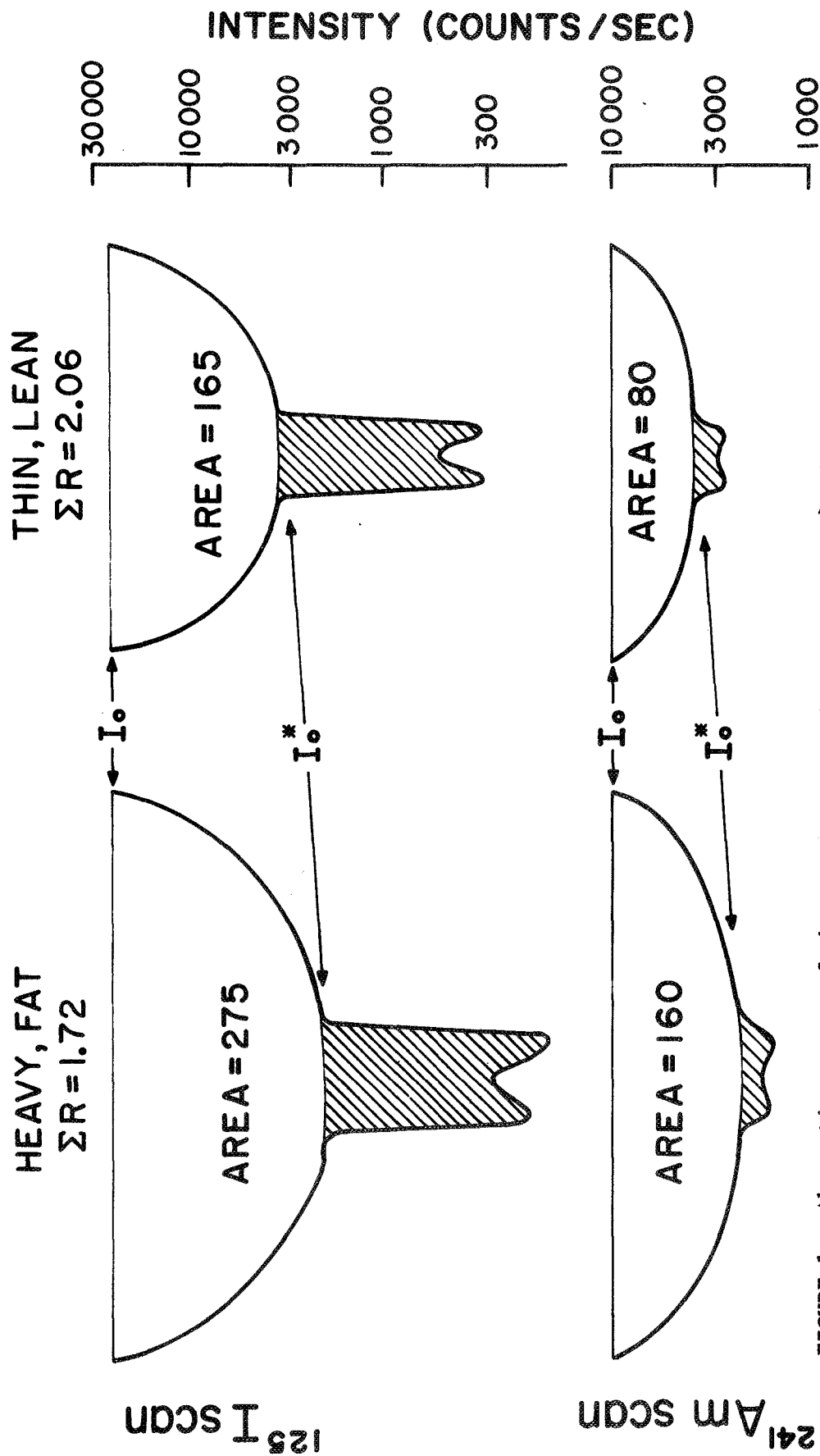
FIGURE 1. Absorption scans of the upperarm in a heavy, fat person (left) and a thin, lean person (right). The unshaded area represents soft-tissue absorption and is proportional to the tissue mass; the shaded portion represents the absorption by bone and is proportional to the bone mineral mass. The fat person has greater soft-tissue absorption, particularly with americium; consequently the ratio of the iodine-125 scan to the americium-241 scan is lower in the fat person (1.72) than in the thin person (2.06). A ratio of 1.52 indicates 100% fat (0% lean) while a ratio of 2.10 indicates 0% fat (100% lean).

A PORTABLE UNIT FOR DETERMINATION OF BONE
MINERAL CONTENT BY PHOTON ABSORPTIOMETRY
Richard B. Mazess and John R. Cameron

In last years progress report we described our initial
work on the portable bone mineral unit (COO-1422-39). In
nearly all work in this laboratory over the past 10 years the
digital count data for bone mineral absorptiometry was obtained
from a scaler/timer and analyzed on a desk-top calculator or
computer. This procedure was time-consuming, required expensive
interfacing and output equipment, and was error-prone. A
technician or programmer was needed to handle the data and
inspection of data was delayed. The new portable system uses
analog rather than digital techniques; immediate direct digital
readout of bone mineral content and bone width is provided.

The portable electronics system consists of a high voltage
supply for the photomultiplier tube, preamplifier-amplifier, and
single channel analyzer. Instead of a scaler/timer, however, the
analyzer output goes to a ratemeter and then to a novel logarithmic
converter-integrator unit (Figure 1). This unit provides
logarithmic conversion of the ratemeter signal. An initial
adjustment is made for each bone scan to compensate for the
varying baseline level (reflecting soft-tissue absorption).
The deflection from the baseline level is detected by a comparator
which activates a reed relay to start and stop integration.
This threshold level can be adjusted for use with different
photon sources. Mineral content and bone width are determined
with the integrator circuits; integration is linear over the
useful range, leakage is low, and the values obtained are displayed

on a digital panel meter with high input impedance.

In one experiment 6 ashed bone sections were scanned repeatedly (10 times each) at both fast and slow speeds (1 and 0.5 mm/sec). The bones were scanned under 5 cm of water to simulate actual scanning conditions and to maintain an equal "soft-tissue" thichness across the bone. The immediate precision of the scans was very high (Table 1); similar values for

. . . .

Table 1. Precision of repeat measurements on ashed bone sections.

	MINERAL	WIDTH
Slow-speed	0.93%	0.64%
Fast-speed	1.32%	0.76%
Average	1.12%	0.70%

. . . .

precision were observed in other work over several months. On larger bones, or with slower-speed scans, the precision is increased. Typically the uncertainty in measuring bones would be half these figures since we routinely make 4 repeat measurements at each scan site.

The absorptiometric measurement of mineral content was highly correlated (r= 0.998) for both fast and slow-speed scans. for fast-speed scans the standard error of estimate was 0.028 grams (or 2.6%). This is slightly better accuracy than obtained on ashed sections using our previous digital output techniques. It should be noted that part of the error is associated with nonuniformities in the ashed bone sections, rather than in uncertainities of the method. Scans on Al standards of uniform

shape demonstrate an uncertainty of about 1.0%; this indicates that the accuracy of the method is limited by precision which in turn reflects photon counting statistics.

Over the past year we have been collaborating with the Instrumentation Systems Center of the University of Wisconsin in design and construction of the electronics of a portable direct readout system similar to the unit described above. This unit could be readily constructed by other investigators; also the schematics will be made available to any laboratories of firms wishing to produce this instrument. We have cooperated with one such firm, Norland Associates of Fort Atkinson, Wisconsin in their efforts to construct a complete direct readout bone scanning unit. Ready availability of these units will greatly increase their use in biomedical investigations and clinical evaluation.

FIGURE 1

A - Ratemeter, output
B - Log. output and
    baseline set
C - Bone width
D - Bone mineral
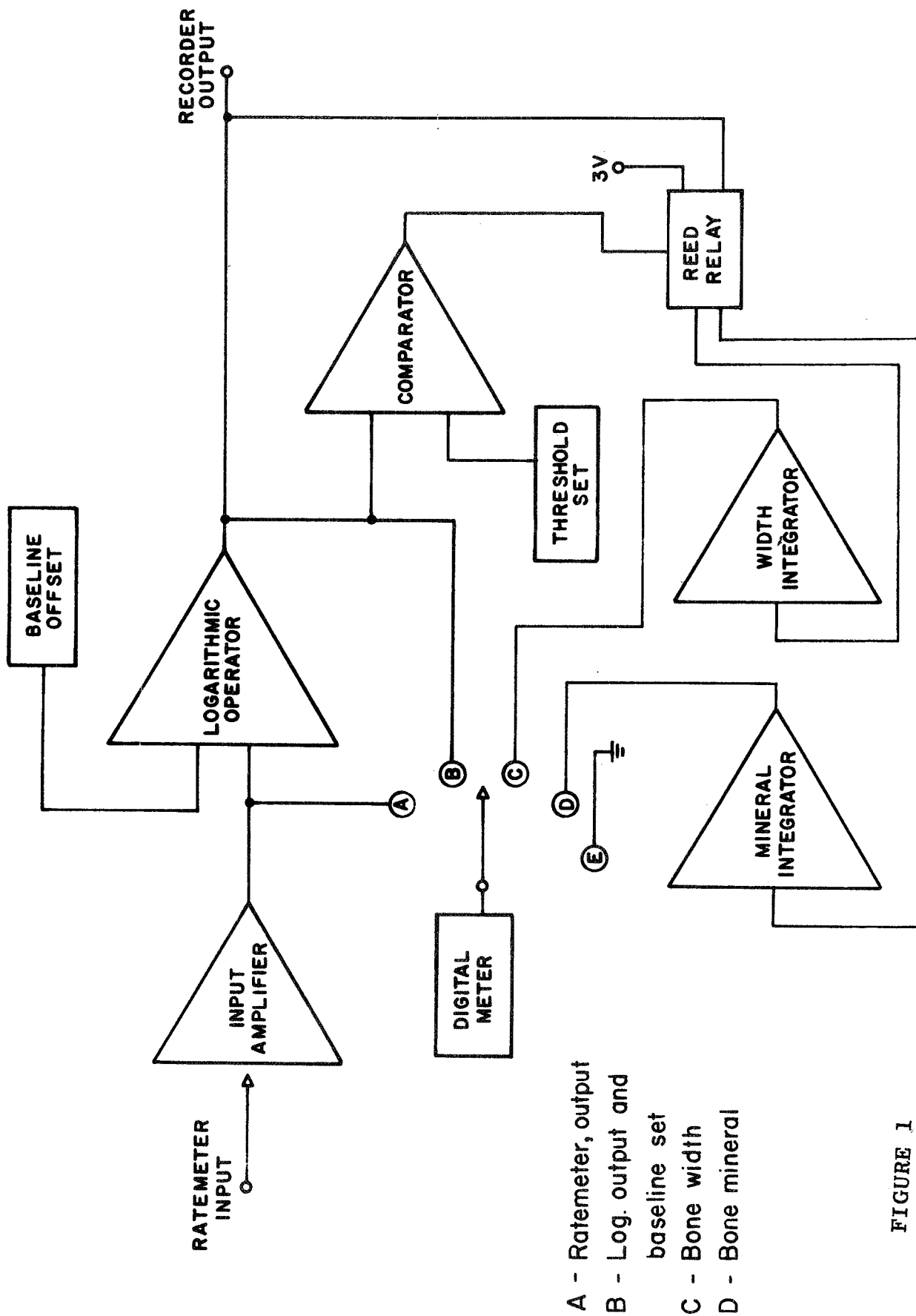
BONE AND SOFT-TISSUE CHANGES DURING
PROTEIN-CALCIUM RESTRICTION

Richard B. Mazess

A study was initiated by Vivian Bruce (Dept. of Foods
and Nutrition, University of Wisconsin) to ascertain nutrient
balance in man on a low calcium (500 mg/day) low protein diet.
All of the dietary protein was derived from vegetable and
cereal sources. A 10-day control period preceded the dietary
modification, and the special diet was given for 36 days.
Complete nutrient balance determinations were made on 6 young
adult males throughout the control and diet periods. Bone
mineral content, and soft-tissue mass and composition, were
monitored using photon absorption methods. The subjects were
measured on 6 occasions – twice during the control period, and
on days 7, 16, 25, and 36 of the special diet.

Bone mineral content was measured on the forearm bones
using an ^{125}I photon source; the locations were at "midshaft"
(33% from the distal end of the bone) and distal (20% from
the distal end) of the radius and ulna. In addition, scans
were made across the entire middle upperarm with both ^{125}I
and ^{241}Am sources. This permitted measurement of the mineral
content at mid-humerus; soft-tissue mass and the relative fat-
lean cellular composition of the upperarm also could be calcu-
lated from these scans.

RESULTS

The bone changes at the 5 sites on the 3 bones are
given in Table 1. The values for the two control period obser-

Table 1 - Bone mineral changes in 6 subjects during dietary period; mineral (grams/cm), width (cm).

		MIDSHAFT			DISTAL		
		Mineral	Width	Min/Width	Mineral	Width	Min/Width
RADIUS	Control	1.308	1.416	0.924	1.366	1.652	0.827
	day 7	1.337	1.443	0.926	1.367	1.682	0.813
	day 16	1.317	1.445	0.911	1.338	1.676	0.798
	day 25	1.297	1.432	0.906	1.327	1.677	0.791
	day 36	1.320	1.442	0.915	1.323	1.652	0.801
ULNA	Control	1.174	1.296	0.908	0.882	1.142	0.772
	day 7	1.172	1.285	0.912	0.888	1.155	0.769
	day 16	1.167	1.333	0.875	0.875	1.145	0.764
	day 25	1.172	1.312	0.893	0.873	1.167	0.748
	day 36	1.173	1.347	0.871	0.855	1.150	0.743
HUMERUS	Control	1.780	1.422	1.252			
	day 7	1.759	1.414	1.244			
	day 16	1.755	1.414	1.241			
	day 25	1.755	1.390	1.262			
	day 36	1.757	1.418	1.239			

vations were averaged. There did not appear to be systematic changes in the mineral content at the midshaft of the radius, ulna or humerus; probably relocation errors at these sites overshadowed any real changes. In contrast the distal radius and ulna sites showed gradual decreases of mineral content (2 to 3% loss) during the diet period. Expressing the mineral content per unit bone width tends to remove some of the effects of relocation error; when this is done a fairly gradaul decrease in bone mineral is evident at all sites. The loss amounts to 2 to 3% on the radius, about 4% on the ulna and about 1% on the humerus (excepting the aberrant value from day 25). Apparently some bone mobilization did occur during the diet period, but this was not uniform on all bones. Even a calcium loss of 1 to 2% (10 to 30 g) would appear highly improbable in this short period of time.

The values for body weight, fatfold (Lange constant tension calipers), and arm circumference are given in Table 2 together with the calculated cross-sectional area of the arm. During the control period there was about a 1-kg loss of body weight which probably can be ascribed to hypohydration. This was remedied during the dietary period through adequate liquid intake; consequently the total 2-kg loss of weight can probably be ascribed to loss of fat and cellular material. The fatfold measurements were very unreliable, as has been the general experience with this technique. The changes in the fatfold values may wholly reflect measurement error. Arm circumference decreased during the study; the decrease in the cross-sectional

areas of the arm, derived from circumference, probably more closely reflects the changes occurring. Still arm circumference, and the derived area, are relatively unreliable and indirect measurements.

....

TABLE 2 - Weight, fatfold, arm circumference and arm cross-sectional area in 6 subjects during dietary period.

	WEIGHT	FATFOLD	CIRCUMFERENCE	AREA
Control (1)	73.7	9.70	27.4	59.74
Control (2)	72.8	8.60	27.1	58.44
day 7	72.4	7.25	27.5	60.18
day 16	72.1	7.67	27.3	59.31
day 25	71.8	7.33	27.1	58.44
day 36	71.7	8.00	26.8	57.16

....

The absorptiometric scan data is given in Table 3. Both ^{125}I and ^{241}Am soft-tissue scan values decreased during the dietary deprivation period, but the decrease in the ^{125}I values was only about 4% compared to the 6% decrease in ^{241}Am values. Consequently the ratio of ^{125}I to ^{241}Am, which reflects relative composition, changed from an initial value of 2.00 to about 2.04. This corresponded to a change from 16.5% fat to about 9.5% fat. A ratio of 1.52 indicates 100% fat, while a ratio of 2.10 indicates 100% lean cellular matter.

The calculations indicated that initially (during the control period) there was a transient decrease of absorption and decrease in the $^{125}I-^{241}Am$ ratio. This increase of relative fatness with loss of tissue probably corresponds to the transient water loss during the control period. The absorption characteristics of water make it appear essentially the same as muscle. It is interesting that this small decrease (about 2%) in total body water was detectable in the upperarm measurement.

The scan values can be converted to tissue mass using experimentally derived constants; a constant of 0.287 is used for ^{125}I scans and 0.575 with ^{241}Am scans (the ^{125}I constant varies with composition). The tissue composition of the upperarm can be readily calculated, for example; bone mineral 1.78 g; soft-tissue mass 56 g; fat mass 9.3 g; lean cellular mass 46.7 g; fatfree mass 48.5 g. The bone mineral was about 3.7% of the fatfree mass; this is similar to the value expected for the total body (about 4%). These calculations also showed that the calculated cross-sectional areas were close to the areas expected when account is taken of the bone mineral content and the density of the soft-tissue. However, the calculated tissue loss based on area would be about 2.8 g if this loss were mostly fat (as appeated to be the case). In contrast the loss based on absorption measurements was about 3.6 g. The absorption measurements also indicated that the 3.6 g net change consisted of 4.3 g decrease of fat, and a 0.7 increase of the cellular component (presumably water).

. . . .

Table 3 – Absorptiometric determinations of upperarm composition in 6 subjects during the dietary period.

	^{241}Am scan	^{125}I scan	^{125}I/^{241}Am	% fat
Control (a)	97.72	195.83	2.004	16.55%
Control (b)	96.56	191.82	1.986	19.59
day 7	95.97	194.56	2.027	12.55
day 16	92.43	188.47	2.039	10.52
day 25	91.81	187.85	2.046	9.33
day 36	91.37	186.76	2.044	9.66

. . . .

CONCLUSIONS

These studies show the feasibility of monitoring bone and soft-tissue alterations in nutritional studies through use of

photon absorption methods. In the present study measurement reliability was adversely affected by changes of sources, detectors, detector collimation, and scanners. In continuing studies newer techniques should be used to minimize relocation of the measurement sites, and calibrated standards would minimize errors due to equipment variation. Despite these difficulties it was possible to detect rather small decreases in bone mineral content and soft-tissue composition. However, these local changes may not reflect the magnitude of total body changes; a 2% loss of total body mineral or a change from 16 to 9% body fat were not realistic. One major conclusion appears to be that changes of body composition may not be uniform at all sites and that some areas could serve as sensitive indicators of processes occurring with lesser intensity in the body as a whole.

EVALUATION OF RADIONUCLIDE SOURCES FOR TRANSMISSION SCANNING

By James A. Sorenson and John R. Cameron

Transmission imaging using scanning and counting techniques was demonstrated by Mayneord in 1954 (1) and subsequently developed by Kuhl and co-workers (2) as a method of obtaining anatomic information for accurate keying of radionuclide emission images obtained on a rectilinear scanner. Techniques have also been developed for transmission imaging with a scintillation camera (3). Transmission images have been reported to be of value for outlining air spaces and organs in the chest for the interpretation of lung and heart scans, and for outlining bony structures in the head and the pelvis for the interpretation of brain scans and bone scans, respectively (2,4,5). Transmission scanning of small animals and of the extremeties was also reported by Kuhl (2). The advantage of transmission scans over roentgenographic images is the lack of geometric distortion relative to the emission image.

Various radionuclide sources have been used for obtaining transmission images on rectilinear scanners and scintillation cameras, principally I-125 (30 keV), Am-241 (60 keV), and Tc-99m (140 keV). Of these, only Tc-99m has been shown to be useful for scintillation camera studies, primarily because of the loss of spatial resolution with this device at lower photon energies. Rectilinear scanners do not have this limitation, and consequently any of the above mentioned sources and a variety of others are potentially useful for transmission imaging with a scanner.

The purpose of this paper is to provide an evaluation of a

number of transmission scanning sources for various transmission imaging procedures.

I. THEORETICAL CONSIDERATIONS

The properties of a radionuclide photon source which affect the quality of the tranmission image are listed in Table I. Photon energy affects the image contrast since the absorption differential between objects of different elemental composition (e.g. bone vs. soft tissue) increases with decreasing photon energy. Image information density decreases with decreasing photon energy for sources of the same activity, because transmission decreases. Slower scanning speeds can be used with lower energy sources to improve information density but practical limits may exist especially when working with very ill or uncooperative patients. Image definition or spatial resolution may be affected if a high energy photon source is used because of difficulties in collimating the photon beam. The latter is not a problem, however, at photon energies below about 200 keV when lead is used for the collimator material.

Image contrast and definition are also dependent on the monochromaticity of the photon source, especially when a low energy source with an apparently small number of higher energy emissions is used. The lower energy radiations are more easily absorbed and in fact may be almost completely stopped in thicker sections, with only the higher energy photons being transmitted. In this situation, the transmission source behaves as if only the higher energy photons were being emitted, and image contrast and definition are characteristic of a source emitting the higher energy radiations.

The amount of activity obtainable, or more specifically, the photon emission rate of the source, affects image information density unless an unlimited scanning time is available.

Source dimensions affect image definition in the same way as does the detector collimating aperture diameter, with a larger source diameter resulting in an image with poorer definition. Source dimensions and resultant resolution loss may be a problem with radionuclides having a low specific activity and a high atomic number. An example is Am-241 (Z = 95) which has a long half-life (463 years) and consequently a low specific activity (3.4 Ci/gm). Am-241 behaves as a surface emitter, since the 60 keV γ-ray emissions are almost totally absorbed by a fraction of a mm of overlying americium (HVL = 0.065 mm for ρ = 11.7 gm/cm^3, Z = 92, at 60 keV) (6). Because of this an increase in source emission rate requires an increase in source emission area, rather than source thickness. Consequently image definition may be lost if source activity must be increased.

The important parameters of image quality, namely contrast, definition, and information density, are all affected by the photon energy of the transmission source. The effects of photon energy on contrast and information density are shown quantitatively in Figure 1. Percent transmission through the various body regions from 30 to 140 keV was calculated assuming the lungs to have a transmission equivalent to 10 gm/cm^2 of water, abdominal areas 20 gm/cm^2 of water, and the abdominal spine and pelvis 20 gm/cm^2 of water plus 1-2 gm/cm^2 of bone mineral (calcium hydroxyapatite)(7). The curves are presented semi-logarithmically, so that contrast between various body regions

is reflected by the separation between the various curves.
For example, the separation between curves labelled lung and
abdomen reflects the contrast between air spaces in the chest
and soft tissue masses, while the separation between the curves
for the abdomen and the spine and pelvis reflects the contrast
between bony structures and soft tissue in abdominal areas.

From these curves, it is apparent that adequate contrast
is obtainable in transmission imaging of the lungs at practically
all photon energies. Thus it would be profitable to choose a
higher photon energy for lung imaging which maximizes transmission
rate and image information without giving collimation and
shielding problems, i.e., 100 - 200 keV. Contrast between
bony structure and soft tissue in the abdominal spine and pelvis
on the other hand is much less at all photon energies, and
transmission imaging in the area may require the use of a lower
energy photon source with a consequently less transmission and
information density in order to obtain adequate image contrast.
The lowest photon energy usable for transmission scanning
procedures is probably about 30 keV for thick sections (>10 cm)
although lower energies may be usable for thin sections and
small animals.

With these considerations in mind, it is convenient to
categorize photon sources into different photon energy ranges.
The curves in Figure 1 are each composed of two essentially
straight-line portions; a low energy range from about 20-40
keV in which contrast is high and transmission relatively low,
and a high energy region (80 keV and up) of low contrast and

relatively high transmission. In the low energy region a small keV difference in energy results in a relatively large difference in contrast and transmission while in the high energy region, the behavior is rather constant with energy. Between the straight line portions is a curved transitional region of inter-mediate energy (40-80 keV) in which the behavior of contrast and transmission are intermediate to that of the low and high energy regions. For the remainder of this discussion, trans-mission sources will be dicussed according to whether they fall into low (20-40 keV), intermediate (40-80 keV) or high (80 keV and up) energy regions.

II. EXPERIMENTAL EVALUATION OF RADIONUCLIDE SOURCES FOR TRANSMISSION SCANNING

Methods and Materials

An experimental evaluation of various source materials was carried out by obtaining transmission images of phantoms and human subjects on a dual-headed rectilinear scanner with 5" dia x 2" thick NaI(Tl) detectors (Model 54FD, Ohio-Nuclear Inc., Cleveland, Ohio)(Figure 2). The anterior or upper detector was used for transmission studies, and was collimated with a 3 mm or 6 mm dia x 70 mm thick straight bore lead collimator. The transmission source was placed directly over the center holes of the focussed collimator on the posterior or lower detector. The transmission source-detector separation was 30 cm.

Transmission sources studied were as follows:

I-125 (30 keV): 100-200 mCi plated on the hemispherical end of a 1 mm dia silver wire and encapsulated in a 0.56 mm

wall thickness aluminum container. The source had a
measured contamination of about 2 mCi I-126, a 386 keV
and 667 keV γ-emitter with a 13 day half-life (8)(Atomic
Energy of Canada, Limited, Ottawa, Ontario, Canada).

Pb-210 (46 keV): nominal activity 100 mCi, 4 mm emission
diameter, encapsulated in steel with a 1 mm thick aluminum
emission window (Source #RBC.6, The Radiochemical Center,
Amersham, England).

Am-241 (60 keV): nominal activity 125 mCi with 5 mm
emission diameter, encapsulated in steel with 0.8 mm
aluminum emission window; source fabrication in our
laboratory.

Tc-99m (140 keV): a rechargable "point" source, with the
active element consisting of a 3 mm dia x 6 mm long ion-
exchange resin column. The source was normally used with
an activity of 10-30 mCi Tc-99m. Details of source con-
struction and method of recharging are described elsewhere.(9)

Cs-137 (662 keV): activity 10 mCi in a 3 mm dia bead of
cesium glass, encapsulated in steel with a 1 mm steel
emission window. (Source #CDC-K1, Nuclear Chicago Corp.,
Des Plaines, Illinois.)

Phantom studies were carried out on a phantom consisting
of a sheet of aluminum 3 mm thick in which slots of various
widths (1.5 mm-12 mm wide) were milled to a depth of 2.5 mm.
The slot depth was chosen to provide a contrast between the
slots and the adjacent solid aluminum sections comparable to
that obtained for the lumbar spine (Figure 3). Transmission
scans were obtained with I-125 (low energy), Am-241 (inter-
mediate energy), and Tc-99m (high energy) with the phantom in
air, and with I-125 with the phantom under 10 cm of water.
Image information densities were 600-1000 c/cm^2.

Transmission images of human subjects were also obtained

with the various sources on a number of body areas including
the head, the chest, the lumbar spine and pelvis, and the
extremities. The information density of the images varied
from 100-600 c/cm^2 depending on the source and the scanning
speed. The scanning speed was chosen to approximate the speed
used in the accompanying radionuclide emission procedures.
For transmission images of the chest the speed was typically
3 cm/sec with 1/8" line spacing (lung scan) while for images
of the pelvis it was typically 0.5 cm/sec (bone scans).

Pulse height analysis of the transmitted beam using a
20 keV window centered on the principle photopeak was used for
all scans.

Results and Comment

Transmission images obtained on the aluminum phantom are
shown in Figure 4. Scans of the phantom in air indicate that
the best contrast and definition are obtained with I-125, which
has the lowest energy principle γ-emission, and also the
smallest active diameter (1 mm). Only gross detail is visible
in the Am-241 image, while the Tc-99m scan shows no contrast
at all. By comparison, the roentgenographic image has a contrast
intermediate to the I-125 and Am-241 scans. The use of I-125
or of a low energy source for transmission imaging of bony
structures in the pelvis is not indicated by these results,
however, because of the effects of a relatively small amount
of higher energy contamination. Also shown in Figure 4 is an
I-125 scan of the aluminum phantom under 10 cm of water. Much
of the contrast was already lost in this thickness of water
because of the selective absorption of the 30 keV photons and

transmission of 386 and 667 keV photons, in spite of the use
of a low energy pulse height analyzer window. The effect is
further exemplified by a transmission image of the pelvis
obtained with the same I-125 source (Figure 5). The resulting
image shows no contrast at all and is similar to that expected
from a transmission source of essenially pure I-126 of about
2 mCi activity. Transmission images with good contrast and
resolution were obtained on thinner sections such as the wrist
(Figure 6), where the penetration of the 30 keV photons was
considerably greater and the effects of I-126 contamination
were consequently less severe.

Transmission images of the pelvis obtained with an inter-
mediate energy source provided barely adequate visualization
of bony structure in the abdominal spine and pelvis, but the
image was definitely superior to that obtained with I-125
(Figure 7). An information density of 100-200 c/cm^2 was
obtainable at bone scanning speeds with the 125 mCi Am-241
source, which was felt to be adequate considering the relatively
poor resolution which could be obtained. It should be noted,
however, that because of the high self-absorption of 60 keV
photons within the Am-241 source, and because of the relatively
low photon yield (0.36 photons/ dis) of this material, that
the 125 mCi source actually emitted as a source with an apparent
activity of only about 40 mCi. An intermediate energy source
of 40 mCi activity which does not have the same limitations
as Am-241 might thus be usable for transmission imaging of the
pelvis.

Transmission images of the lungs showed adequate contrast,

but relatively poor resolution and information density (100-200 c/cm^2) when performed at lung scanning speeds (Figure 8).

Another intermediate energy source, Pb-210, was also evaluated as a transmission scanning source, but was found to be inadequate for imaging of the chest or pelvis. Although it has a convenient principle photon energy and half-life (46 keV, 22 years), its usefulness is limited by a very low photon yield (0.04 photons/dis). The 100 mCi source used thus had an apparent activity of only 4 mCi, which was considerably less than the minimum usable activity of 40 mCi suggested by the Am-241 experiments. No satisfactory transmission images on humans were obtained with the Pb-210 source.

Transmission images of the pelvis obtained with a high energy source, Tc-99m, displayed no bony structures (Figure 9). The small areas of decreased transmission seen in the image were produced by a belt buckle and a metal clip on a film badge. The use of metal objects placed at specified locations on the subject to provide negative shadows on a transmission image, such as is sometimes done in emission imaging procedures on the scintillation camera, would be the only way to obtain anatomic reference from transmission images of the pelvis using this source.

Good quality transmission images of the chest were obtained with the Tc-99m source with adequate visualization of the heart, the rib cage, the air space of the trachea and occasionally the aortic arches. A source activity of 20 mCi routinely resulted in an image information density of 600 c/cm^2 at a speed of 3 cm/sec and a line spacing of 3 mm.

Satisfactory transmission images of the skull were obtained with both the 125 mCi Am-241 source, and a 20 mCi Tc-99m source at typical brain scanning speeds (2 cm/sec) (Figure 11). Better definition and a higher information density were obtained with Tc-99m because the source emission diameter was smaller and the transmission rates were higher. Definition was also enhanced in the Tc-99m image because a smaller collimator aperture diameter could be used (3 mm for Tc-99m vs 6 mm for Am-241), while still maintaining a higher information density (600 c/cm^2, vs 150 c/cm^2) at the same scanning speed.

A transmission image of the chest obtained with Cs-137 was of poor quality (Figure 12). Although contrast was poor, it might have been adequate for outlining the air spaces of the lungs and the heart shadow. Resolution was very poor however, primarily because of difficulties in collimating the 662 keV photon beam. Cs-137 was also found to be unusable in any simultaneous transmission-emission procedure. Placing the 10 mCi Cs-137 source anywhere near the collimated emission detector resulted in count rates of the order of 100,000 c/min in any 40 keV pulse height window below the 660 keV, even when the source was shielded with 2 cm of lead. This background counting rate could not be tolerated in any emission scanning procedure.

Conclusions

Low energy transmission sources, such as I-125, provide high contrast and would thus be useful for transmission imaging of small bones and animals. Because of low transmission through thick sections, however, source activities of the order of a

Curie or more would be necessary for transmission imaging of the pelvis or lungs. This source would have to be very clean with respect to higher energy emissions, since low energy sources are particularly affected by relatively small amounts of higher photon energy contamination (~1.0%) when thick sections such as the pelvis are imaged.

Low energy sources other than I-125 which might be usable on small animals or thin sections are Cd-109 (22 keV, half-life 460 days) and Pm-147 (20-60 keV, half-life 2.6 years). The latter is a bremsstrahlung source which can be fabricated with various "target" materials to provide a variety of emission spectra (10). Both are commercially available as sealed sources (The Radiochemical Center, Amersham, England) but neither at present is available with an adequate photon yield for transmission imaging of the chest and pelvis.

Intermediate energy sources, such as Am-241, provide transmission images of the chest, pelvis, and skull with adequate contrast and information density when the source activity is equivalent to 40 mCi or more.

High energy sources, such as Tc-99m, provide the best images of the chest and skull but are not adequate for outlining bony structures in the pelvis. The use of metal objects overlying anatomic references may permit the application of this source in the pelvic area in some instances. Activities of the order of 10-20 mCi are adequate to provide information densities of about 300-600 c/cm^2 at lung scanning speeds.

Another possible high energy transmission source is Co-57 (120 keV, half-life 270 days). This material has the advantage

of a long half-life relative to Tc-99m, and also would be
simpler to use in simultaneous transmission-emission procedures
with Tc-99m as the transmission source because of the difference
in the photon energies. The latter is not a serious problem
with Tc-99m, however, when a dual-headed scanner is used, since
the transmission source is easily shielded from the emission
detector by a few mm of lead. (9)

Very high energy sources such as Cs-137 are not useful
for transmission imaging because of difficulties in collimating
the photon beam. Also, the higher energy sources are not
usable in simultaneous transmission-emission procedures with
a dual-headed scanner, because they cannot be adequately shielded
from the emission detector.

TABLE I

Properties of a Radionuclide Source Affecting the
Quality of the Transmission Image

	Image Parameter Affected		
	Contrast	Definition	Information Density
Photon energy	X	X	X
Monochromaticity	X		
Photon yield			X
Source dimensions		X	

References:

1. Mayneord, W.V.: Radiological Research, British Journal of Radiology 27: 309-317 (1954).

2. Kuhl, O.E., Hale, J., and Eaton, W.L.: Transmission Scanning: A Useful Adjunct to Conventional Emission Scanning for Accurately Keying Isotope Deposition to Radiographic Anatomy, Radiology 87: 278-284 (1966).

3. Anger, H.O., and McRae, J.: Transmission Scintiphotography, Journal of Nuclear Medicine 9: 267 (1968).

4. Briggs, R.C., Wilson, E.B., and Sorenson, J.A.: Combined Emission-Transmission Scanning of the Skeleton, Radiology 90: 348-350 (1968).

5. Westerman, B.R., Quinn, J.L., and Johnson, R.M.: Transmission Scanning as an Aid to the Interpretation of Routine Emission Scans, Journal of Nuclear Medicine 10: 381 (1969).

6. McGinnies, R.T.: X-ray Attenuation Coefficients from 10 KeV to 100 MeV, National Bureau of Standards Supplement to Circular 583, U.S. Department of Commerce (1959).

7. Ömnell, K.A.: Elemental Composition of Certain Animal Tissues, Acta. Radiol. Suppl. 148: 22 (1957).

8. Lederer, C.M., Hollander, J.M., and Perlman, I.: Table of Isotopes, 6th Edition, John Wiley and Sons, Inc., New York, (1967).

9. Sorenson, J.A., Briggs, R.C., and Cameron, J.R.: ^{99m}Tc Point Source for Transmission Scanning, Journal of Nuclear Medicine 10: 252-253 (1969).

10. Preuss, L.E.: A Compilation of Beta Excited X-ray Spectra, USAEC Document TlD-22361 (1966).

PERCENT TRANSMISSION

LUNG

ABDOMEN

SPINE-PELVIS

Figure 1.
Variation of transmission and image contrast with photon energy. Lung = 10 gm/cm^2 water, abdomen = 20 gm/cm^2 water, spine and pelvis = 20 gm/cm^2 water plus 1-2 gm/cm^2 calcium hydroxyapatite.

PHOTON ENERGY (keV)

20   40   60   80   100   140
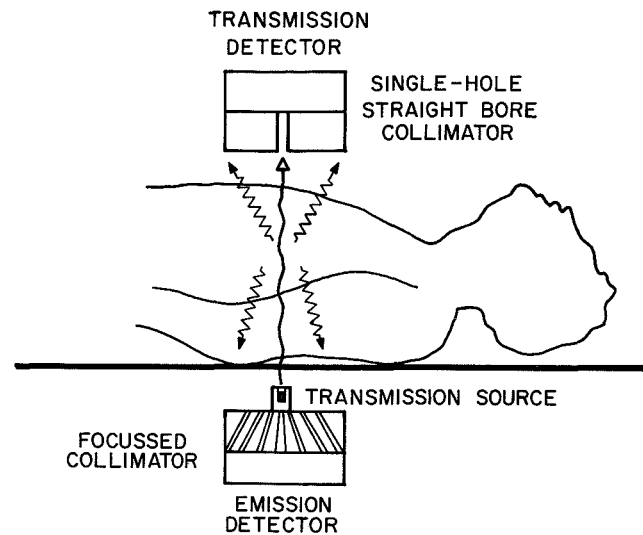
SIMULTANEOUS TRANSMISSION-EMISSION
SCANNING WITH A DUAL-HEADED SCANNER

Figure 2.   Use of a dual-headed scanner for transmission
scanning.   Simultaneous transmission-emission
procedures are possible.

**ALUMINUM PHANTOM
IN 10 CM WATER
100 KVP X-RAY**
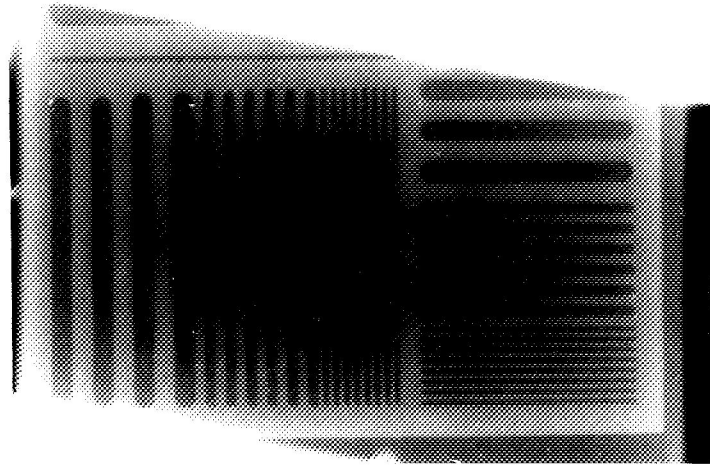
Figure 3. Roentgenograph of aluminum phantom.
Contrast is comparable to that obtained
for bony structures in the pelvis.
Line spacings are 1.5-12 mm.
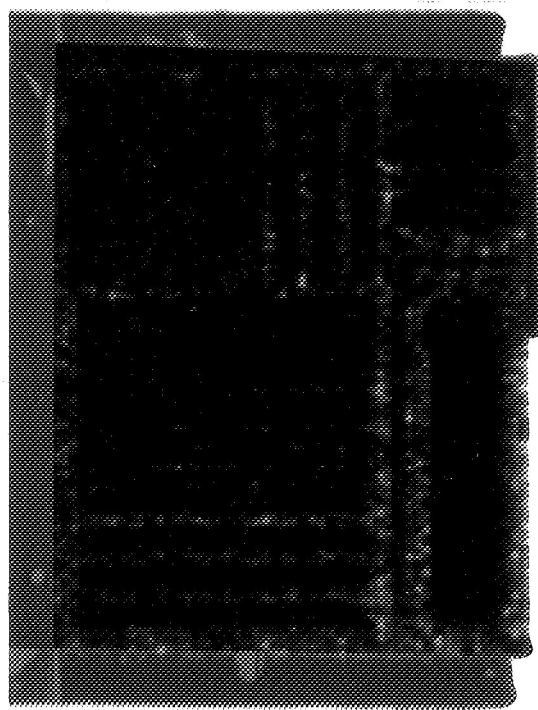
ALUMINUM PHANTOM
IN AIR, Am-241
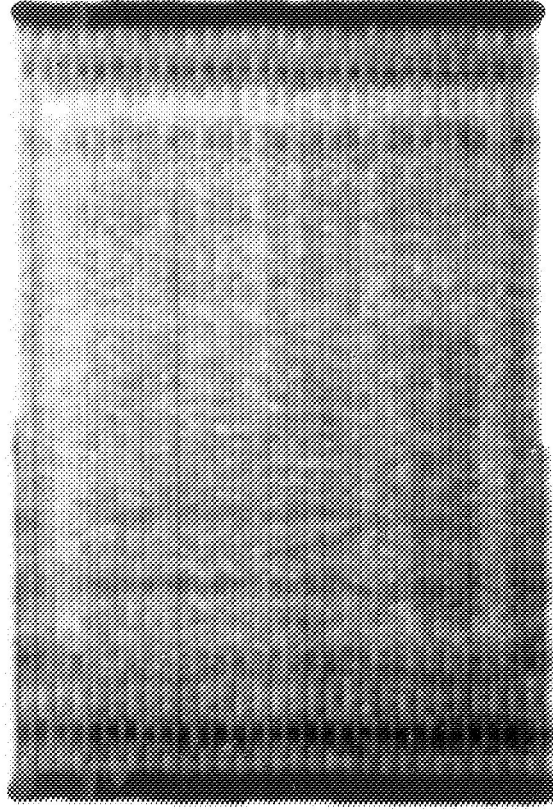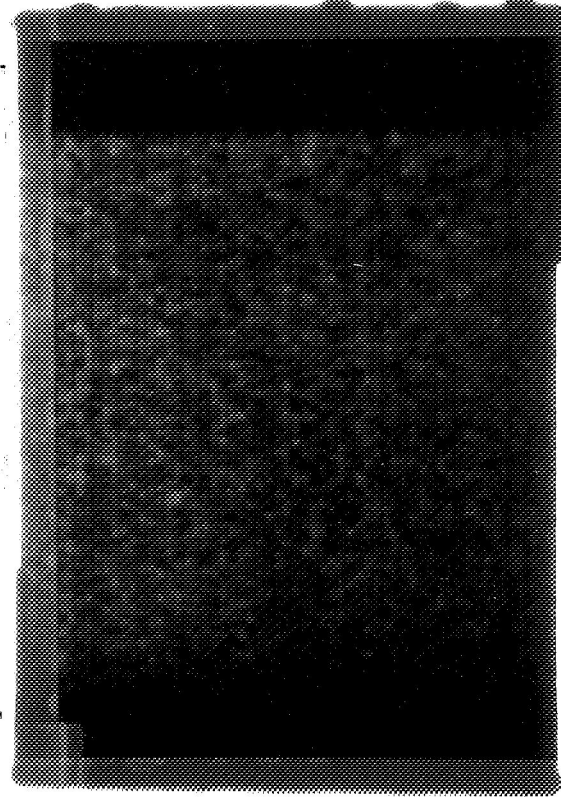
ALUMINUM
PHANTOM I-125

UNDER WATER

ALUMINUM I-125 IN AIR
PHANTOM

ALUMINUM PHANTOM
IN AIR, Tc-99m
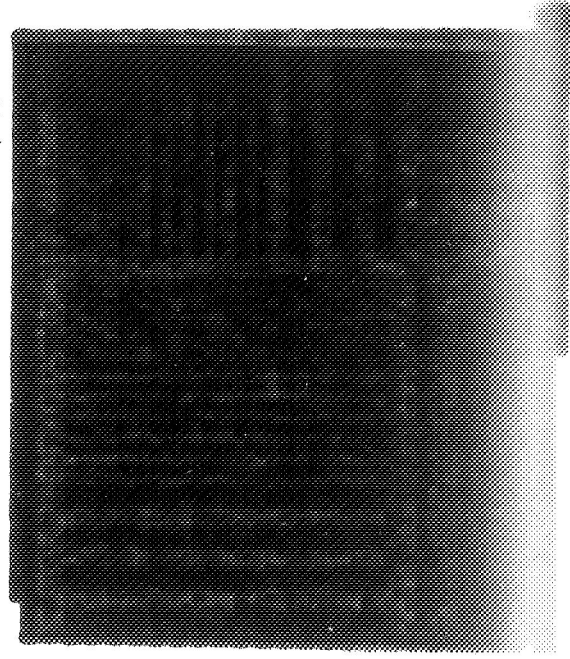
Figure 4. Transmission scans of the aluminum phantom in air with a) I-125,
b) Am-241, and c) Tc-99m, and d) of the phantom under 10 cm of
water with I-125.
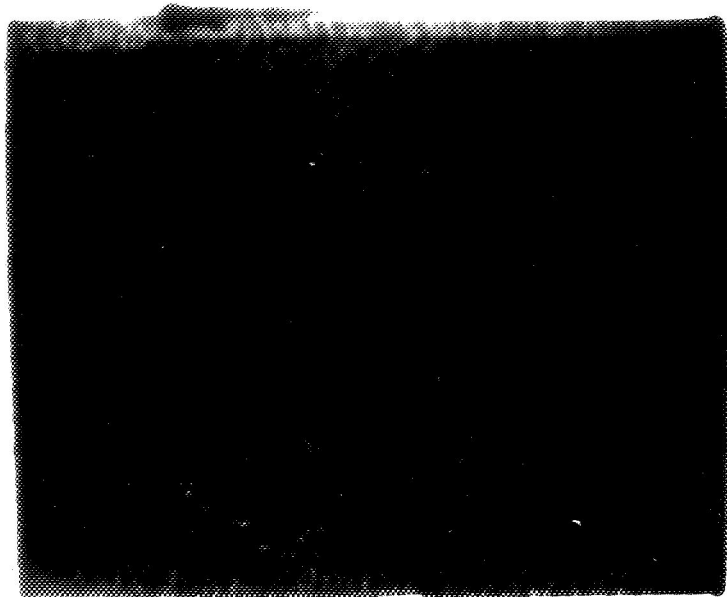
I-125 SCAN OF PELVIS

Figure 5. Transmission scan of the pelvis of an
average adult with I-125. Approximately
1% I-126 contamination was sufficient to
wash out contrast in this thick body
section.

I-125 SCAN OF DISTAL RADIUS AND ULNA

Figure 6. Distal forearm with I-125. Resolution
and contrast are adequate for visualization
of the medullary canal and of a mineral
deposit in the wrist.
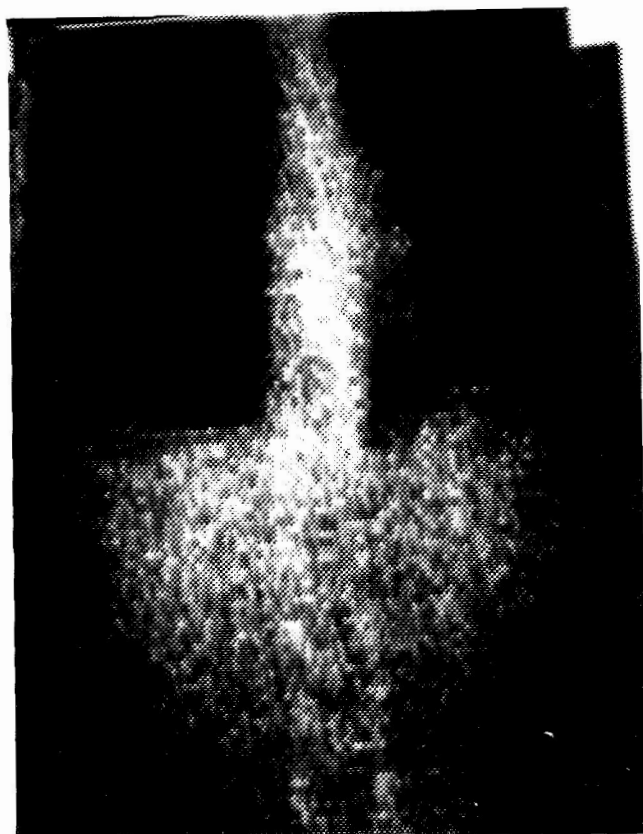
Figure 7. Transmission image of the abdominal spine
and pelvis with Am-241. Bony structures
are barely seen.
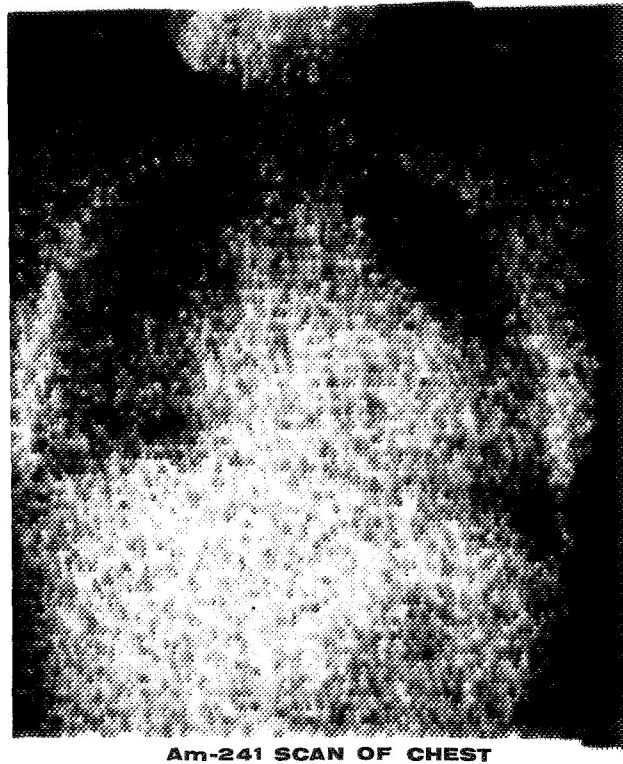
Am-241 SCAN OF CHEST

Figure 8.   Transmission of the chest with Am-241.
            Good contrast between air and tissue is
            obtained.   Resolution is poor but adequate.
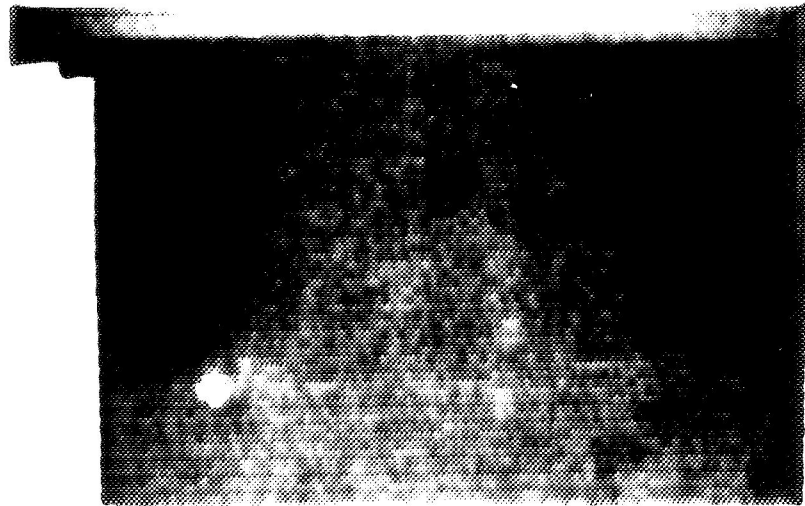
Tc-99m SCAN OF PELVIS

Figure 9.   Transmission scan of pelvis with Tc-99m.
            Objects seen are a belt buckle and a metal
            clip.   No bones are seen.
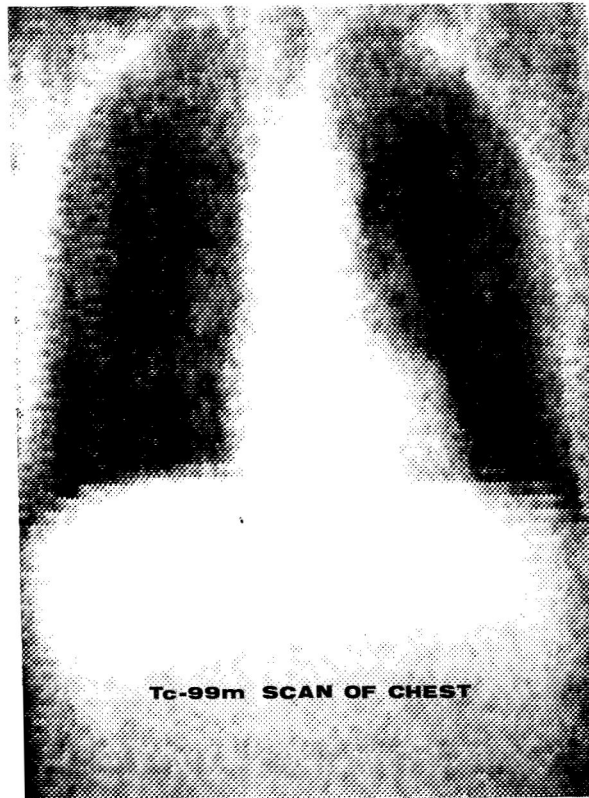
Tc-99m SCAN OF CHEST

Figure 10. Transmission scan of chest with Tc-99m.
Resolution and information density are
better than with Am-241. Contrast is
more than adequate.
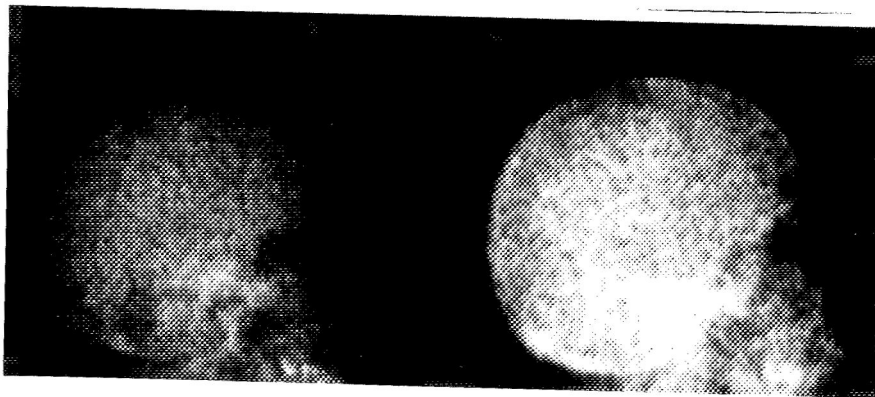
Figure 11. Comparative transmission images of the
skull with Am-241 (left) and Tc-99m
(right). Tc-99m image has better resolution
and information density.
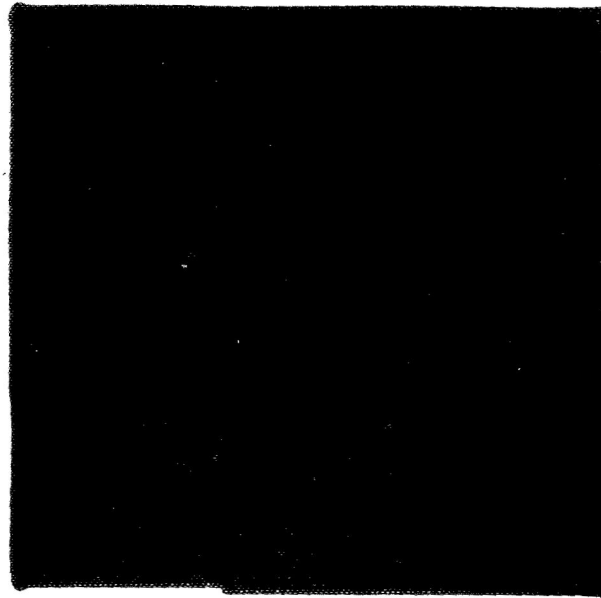
Cs-137, 662 Kev, Transmission
Scan of the Chest

Figure 12.   Transmission image of the chest with Cs-137.
             Contrast may be enough to outline air spaces
             and the heart shadow, but resolution is
             very poor because of beam collimation
             difficulties.

Computer Programs for Bone Mineral Calculations

By: Kianpour Kianian

The main purpose of this report is to familiarize those who are using our computer programs to calculate Bone Mineral.

These programs are available for both remote terminals (connected to the G. E. Time Sharing System) and, by modification, for any other digital computer. Because we have developed and used many programs, I will enumerate only the extensively used programs.

BONE 2 AND BONE 3

Two programs named BONE 2 and BONE 3, which are modified versions of the BONE 2 program described previously (1), are ' very useful if the turn around time of the computer is important.

Both programs have been written in MK II BASIC and are very similar, except that BONE 2 is used for data collected at full scanner speed and BONE 3 at half scanner speed. The effect of scanner speed appears in the experimental proportionality constants which are used to determine bone mineral content.

The basic procedures for making and interpreting the measurements have been previously described (2) and will not be discussed any further. The data used by these programs are punched on paper tape. We punch I_o^* on a paper tape after choosing it from the line printer output, i.e., we select where the edge has to lie. Figure 1 shows how this is done.

These programs are sometimes stored in the G. E. user's library and, for those who are interested, can be obtained by special arrangement. A listing of BONE 2 along with a sample run is attached to this report.

START

A more efficient version of BONE 2 and BONE 3, called
START, was used extensively until last year on the CDC 1604
and is now being used on the CDC 3600. The program is a mixture
of FORTRAN language and CDC 3600 COMPASS assembly language
operating under the control of the SCOPE supervisory system.
The program consists of four subroutines, two in FORTRAN, two
in machine language and the main program, START, in machine
language.

Program START has many features; one of the most important
is the programmed selection of I_o^* and I. START does this by
comparing the successive counts of each scan. If the I th count
is 70% greater than the $(I + 1)$ th count, the program will check
to see if it is also 70% greater than the $(I + 2)$ th count. If
it is, the program will take I th count as the leading edge of
the bone. This process is reversed to obtain the other edge
of the bone. Two adjacent counts are compared in order to
eliminate the effects of a random very low or very high count.
The program is able to recognize both edges of the bone, and
hence calculate all of the desired values.

Another feature of this program is its capability for
processing a large set of data at one time. This is because it
uses magnetic tape for data input. First, after punching all
the scans on paper tape with a tally punch, we convert the paper
tapes to magnetic tape in Binary mode with a CDC 940, then we can
use the magnetic tape later. A sample run of the program is
attached with this literature. The coding for this program is
extensive, and is therefore not listed here. If needed, copies
can be supplied upon request.

In regard to paper tape coding, this program uses the same coding (2) with one exception--the conversion is done with CDC 940.

DISCUSSION

During the past few years we have run thousands of scans and have gathered a great deal of new information about our applied technique. This information has been put on IBM cards in a simple coded form for further analysis with the computer. For the accumulated data from individuals, we have developed a plotting program, which is capable of doing any kind of correlation between bone mineral width, diameter, age, height, etc. The program uses the method of least squares for objectively fitting lines and curves.

The analysis of least squares is by far the most general and can be followed with the use of any introductory statistic text. This type of analysis is mostly used as a tool in the diagnosis of osteoporosis or other demineralization of bone.

The last three pages of this report show the CDC FORTRAN 63 copy of this program, called NIK, which can be used on CDC 3600. Note that this program uses CALCOM Plot with the routine GRAPH. However, this routine may not be the same on other CDC machines.

REFERENCES:

1. K. Kianian and James A. Sorenson
    Program for Bone Mineral Computation Using General Electric
    Time-Sharing Service, Progress Report, 1968, U. of Wis.

2. J. Sorenson, P. Judy, R. Witt and J. R. Cameron
    Progress in the Measurement of Bone Mineral Content By
    Direct Photon Absorption Technique, USAEC COO-1422-7
    (1966).

0 0 0 6 6 3
0 0 0 6 5 9
0 0 0 7 1 1
0 0 0 7 4 2
0 0 0 7 0 3
0 0 0 7 3 3
0 0 0 6 7 8
0 0 0 6 8 6
0 0 0 6 7 0
0 0 0 6 9 5
0 0 0 5 3 8
0 0 0 1 6 5
0 0 0 0 8 3
0 0 0 0 6 6
0 0 0 0 3 7
0 0 0 0 7 3
0 0 0 0 9 2
0 0 0 0 8 7
0 0 0 1 1 5
0 0 0 1 0 5
0 0 0 1 2 9
0 0 0 1 1 8
0 0 0 0 9 7
0 0 0 0 9 1
0 0 0 0 6 1
0 0 0 0 8 8
0 0 0 1 3 0
0 0 0 2 0 6
0 0 0 3 5 1
0 0 0 6 5 7
0 0 0 6 9 4
0 0 0 6 8 9
0 0 0 6 1 0
0 0 0 6 2 5
0 0 0 6 4 4

I_o I_o^*

Line printer output

Figure 1

Here is shown a line printer output with markers showing how I_o^* and I_o values have been chosen. Below is the teletype printed copy of the same scan which shows how the corresponding I_o^* and I_o values have been punched on paper tape. BONE 2 program was run with this data. The result is shown in output file name output. The total run time was 60 seconds and the whole program was about 200 characters long.

100 11:22:69:678:686:670:689:610:625:165:83:66:37:73:92:87:115
102 105:129:118:97:91:61:88:130:206:351:0:663:656:660:701:647
104 731:430:254:173:109:61:72:107:111:112:139:138:110:62:68:49
106 53:73:144:364:0:0

Teletype output

```
5 FILES IN;OUTPUT
6 SCRATCH #2
7 RESTORE #1
8 DELIMIT #2,( )
9 DELIMIT #1,(:)
10 FOR K=1 TO 3
20 READ #1,C(K)
22 IF END #1 THEN 9999
25 NEXT K
26 LET O=1
28 WRITE #2,"*******************************************************"
30 WRITE #2,"PATIENT"C(1);TAB(24);"POSITION"C(2);TAB(48);"DATE"C(3)
40 WRITE #2,"(IZERO)  (.70*IZERO)  (INTEGRAL)  (WIDTH)  (WID)  (B.M.)"
50 WRITE #2,"                                          (.139)  (G/C) "
55 WRITE #2,"----------------------------------------------------------"
60 LET L=0
70 LET N=6
80DIM A(150),B(150),C(150)
85 DIM G(7),H(7),N(7),Y(7),X(7),C(7)
90 LET M=1
100 FORI=M TO N
110 READ #1,A(I)
120 NEXT I
130 LET G=0
140 FOR I=1 TO N
150 LET G=G+A(I)
160 NEXT I
170 LET G=G/N
180 LET I=1
190 READ #1,B(I)
200 IF B(I)=0 THEN 230
210LETI=I+1
220 GO TO 190
230 LET L=L+1
240 LET N=I-1
250 LET Y=N*0.162
260 LET X=Y*0.855
270 LET T=N*LOG(G)
275 LET S=0.70*G
280 LET F=0
290 FOR J=1 TO N
300 LET O=B(J)
310 LET F=F+LOG(O)
320 NEXT J
321 LET H=T-F
322 LET C=H*.0617+.0554
323 WRITE #2,"SCAN NO."L
324 WRITE #2,G;TAB(10);S;TAB(22);H;TAB(36);N;TAB(42);X;TAB(52);C
326 IF S>=B(1) THEN 329
327 WRITE #2,"LEFT EDGE WRONG"
328 GO TO 330
329 WRITE #2,"LEFT EDGE CORRECT"
330 IF S>=B(N) THEN 340
```

Program BONE 2 for 70% edge determination at full speed.   CONTINUE

```
331 WRITE #2,"RIGHT EDGE WRONG"
335 GO TO 341
340 WRITE #2,"RIGHT EDGE CORRECT"
341 LET G(O)=G
342 LET H(O)=H
343 LET N(O)=N
344 LET Y(O)=Y
345 LET X(O)=X
346 LET C(O)=C
350 READ #1,B(I+1)
355 IF B(I+1)<>0 THEN 375
356 LET G1=0
357 LET G2=0
358 LET G3=0
359 LET G4=0
360 LET G5=0
361 LET G6=0
362 FOR K=1 TO O
363 LET G1=G1+G(K)
364 LET G2=G2+H(K)
365 LET G3=G3+N(K)
366 LET G4=G4+Y(K)
367 LET G5=G5+X(K)
368 LET G6=G6+C(K)
369 NEXT K
370 WRITE #2,"AVERAGES:"
371 WRITE #2,G1/O;TAB(22);G2/O;TAB(36);G3/O;TAB(42);G5/O;TAB(52);G6/O
373 GO TO 10
375 LET A(1)=B(I+1)
380 LET M=2
385 LET N=6
387 LET O=O+1
390 GO TO 100
9999 END
```

Program BONE 2 for 70% edge determination at full speed.

```
OUTPUT          11:05        06/12/69

100  ****************************************************
110  PATIENT   11            POSITION  22            DATE    69
120  (IZERO)   (.70*IZERO)  (INTEGRAL)    (WIDTH)   (WID)   (B.M.)
130                                                 (.139)  (G/C)
140  ----------------------------------------------------
150  SCAN NO.   1
160   659.667    461.767     33.4883        18     2.49318  2.12163
170  LEFT EDGE CORRECT
180  RIGHT EDGE CORRECT
190  SCAN NO.   2
200   676.333    473.433     33.9545        19     2.63169  2.15039
210  LEFT EDGE CORRECT
220  RIGHT EDGE CORRECT
230  AVERAGES:
240   668.                   33.7214       18.5    2.56243  2.13601
```

TIME,   0   0   0

GOOD SCAN, NUMBER 1

1191.00	1228.00	1177.00	1164.00	1182.00	1157.00	1130.00	1176.0
1134.00	1062.00	1128.00	1081.00	1089.00	1077.00	1064.00	1137.0
1056.00	1067.00	1102.00	1073.00	1045.00	1078.00	1097.00	1111.0
1045.00	1046.00	1013.00	999.00	1068.00	1055.00	1025.00	1048.0
505.00	296.00	157.00	105.00	113.00	82.00	98.00	74.0
141.00	139.00	127.00	121.00	102.00	109.00	97.00	102.0
350.00	572.00	689.00	884.00	982.00	992.00	970.00	1041.0
997.00	980.00	983.00	1006.00	1004.00	1037.00	861.00	

CURRENT I-ZEROSTAR (LEFT = 1033.000)(RIGHT = 1003.000)   INTEGRATION B

GOOD SCAN, NUMBER 2

1058.00	984.00	1018.00	1019.00	1007.00	982.00	960.00	1003.0
706.00	500.00	317.00	204.00	157.00	114.00	113.00	116.0
116.00	133.00	152.00	151.00	111.00	114.00	89.00	72.0
278.00	508.00	766.00	954.00	1007.00	1014.00	1026.00	1050.0
735.00							

CURRENT I-ZEROSTAR (LEFT = 1000.500)(RIGHT = 1022.250)   INTEGRATION B

GOOD SCAN, NUMBER 3

1021.00	1020.00	1063.00	1014.00	1069.00	1044.00	1008.00	1064.0
158.00	116.00	86.00	77.00	93.00	100.00	118.00	134.0
117.00	95.00	99.00	95.00	114.00	106.00	148.00	164.0
868.00	994.00	1004.00	984.00	995.00	990.00	1007.00	1007.0
857.00							

CURRENT I-ZEROSTAR (LEFT = 1033.750)(RIGHT = 994.000)   INTEGRATION B
  0.00   1018.00   1011.38   1013.88

0	1131.00	1171.00	1075.00	1087.00
0	1059.00	1086.00	1075.00	1101.00
0	1045.00	980.00	1053.00	1027.00
0	1004.00	1010.00	953.00	731.00
0	82.00	118.00	126.00	135.00
0	108.00	143.00	188.00	277.00
0	983.00	1018.00	945.00	963.00

EGAN WITH 505, AND ENDED WITH 689.

)	1021.00	1018.00	905.00	879.00
)	97.00	104.00	132.00	138.00
)	84.00	108.00	115.00	145.00
)	999.00	1031.00	1000.00	1010.00

EGAN WITH 500, AND ENDED WITH 508.

	973.00	780.00	521.00	327.00
	32.00	146.00	149.00	116.00
	234.00	331.00	508.00	684.00
	984.00	1000.00	972.00	955.00

GAN WITH 521, AND ENDED WITH 684.

PATIENT RUP

PATIENT NUMBER 2013

POSITION 30.

I-ZEROSTAR = 1014.417

SCANNER IDENTIFICATION NUMBER = 1002

LINEAR SCANNER(I-125),AT HALF SPEED,

MIN(GM/CM)=.0205*(INTEGRAL)+.037   AND   WIDTH(CM)=0.046(WIDTH,CORR.)

SCAN NO.	INTEGRAL	WIDTH (CORR.)	WIDTH	MIN. (GM/CM)	WIDTH (CM)	IOSTAR
1	5.1137+001	26.86	27	1.0899+000	1.24	1018.0
2	4.8794+001	25.79	25	1.0417+000	1.19	1011.3
3	4.8892+001	25.88	26	1.0437+000	1.19	1013.6
AVERAGES =	4.9607+001	26.18		1.0584+000	1.21	
STD. DEV. =	1.0822+000	0.49		2.2282-002	0.02	
PER CENT STD. DEV. =	2.2	1.9		2.1	1.9	
STD. DEV. OF MEAN =	0.6	0.3		0.0	0.0	
PER CENT STD.MEAN =	1.3	1.1		1.2	1.1	

```
      PROGRAM NIK
      DIMENSION X(200),Y(200),SUB(200)
      DIMENSION BM(200),DIA(200),WEI(200),HEI(200)
      DIMENSION E(200),F(200),CM(200),CD(200)
      DO 333 J=1,2
      MCR=0
      READ 11,N
      DO 1000 I=1,N
      READ 110,BM(I),DIA(I),SUB(I),WEI(I),HEI(I),E(I),F(I)
 110  FORMAT(42X,F4.2,1X,F3.2,A4,F3.0,F2.0,2X,A8,A8,2X)
1000  CONTINUE
  12  MCR=MCR+1
      SUM1=0 $ SUM2=0 $SUM3=0 $ SUM4=0 $ SUM5=0 $ SUM6=0 $SUM7=0
      SUM8=0 $ SUM9=0
      GO TO (40,41,42,43,44),MCR
  40  X(1)=0.0  $ X(2)=3.0  $ Y(1)=0.0  $ Y(2)=2.0
      CALL GRAPH1(X,Y,-2,4H8X10,4HEXTN,0.0,0.3,0.0,.25,48H  BONE MINERAL
     1-.VS.DIAMETER                       ,14H  DIAMETER   ...,14HBONE MINER
     2AL..)
      PRINT 1
   1  FORMAT(1H0,*B.M.*,1X,*DIAM.*)
      NTEMP=N
      DO 51 K=1,N
      Y(K)=BM(K)
      X(K)=DIA(K)
      PRINT 2,Y(K),X(K),E(K),F(K),SUB(K)
   2  FORMAT(1H0,F4.2,1X,F4.2,1X,A8,A8,2X,A4)
  51  CONTINUE
      M=N
      GO TO 99
  41  X(1)=0.0  $ X(2)=80.0 $ Y(1)=0.0  $ Y(2)=2.0
      CALL GRAPH1(X,Y,-2,4H8X10,4HEXTN,0.0,8.0,0.0,.25,48H  BONE MINERAL
     1-.VS.HEIGHT                        ,14H  HEIGHT      ...,14HBONE MINER
     2AL..)
      PRINT 3
   3  FORMAT(1H0,*B.M.*,1X,*HEIGHT*)
      M=0
      DO 52 K=1,N
      IF(HEI(K).EQ. 0.) GO TO 52
      M=M+1
      Y(M)=BM(K)
      X(M)=HEI(K)
      PRINT 4,Y(M),X(M),E(K),F(K),SUB(K)
   4  FORMAT(1H0,F4.2,1X,F5.2,1X,A8,A8,2X,A4)
  52  CONTINUE
      GO TO 99
  42  X(1)=0.0  $ X(2)=200.0$ Y(1)=0.0  $ Y(2)=2.0
      CALL GRAPH1(X,Y,-2,4H8X10,4HEXTN,0.0,20.,0.0,.25,48H  BONE MINERAL
     1-.VS.WEIGHT                        ,14H  WEIGHT      ...,14HBONE MINER
     2AL..)
      PRINT 5
   5  FORMAT(1H0,*B.M.*,1X,*WEIGHT*)
      M=0
      DO 53 K=1,N
      IF(WEI(K).EQ. 0.) GO TO 53
      M=M+1
```

```
         Y(M)=BM(K)
         X(M)=WEI(K)
         PRINT 6,Y(M),X(M),E(K),F(K),SUB(K)
   6 FORMAT(1H0,F4.2,1X,F5.0,1X,A8,A8,2X,A4)
  53 CONTINUE
         GO TO 99
  43 X(1)= .0   $ X(2)=80.0 $ Y(1)=0.0   $ Y(2)=4.0
         CALL GRAPH1(X,Y,-2,4H8X10,4HFXTN,0.0,8.0,0.0,0.5,48H   BONE MINERAL
        1/DIAMETER.VS.HEIGHT                    ,14HHEIGHT       ..,14H BM/DIAMET
        2ER..)
         PRINT 7
   7 FORMAT(1H0,*B.M./DIA*,1X,*HEI*)
         M=0
         DO 54 K=1,N
         IF(HEI(K).EQ..0)GO TO 54
         M=M+1
         Y(M)=BM(K)/DIA(K)
         X(M)=HEI(K)
         PRINT 8,Y(M),X(M),E(K),F(K),SUB(K)
   8 FORMAT(1H0,F6.3,1X,F5.2,1X,A8,A8,2X,A4)
  54 CONTINUE
         GO TO 99
  44 X(1)= .0   $ X(2)=200.0$ Y(1)=0.0   $ Y(2)=4.0
         CALL GRAPH1(X,Y,-2,4H8X10,4HFXTN,0.0,20.,0.0,0.5,48H   BONE MINERAL
        1/DIAMETER.VS.WEIGHT                    ,14HWEIGHT       ..,14H BM/DIAMET
        2ER..)
         PRINT 9
   9 FORMAT(1H0,*B.M./DIA*,1X,*WEIGHT*)
         M=0
         DO 55 K=1,N
         IF(WEI(K).EQ..0) GO TO 55
         M=M+1
         Y(M)=BM(K)/DIA(K)
         X(M)=WEI(K)
         PRINT 10,Y(M),X(M),E(K),F(K),SUB(K)
  10 FORMAT(1H0,F6.3,1X,F5.0,1X,A8,A8,2X,A4)
  55 CONTINUE
  49 N=M
         DO 100 I=1,N
         SUM1=SUM1+X(I)*Y(I)
         SUM2=SUM2+X(I)
         SUM3=SUM3+Y(I)
         SUM4=SUM2*SUM3
         SUM5=SUM5+X(I)**2
         SUM6=SUM2*SUM2
         SUM7=SUM3*SUM3
         SUM8=SUM8+Y(I)**2
 100 CONTINUE
         B=(N*SUM1-SUM4)/(N*SUM5-SUM6)
         PRINT 101,B
         A=(SUM3-B*SUM2)/N
 101 FORMAT(1H1,40X,16H REGRESION LINE ,////30X,7H Y=BX+A,///20X,5H B =
        1 ,F10.5)
         PRINT 102,A
 102 FORMAT(2X,///20X,5H A = ,F10.5)
         S2X=(N*SUM5-SUM6)/(N*(N-1))
```

```
      S2Y=(N*SUM8-SUM7)/(N*(N-1))
      SX = SQRTF(S2X)
      SY=SQRTF(S2Y)
      PRINT 301,SX,SY
301 FORMAT(1H0,19H SUMS AND VARIANCES,///25X,7H SX  = ,F10.5,///25X,7H
   2 SY  = ,F10.5)
      T=(N-1)/(N-2)
      S2YX=T*(S2Y-(B**2)*S2X)
      SYX = SQRTF(S2YX)
      PRINT 302,SYX
302 FORMAT(12X,29H STANDARD ERROR OF ESTIMATE =,F10.5)
 11 FORMAT(I2)
      SP=(SYX)/(SX*(N-1)**.5)
      PRINT 303,SP
303 FORMAT(1H0,25X,44H STANDARD ERROR OF REGRESSION COEFFICIENT B=,F10
   3.6)
      R2 = (N*SUM1-SUM2*SUM3)**2/((N*SUM5-SUM6)*(N*SUM8-SUM7))
      R=SQRTF(R2)
      PRINT 304,R
304 FORMAT(20X,5H R = ,F10.5)
      PRINT 21 ,N
 21 FORMAT(1X,*N= *,I2)
      PN = N
      AVERX = SUM2/PN
      AVERY = SUM3/PN
      PRINT 28,AVERX,AVERY
 28 FORMAT(///15X,9H AVERX=   ,F10.5,18X,9H AVERY = ,F10.5)
      CALL GRAPH1(X,Y,-N,7HOVERLAY,4HSAME,4)
      XX=SUM2/N
      YY=SUM3/N
      STDX=SQRTF(SUM5/N-(XX)**2)
      STDY=SQRTF(SUM8/N-(YY)**2)
      STDEX=STDX/SQRTF(PN)
      STDEY=STDY/SQRTF(PN)
      PRINT 341
      PRINT 342,XX,YY,STDX,STDY,STDEX,STDEY
341 FORMAT(1H0,*XMEAN*,8X,*YMEAN*,8X,*STD DEV X*,3X,*STD DEV Y*,3X,*ST
   1D ERR X*,3X,*STD ERR Y*)
342 FORMAT(1H0,4(F10.3,3X),2(E20.6,3X))
      DO 400 I=1,N
      Y(I)=0.0
      X(I)= .0
400 CONTINUE
      N=NTEMP
      IF(MCR.NE.5) GO TO 12
333 CONTINUE
      END
```

A DICHROMATIC ABSORPTION METHOD FOR THE MEASUREMENT OF BONE MINERAL CONTENT

Philip F. Judy and John R. Cameron

The transmission of the essentially monochromatic photon beams from ^{125}I and ^{241}Am through various paths of the body has been used to determine the bone mineral components and soft tissue components of the paths. The method is being investigated because of its simplicity and its potentially good precision. Good precision will permit the determination of smaller bone mineral changes. This report discusses the theory of the method and some preliminary results.

The use of photon beams of two energies to measure body composition has been studied by various investigators (1,2,3,4). Dichromography has been used to describe this method (5), but this term suggests an "image" is the result of the measurement, which is misleading. We prefer "dichromatic absorptiometry" to describe the method.

THEORY

The transmission of two monochromatic x-ray or γ-ray beams through a path of the body, that is assumed to be composed of two substances, bone mineral and soft tissues, is described by equations (1) and (2):

$$I_1 = I_{o,1} \exp (-\mu_{BM,1} M_{BM} - \mu_{ST,1} M_{ST}) \qquad (1)$$

$$I_2 = I_{o,2} \exp (-\mu_{BM,2} M_{BM} - \mu_{ST,2} M_{ST}) \qquad (2)$$

where: I_o = unattenuated intensity

I = transmitted intensity

μ = mass attenuation coefficient

"M" = mass in g/cm^2

ST = subscript referring to soft tissue component

BM = subscript referring to bone mineral component

The numbered subscript identifies the photon beam. The solutions of these simultaneous equations for M_{ST} and M_{BM} are:

$$M_{BM} = K_1 \log_e (I_{o,1}/I_1) + K_2 \log_e (I_{o,2}/I_2) \qquad (3)$$

$$M_{ST} = K_3 \log_e (I_{o,1}/I_1) + K_4 \log_e (I_{o,2}/I_2) \qquad (4)$$

The expressions for K_i are:

$$K_1 = \mu_{ST,2}/D$$

$$K_2 = \mu_{ST,1}/D$$

$$K_3 = \mu_{BM,2}/D$$

$$K_4 = \mu_{BM,1}/D$$

where: $D = \mu_{BM,1} \mu_{St,2} - \mu_{BM,2} \mu_{ST,1}$

MEASUREMENT SYSTEM

The components of the measurement system are illustrated in Figure 3. The collimated sources, ^{125}I and [241]Am (7), are mounted on a wheel which can reproducibly place either source in the counting position. A 1/4" diameter collimated detector is permanently fixed above the counting position. Collimators from 1/16" to 3/8" are also available for use with the system. Preliminary measurements indicate little variation of the measurement of the bone mineral component as a function of collimation size. The detector used is a commercially available integral mount NaI (Tl) scintillation detector (8). The pulses from the photomultiplier tube are analyzed and recorded with a

spectrometer (Baird Atomic, Model 530). The part of the body
being examined (preliminary work has been restricted to bones
of the hand) is held in place between the source and the detector
by a plaster of paris mold of that part of the body. The mold
is securely and reproducibly held by guide pines attached to
the apparatus.

The unattenuated intensity of the photon beams is not
measured directly, rather a standard of copper and lucite has
been constructed that has about the same attenuation for ^{125}I
and ^{241}Am as the part of the body examined. A comparison with
the transmission of this standard is made instead of a measure-
ment of the unattenuated intensity. This comparison measurement
reduces the correction on the ratio associated with dead time
because approximately the same correction is made on each count
rate. This procedure also minimizes the changes of gain of the
photomultiplier tube associated with sudden large changes of
intensities. The sequence of measurements (I, II, III, IV)
made for each determination of the bone mineral component is
illustrated in Figure 4.

ESTIMATE OF PRECISION

The above procedures have been investigated initially with
an older apparatus. The bone mineral component of midshaft of
the third proximal phalanx of a normal 26 year old was measured
on 15 different days over a period of six weeks. Measurements I,
II, III, IV were repeated five times each day. The determination
of the bone from each of the five measurements was averaged.
The standard deviation of this average over the six week period
was 1%. The results are summarized in Table I.

At the same time measurements II and III were repeated
five times with no movement of source and the hand being removed
from the mold between each measurement. The analysis of the
variations suggested the major sources of error were the varia-
tion of the position of the sources and the variation of the
position of the bone. The variation of the position of the
sources contributed twice the variation of the position of the
bone. Because of these measurements a new apparatus was con-
structed and preliminary measurements indicate the variation
due to source position is minimal with the new apparatus.

ERROR ANALYSIS

The two major sources of uncertainty in the measurement
of the bone mineral component are: (1) uncertainties of the
counting rate and (2) variation of the bone mineral in the
photon beam due to repositioning errors. The contribution of
the uncertainties in the counting rates has been analyzed using
a standard technique (6). The coefficient of variation of the
bone mineral component (σ_{BM}) due to this source of error is:

$$\sigma_{BM} = \frac{\sqrt{\dfrac{K_1^2 \sigma_1^2}{\exp 2(u_{BM,1} M_{BM} + u_{ST,1} M_{ST})} + \dfrac{K_2^2 \sigma_2^2}{\exp 2(u_{BM,2} M_{BM} + u_{ST,2} M_{ST})}}}{M_{BM}}$$

where most of the symbols have been previously defined and

σ_1 = Coefficient of variation of $I_{o,1}/I_1$

σ_2 = Coefficient of variation of $I_{o,2}/I_2$

To illustrate how σ_{BM} depends on the bone mineral and soft
tissue components it has been calculated for the photon beams

of ^{125}I and ^{241}Am assuming σ_1 and σ_2 are each 1%. For the remainder of this paper, subscript "1" refers to the photon beam from ^{125}I and subscript "2" refers to the photon beam from ^{241}Am. The results are summarized in Figure 1. Experimentally σ_1 and σ_2 are less than 1% in a few minutes total counting time. The values of σ_{BM} are listed in Table II for typical values of M_{BM} and M_{ST} of various sites for $\sigma_1 = \sigma_2 = 1\%$. If σ_1 and σ_2 are less than 1%, then σ_{BM} is improved proportionately.

To evaluate the change in the counting rates due to an actual change in the bone mineral in the beam, the change in $I_{o,1}/I_1$ and $I_{o,2}/I_2$ were calculated assuming a 1% change in the bone mineral in the beam. This change could be due to a repositioning error or an actual change at the original measuring site. The results are summarized in Figure 2. A result of these calculations is that the percentage change in $I_{o,1}/I_1$ is 3 to 20 times larger than the percentage change in $I_{o,2}/I_2$ for a given change in BM. Experimentally, σ_1 has been observed to be two to five times larger than σ_2. This also suggests the primary source of error is the repositioning error.

FUTURE PLANS

Constants K_1, K_2, K_3, and K_4 in the initial investigation have been estimated from published attenuation coefficients (9) and the accuracy of the technique has not been estimated. Therefore the method will be calibrated with ash studies. Excised bones will be milled into regular shapes and the trans-

mission of various photon beams of these sections will be measured under various thicknesses of water. The method can be calibrated and its accuracy estimated by ashing and weighing the bone sections. Other plans are listed below.

1) Investigation of other photon sources.

2) Investigation of effects of collimation.

3) Estimate of variation of mineral as function of position.

4) Development of a scanning mode method.

5) Investigation of the effects of trabeculae on accuracy.

6) Development of software for computer analysis and record keeping for systems.

CONCLUSION

These preliminary investigations indicate the bone mineral component of the finger can be measured with a precision of 1%. The primary source error was the variation of amount of bone mineral in the photon beam caused by some type of repositioning error.

REFERENCES

1. J.R. Cameron and J.A. Sorenson, Science 142, 230 (1963).

2. B. Jacobson, Am. J. Roentg., Radium Therapy Nucl. Med.
   91, 202 (1964).

3. M.J. Cohen and A.J. Gilson, Progress In Development of
   Method in Bone Densitometry, (Scientific and Technical
   Information Division, NASA, Washington, D. C., 1966,
   ed., G.D. Whedon, W.F. Neuman and D.W. Jenkins) p. 103.

4. L.E. Preuss and L.T. Kosnik, J. of Nucl. Med., 10,
   366 (1969).

5. B. Jacobson, Science 128, 1346 (1958).

6. D.C. Baird, Experimentation: An Introduction to
   Measurement Theory and Experiment Design, (Prentice-
   Hall, Inc., Englewood Cliffs, New Jersey, 1962) p. 61.

7. J.A. Sorenson and J.R. Cameron, Comparison of I-125,
   Pb-210 and Am-241 as Radiation Sources for Bone Mineral
   Measurements (U.S. AEC Report, COO-1422-26, July 1968).

8. Harshaw Integral Line, Type M10SH-3M-X
   The Harshaw Chemical Co., Division of Kewanee Oil Co.,
   Cleveland, Ohio.

9. F.H. Attix and W.C. Roesch, Radiation Dosimetry (Academic
   Press, New York, 1968), 2nd Ed., Vol. 1, p. 121.

TABLE I

Summary of Repeat Measurements
of Bone Mineral Component of 3rd Proximal Phalanx

$$M_{BM} = .705 \pm .007 \quad gm/cm^2$$
$$(1\%)$$

$$M_{ST} = 1.822 \pm .035 \quad gm/cm^2$$
$$(2.1\%)$$

$$I_{o,1}/I_1 = 14.1 \pm .3$$
$$(1.4\%)$$

$$I_{o,2}/I_2 = 1.918 \pm .017$$
$$(.9\%)$$

TABLE II

Typical Values of the Bone Mineral Component and Soft Tissue Component for Various Sites

	Bone Mineral Component M_{BM}	Soft Tissue Component M_{ST}	Coefficient of Variation of Bone Mineral Component σ_{BM} *
Midshaft of Proximal Phalanx	$0.7 \ gm/cm^2$	$2 \ gm/cm^2$	0.9%
Distal end of Radius	$0.5 \ gm/cm^2$	$5 \ gm/cm^2$	0.7%
Oscalcis	$0.5 \ gm/cm^2$	$8 \ gm/cm^2$	0.4%

* Coefficient of variation of $I_{o,1}/I_1$ and $I_{o,2}/I_2$ are assumed to be 1%.
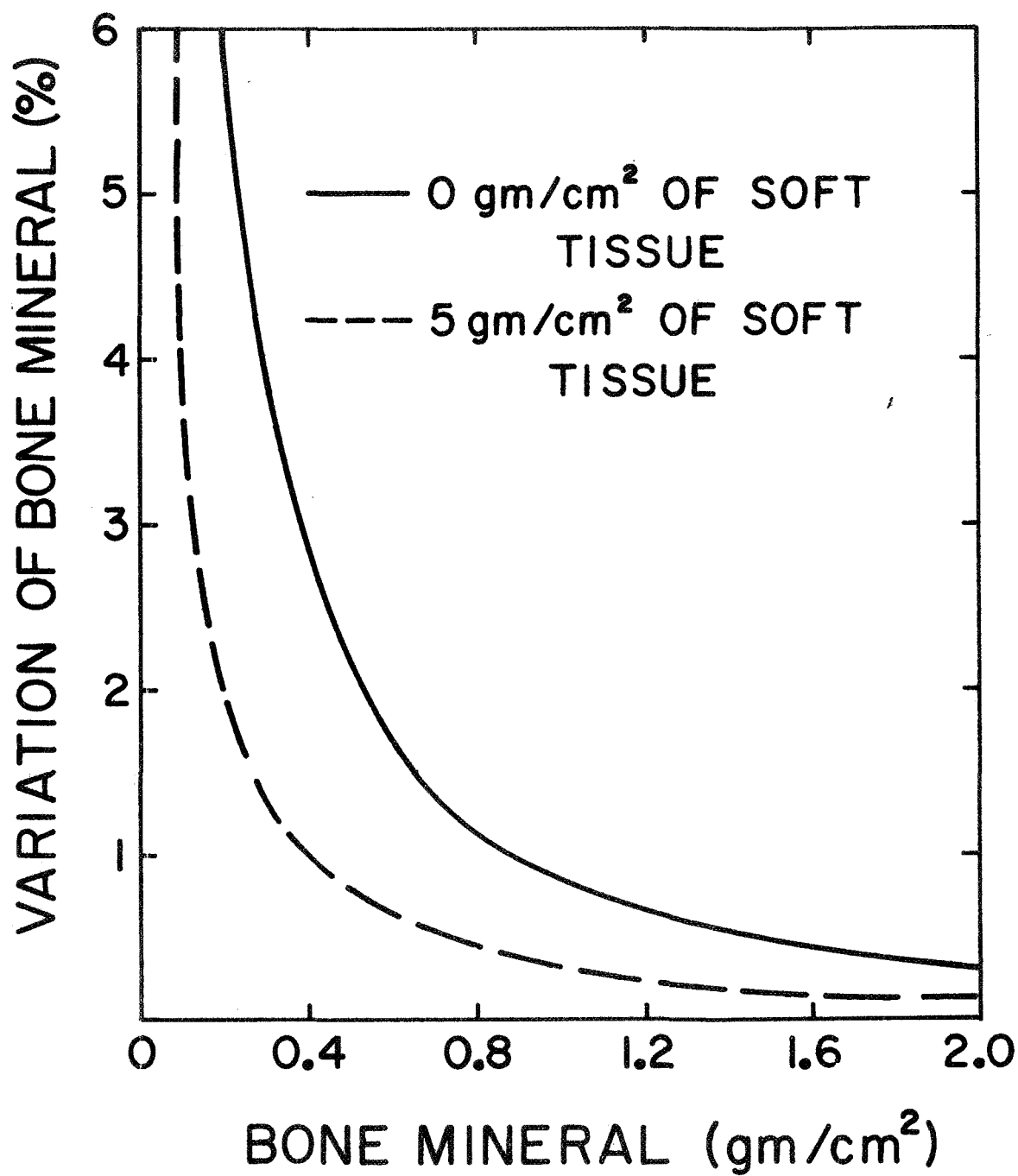
Figure 1   The coefficient of variation of the bone mineral
            component as a function of the bone mineral component
            for a 1% coefficient variation of $I_{o,1}/I_1$ and
            $I_{o,2}/I_2$
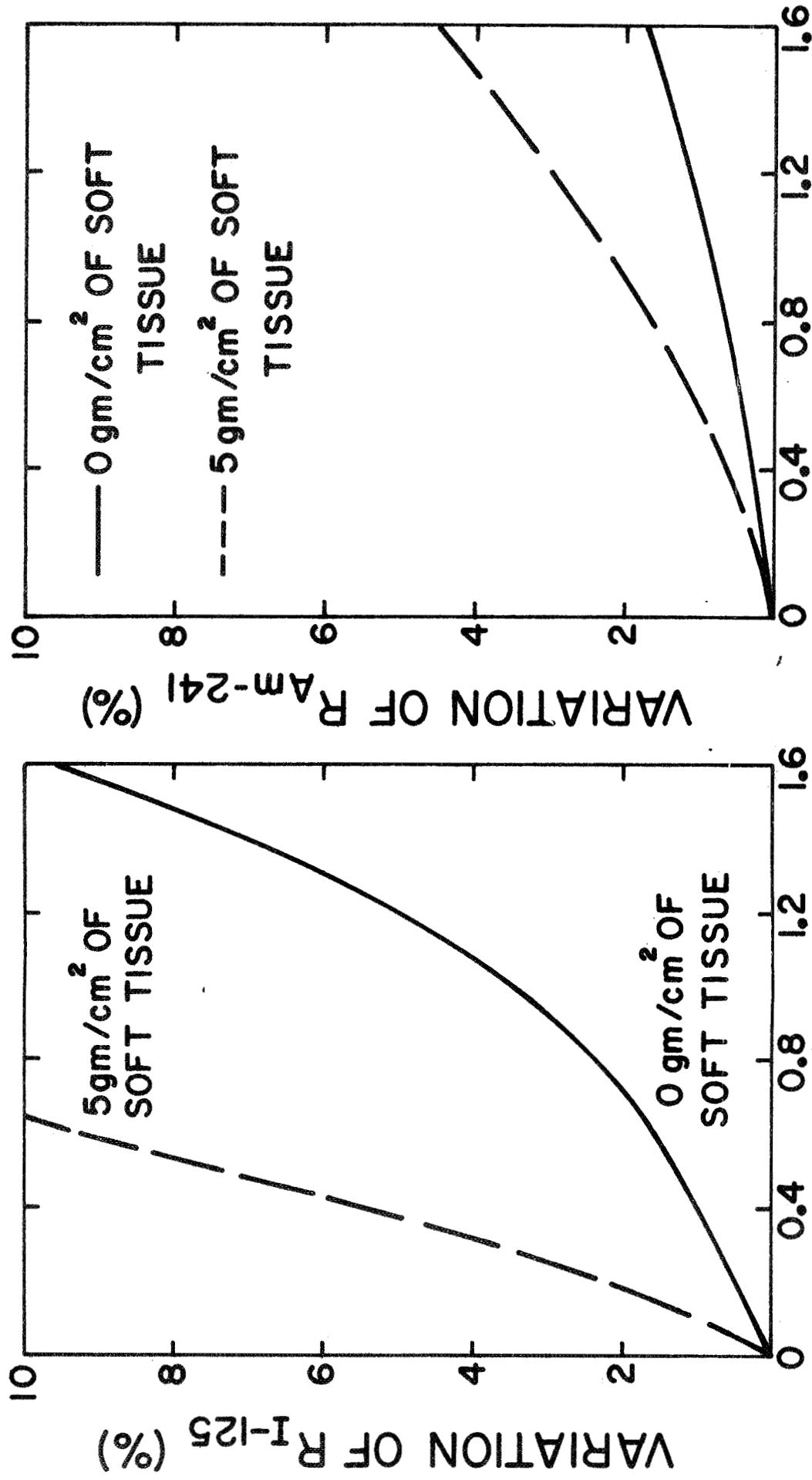
BONE MINERAL (gm/cm^2)

Figure 2   The variation of $I_{o,1}/I_1$ and $I_{o,2}/I_2$ as a function
of the bone mineral component assuming 1% change
in the bone mineral in beam.
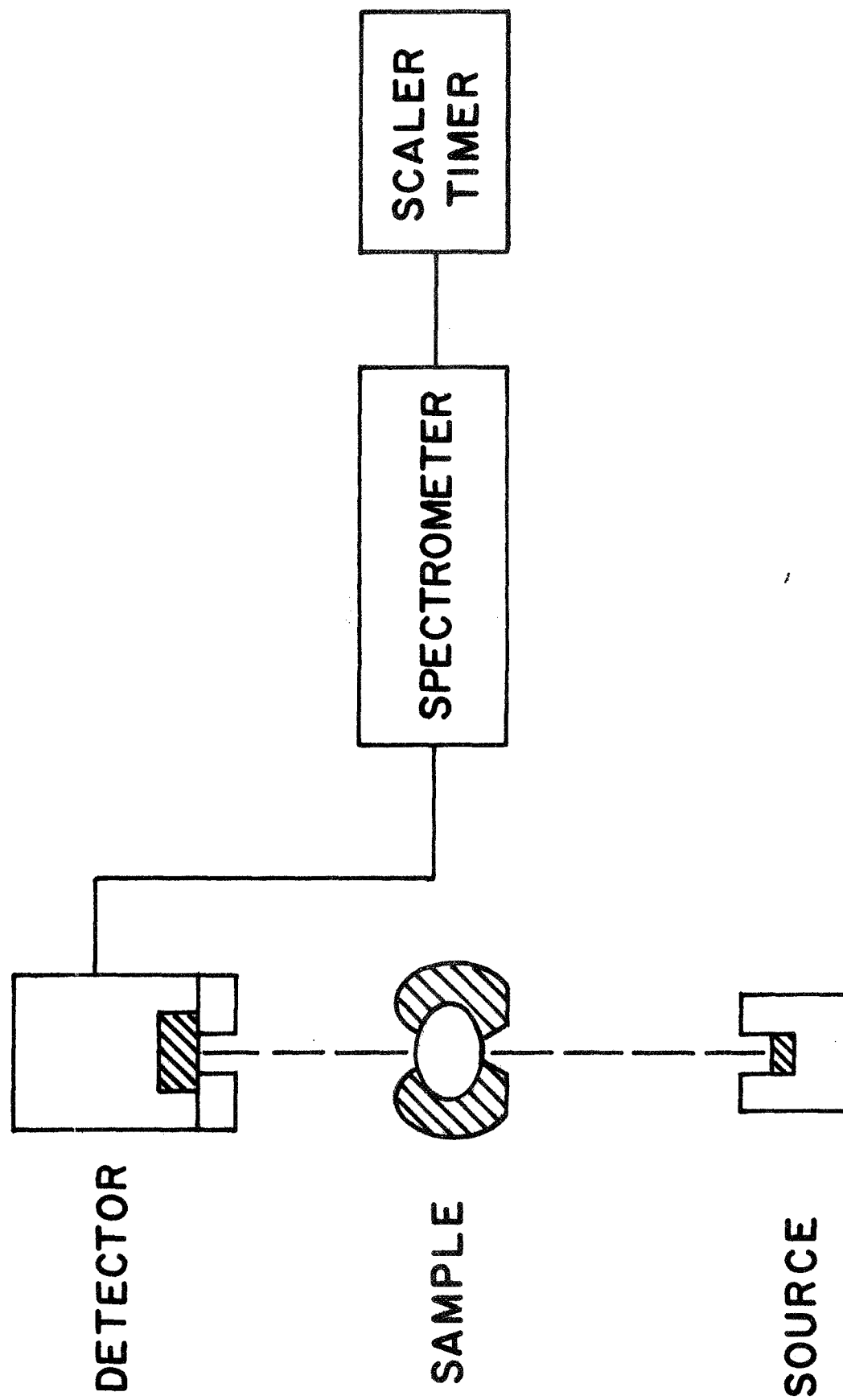
Figure 3   Components of the dichromatic absorption measurement
            system.
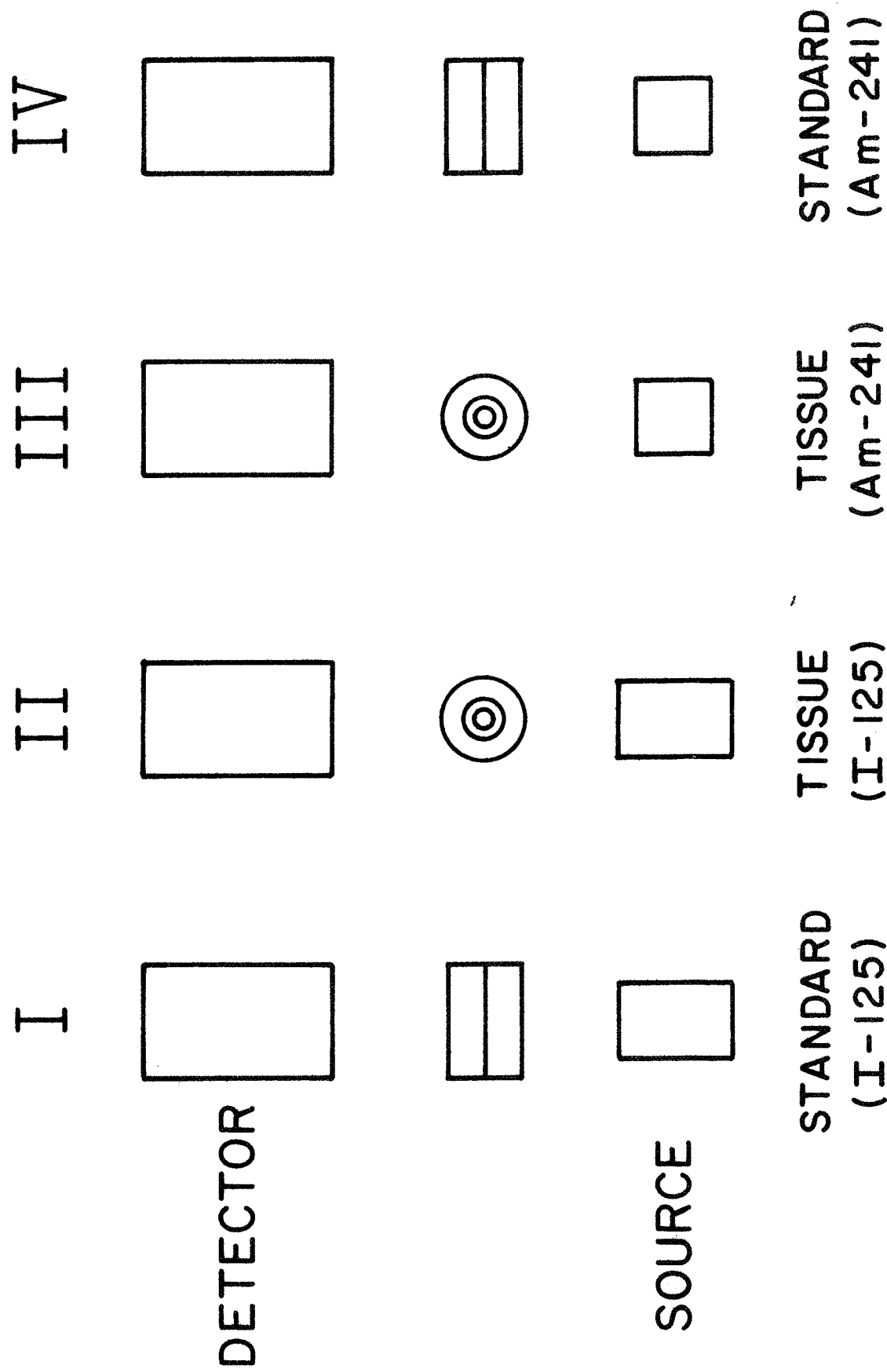
Figure 4   Measurements made in actual determination of the bone mineral component.

Report of the First Bone Mineral Scanning Conference
by - John R. Cameron

Conversations with a number of scientists using the direct photon absorption technique for determining bone mineral mass lead to the organization of a one-day conference held at the Chicago O'Hare Airport on April 25, 1969. It was anticipated perhaps 20 or 25 individuals would be interested in participating in such a conference, primarily to exchange ideas on the technique. The final attendance was approximately 65 with about 10 other individuals who had wanted to come but were unable to for one reason or another. A preliminary survey indicated that the Chicago O'Hare Airport would be the most convenient but not the most congenial location for the meeting. The conference was unusual in several respects, it had no official sponsor, it had no official support and it had no publicity other than contacts with individuals who had instrumentation for this technique or planned to be using the technique in the near future. There were also a number of commercial representatives who have an interest in building instrumentation or furnishing radioactive sources for the instrument. A list of the names and addresses of the attendees together with the names and addresses of a number of individuals who were interested in attending but were not able to is included in the appendix. Also included in the appendix is a list of the various Medical Centers currently using the technique together with the name of an individual who can be contacted to obtain further information on their work. I am sure that there are

other centers that should be included but unfortunately I
do not have that information.

No summary report was written of the meeting. A number
of the speakers did hand out pre-prints or reprints of their
work. Tape recordings were made of the proceedings and these
are available for loan to interested individuals.

There was an extended discussion of acceptable units,
terminology and calibration devices. An informal committee
of several physicists was formed to help clarify the situation.
When their deliberations are complete, they will be circulated
to the participants of the conference for their information.

The interest of a number of commercial concerns in the
development of units or radioactive sources was encouraging
since it should greatly accelerate the application of this
technique. The commercial concerns involved are Norland
Associates, Packard Instrument Company, Atomic Energy of
Canada Limited and Searle-Amershan. The addresses for these
companies are available in the list of attendees.

Because of the favorable response of this meeting and
its general convenience, it is quite likely that similar
meetings will be held in the future.

APPENDIX

MEDICAL CENTERS WHICH HAVE ADOPTED THE PHOTON
ABSORPTIOMETRIC TECHNIQUE FOR SKELETAL EVALUATION

Dr. Eugene Ball-	University of Alabama Medical Center: Birmingham, Alabama
Dr. Jack Edeiken-	Jefferson Medical Center: Philadelphia, Pennsylvania
Dr. Marvin Goldman-	University of Calfornia: Davis, California
Dr. William Harris-	Massachusetts General Hospital: Boston, Massachusetts
Dr. James Johnston-	Kaiser Permanente Hospital: Oakland, California
Dr. C.C. Johnston-	University of Indiana Medical Center: Indianapolis, Indiana
Dr. L.H. Lanzl-	University of Chicago Medical Center: Chicago, Illinois
Dr. Charles Pak-	National Institute of Health: Bethseda, Maryland
Dr. Jaap van der Sluys Veer-	University of Leiden: Leiden, Holland
Dr. F.W. Spiers-	University of Leeds: Leeds, England
Dr. Donald Taves-	University of Rochester Medical Center: Rochester, New York
Dr. John Vogel-	U.S. Public Health Service Hospital: San Francisco, California
Dr. Heinz Wahner-	Mayo Clinic: Rochester, Minnesota

BONE MINERAL SCANNING CONFERENCE

CHICAGO O'HARE AIRPORT, CHICAGO, ILL.

SEVEN CONTINENTS RESTAURANT   APRIL 25, 1969

REGISTRATION AND COFFEE   (9:30-10:00)

SESSION I: Introduction and Clinical Results

10:00   Introductory Remarks by John R. Cameron

10:15   Review of Principles; Summary of Normal Data by J.R. Cameron

11:00   Measurement at Jefferson Medical College, Phiadelphia by
        J. Edeikin, et al.

11:15   Measurements on Bed-Rest Cases at U.S.P.H.S. Hospital,
        San Francisco by J. Vogel, et al.

11:30   Measurements at the Univ. of Indiana, Indianapolis by
        C.C. Johnston, et al.

11:45   Measurements at the Univ. of Alabama, Birmingham by E. Ball

12:00-1:00   LUNCH

SESSION II: Instrumentation, Standards, Etc. G.D. Whedon, Chairman

1:00   "2-Photon" Measurements, Univ. of Wisconsin by P. Judy

1:15   Feasible Physical Methods of the Determination of Bone Mineral
       Content In Vivo by Dr. Reiss, Erlangen, Germany

1:30   Standards, Univ. of Wisconsin by R.M. Witt

1:45   Measurements at the Univ. of Chicago by L. Lanzl

2:00   Discussion of :

       a.   Calibration techniques
       b.   Choice of bone
       c.   Discrimination of osteoporosis
       d.   Units
       e.   Sources
       f.   Other

2:45   A New Portable, Direct Read-out Unit, Univ. of Wis. by R.Mazess

3:00-3:30   BREAK

3:30   Measurement of Density, Elasticity, and Speed of Ultrasound
       Propagation in Excised Strips of Bone by W.F. Abendschien and
       G.W. Hyatt from Georgetown University, Washington, D.C.

4:00   Bone Mineral Changes Induced by Growth Hormones by W. Harris
       from Massachusetts General Hospital, Boston, Massachusetts

4:30   GENERAL DISCUSSION

5:30   ADJOURNMENT

PERSONS WHO ATTENDED BONE SCANNING CONFERENCE
O'HARE AIRPORT CHICAGO, ILLINOIS
APRIL 25, 1969

Dr. Louis Zeitz
Dept. of Biophysics
Sloan-Kettering Instit.
New York, New York

Dr. Louis S. Meharg
University of Texas
Houston, Texas

Dr. Robert Marcus
National Institute of Arthritis
And Metabolic Diseases
National Institute of Health
Bethesda, Maryland   20014

Dr. Jay Shapiro
Washington Hospital Center
Washington, D.C.

Mr. C.M. Hilgers, M.S.
Dept. of Radiology
University of Minnesota
Minneapolis, Minnesota

D.C. Matthes, M.S.
V.A. Hospital
Radiotherapy Center
Wood, Wisconsin

Dr. N. Suntharalingam
Dept. of Radiology
Jefferson Medical College
Philadelphia, Pennsylvania

Dr. John R. Prince
Kansas City Hospital and
Medical Center
24th and Cherry Street
Kansas City, Missouri   64108

Dr. R.E. Rowland
Argonne National Lab.
9700 Cass Avenue
Argonne, Illinois   60439

Dr. Leonard Goodman
Physics Division
Argonne National Lab.
9700 Cass Avenue
Argonne, Illinois   60439

Dr. George Hyatt
Chairman, Orthopedic Surgery
Georgetown Univ. Med. Center
3800 Reservoir Rd.
Washington, D.C.   20007

Dr. W.F. Abendschein
Georgetown University
3800 Resevoir Rd.
Washington, D.C.   20007

Dr. J.T. Langloh
Georgetown University
3800 Reservoir Rd.
Washington, D.C.   20007

Gordon Sims
AECL Commercial Products
P.O. Box 93
Ottawa, Ontario, Canada

Robert Ratz
AECL Commercial Products
P.O. Box 93
Ottawa, Ontario, Canada

Mr. Henrey L. LeMien
Ayerst Laboratories
685 Third Avenue
New York, New York   10017

Dr. G. Donald Whedon
Director
NIAMD-NIH
Bethesda, Maryland   20014

Dr. Jacob Kastner
Argonne National Lab.
9700 Cass Avenue
Argonne, Illinois   60439

Dr. Elizabeth Lloyd
Assoc. Biophysicist
Radiological Physics Div.
Argonne National Lab.
9700 Cass Avenue
Argonne, Illinois   60439

Dr. John Marshall
Argonne National Lab.
9700 Cass Avenue
Argonne, Illinois   60439

Dr. John M. Vogel
Chief, Research Dept.
U.S.P.H.S. Hospital
15th Ave. and Lake St.
San Francisco, California
                    94118

Dr. William Dunnette
Mayo Clinic
Rochester, Minnesota

Dr. Heinz W. Wahner
Mayo Clinic
Rochester, Minnesota

Dr. Anders B. Ness
Mayo Clinic
Rochester, Minnesota

Dr. Fred Rose
Norland Associates
Fort Atkinson, Wisconsin

Robert O. Gorson, Chairman
Dept. of Radiologic Physics
Stein Research Center
Jefferson Medical College
Philadelphia, Pennsylvania   19107

Dr. C. Conrad Johnston, Jr.
Assoc. Prof. Of Medicine
Indiana Univ. Medical Center
Indianapolis, Indiana   46202

Dr. David Smith
Indiana Univ. Medical Center
Department of Medicine
1100 W. Michigan St.
Indianapolis, Indiana   46202

Dr. S.P. Vinograd, Director
Medical Science and Tech.
Space Medicine Division
NASA
Washington, D.C.

Dr. James Johnston
Orthopedic Clinic
Kaiser Hospital
208 W. McArthur
Oakland, California   94611

Dr. Arnold Engel
National Center for Health
Statistics
330 C. St. S.W.
Washington, D.C.

Dr. Marvin Goldman
Radiation Biological Lab.
University of California
Davis, California

Dr. R. Eugene Johnston
Div. of Nuclear Medicine and
Biophysics
Vanderbilt University
Nashville, Tennessee   37203

Dr. Surendra Rishi
V.A. Hospital
Washington, D.C.

Dr. Brian Devine
National Center for Health
330 C. St. S.W.
Washington, D.C.

Miss Hing-Har Lo, M.S.
Radiology Dept. White 2
Massachusetts General Hospital
Boston, Massachusetts

Dr. William Harris
Massachusetts General Hospital
Boston, Massachusetts

Dr. Edward Creighton
Michael Reese Hospital
Chicago, Illinois

Dr. Charles Enerson
Vanderbilt Univ. Hospital
Nashville, Tennessee

Dr. John Wallace
Dept. of Radiology
Jefferson Medical College
Philadelphia, Pennsylvania   19107

Robert F. Curley, M.S.
Dept. of Radiology
Jefferson Medical College
Philadelphia, Pennsylvania   19107

Dr. Jack Edeikin
Chief, Diagnostic Division
Dept. of Radiology
Jefferson Medical College
Philadelphia, Pennsylvania

Dr. K.H. Reiss
Abteilung WW Med ERPL
Siemens AG
D-8520 ERLANGEN
Postfach 40
Federal Republic of Germany

Dr. Eugene Ball
Dept. of Medicine
Univ. of Alabama
School of Medicine
1919 7th Ave. So.
Birmingham, Alabama

Dr. Lawrence Lanzl
Dept of Radiology
Univ. of Chicago Hospital
Chicago, Illinois

Dr. Robert C. Thompson
John Hopkins Hospital
CMSC 9-10108
Baltimore, Maryland 21205

Dr. Helen Clark
Purdue University
School of Home Economics
LaFayette, Indiana 47907

Mrs. Catherine Justice
Graduate Student
Purdue University
School of Home Economics
LaFayette, Indiana 47907

Dr. Francis Spurrell
College of Vet. Medicine
University of Minnesota
Minneapolis, Minnesota

Dr. Bertram Levin
Michael Reese Hospital
Dept. of Radiology
Chicago, Illinois

Dr. A.G. Schrodt
Packard Instrument Co.
2200 Warrenville Rd.
Downers Grove, Illinois

Frank Kubina
Life Science Sales
11752 South Western Ave.
Chicago, Illinois 60643

Mr. C.G. Tapley
Amersham Searle Corp.
333 Howard Ave..
Des Plaines, Illinois 60018

Mr. Ted Hall
Amersham Searle Corp.
333 Howard Ave.
Des Plaines, Illinois

Dr. Donald Taves
University of Rochester
Medical School
Rochester, New York

Mr. James Galvin
Peter Bent Brigham Hospital
Boston, Massachusetts

Participants from the Univ. of Wis.

John R. Cameron, Ph.D.

Richard B. Mazess, Ph.D.

John M. Jurist, Ph.D.

Robert M. Witt, M.S.

Philip F. Judy, M.S.

Everett L. Smith, M.S.

Joyce L. Fischer, R.T.

Charles R. Wilson, M.S.

Gordon Meyer (Poultry Science)

Milton Sunde, Ph.D. (Poultry Sc.)

Gerard Ponchon, M.D. (Biochem)

Steven Babcock, M.D.

PERSONS UNABLE TO ATTEND THE BONE SCANNING CONFERENCE
WHO ARE INTERESTED IN THIS TECHNIQUE

Dr. Frederic Bartter
Chief, Clinical Endocrinology
Branch
NHI-NIH
Bethesda, Maryland 20014

Dr. Bertrand Brill
Div. of Nuclear Medicine-Biophy.
Vanderbilt University
Nashville, Tennessee

Dr. James S. Arnold
Director, Radioisotope Div.
Kansas City General Hospital
Kansas City, Missouri 64108

Dr. John E. Bower
Artery-Kidney Unit
Univ. of Mississippi
Medical Center
Jackson, Mississippi 39216

Dr. David Brown
Dept. of Pediatrics
Univ. of Minnesota
Minneapolis, Minnesota

Mr. Charles Lescrenier
Assoc. Prof. of Radiology
Milwaukee Co. General Hospital
Milwaukee, Wisconsin 53226

Dr. Lawrence Dietlein
NASA, MSC
Medical Research and Operations
Houston, Texas

Dr. Hugh Hickey
Orthopedic Surgery
4611 N. Oakland Ave.
Milwaukee, Wisconsin 53211

Dr. Ladislaw Novak
Clinical Pathology
Mayo Clinic
Rochester, Minnesota

Dr. Robert G. Waggener
Assist. Prof. of Radiology
Univ. of Texas Medical School
7703 Floyd Curl Drive
San Antonio, Texas 78229

Dr. Lester Goodman, Chief
Biomedical Eng. and Inst. Branch
Dept. of Health, Educ. and Welfare
NIH
Bethesda, Maryland 20014

Luther E. Pruess, Head
Div. of Nuclear Medicine
Edsel B. Ford Inst. for Medical
Research
Henry Ford Hospital
Detroit, Michigan 48202

Dr. Paul Rambout
Medical Research and Operation
Directorate
NASA
Houston, Texas

Dr. Donald Young ,
NASA-Ames Research Center
Biotechnology Division
Moffett Field, California

Dr. Charles Pak
NHI-NIH
Bethesda, Maryland 20014

Dr. Robert Coifman
Univ. of Minn. Medical School
Dept. of Pediatrics.
Box 494
Minneapolis, Minnesota 55455

Dr. Naomi Goldsmith
Orthopedic Clinic
Kaiser Hospital
208 W. McArthur
Oakland, California 94611

Dr. Lawrence Riggs
Mayo Clinic
Rochester, Minnesota

Dr. Justin Wolfson
Dept. of Radiology
University of Minnesota Hospital
Minneapolis, Minnesota 55455

Jerry Anderson, M.D.
U.S.P.H.S. Hospital
San Francisco, California

Dr. Ann Cox
Dept of Radiology
University of Chicago Hospital
Chicago, Illinois

Dr. Harold Hodge
University of Rochester
Rochester, New York

Tom Rauterkus
Systems Research Laboratories
500 Woods Dr.
Dayton, Ohio 45432

A QUANTITATIVE MEASURE OF SKIN TRANSPARENCY

John R. Cameron, Gary Fullerton and Mark Mueller

I. INTRODUCTION

It has been observed that there is a correlation between the occurrence of osteoporosis and transparent skin, which is particularly marked among women with rheumatoid disease (1,2,3). It has been suggested that a disorder of the connective tissue (collagen disturbance) could underlie both the phenomena of transparent skin and certain forms of osteoporosis (4).

The skin transparency in the above mentioned studies was determined by a qualitative judgment of the visual appearance of the skin of the back of the hand. In order to determine the extinction coefficient of skin we have developed equipment to obtain a quantitative measure of of the light transmission of a skinfold together with the thickness of the fold. Extinction coefficients calculated from these measurements will be correlated with bone mineral measurements on the same individual using the technique developed at the University of Wisconsin (5,6).

Since the instrumentation for measuring skin transparency and thickness is basically simple, it is hoped that this technique might prove to be a reliable screening procedure for osteoporosis.

II. METHOD

A Lange skinfold caliper was modified so that one

of its jaws contains a small light source[*] and the opposing jaw a CdS light sensor.[**] With this instrument it is possible to obtain a simultaneous measure of the thickness of a skinfold and the attenuation of a light beam through the skinfold.

Measurements are at present being taken on the back of the hand over the midshaft and distal end of the fourth metacarpal and on the web between the index finger and thumb on both hands. These sites were chosen because:

1) they allow comparison with the data of McConkey et al. (1,2,3) which were also taken on the back of the hand,

2) clinical observers first noted the relationship of transparent skin and osteoporosis in their observations of skin on the back of the hand,

3) a skinfold which includes little subcutaneous fat is normally found in these locations,

4) these areas are readily accessible for measurement.

III. RESULTS

Our preliminary data on 30 elderly nuns does not allow satisfactory statistical interpretation but does permit the following tentative conclusions:

1) Individual differences in skinfold thickness and skin transparency are measurable by this method.

* Type 2102, 18V, 0.040 amp., Chicago Miniature Lamp Works, Chicago, Illinois.

** Clairex, Model CL 907, Allied Radio Electronics, Chicago, Illinois.

2) Skinfold transparency is primarily dependent on the thickness of the fold.

3) Bone mineral measurements of the radius correlate better with skinfold transparency than with skinfold thickness.

4) There is an even higher correlation between the extinction coefficient of the skinfold (i.e. light transmission corrected for skin thickness) and the bone mineral content of the radius.

5) A more accurate measure of skinfold thickness is necessary to clearly delineate the relationship between skin transparency and bone mineral content.

IV. DISCUSSION

The results of initial measurements indicate that our goal of quantifying skinfold thickness and skin transparency is obtainable. Using optical density standards it is possible to obtain standardized, reproducible measurements. Current effort is directed towards obtaining sufficient data to determine the correlation coefficient of the degree of osteoporosis to the extinction coefficient of the skin.

A new instrument is under construction which uses a Harpenden skinfold caliper (7) which not only will permit a much more precise measure of skinfolds encountered on the back of the hand but will also permit the measurement of the skin transparency at two closely spaced locations. This modification will also permit studies to determine the optimum wavelength of light to be used in the absorption studies. The study will concentrate on patients with rheumatoid arthritis.

REFERENCES

1. McConkey, B., Fraser, G.M. and Bligh, A.S.,
   "Osteoporosis and Purpura in Rheumatoid Disease,"
   Quart. J. Med. 31, 419, (1962).

2. McConkey, B., Fraser, G.M., Bligh, A.S. and Whitely, H.,
   "Transparent Skin and Osteoporosis," Lancet 1, 693, (1963).

3. McConkey, B., Fraser, G.M. and Blight, A.S., "Transparent
   Skin and Osteoporosis," Ann. Rheum. Dis. 24, 219, (1965).

4. Shuster, S. and Bottoms, E., "Senile Degeneration of
   Skin Collagen," Clin. Sci. 25, 487, (1963).

5. Cameron, J.R. and Sorenson, J.A., "Measurement of Bone
   Mineral In Vivo: An Improved Method," Science, 142:
   230-232, (1963).

6. Sorenson, J.A. and Cameron, J.R., "A Reliable In Vivo
   Measurement of Bone Mineral Content," J. of Bone and
   Joint Surg., Vol. 49-A, No. 3, April, 1967.

7. Tanner, J.M. and Whitehouse, A., "The Harpenden Skinfold
   Caliper," Am. J. Phys. Anthro. 13: 743, (1955).

AN IMPROVED METHOD OF REPOSITIONING DISTAL END SITES
ON THE LINEAR BONE MINERAL SCANNER

By: Mira Binder
     Joyce L. Fischer
     James A. Sorenson

Introduction

A method for improving the precision of bone mineral measurements at the distal end of the radius using our present linear scanning device[1] has been developed. The fact that the shape of the radius near its distal end is rapidly changing makes relocation of the scanning site critical. Previously, improved precision was obtained by scanning at three closely spaced intervals at this site, and using the average of the three measurements. The closely spaced intervals were located by moving the scanning mechanism, which was fixed to a traveling microscope platform in 3 mm steps along the length of the bone.[2] This technique was not readily adapted to our present linear scanning device. The presently used technique requires that the subject remove and reposition his arm between successive scan measurements.

Methods

Three subjects were studied in the investigation. Their arms at the scanning site were enveloped in tissue equivalent material, the source-finger tip distances were 22.5 cm, 23 cm and 19 cm, respectively. Three scans were made on each subject while his arm was in position. Then, the tissue equivalent material was removed and the subject withdrew his arm. This process was repeated two more times. Thus, a total of nine scans were obtained for each subject with repositioning between scans No. 3 and 4, and scans No. 6 and 7. These measurements

were repeated under the same conditions for nine additional days.

Results

The following data reduction procedures were used to see if repositioning between scans improved precision.

A. Stationary Measurements

For each subject the average bone mineral content (in calculator units) was calculated for scans 1, 2 and 3 of the first day of measurement. The same was done for the first three scans of each of the following nine days. Thus, the averages of the first three scans each day were obtained. The standard deviation of the ten mean values was found to be 4.02% for Subject A; 2.32% for Subject B; and 3.95% for Subject C.

B. Repositioned Measurements

For each subject the average bone mineral content (in calculator units) was calculated for scans 1, 4 and 7 of the first day. (Repositioning took place between each of these scans). The same was done for scans 1, 4 and 7 made on each of the following nine days. The standard deviation of the ten mean values of scans 1, 4 and 7 of each day were found to be 2.70% for Subject A; 2.62% for Subject B; and 2.07% for Subject C.

Table 1 summarizes these results.

Discussion and Conclusions

An improvement in precision of measured bone mineral was demonstrated by removing the arm in between each of the three routine measurements on the distal end of the radius in two (Subjects A and C) of three cases; no significant improvement was found for Subject B.

These findings are now being used in our daily patient work. While the patient's arm is not repositioned for the three

routine scans near the midshaft of the radius, it is removed and repositioned for each of the three routine scans near the distal end of the radius.

Table 1

% Standard Deviation for the Daily Mean Mineral Content Measurement
of the Distal End of the Radius

	Scans 1, 2 and 3 averaged (No Repositioning)	Scans 1, 4 and 7 averaged (Repositioning between scans)
Subject A	4.02 %	2.70 %
Subject B	2.32 %	2.62 %
Subject C	3.95 %	2.07 %

REFERENCES:

1. R.M. Witt, J.A. Sorenson and J.R. Cameron, An Improved
    Bone Mineral Scanner (Progress Report, AEC Contract
    No. AT(11-1)-1422, August 1968)

2. J.A. Sorenson and J.R. Cameron, A Reliable In Vivo
    Measurement of Bone Mineral Content (Journal of Bone
    and Joint Surgery, Vol. 49-A, 1967)

BONE MINERAL DETERMINATION: RADIOGRAPHIC PHOTODENSITOMETRY AND DIRECT PHOTON ABSORPTIOMETRY

C. Colbert and R. B. Mazess

ABSTRACT

The accuracy of predicting bone mineral content was assessed using two radiological methods. Direct photon absorptiometry used a monoenergetic radionuclide source (^{125}I at 27.4 Kev) with a scintillation detector-pulse height analyzer system for direct bone scans. Radiographic photodensitometry used an X-ray tube source with film as the detector; the bone image on the radiograph was scanned with a photodensitometer-computer system. Mineral weight of standard bone sections (n=85) was predicted with a 3% standard error using photon absorptiometry and with a 6% error using photodensitometry.

Photodensitometric measurement of the bone image on a radiograph has been used for over 30 years as a quantitative indicator of bone mineral content,[1] but photodensitometry has been viewed with skepticism by many workers and very high inaccuracies (20 to 50%) have been reported.[2] Among the problems usually cited are: (a) the contribution of scattered radiation from the broad X-ray beam is a major source of error, (b) variability in film exposure, film response, and film development cause errors, (c) the energy spectrum from the X-ray tube is broad and often variable, leading to large uncertainties in the effective absorption coefficients of bone and soft tissue, and (d) the energy spectrum from the X-ray tube is "hardened" in passing through soft tissue and bone since the lower energy component is preferentially absorbed. In 1967 an improved photodensitometric method was developed at the Fels Research Institute using a Joyce-Loebl Mark III microdensitometer connected on-line to a LINC-8 computer.[3] This method tends to minimize errors associated with scattered radiation and film variability. The image of an aluminum reference wedge, exposed on the same film as the bone of interest, is first scanned to determine film background density and level of exposure. The bone image is then scanned in line-by-line fashion and the computer calculates a bone index [μV] proportional to the bone mineral mass in the scanned image. The time required to measure the bone index for a 1-cm length of a phalanx or metacarpal is about seven minutes; this includes the scan of the reference wedge which need be done only once per film.

In contrast to photodensitometry, the direct photon absorption method developed by Cameron and Sorenson[4] at the University of Wisconsin is relatively free of errors since the problems given above for photodensitometry are not encountered.

Absorptiometry uses a monoenergetic radionuclide (usually tin-filtered ^{125}I at

27.4 Kev) as a photon source and a scintillation detector-pulse height analyzer

system. The source and detector are highly collimated (3 mm) to eliminate

effects of scattered radiation. The mechanically linked source and detector

are passed across the bone of interest, and the measured absorption ("scan in-

tegral") is directly proportional to the bone mineral mass in the scan path.

Technical improvements reported by the Wisconsin[1] group gave direct photon

absorptiometry a vastly superior precision and accuracy compared to previously

reported values for radiographic photodensitometry.[5] We evaluated the accuracy

attained with the Fels photodensitometric method, and found it more nearly

. comparable to that of absorptiometry.

Eight-five bone sections, 1-cm in axial length, were taken from extremities

of human cadavers. The sections were ashed at 600°C for 24 hours, weighed to

0.1 mg, and impregnated with paraffin. Radiographs of these sections were made,

half on one film and half on another, with a conventional X-ray set (50 Kvp and

3.4 mm Al filtration) using no-screen film. One set of films was made at 50 mas

and another at 70 mas to evaluate reliability with varying exposure. The bones

were prepared and the films were taken in Wisconsin, but the films were sent to

Fels for automatic processing and photodensitometric analysis.[3] Determinations

of bone mineral content using photon absorptiometry were done on the same sections

at Wisconsin. The absorptiometric scans, and the radiographs, were made with the

sections under 5-cm of water; this was necessary to eliminate the effect of organic

matter (paraffin) and to simulate soft tissue cover.

The precision of repeat absorptiometric measures on the same section, or of

repeat photodensitometric traces on the same film, was high (1 to 2% error).

Measurements of the same sections from films at 50 mas and 70 mas exposures gave

a high correlation (r=0.99) and the standard error of estimate indicated an uncertainty of 4.4%. In a subsequent experiment, twenty of the eighty-five bone images were each rescanned five times. Average bone indexes were determined from the 50 mas and 70 mas films. The correlation between bone indexes from these two films was r=0.993; the average bone index from the 70 mas film can be predicted from the average bone index from the 50 mas film within 3.8%. Other workers using photodensitometry report between-film uncertainties of from 5 to 10%.[6] Since our films were taken at a single time and developed together, low variability in film exposure and development may be responsible for our somewhat higher precision. The long-term precision reported for photon absorptiometry is about 1% for measurements on standards and 2% for measurements of bones *in vivo*.[5]

The regression equations (plotted in Figures 1a and 1b) and correlations relating the radiological measures to bone mineral content were:

FELS: 50 MAS   Ash weight(g) = 1.0969 Bone Index + 0.0582; r = 0.983

FELS: 70 MAS   Ash weight(g) = 1.0906 Bone Index + 0.0578; r = 0.979

WISCONSIN   Ash weight(g) = 0.0377 Scan Integral + 0.0747; r = 0.995

The correlation between the two methods also was high (r=0.97 to 0.98) and the uncertainty in estimating one index from the other was about 7%. The uncertainty in prediction (standard error of estimate) of the ash weight using absorptiometry was 3% while the uncertainty using the Fels method of photodensitometry was 6%. Apparently the correction for film background density and scattering used in the Fels method allowed a much higher accuracy than achieved by other photodensitometric approaches.[2] Some of the error using photon absorptiometry results from use of a narrow (3-mm) beam which does not measure the entire 1-cm bone section; on standards of uniform shape the accuracy of absorptiometry is limited by photon counting statistics and is typically about 1 to 2%.

Some of the uncertainty in the photodensitometric prediction of ash weights may be due to uncertainties in the ash weight determinations rather than to errors of the photodensitometric method and hence the 6% error may be an overestimation.

Even though the precision and accuracy of the Fels photodensitometric method are probably slightly lower than attained with direct photon absorptiometry, the radiographic method offers some advantages: (a) films can be made rapidly, (b) location and relocation of measurements are facilitated, (c) a visible record is maintained on which the entire bone can be scanned in a line-by-line fashion, (d) examination of the axial skeleton may be facilitated and (e) X-ray machines are readily available. Correction for background density of the radiograph allows photodensitometry to achieve an accuracy suitable for use in surveys of skeletal status and for certain longitudinal studies and clinical and diagnostic applications.

Charles Colbert

The Fels Research Institute

Yellow Springs, Ohio 45387

Richard B. Mazess

Departments of Anthropology and Radiology

University of Wisconsin
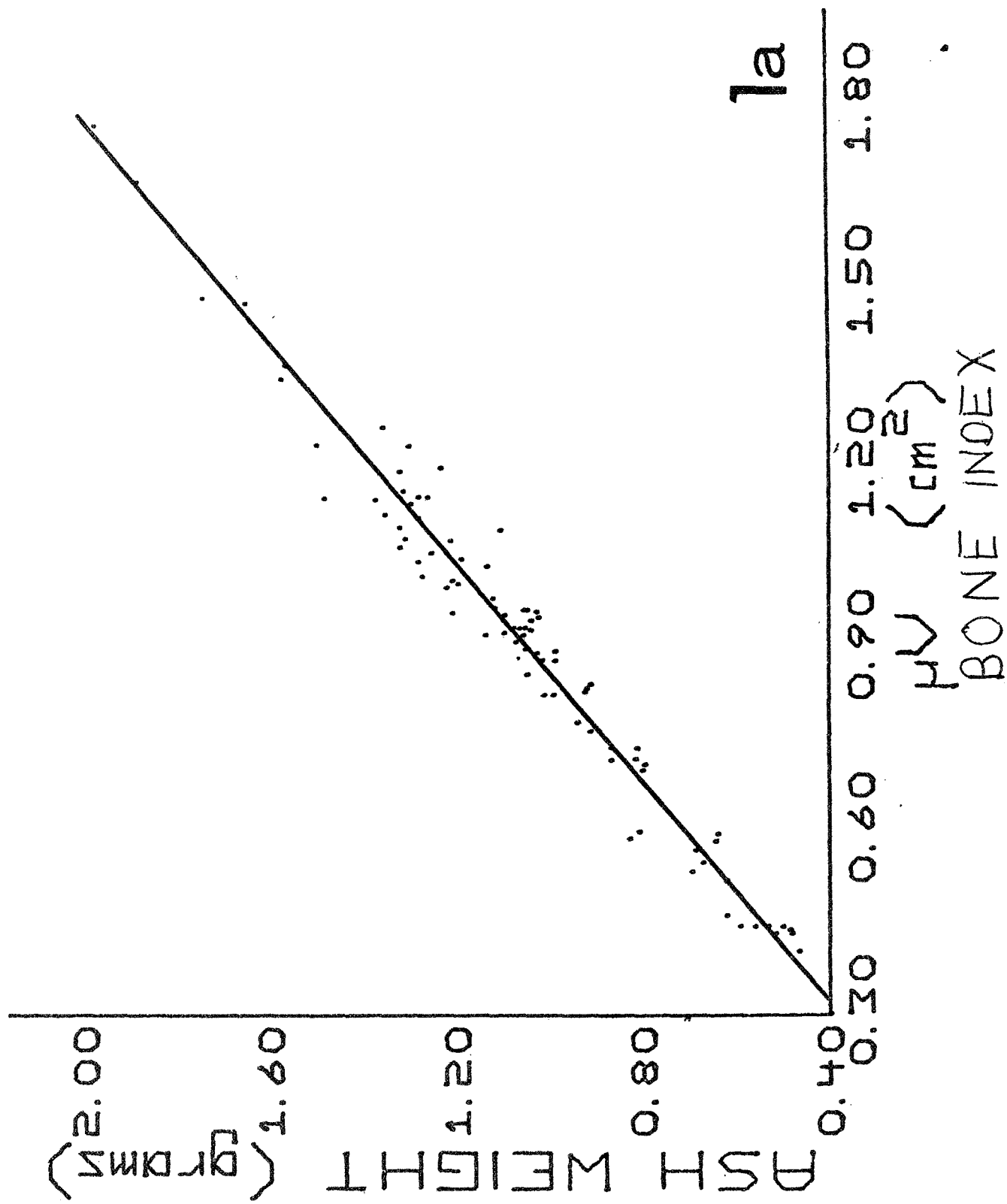
Madison, Wisconsin 53706.
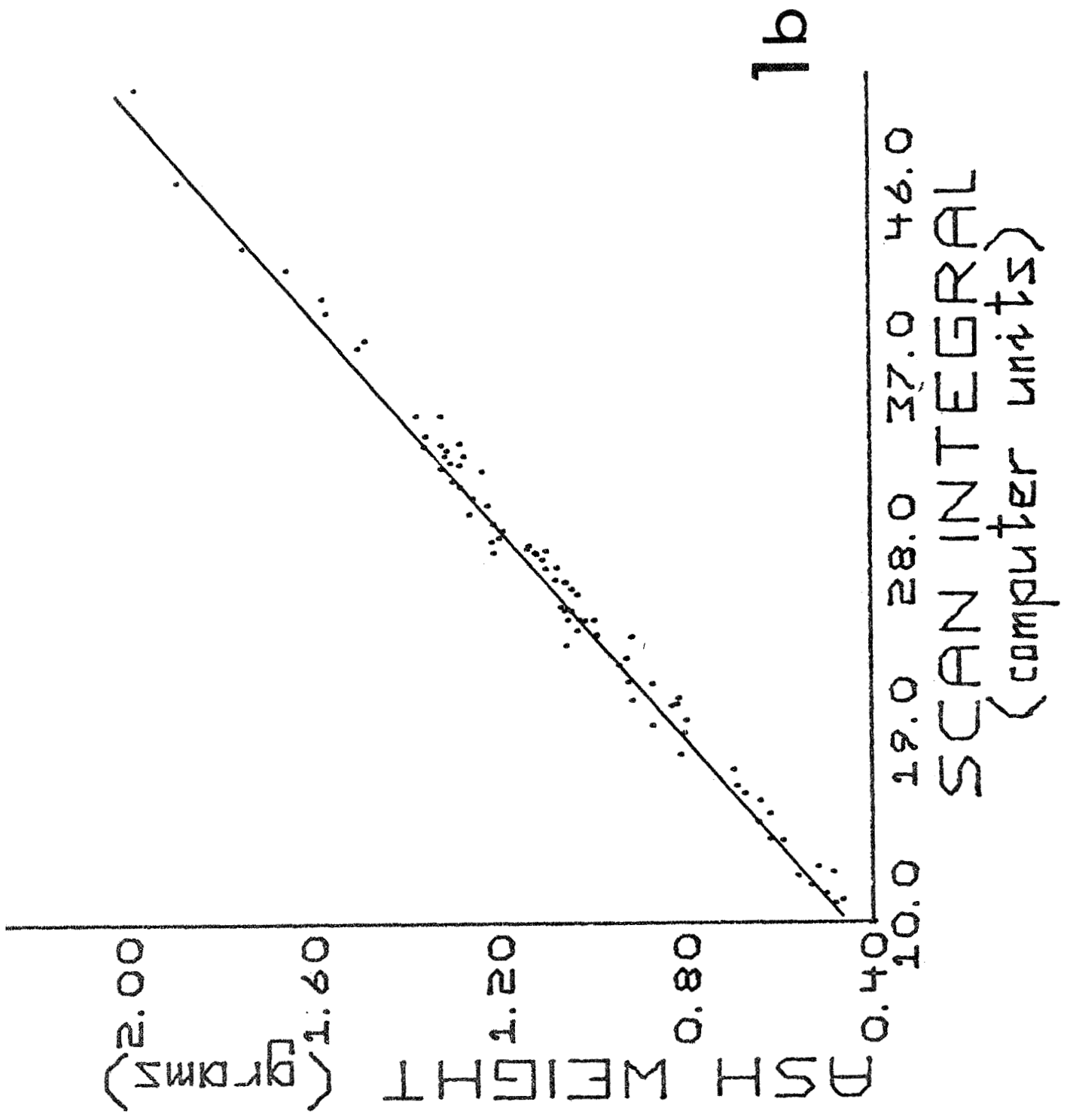
REFERENCES AND NOTES

1. P.B. Mack, A.T. O'Brien, J.M. Smith, *Science* 89, 467 (1939); P.B. Mack, W.N. Brown, H.D. Trapp, *Am. J. Roentgenol.* 61, 808 (1949); W.N. Brown, *Proc. Nat'l Electronics Conf.* 5, 64 (1949); K.A. Omnell, *Acta Radiol. Suppl.* 148 (1957); H. Schraer, *J. Pediatr.* 4, 416 (1958); D.E. Williams and R.L. Mason, *Science* 138, 39 (1962); G.D. Whedon, W.F. Neumann, and D.W. Jenkins, eds., *Progress in the Development of Methods in Bone Densitometry,* (NASA Report SP-64, Washington, D.C.: 1966); R.B. Pridie, *Brit. J. Radiol.* 40, 251 (1967).

2. P.T. Baker, H. Schraer, R.G. Yalman, *Photogrammetric Eng.* 25, 456 (1959): H. Schraer, R. Schraer, H.G. Trostle, A. D'Alfonso, *Arch. Biochem. Biophys.* 83, 486 (1959); D.J. Baylinck, G.P. Vose, W.E. Dotter and L.A. Hurxthal, *Lahey Clin. Bull.* 13, 217 (1964); G.P. Vose, S.A. Hoerster, Jr., and P. Mack, *Am. J. Med. Electron.* 3, 181 (1964); G.P. Vose and R.E. Pyke, *Invest. Radiol.* 1, 371 (1966).

3. C. Colbert, J.J. Spruit, and L.R. Dávila, *Trans. N.Y. Acad. Sci.* II, 30, 2:271 (1967).

4. J.R. Cameron and J. Sorenson, *Science* 142, 230 (1963); J.A. Sorenson and J.R. Cameron, in G.D. Whedon *et al, op cit* (1966).

5. R.B. Mazess, J.R. Cameron, B. O'Connor and D. Knutzen, *Science* 145, 388 (1964); J.A. Sorenson and J.R. Cameron, *J. Bone Jt. Surg.* 49-A, 481 (1967); J.R. Cameron, R.B. Mazess, and J.A. Sorenson, *Invest. Radiol.* 3, 141 (1968).

6. W. McFarland, *Science* 119, 810 (1954): J.B. Anderson, J. Shimmins and D.A.

Smith, *Brit. J. Radiol.* 39, 443 (1966); E.H. Mayer, H.G. Trostle, E. Acker-

man, H. Schraer, O.D. Sittler, *Radiation Research* 13, 156 (1960); D.B. Morgan,

F.W. Spiers, C.N. Pulvertaft and P. Fourman, *Clin. Radiol.* 18, 101 (1967).

LEGENDS

Figure 1a   Ash weight (g) plotted against Fels bone mineral index [μV];

                 for 85 standard 1-cm sections of human bone.

Figure 1b   Ash weight (g) plotted against absorptiometric bone mineral

                 index (scan integral); for 85 standard 1-cm sections of

                 human bone.

8

1a

ASH WEIGHT (grams)

BONE INDEX

HV (cm²)

1b

SCAN INTEGRAL
(computer units)

ASH WEIGHT (grams)

9

PRELIMINARY REPORT

BONE MINERAL CONTENT OF WAINWRIGHT ESKIMO

JANUARY 1969

R. B. Mazess

PRELIMINARY REPORT

BONE MINERAL CONTENT OF WAINWRIGHT ESKIMO

JANUARY 1969

R. B. Mazess

Measurements of bone mineral content were made,
using a radiometric method, on inhabitants of Wainwright,
Alaska, during July 1968. The direct photon absorption
method for bone mineral measurement was used to evaluate
skeletal status in this Eskimo community.

Methods

Direct photon absorptiometry has been extensively
developed at the Radioisotope Laboratory of the University
of Wisconsin, and has been shown to be an accurate and pre-
cise method for measurement of bones in vivo (Cameron
and Sorenson, 1963; Cameron et al., 1968; Sorenson and
Cameron, 1967). A monoenergetic radionuclide photon source
is passed across the measurement site and the transmitted
radiation measured with a scintillation detector-pulse
height analyzer system. In the Madison laboratory the
results are usually punched on paper tape for computer
analysis, but for the Wainwright measurements a new device
for logarithmic conversion of a ratemeter signal was used
and the resultant data recorded on a poteniometric chart
recorder. The recorder data was analyzed later in Madison.

On each of the Wainwright subjects absorptiometric
scans were made on the shaft of the radius and of the
ulna using a ^{125}I source; scans were also made with ^{241}Am
on the humerus midshaft. Two or three repeat measurements
were made at each location on most subjects. This pre-
liminary analysis deals only with the radius data.

Initially 93 people were measured including 31
female and 28 male children, and 8 adult males. Five of
the youngest children had poor results, probably due to

movement during the measurements, and their data were
eliminated. Of the adults one elderly male (age 80)
and one elderly female (age 62) were clearly osteoporotic
and their data were not included in the analysis.
Another younger male (age 21) with reported endocrine
abnormalities and very aberrant bone mineral was also
excluded. The final sample is outlined in Table 1

TABLE 1
Outline of Wainwright Eskimo Samples

	MALES		FEMALES	
	n	Age Range	n	Age Range
CHILDREN	28	5-17 years	26	6-17 years
ADULTS	24	19-66 years	7	20-54 years

Precision of the measurements was examined by
measuring a standard in both Madison and Wainwright using
the same system. There was virtually no systematic
difference between results from the two locations, but
there was more measurement variability in Alaska (Table 2).
The nature and extent of the differences between results
with the ^{125}I and ^{241}Am sources were similar to those
theoretically expected.

TABLE 2
Comparison of Absorptiometric Scans on an Al Standard In
Wisconsin and Alaska

		INTEGRAL		WIDTH	
		Mean	CV	Mean	CV
^{125}I	Wainwright	121.35	3.24%	8.374	2.03%
	Madison	121.27	1.03	8.400	0.91
^{241}Am	Wainwright	38.638	3.58	8.151	1.98
	Madison	38.430	2.32	8.190	1.39

Results

Adults: The bone measures for the Eskimo adults
are compared with those for U. S. whites in Table 3.
Both male and female Eskimos have values for bone
mineral content and bone width almost the same as the
mean values for the whites. Regression analysis showed
that at a bone width of 1.4 cm the estimated mineral
content for the Eskimo males was 1.17 g/cm while for
the whites it was 1.21 g/cm; the corresponding values for
females were 1.10 g/cm and 1.06 g/cm. Given their small
body size, the Eskimos have a relatively high bone mineral
content. However, this may result from the greater
body weight and heavier body build of these Eskimos
compared to U. S. whites. The sex difference in bone
mineral content was somewhat smaller in the Eskimo than
in the whites; this may be due to the smaller sexual
dimorphism for body build in the Eskimos.

TABLE 3
Comparison on Bone Measures For
Eskimo and White Adults

	MINERAL			WIDTH		
MALES:	Mean	SD	CV	Mean	SD	CV
Eskimo	1.22	0.12	10.1%	1.47	0.10	6.9%
White	1.28	0.17	13.5	1.50	0.14	9.4
FEMALES:						
Eskimo	0.95	0.15	15.7	1.22	0.22	18.1
White	0.92	0.12	13.2	1.25	0.13	10.6

Children: The morphological characteristics and
bone measures for Eskimo children are compared with those
for U. S. white school children in Table 4. The U. S.
white children, particularly the males, were younger than
their Eskimo counterparts. These age differences were
reflected in part by differences of body size. The pattern
of height and weight differences indicated that the Eskimo
children were relatively heavier than white children per

unit of stature. Since arm circumference and skinfold did not show the Eskimos to be fatter than the whites, the difference seemed to indicate a generally heavier body build for the Eskimos.

TABLE 4
Morphology and Bone Measures For
White and Eskimo Children

	ESKIMO			WHITE		
	Mean	SD	CV	Mean	SD	CV
Male Children:						
AGE (months)	147.4	45.9	32.2%	121.6	27.6	22.7%
STATURE (cm)	146.8	22.1	15.0	142.3	13.7	9.6
WEIGHT (kg)	45.1	16.5	36.7	35.6	12.6	35.3
ARM CIRCM. (cm)	21.8	3.4	15.4	20.7	3.9	18.9
ARM SKINFOLD (mm)	7.5	1.9	26.1	10.3	4.8	46.9
BONE MINERAL (g/cm)	.801	.234	29.2	.636	.145	22.9
BONE WIDTH (cm)	1.17	.179	15.3	1.11	.145	13.0
Female Children:						
AGE (months)	142.3	38.6	27.5	128.8	28.0	21.7
STATURE (cm)	143.7	15.6	10.8	144.6	14.7	10.2
WEIGHT (kg)	45.3	15.7	34.7	35.6	12.2	34.3
ARM CIRCUM. (cm)	22.1	4.3	19.5	20.4	3.0	14.9
ARM SKINFOLD (mm)	13.9	6.8	49.0	11.3	4.6	40.4
BONE MINERAL (g/cm)	.726	.181	24.9	.610	.149	24.4
BONE WIDTH (cm)	1.07	.167	15.7	1.04	.143	13.7

The Eskimo children had a higher bone mineral content than the whites, but this reflected in part group differences in age, height, weight and bone width. In both Eskimos and whites these factors were highly correlated with bone mineral (Table 5). Regression analysis was therefore used to assess the import of these factors.

TABLE 5
Correlations of Bone Width, Height, Weight, and with
Bone Mineral Content in Eskimo and White Children

	ESKIMO		WHITE	
	Male	Female	Male	Female
n	26	28	108	86
STATURE	0.84	0.89	0.85	0.84
WEIGHT	0.93	0.82	0.81	0.86
STATURE & WEIGHT	0.94	0.89	0.86	0.88
BONE WIDTH	0.84	0.85	0.84	0.86
AGE	0.90	0.84	0.74	0.81

The conventional measure used for evaluation of skeletal status by the Radioisotope Laboratory is the bone mineral content per unit of bone width. Regression analysis indicated that Eskimo children have a higher bone mineral content per unit bone width than the whites, and consequently their skeletal status would be considered adequate. For example, at a bone width of 1.0 cm the mineral content for Eskimo boys would be 0.616 g/cm compared to 0.541 g/cm in whites; the corresponding values for girls were 0.663 and 0.570 g/cm. This would indicate about 10 to 15% greater mineral content in Eskimo children, but would not take into account the heavier body build of the Eskimos. Regression analysis, taking into account height and weight, was used to assess the effect of body build on bone mineral. The results indicated that in smaller children there would be little or no difference of bone mineral content if body build were identical for the two groups; in persons of larger body size there would be a group difference and the Eskimos would have 10 to 15% greater bone mineral content than the whites (Table 6). Consequently the higher bone mineral content in Eskimo children seems not to merely reflect differences of body build since the difference is at least partially evident for the hypothetical case of identical body builds.

TABLE 6
Estimated Bone Mineral Content For Children of Two Body Sizes

		Weight Stature	127 cm 25 kg	152 cm 50 kg
MALES ----		ESKIMO	0.518	0.869
		WHITE	0.505	0.746
FEMALES ----		ESKIMO	0.548	0.819
		WHITE	0.582	0.734

This same analysis (Table 6) also shows that sex differences in bone mineral content are partially dependent

on body size. Smaller females of both groups have a greater mineral content than the corresponding males, but with growth the situation is reversed and the males come to have a greater mineral content than the females.

Discussion and Conclusions

The preliminary results indicated that the bone mineral content of the Eskimo sample was similar to, or higher than the values for corresponding age and sex groups of U. S. whites. Both Eskimo adults and children had a surprisingly high mineral content relative to their small stature. This apparent "excess" of bone mineral in the Eskimo may be explained by the greater body weight, and heavier body build, of the Eskimos compared to U. S. whites. Larger samples will be needed to establish normative standards for the Eskimo shich take into account body build as well as age, sex, and bone width. Establishment of such standards for the Eskimo may aid in the diagnosis of metabilic bone diseases. Even though the mineral content of healthy Eskimos is adequate, pathologies are not absent. Two older subjects of this investigation were definitely osteoporotic and two others showed signs of diminished bone mineral content. In addition, one subject may have exhibited osteosclerosis. The completed analysis of the 1968 Eskimo data will serve as a guideline for subsequent investigations in Eskimo communities.

References

Cameron, J. R. and J. A. Sorenson 1963. Measurement of bone mineral in vivo: an improved method. SCIENCE 142: 230-232.

Cameron, J. R., R. B. Mazess, and J. A. Sorenson 1968. Precision and accuracy of bone mineral determination by direct photon absorptiometry. INVEST. RADIOL. 3: 141-150.

Sorenson, J. A. and J. R. Cameron 1967. A reliable in vivo measurement of bone mineral content. J. BONE. JT. SURJ. 49-A: 481-497.

Acknowledgements

nm/PRELIMINARY NOTE

^{99m}Tc POINT SOURCE FOR TRANSMISSION SCANNING

J. A. Sorenson, R. C. Briggs* and J. R. Cameron, Ph.D.

University of Wisconsin, Madison, Wisconsin

Simultaneous transmission-emission scanning was introduced by Kuhl as an aid to accurate keying of the emission image to patient anatomy (1). The commonly used radiation sources for transmission scanning have been ^{125}I (27-keV x-rays, 60-day half-life) and ^{241}Am (60-keV gamma rays, 460-yr half-life). Transmission imaging with the scintillation camera using ^{99m}Tc (140 keV gamma rays, 6-hr half-life) as the transmission source was recently reported by Anger and McRae (2). The transmission source consisted of a uniform distribution of ^{99m}Tc solution covering the full field of view of the camera crystal. We have developed a technique for making point sources of ^{99m}Tc usable for transmission imaging in rectilinear scanning procedures.

MATERIALS AND METHODS

The ^{99m}Tc source activity is contained on a small column of ion-exchange resin (Dow 21K, 50–100 mesh, J. T. Baker Chem. Co., Phillipsburg, N.J.) at the center of a lead and stainless-steel holder (Fig. 1). The holder is cylindrical with an outside diameter about 2.5 cm and length about 3.2 cm. The dimensions of the resin column are 3-mm dia $\times$ 6-mm long. A piece of 150-mesh stainless-steel

screen at each end of the column holds the resin in place. The chambers at the ends of the column and the column itself are sealed in an air-tight manner with rubber O-rings and diaphragms as shown in Fig. 1.

The resin is activated by passing the eluate from a ^{99m}Tc generator (from Squibb or Neisler) through the column. Radioactive solution is injected through the rubber diaphragm and into the chamber at one end of the column with a syringe and needle and is continuously withdrawn from the chamber at the opposite end with another syringe and needle or with a needle and flexible tubing connected to an evacuated collection vial. A 30-cc sample of ^{99m}Tc solution passes through the column in about a minute when a 30-cc evacuated collection vial is used.

Lead was used in the fabrication of the source holder to reduce radiation leakage through the sides of the holder. The lead pieces are press-fitted into the stainless-steel outer shell to maintain the air-tight seal. The remaining metal components are stainless steel to eliminate rusting.

The construction of the source holder permits easy replacement of the rubber diaphragms, stainless-steel screens or the resin column itself, should this be necessary. A ^{99m}Tc transmission source of the type described has been in use in our laboratory for about 3 months. After about 20 activations it was necessary to replace the rubber diaphragms at each end of the source column, but it has not yet been necessary to replace any of the other components of the source or of its holder.

The extraction efficiency of the resin column was determined at each activation of the source by measuring the activity of the ^{99m}Tc solution before and after passage through the resin column. The range was 35–65%, and typically it was about 50%. There was no systematic change in the efficiency with use. Passing the eluate through the column the second time increased the over-all efficiency to about
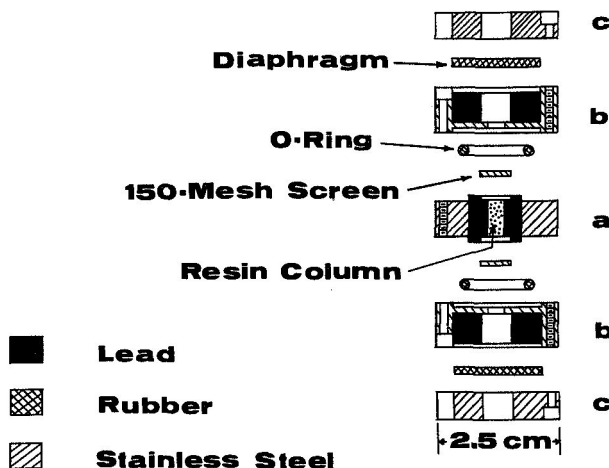

FIG. 1. Cross-section view of ^{99m}Tc point source. Piece b fastens to piece a, and piece c fastens to b, each with three Allenhead screws on common diameter.
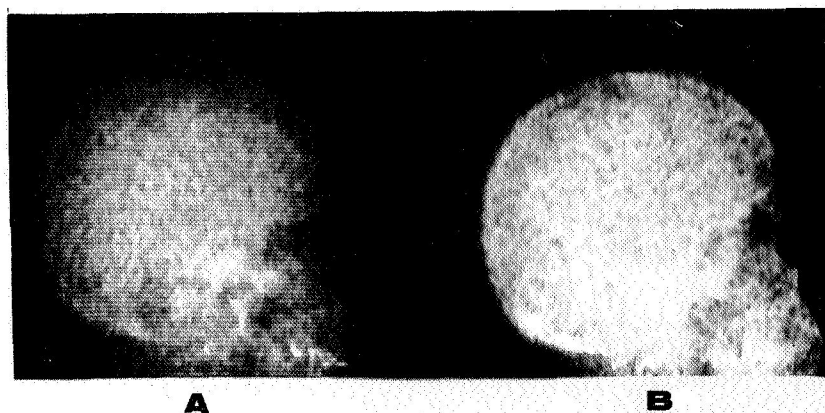
FIG. 2. Comparative transmission scans of skull with 30 mCi ^{99m}Tc (A) and 125 mCi ^{241}Am (B) on rectilinear scanner.

75%. The efficiency could be increased by using a column with a larger resin volume. In an earlier version of the source the size of the resin column was ¼-in. dia × ¼-in. long, and the extraction efficiency was consistently 80–90%. The size of the column was subsequently made smaller to improve the resolution of transmission images.

RESULTS

Comparative transmission images of the skull were obtained with a 30-mCi ^{99m}Tc source and with a 125-mCi ^{241}Am source on a conventional dual-headed rectilinear scanner (Ohio-Nuclear Model 54FD) (Fig. 2). The source-detector separation was about 30 cm for both scans. A straight-bore collimator, 3-mm dia × 50-mm long, was used on the detector for the ^{99m}Tc scan. Transmitted counting rates averaged about 15,000 cpm through the skull. The ^{241}Am source gave only about 1,000 cpm under the same conditions so the collimator aperture diameter was increased to about 6 mm for the ^{241}Am scan to give a more usable level of 4,000 cpm. The scanning speed was 250 cm/min for both scans, and the comparative information densities of the two scans were 100 counts/cm^2 (^{241}Am) and 400 counts/cm^2 (^{99m}Tc).

The information density of the ^{99m}Tc scan could be increased significantly by loading the source with more activity. Our present source was activated to 70-mCi activity without difficulty. The activity of available ^{241}Am sources is limited to about 125 mCi. This is an inherent limitation of the ^{241}Am source material because of its low specific activity and high self-absorption of 60-keV gamma rays.

The ^{99m}Tc point source was also used to obtain good-quality transmission images of the chest. However, attempts at outlining bony structures in the pelvis were not successful because of the low differential in absorption between bone and soft tissue. The usefulness of ^{99m}Tc as a transmission source thus appears to be best for outlining dense bones such as the skull and for outlining air spaces such as those in the chest.

To use ^{99m}Tc as the transmission source in conjunction with ^{99m}Tc emission scanning it would be necessary to use a dual-headed scanner with opposing detectors. A separate detector is required for each image since there would be no way of distinguishing transmitted from emitted photons with a single detector. To obtain directly superimposable transmission and emission images with a dual-probe scanner, the transmission source would be placed directly over the center holes of the focusing collimator on the emission detector. This would require careful shielding of the emission detector from the transmission source.

For this reason a 5-mm thick × 25-mm dia lead shield was made to be placed over one end of the transmission source. With this shield in place it was observed that the ^{99m}Tc source could be placed directly over the center holes of the emission-detector focusing collimator with a negligible increase in background counting rates. The focusing properties and efficiency of the collimator were somewhat disturbed in this arrangement with the efficiency of the collimated 5-in. dia emission detector being reduced by about 15%. The results suggest, however, that simultaneous transmission-emission scanning with ^{99m}Tc as the only source is possible on a dual-headed scanner.

REFERENCES

1. KUHL, D. E., HALE, J. AND EATON, W. L.: Transmission scanning: A useful adjunct to conventional emission scanning for accurately keying isotope deposition to radiographic anatomy. *Radiology* **87**:278, 1966.
2. ANGER, H. O. AND McRAE, J.: Transmission scintiphotography. *J. Nucl. Med.* **9**:267, 1968.

DRILL THRU 3-HOLES 1/8"DIA.
EQUALLY SPACED ON 3/4"DIA.CIRCLE

— Piece A, Number Req. 2 —

7/8" DIA

7/32"

3/16"

STAINLESS

DRILL AND C'BORE 3-HOLES
EQUALLY SPACED ON 3/4"DIA.
CIRCLE FOR 3-48 M.S. SOCKET
HEAD CAP.

7/8" DIA

5/6" DIA

7/32"

1/32"

1/8"

13/64"

0.080"

0.345"

LEAD

— Piece B, Number Req. 2 —

— Piece C, Number Req. I —

DRILL AND TAP 3-HOLES
EQUALLY SPACED ON 3/4"
DIA. FOR 3-48M.S.

Stainless

7/8" DIA.

LEAD

0.011"

0.080"

1/8"

1/4"

3/8"

0.080"

0.250"

0.080"

0.410"

UNIVERSITY OF WISCONSIN
BONE MINERAL LABORATORY

99mTc Source Holder

Scale: Enlarge	Material: As noted
Drawing by Orlando	Designed by J.A.Sorenson
	Checked by J.A.S.

Drawing No. O-69   Sheet No I OF 2

NOTE: Lead pieces should press fit into the steel
All holes should be oriented as shown above.

8 3/8 x 9/16 Rubber gasket

A   B   C   B   A

ASSEMBLY

UNIVERSITY OF WISCONSIN
BONE MINERAL LABORATORY

99mTc Source Holder

Scale: Enlarge	Designed by J.A.Sorenson
Drawing by Orlando	Checked by J.A.S.
Drawing No. OO–69 Sheet No 2 of 2	

DETECTION OF OSTEOPOROSIS BY MEASUREMENT OF
MONOENERGETIC PHOTON ABSORPTION

E. L. Smith, S. W. Babcock and J. R. Cameron

One of the common disorders of the ageing white population is osteoporosis. It is one of the most elusive diagnostic problems for the present day clinician. Due to the gradual onset of the condition, it is difficult to diagnose at an early stage. Therefore the presence of osteoporosis is often not diagnosed until the spontaneous collapse of a vertebra or fracture of the femoral neck has occurred. When spontaneous fractures occur, the bone mass may be 40 to 50% less than that present at age thirty. Spontaneous fractures require bed rest and immobilization which increases the bone mineral loss rate. The greater longevity of the human population, suggests that osteoporosis will be an increasing medical problem.

Using present radiographic techniques, osteoporosis is observed frequently in postmenopausal women. Therefore, a hormonal decrease is being investigated by a number of laboratories as a possible cause of osteoporosis in post-menopausal women. At the present time little definite evidence is present to demonstrate changes of human osteoporotic bone metabolism when either estrogen or androgen is given. Davis (5) and associates have shown some evidence using the Cameron and Sorenson photon absorption method (4,12) that osteoporosis in females is retarded by extrogenic replacement therapy. The therapy group showed less bone loss than the control group

in the first part of the study. Later the bone loss of the therapy group paralleled the control group.

In a review article, Nordine (10) indicates that calcium deficiency over a long period of time will cause osteoporosis. Rats on calcium deficient diets with adequate supply of Vitamin D have been shown to develop osteoporosis. This type of calcium deficient induced osteoporosis cannot really be compared with that found in man. Garn demonstrated that the quantity of calcium in the diet has little or no effect on the development of osteoporosis in man. The problem of osteoporosis is apparently widespread as seen in similar patterns of bone loss in El Salvador, Guatemala, and the United States (7).

Another possible cause of osteoporosis is immobiliza-tion (8). It has been demonstrated numerous times that bed rest and limb immobilization will cause disuse osteoporosis, while physical activity may aid in bone maintenance and mineralization. Smith and Felts (11) found that mice exercised on a treadmill had stronger bone structures with increased organic and inorganic components compared to non-exercised control animals.

METHODS

Fifty clinically osteoporotic women from the ages of 52-97 were selected as a study group. The criteria used to define clinical osteoporosis were; a spontaneous fracture of the femoral neck and/or collapsed vertebra. These women were compared to 50 age matched controls.

In the control group there was no medical history of chronic endocrine, renal, pulmonary or hepatic disease, congestive heart failure, radiotherapy treatment, metabolic calcium or phosphorus disorders, or prolonged bed rest.

The midshaft of the radius of the 100 women was measured with the monochromatic photon absorption technique which has been described in earlier papers (4,12). The amount of mineral in the bone at the scanning site was obtained by measuring the difference between the photon absorption of the bone and soft tissue. The amount of mineral in bone (gm/cm) at the scanning site can then be determined with an accuracy and precision at the 2% level. The estimated values obtained showed a correlation of .99 with the actual mineral present in bone when ashed at $600^{o}C$. for 72 hours (4).

RESULTS

The mean radius bone mineral content of the osteoporotic patients was significantly lower than that of the control group as indicated by a paired t-test, t = 5.54 (Table I). The bone width of the two groups showed no significant differences (Table II). The mean ratio of bone mineral divided by the width of the osteoporotic patients was significantly lower than that of the control group, t = 5.11 (Table II). Discriminant analysis showed that 74% of the control subjects were above, and 78% of the osteoporotic patients were below a bone mineral discriminant value of 0.68 g/cm (Fig. I) (Table IV). Discriminant analysis also showed that 70% of the control subjects were above, and 76% of the osteoporotic

patients were below a bone mineral/width ratio discriminant value of 0.55 g/cm^2 (Fig. 2) (Table V).

An analysis of these data indicate that using a discriminant value of 0.68 g/cm for bone mineral, the diagnostic accuracy would be 76% using the definition of osteoporosis given above. If a bone mineral/width discriminant of 0.55 gm/cm^2 is used, the photon absorption technique would be correct ~ 73% of the time on the same basis as above. A different criteria for the diagnosis of osteoporosis would of course change these figures.

DISCUSSION

A quantitative technique is needed for rapid scanning of large groups of people to aid in early detection of osteoporosis. Such a technique should become as much a part of the senior citizen's physical health maintenance as a regular medical examination.

With the increasing mechanization of our environment, we are becoming physically inactive. Disuse of the human body over a period years may be a part of the unknown etiological factor of osteoporosis.

How should osteoporosis be defined? Too often the term osteoporosis has been defined and redefined to the point where confusion rests with the use of the word. Many clinicians define it as a disease or a syndrome. If one confines the word to mean porous bone, it is neither a disease or a syndrome; but rather a condition. The word osteoporosis itself refers to porous bone where the bone that is present reveals the same balance of phosphorus and calcium as other

bone and seems to show no biological abnormalities in the
organism other than too little bone. The bone mineral loss
is primarily from the endosteal surface of the bone in the
diaphysis thus reducing the cortical thickness of the bone.
While there is some increase in porosity, the primary cause
of bone weakness in osteoporosis is due to thinning of the
cortex. In the metaphysis the cancellous bone is also greatly
reduced weakening its structural support. There are three
main classifications of bone condition:

1) Non-osteoporotic or normal bone,

2) Gerontological (senile) osteoporosis where for
reasons yet unknown, bone loss occurs with increasing
age; and

3) Pathological osteoporosis in which there is advanced
bone loss to the point where spontaneous fractures
occur.

The two terms Gerontological and Pathological osteoporosis
may both be considered to deviate from the normal process of
homeostasis where the rate of bone formation equals the rate
of bone resorption.

The data from this study indicates the usefulness of the
monoenergetic photon absorption technique as an aid in the
diagnosis of pathological osteoporosis and gerontological
osteoporosis. The ability to separate 76% of the osteoporotics
from the control group demonstrates the discriminant value of
the system. It is necessary to emphasize that the age matched
control group was randomly picked from a larger group of women
not showing clinical symptoms of osteoporosis, but these women
do in fact have less bone mineral when compared to younger

females. Those in the control group who overlap the osteo-
porotic group give cause for concern. Their bone mineral
content indicates that the skeletal system shows bone loss
to such an extent that they may be considered more fracture
prone. In a separate study 30 "normal" subjects were found
with bone mineral below the discriminant value of 0.68 gm/cm.
Between the first measurement and one taken six months later,
four of these women broke bones, three were hip fractures
and one was the proximal head of the humerus. The criteria
used for defining osteoporosis in this study are not clearly
satisfactory. We would like to suggest use of the photon
absorption discriminant of 0.68 gm/cm at the midshaft of the
radius in conjunction with other clinical conditions as an
early and more definitive diagnosis of osteoporosis.

The authors would like to acknowledge the aid of John
Jurist and his willingness to give statistical counsel on
analysis of the data. Also, we wish to thank Dick Mazess
and Robert Purvis for their aid in the project.

BIBLIOGRAPHY

1. Arnold, James S., M.D., "Quantitation of Mineralization of Bone as an Organ and Tissue in Osteoporosis," Clin. Orth., No. 17, 1960.

2. Arnold, J.S., M.D., Bartley, M.H., D.D.S., Tont, S.A., and Jenkins, D.P., "Skeletal Changes in Aging and Disease," Clin. Ortho., No. 48, 1966.

3. Casuccio, C., "Concerning Osteoporosis," J. Bone and Joint Surg., 44B, 453-463, 1962.

4. Cameron, J.R. and Sorenson, J.A., "Measurement of Bone Mineral in vivo: An Improved Method," Science, 142: 230-232, 1963.

5. Davis, M. Edward, M.D., Strandjord, Nels M., M.D. and Lanzl, Lawrence H., Ph.D., "Estrogens and the Aging Process," JAMA, April 18, 1966, Vol. 196, No. 3.

6. Frost, Harold M., M.D., "The Bone Dynamics in Osteoporosis and Osteomalacia," Charles C. Thomas Pub., Springfield, Ill., 1966.

7. Garn, Stanley M., Rohmann, Christabel G. and Wagner, Betty, "Bone Loss As A General Phenomenon In Man," Federation Proc., Vo. 26, No. 6, Nov.-Dec., 1967.

8. Hattner, R.S., M.D. and McMillan, D.E., M.D., "Influence of Weightlessness Upon the Skeleton: A Review," Aerospace Medicine, August, 1968.

9. Jowsey, J., "Age Changes In Human Bone," Clin. Ortho., 17, 210-218, 1960.

10. Nordin, B.E.C., "Osteomalacia, Osteoporosis and Calcium Deficiency," Clin. Ortho. Related Res., 17: 235, 1960.

11. Smith, Everett L., and Felts, William J., "The Effects of Physical Activity on Bone," In Press.

12. Sorenson, James A. and Cameron, J.R., "A Reliable In Vivo Measurement of Bone Mineral Content," J. Bone and Joint Surg., Vol. 49-A, No. 3, pp. 481-497, April, 1967.

13. Urist, M.R., MacDonald, N.S., Noss, M.J., and Skoog, W.A., "Rarefying Disease of the Skeleton: Observation dealing with , aged and dead bone in patients and osteoporosis, in mechanisms of hard tissue destruction," Pub. No. 75, Amer. Assoc. for the Advancement of Science, Washington, D.C., 385-446, 1963.

14. Whedon, G.D., Deitrick, J.E. and Shorr, E., "Modification of the Effects of Immobilization upon Metabolic and Physiologic Functions of Normal Men by the Use of an Oscillating Bed," Am. J. of Med. 5: 684, 1949.

15. George, P., "Quantitative Microradiography of Osteoporotic Compact Bone," Clin. Ortho. 24, 206-212, 1962.

TABLE I

BONE MINERAL CONTENT OF THE MID-SHAFT OF THE RADIUS FOR 50

OSTEOPOROTIC WOMEN AND 50 AGE MATCHED NORMAL WOMEN

N = 50	Mean	S.D.	S.E.	t-test	Sign
Age	74.1	11.1			
Control	0.76 g/cm	0.13	0.02	5.54	P<0.001
Osteoporotic	0.62 g/cm	0.12	0.02		

$$\text{Mean } \bar{x} = \frac{\Sigma x}{N} \qquad \text{S.D.} = S^2 \quad \text{Standard Deviation} \qquad \text{S.E.} = \frac{SD}{N} \quad \text{Standard Error}$$

$$dF = (N - 1)$$

$$t = \frac{\bar{d}}{\frac{Sd^2}{N}}$$

Here $\bar{d}$ is the mean difference between paired measurements.

Sd^2 is the variance of these differences and N is the number of specimens.

N = Number of pairs

TABLE II

BONE WIDTH OF THE MID-SHAFT OF THE RADIUS FOR

50 OSTEOPOROTIC WOMEN AND 50 AGE MATCHED NORMAL WOMEN

N = 50	Mean	S.D.	S.E.	t-test	Sign.
Control	1.27 cm	0.14	0.02		
Osteoporotic	1.27 cm	0.15	0.02	0.03	None

$$\text{Mean } \bar{x} = \frac{\Sigma x}{N} \qquad \text{S.D.} = S^2 \text{ Standard Deviation} \qquad \text{S.E.} = \frac{SD}{N} \text{ Standard Error}$$

$$dF = (N - 1)$$

$$t = \frac{\bar{d}}{\frac{Sd^2}{N}}$$

Here $\bar{d}$ is the mean difference between paired measurements.

Sd^2 is the variance of these differences and N is the number of specimens.

N = Number of pairs

TABLE III

BONE MINERAL DIVIDED BY BONE WIDTH OF THE MID-SHAFT OF THE RADIUS

FOR 50 OSTEOPOROTIC WOMEN AND 50 AGE MATCHED NORMAL WOMEN

N = 50	Mean	S.D.	S.E.	t-test	Sign
Control	0.60 g/cm^2	0.09	0.01		
Osteoporotic	0.49 g/cm^2	0.09	0.01	5.11	P<0.01

Mean $\bar{x} = \dfrac{\Sigma x}{N}$ S.D. = S^2 Standard Deviation   S.E. = $\dfrac{SD}{N}$ Standard Error

dF = (N - 1)

$t = \dfrac{\bar{d}}{\dfrac{Sd^2}{N}}$ Here $\bar{d}$ is the mean difference between paired measurements.

Sd^2 is the variance of these differences and N is the number of specimens.

N = Number of pairs

TABLE IV

BONE MINERAL DISCRIMINANT ANALYSIS OF THE MID-SHAFT OF THE RADIUS

FOR 50 OSTEOPOROTIC WOMEN AND 50 AGE MATCHED NORMAL CONTROLS

N = 100 Cases	Normal	Osteoporotic
BM $\geq$ 0.68 g/cm	37	11
BM < 0.68 g/cm	13	39

Discriminant is 0.68 g/cm $\quad \hat{S} = \dfrac{37 + 39}{37 + 11 + 13 + 39}$ x100 $\quad \hat{S} = 76\%$

$\hat{S}$ = Correct diagnosis

TABLE V

BONE MINERAL DIVIDED BY BONE WIDTH DISCRIMINANT ANALYSIS

OF THE MID-SHAFT OF THE RADIUS FOR 50 OSTEOPOROTIC

WOMEN AND 50 AGE MATCHED NORMAL CONTROLS

N = 100 Cases	Normal	Osteoporotic
BM/W > 0.55 gm/cm^2	35	12
BM/W < 0.55 gm/cm^2	15	38 $\bar{S}$=73%

$$\bar{S} = \frac{35 + 38}{35 + 12 + 15 + 38} \times 100 = 76\%$$

Discriminant is 0.55 gm/cm^2

$\bar{S}$ = Correct diagnosis

NORMALS

DISCRIMINANT=0.68g/cm

OSTEOPOROTICS

FIGURE 1

NUMBER OF SUBJECTS

MIDSHAFT RADIUS BM (g/cm)

FIGURE 2